THE ELECTRICAL PROPERTIES OF CONCRETE

by

John Wilson B.Sc.

THESIS SUBMITTED TO THE UNIVERSITY OF EDINBURGH

FOR THE DEGREE OF DOCTOR OF PHILOSOPHY

1986

UNIVERSITY OF EDINBURGH

DEPARTMENT OF ELECTRICAL ENGINEERING

ABSTRACT

This thesis describes research into the electrical properties of concrete for frequencies up to 1000 MHz. The general properties of concrete, and non-electrical methods of testing structural concrete are described.

A theoretical description of the electrical behaviour of concrete is synthesised from the behaviour of its constituents, and the work of other authors in the field of electrical measurements on concrete is reviewed.

The development and performance of equipment to measure the resistivity of a large number of samples of concrete at 2 kHz, is described, and the application of the results obtained is discussed. There is a possibility of determining the basic mix ratios of samples within one day of mixing.

The results of experiments to measure the electrical impedance of concrete over the frequency range 1 - 1000 MHz are presented. These indicate that the equipment is sufficiently sensitive to measure variations in the constituents of concrete. The resistivity and dielectric constant of various concrete samples are calculated from impedance data using an approximate technique, and might prove valid indicators of the constituents of concrete.

Suggestions for further research in this field are presented.

DECLARATION.

I declare that this thesis was written by me, and that the work described was carried out by me unless otherwise acknowledged.

ACKNOWLEDGEMENTS.

The author wishes to thank both Professor J.H. Collins and Professor J. Mavor of the Department of Electrical Engineering at the University of Edinburgh, and also Mr. P.H. Beards of the Department of Electrical and Electronic Engineering at Napier College, and Professor A.W. Hendry of the Department of Civil Engineering and Building Science at the University of Edinburgh, for placing the facilities of their respective departments at his disposal.

The author is grateful to Dr. H.W. Whittington for his supervision and guidance through the unsuspected pitfalls and minefields of multidisciplinary research. The contribution of Dr. M.C. Forde in assisting in the setting up of the project, and as second supervisor in the early stages, is also acknowledged.

The author would also like to thank the following fellow students for their helpful discussions and assistance; Dr. Roberto Morelli who was working on parallel research in the Department of Civil Engineering and Building Science, and who was largely responsible for the construction of the environmental control system and the supporting structure for the hoist for the initial low frequency system; Dr. Bijan Kiani-Shabestari for discussion on the implementation of the IEEE bus interface system used in the developed low frequency resistivity system; and Mr. Henry Young, now an honours graduate of the University of Edinburgh, for discussions on the Maxwell-Wagner effect, and the application of suitable models to concrete.

The author would also like to thank Dr. M. Jack and Dr. J. Robertson of the Department of Electrical Engineering, University of Edinburgh, and their associates, for their assistance during the development of the microelectronic circuits for the developed low frequency system.

The advice and assistance of the heads and staff of the following departments at Napier College are gratefully acknowledged:-

Civil Engineering

Mechanical Engineering

Industrial Engineering

Applied Chemical Studies

Library Services Unit

Computer Services Unit

The author is particularly indebted to his wife Ann for her patience during his involvement in a part time degree, and also for reading the manuscript. He is also indebted to the rest of his family, and to his colleagues in the Department of Electrical and Electronic Engineering at Napier College, for their forbearance.

Funding for this work has been provided by the Science and Engineering Research Council, and by Lothian Regional Council, and is gratefully acknowledged.

CONTENTS.

NOTATION.

The following symbols are used in this thesis:-

A	Al_2O_3
A	a constant
A	area of plate (m^2)
A	real part of the propagation constant (neper/m)
A_a	depolarising factor
A_b	depolarising factor
A_c	depolarising factor
A/D	analogue to digital
a	a constant
a	length of major axis (m)
a	separation of plates (m)
B	imaginary part of the propagation constant (rad/m)
BASIC	computer programming language
b	maximum diameter (m)
b	width of plates (m)
C	CaO
C	capacitance (F)
C	capacitance per unit length (Fm^{-1})
CAPO	an in-situ mechanical test
C_X	values of capacitance (F)

C/S/A	cement/sand (fine aggregate)/coarse aggregate ratios
c	length of macro-defect (m)
c	velocity of light $3x10^8$ ms^{-1}
c	concentration (M)
c_s	ion concentration (N)
D_1	amplitude of the in-phase component of the electric flux density (Cm^{-2})
D_2	amplitude of the quadrature component of the electric flux density (Cm^{-2})
d	thickness (m)
d	plate separation (m)
d_1	thickness of insulating layer (m)
d_1	thickness of medium 1 (m)
d_2	thickness of medium 2 (m)
E	amplitude of the applied electric field intensity (Vm^{-1})
E	activation energy (J)
EOI	end or identify
E_o	a constant
EPROM	erasable programmable read only memory
F	Fe_2O_3
FET	field effect transistor
f	frequency (Hz)
f_r	relaxation frequency (Hz)
G	conductance (S)
G	conductance per unit length (Sm^{-1})

G	amplifier voltage gain
H	H_2O
$\underset{\sim}{I}$	complex current (A)
IEEE	Institute of Electrical and Electronic Engineers (USA)
IRQ	interrupt request
k	a constant
k	Boltzmann's constant 1.38×10^{-23} JK^{-1}
k_1	a constant
k_2	a constant
L	physical length (m)
L	inductance per unit length (Hm^{-1})
LED	light emitting diode
LOK	an in-situ mechanical test
LSI	large scale integration
L'	apparent conduction length (m)
l	length of side of sample cube (m)
l	length of transmission line (m)
MAJIC	name of cell library
m	a constant
m	mass (kg)
N	integer values
NMI	non-maskable interrupt
PUNDIT	ultrasonic test equipment
p	porosity
q	charge (C)
R	resistance (Ω)

R	real part of measured impedance (Ω)
RAM	rapid analysis machine
RAM	random access memory
R_c	calibration resistance (Ω)
R_o	a constant
R_o	real part of the characteristic impedance (Ω)
R_o	resistance at 0 °C (Ω)
R_T	resistance at temperature T (Ω)
R_x	values of resistance (Ω)
r	frictional constant
r_a	cement/aggregate ratio
r_w	water/cement ratio
S	SiO_2
SRQ	service request
s	compressive strength (Pa)
s_a	specific gravity of aggregate
s_c	specific gravity of dry cement powder
T	temperature (°C,K)
T	period of waveform (s)
T_o	temperature (°C)
T_o	reference temperature (°C)
TTL	transistor/transistor logic
t	time (s)
t_o	time from start of half cycle (s)
$\underset{\sim}{V}$	complex voltage (V)
V_a	volume of air (m^3)

V_c	volume of cement (m^3)
V_o	amplitude of output voltage (V)
V_{or}	amplitude of output reference voltage (V)
V_r	amplitude of energising voltage (V)
V_w	volume of water (m^3)
VIA	versatile interface adaptor
v	fractional volume of pore water
v	velocity (ms^{-1})
v	fractional volume of imbedded particles
v	fractional volume of cement paste
v_o	output voltage as a function of time (V)
v_r	energising voltage as a function of time (V)
W/C	water/cement ratio
w/c	water/cement ratio
X	imaginary part of measured impedance (Ω)
X_o	imaginary part of the characteristic impedance (Ω)
x	fractional volume of water channel
Z	impedance (Ω)
Z_o	characteristic impedance (Ω)
α	relaxation time spread parameter
α	temperature coefficient of conductance (/^oC)
α	fractional deviation in output voltage

α_L	effective length ratio
α_n	conductance ratio
γ	propagation constant
ΔR_x	changes in resistance values (Ω)
ΔV_o	change in amplitude of output voltage (V)
ΔV_{or}	change in amplitude of output reference voltage (V)
$\Delta\varepsilon$	increment in dielectric constant
$\Delta\sigma$	percentage elevation in conductivity
$\Delta\lambda$	increment in relaxation wavelength (m)
δ	phase lag (rad)
δ	dielectric increment
$\delta\lambda$	wavelength increment (m)
$\underset{\sim}{\varepsilon}$	complex dielectric constant
ε_{As}	low frequency dielectric constant of the water channel
$\varepsilon_{A\infty}$	high frequency dielectric constant of the water channel
ε_{Bs}	low frequency dielectric constant of the needle channel
$\varepsilon_{B\infty}$	high frequency dielectric constant of the needle channel
ε_o	permittivity of free space 8.85×10^{-12} Fm^{-1}
ε_r	dielectric constant
ε_s	static dielectric constant
ε_s	dielectric constant of solution

ε_w	dielectric constant of water
ε_1	dielectric constant of insulating layer
ε_1	dielectric constant of medium 1
ε_2	dielectric constant of bulk material
ε_2	dielectric constant of medium 2
ε_∞	dielectric constant at infinite frequency
ε'	real part of dielectric constant
ε''	imaginary part of dielectric constant
Λ_{oT}	equivalent conductance at infinite dilution at T ^oC (Sm^{-1}/N)
Λ_{on}	equivalent conductance at infinite dilution (Sm^{-1}/N)
Λ_{o25}	equivalent conductance at infinite dilution at 25 ^oC (Sm^{-1}/N)
λ	wavelength (m)
λ_r	relaxation wavelength (m)
λ_s	relaxation wavelength of solution (m)
λ_w	relaxation wavelength of water (m)
μ	ion mobility
μ_o	permeability of free space 1.26×10^{-6} Hm^{-1}
ρ	resistivity (Ωm)
ρ_T	resistivity at temperature T (Ωm)
ρ_o	resistivity at temperature T_o (Ωm)
ρ_p	resistivity of cement paste (Ωm)
ρ_{20}	resistivity at 20 ^oC (Ωm)
σ	flexural strength (Pa)

σ	conductivity (Sm^{-1})
σ	standard deviation
$\sigma_{A\infty}$	high frequency conductivity of the water channel (Sm^{-1})
$\sigma_{B\infty}$	high frequency conductivity of the needle channel (Sm^{-1})
σ_D	change in conductivity (Sm^{-1})
σ_c	compressive strength (Pa)
σ_m	conductivity of aggregate/cement matrix (Sm^{-1})
σ_o	a constant (Sm^{-1})
σ_O	standard deviation of output voltage (V)
σ_{or}	standard deviation of output reference voltage (V)
σ_s	static conductivity (Sm^{-1})
σ_w	conductivity of pore water (Sm^{-1})
σ_x	values of standard deviation
σ_1	conductivity of medium 1 (Sm^{-1})
σ_2	conductivity of medium 2 (Sm^{-1})
σ_∞	conductivity at infinite frequency (Sm^{-1})
τ	dielectric relaxation time (s)
τ	time constant (s)
τ_x	values of time constants (s)
τ_1	relaxation time for layer structure (s)
ω	radian frequency (rad/s)
ω_r	relaxation frequency (rad/s)

1. STRUCTURAL CONCRETE.

1.1. Introduction.

Concrete is made by adding water to a mixture of cement, sand (fine aggregate), and coarse aggregate. Hydration takes place between the water and cement, producing a matrix of compounds, which is known as cement paste. This matrix locks together the coarse and fine aggregate particles to form a material with considerable compressive strength.

The coarse and fine aggregates are cheap, high strength fillers, and are not normally regarded as active constituents, these being limited to cement and water.

In the United Kingdom, the cement used most frequently is ordinary Portland cement. This is manufactured by mixing together calcereous (chalk or limestone) and argillaceous (clay) materials, burning them at high temperature so that clinkering occurs, and then grinding the resultant clinker to a fine powder. Portland cement gets its name from its similarity in colour and texture to Portland stone which is quarried in Dorset.

A concrete mix is normally defined by the mass ratios of constituents:-

(a) water/cement ratio

(b) cement/sand/aggregate ratio

or cement/total aggregate ratio.

The compressive strength of concrete is largely dependent on the cement matrix, and is given empirically by Abram's Law:-

$$s = \frac{k_1}{k_2^{w/c}}$$

where s = compressive strength

k_1, k_2 = constants

w/c = water/cement ratio.

Concrete is a brittle material, and figures presented by Neville [1] suggest that the direct tensile strength can be as low as 0.1 of the strength in compression. When concrete is used in a load bearing structure such as a beam or a pillar, tensile strength is obtained by reinforcing the concrete with steel bars.

1.2. Chemistry and Structure of Cement Paste.

1.2.1. Chemistry of Cement Hydration.

The chemistry of cement has been studied extensively. Summaries are given by Neville [1] and Double [2].

The materials used to manufacture cement are impure, but consist mainly of lime, silica, alumina, and iron oxide. During the manufacturing process these compounds react to form more complex products. The process is further complicated in that, during cooling, both crystalline and amorphous products are obtained, and the properties of these forms are different. Whether a particular batch of cement is acceptable is normally determined by direct physical testing of the properties considered of practical importance.

Cement chemists use a shortened notation to refer to oxides; thus $CaO = C$, $SiO_2 = S$, $Al_2O_3 = A$, $Fe_2O_3 = F$, and $H_2O = H$.

The main constituents of cement are:-

Compound	Oxide Composition	Abbreviation
Tricalcium silicate	$3CaO.SiO_2$	C_3S
Dicalcium silicate	$2CaO.SiO_2$	C_2S
Tricalcium aluminate	$3CaO.Al_2O_3$	C_3A
Tetracalcium aluminoferrite	$4CaO.Al_2O_3.Fe_2O_3$	C_4AF

These compounds are generally referred to by their abbreviations. A number of minor compounds such as MgO, TiO_2, Mn_2O_3, K_2O, and Na_2O are also present, but each amounts to only a few percent of the total mass of the cement. Na_2O and K_2O are known as "the alkalis" and have been found to react with certain aggregates in concrete. The products of the reaction can cause disintegration of the concrete.

C_2S can take a number of different forms depending on the temperature conditions during the manufacture of the cement. C_4AF is actually a solid solution with constituents ranging from C_2F to C_6A_2F, C_4AF being a convenient simplification.

When water is added to cement, two different hydration reactions can take place. The first is the direct addition of water molecules which is a true hydration process. The second reaction is hydrolysis. Both are considered part of cement hydration.

The hydration of both tricalcium silicate and dicalcium silicate give rise to similar calcium silicate hydrates, with approximate composition $C_3S_2H_3$. Since this is an approximation it

cannot strictly be used in a stochiometric formula, but it gives realistic results [1].

For tricalcium silicate

$$2C_3S + 6H \leftrightarrow C_3S_2H_3 + 3Ca(OH)_2$$

The corresponding masses are

$$100 + 24 \leftrightarrow 75 + 49$$

For dicalcium silicate

$$2C_2S + 4H \leftrightarrow C_3S_2H_3 + Ca(OH)_2$$

and the corresponding masses are

$$100 + 21 \leftrightarrow 99 + 22$$

Thus while both silicates require approximately the same amount of water, tricalcium silicate produces much more calcium hydroxide ($Ca(OH)_2$).

The reaction of tricalcium aluminate with water is very rapid, and gives rise to immediate stiffening of the cement paste, which is undesirable in normal cement; this is known as flash set. To prevent this rapid reaction, gypsum ($CaSO_4.2H_2O$) is added to the cement clinker during manufacture. Gypsum and tricalcium aluminate react to form insoluble calcium sulphoaluminate. The sulphate content then gradually reduces until eventually a tricalcium aluminate hydrate is obtained. Ignoring the intermediate stages, an approximate formula is:-

$$C_3A + 6H \leftrightarrow C_3AH_6$$

with corresponding masses

$$100 + 40 \leftrightarrow 140$$

Thus the tricalcium aluminate requires considerably more water than the silicates.

Gypsum reacts with tetracalcium aluminoferrite to form calcium sulphoferrite and calcium sulphoaluminate.

The amount of gypsum added to cement must be very carefully controlled, since too much gypsum can cause expansion and disruption of the cement paste.

The products of hydration of cement have low solubility in water, which gives hardened cement paste good stability in water.

Because hydration processes are exothermic, rates of reaction can be assessed by measurement of the rate of heat evolution. There is an initial peak in heat generation in the first few minutes after water is added to the cement. This is believed to be due to the heat of wetting the C_3S powder and the hydration of free lime [2]. The heat generated then falls to a low value for the period between 1 to 3 hours after water is added. The rate of heat production then increases again and reaches a maximum after between 8 and 10 hours, and then falls gradually. The time at which the second maximum is reached can be reduced by increasing the ambient temperature. Figure 1.1 after Double [2] shows the heat evolution graph for the hydration of C_3S, which shows similar characteristics.

The relative rates of hydration of C_3S and C_2S have been determined by examining the reactions of pure C_3S and C_2S [1]. C_3S hydration is largely complete within a day, but hydration of C_2S only becomes significant after about 7 days.

The variations in ionic concentrations in free water in the cement paste are shown in Figure 1.2 after Double [2]. Initially the most numerous species are calcium and sulphate ions, their concentrations reaching a peak a few minutes after the mixing of

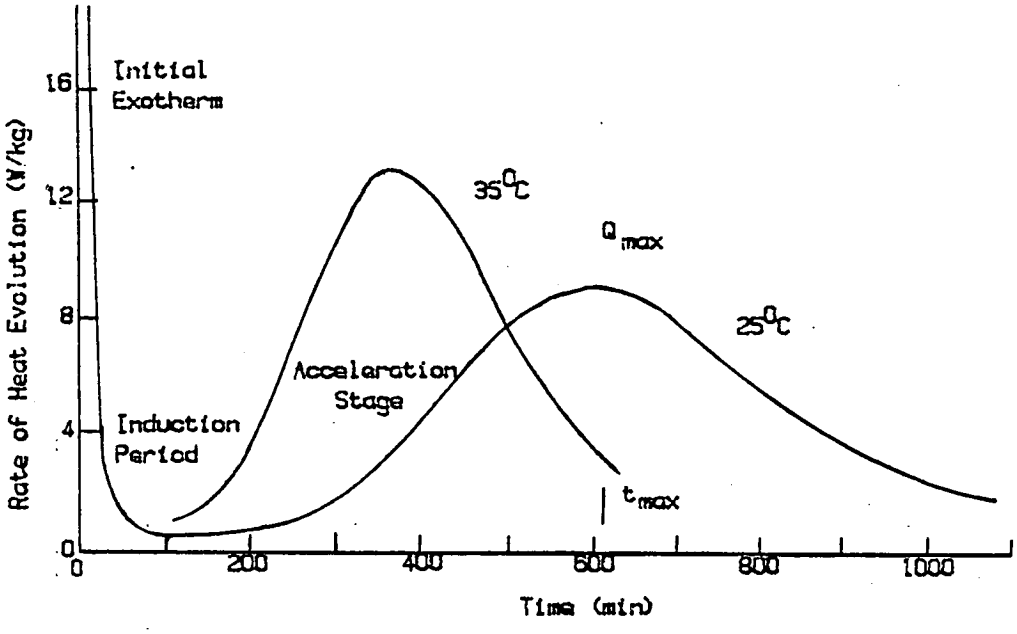

Figure 1.1
Heat Evolution for the Hydration of C_3S after Double

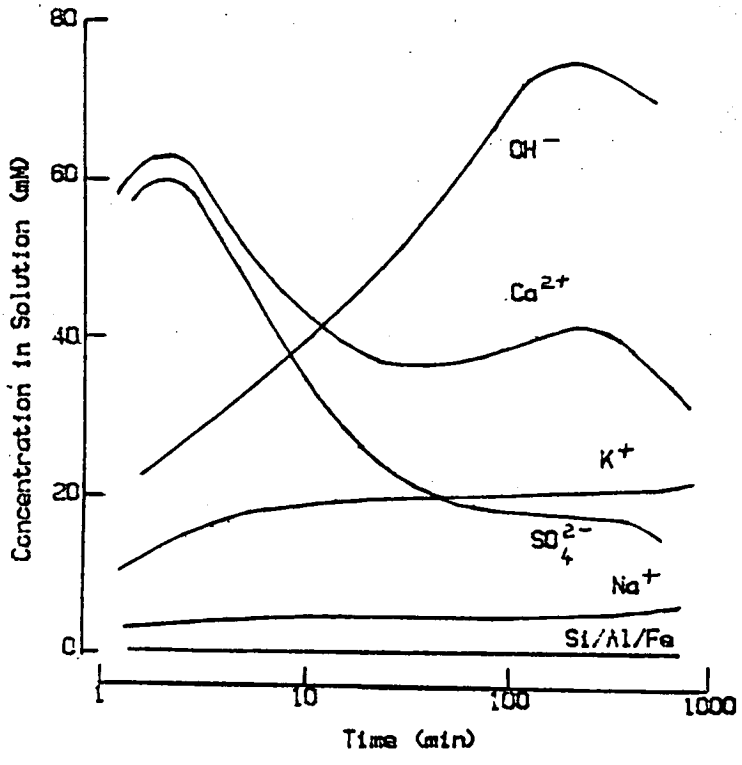

Figure 1.2
Ionic Concentrations in Free Water in Cement
Paste after Double

cement and water. The sulphate ion concentration then falls rapidly, and, by approximately 2 hours, has dropped to a relatively low value. This is probably related to the aluminate and aluminoferrite reactions with gypsum. The calcium ion concentration also falls, but then rises again to reach a second broad but lower peak sometime after 2 hours. The concentration of hydroxyl ions is initially relatively low, but increases progressively until it also reaches a maximum after about 2 hours, by which time it is the most numerous species.

The ionic concentration is still high after 16 days. This probably reflects the presence of unhydrated cement.

At all times the silicate ion concentration is low.

1.2.2. Structure of Hydrating Cement Paste.

The process of cement hydration is usually divided into two sections; setting, which is the period during which the cement changes from a fluid to a solid state; and hardening, which is the subsequent period during which the cement develops strength. Setting is sometimes defined in terms of the changes in temperature as a result of hydration. Initial set includes the initial peak in temperature. Final set is when the second maximum is obtained following the relatively constant low temperature.

Double [2] describes the development of the paste microstructure during the setting period based on electron microscopy studies by a number of workers. Two models have been proposed to explain the relatively long induction period between the

initial set and the point where the temperature starts to rise once more.

The delayed nucleation theory suggests that there is a mechanism preventing the hydration of silicates, and that this is associated with delayed nucleation of $Ca(OH)_2$ and the resultant increase in lime in solution which inhibits the silicate reaction.

The protective coating theory suggests that rapid precipitation of calcium silicate hydrate round the cement grains during initial set, provides a barrier which slows the access of water, and retards hydration during the induction period. The coating is seen as a membrane which allows inward diffusion of water to the cement grains, and outward diffusion of calcium and hydroxyl ions, but no outward diffusion of the larger silicate ions. This results in an increasing osmotic pressure within the coating which eventually causes rupture of the coating. The silicate ions are then released into the solution, which immediately causes calcium silicate hydrates to be precipitated because of the high concentration of lime in solution.

Double suggests that the protective coating theory is the better model, in that it explains the variations in ion concentration in the free water in the cement paste, and has similarities with other silicate reactions. In addition, Pratt and Ghose [3] have obtained electron micrographs of cement, which appear to show fractured shells with the remains of the unhydrated cement grain inside.

Double [2] describes the structure of the cement gel as consisting of irregular fibres of silicate growing from the surface

of the cement grains and bridging the spaces between them. Plate-like crystals of calcium hydroxide also appear in the structure. The initial gelatinous coating of hydrates on the cement grains is of the order of 0.1 - 1.0 μm thickness. In fully aged cement there is considerable in-filling of the structure by fine grained silicate hydrate gel and by growth of crystalline hydration products. Structures are also formed on the inside of the grain coating. These usually have a fine grained and compact texture.

Because of the initial random distribution of cement grains and water, there will be zones in the matrix which are not filled with cement gel. These are called capillary pores, and are approximately 1.3 μm in diameter [1], and form an interconnected system randomly distributed throughout the structure.

Because the gel is not a continuous amorphous structure, it contains a relatively large volume of much smaller voids called gel pores. These are between 1.5 and 2.0 nm in diameter, which is only an order of magnitude greater than the diameter of the water molecule. The gel pores account for approximately 28% of the total volume of the gel.

If the water/cement ratio of the paste is sufficiently low, and the paste is allowed to undergo moist curing for a long period of time, it is possible for the capillary pores to be blocked by gel, and to become segmented such that the pore structure consists of segmented capillary pores interconnected by gel pores. This cannot occur for water/cement ratios greater than 0.7.

Neville [1] describes the distribution of water in the cement paste. Water is held in three major ways. There is the chemically

combined water forming part of the hydrated compounds, adsorbed water which is held by the surface forces of the gel particles, and pore water which is contained within the gel and capillary pores.

The water content is sometimes classified into evaporable and non-evaporable water. In well hydrated cement, the non-evaporable water is about 18% of the mass of original unhydrated cement. This figure rises to about 23% in fully hydrated cement.

Neville [1] gives the volume distribution for products in a cement paste of water/cement ratio 0.475, where the system has been sealed to prevent inward or outward flow of water. The distribution is:-

(i) No hydration

Water 60%

Unhydrated cement 40%

(ii) 50% hydration

Empty capillary pores 3.7%

Capillary water 33.5%

Gel water 12.0%

Products of hydration 30.8%

Unhydrated cement 20%

(iii) 100% hydration

Empty capillary pores 7.4%

Capillary water 7.0%

Gel water 24%

Products of hydration 62.6%

In normal cement, the amount of water in the capillary pores can vary depending on the relative humidity. If the relative

humidity falls below about 45%, the capillary pores will empty, but this will depend on the degree to which the capillary pores have become segmented.

1.2.3. Admixtures.

Substances are frequently added to concrete at the time of mixing to modify its characteristics. Such admixtures and their effects are described by Neville [1], Double [2], and Schutz [4]. The usual effects required are, acceleration of hardening (accelerators), retardation of setting (retarders), and improvement in workability (plasticizers and superplasticizers).

Accelerators are usually used when concrete is to be placed at low temperatures (2 - 4 ^{o}C), to minimise the possibility of frost damage, and during repair work which must be completed in a short time. The most commonly used accelerator is calcium chloride. The amount added is unlikely to exceed 2% of the cement by mass. The effect of calcium chloride is not known in detail, although it is thought that it acts as a catalyst in the hydration of C_3S and C_2S [1].

The presence of calcium chloride can have deletereous effects on the durability of hardened concrete, including reduction in resistance to sulphate attack, and can result in increased corrosion of reinforcement, although this is still a subject of controversy.

Retarders are used when concreting in hot weather to delay the rapid onset of hardening caused by the elevated temperature, and to obtain certain architectural finishes. The admixtures are usually

soluble organic compounds similar to sugar. The amount of sugar added is usually about 0.05% of the cement by mass. Addition of large quantities of sugar in the range 0.2 - 1% will completely prevent setting of the cement. The chemical effect of sucrose is also the subject of speculation. It is thought to affect the hydration of C_3S, although there might also be reaction with aluminates. One theory suggests that the organic compounds have the capability of binding calcium, resulting in an increase in silicates in solution, and delaying the precipitation of silicate hydrates.

The early strength of cement incorporating retarders is reduced, but beyond 7 days, the strength is increased by a few percent. This is probably due to a denser gel caused by the delay in setting.

Plasticizers are used to improve the workability of a given mix, or to allow a reduction in water/cement ratio for a given workability, and so improve the basic strength. The admixtures used are usually complex organic acids or their salts. These substances may also have retarding or accelerating properties. The admixtures are surface-active, and are adsorbed onto the cement grains giving them a negative charge. This causes repulsion between the grains, and stabilizes their dispersion. The charge on the grains also causes a sheath of oriented water molecules to form round each grain, preventing the particles coming into direct contact. The cement grains have therefore a greater mobility, and the existing water in a mix becomes a more efficient lubricator giving improved workability.

The dispersion of the cement grains exposes a greater surface

area of cement to hydration, which may therefore proceed faster at an early stage. An increase in strength is therefore obtained with young concretes which might persist for a considerable time.

The effects of admixtures are very much dependent on the composition of the cement. It is necessary therefore to carry out a series of tests to determine the correct proportion of the admixture for the particular cement being used.

1.3. Strength and Durability of Concrete.

1.3.1. Strength of Cement Paste.

From Abram's Law, it can be seen that the strength of concrete is generally dependent on the characteristics of the cement paste.

At the microscopic level, the paste consists of a combination of a gelatinous mass and interlaced elongated crystals of hydrated compounds. The strength of the paste will dependent on the forces acting between the hydrated material which has been precipitated, and also between the unhydrated cement and the hydrated material. Neville [1] suggests two forces which contribute to the strength of the gel. These are, the van der Waal forces which are the forces of attraction between surfaces separated by very small distances e.g. across gel pores, and the force of the chemical bond. The chemical bond is of much greater magnitude than the van der Waal forces, but can exist only between gel particles which are in contact, and can therefore act only over a small fraction of the boundary area of a gel particle.

The early strength of the paste is largely due to the hydration of C_3S, but after about 14 days, the products due to C_2S become significant, and a progressive increase in strength due to these components is obtained over a period of many months. Aluminates contribute to strength in the very early stages, but as the hydration process continues, their contribution becomes of little significance.

Hardened cement is a relatively weak material, with the tensile strength being much lower than the compressive strength. Kendall, Howard, & Birchall [5] quote a flexural strength of 7 MPa and a compressive strength of 40 MPa. Feret's empirical law for the compressive strength of cement [5] gives

$$\sigma_c = A\left\{V_c/(V_c + V_w + V_a)\right\}^2$$

where σ_c = compressive strength

A = a constant

V_c = volume of cement

V_w = volume of water

V_a = volume of air

Thus the compressive strength is related to the porosity of the cement.

Neville [1] suggests that failure in compression is caused by an initial failure in tension, since if a compressive strain is present, there must also be a tensile strain at right angles to it because of Poisson's ratio. Thus it can be expected that for a porous material like cement, where the tensile strength is low, the

compressive strength will also be low, but will be much higher than the tensile strength.

Kendall et al [5] demonstrated that by reducing the occurrence of macro-defects in cement i.e. the occurrence of voids or pores with dimensions in the region of 1 mm, the flexural strength can be increased to 70 MPa, and by reducing the basic porosity, after removing these defects, the flexural strength can be further increased to 150 MPa, with a corresponding compressive strength of 300 MPa. Kendall et al [5] accept that a proportion of the increase in strength is due to the presence of a polymer additive used in the process.

On the basis of these results, an equation has been developed for the flexural strength of a brittle material which contains macro-defects of a constant size, and which is also porous. The equation is:-

$$\sigma = \left\{ \frac{E_o R_o (1 - p)^3 \exp(-kp)}{\pi c} \right\}^{\frac{1}{2}}$$

where σ = flexural strength

E_o, R_o, and k are constants

p = porosity

c = length of macro-defect

This equation is derived from the Griffiths' formula [6], which considers flexural failure as being due to stress concentration at the ends of cracks or pores.

Assuming that the compressive strength is related to the flexural strength, and by comparing this equation with Feret's

equation, it can be deduced that the macro-defect length in normal cement must be in the region of 2 mm, and that the maximum size of such defects using the normal mixing process must be approximately constant. Assuming this size of defect, the derived equation corresponds closely to Feret's law with variation in porosity.

1.3.2. Strength of Concrete.

The strength of concrete must depend on:-

(i) the strength of the cement paste

(ii) the strength of the aggregate

(iii) the strength of the bond between the cement and the aggregate,

and (iv) the degree of voiding which occurs.

The compressive strength of aggregates is generally greater than 110 MPa [1] compared with a compressive strength of 40 MPa for cement paste. The basic strength of the aggregate is therefore unlikely to be a limiting factor in the strength of concrete.

The bond between the cement and aggregate depends on the state of the surface of the aggregate and the kind of aggregate [1]. The bond is greater with crushed rock than with gravel, which has a smoother surface. A better bond is also obtained with aggregate which is porous and heterogeneous.

One failure theory suggests that failure occurs in the interface between mortar and coarse aggregate, and that fine cracks exist in this interface region even before load is applied [1]. At 30% of ultimate load, the extent of the cracks increases, and at

approximately 80% of ultimate load, cracks open up through the mortar.

Frohnsdorff & Skalny [7] suggest however, that while cracks exist at the interface, they are not necessarily the initial cause of failure.

The presence of air voids in concrete caused by poor compaction, can result in a serious reduction in strength. 5% of voids can result in a 30% fall in strength [1]. A reduction in strength is predicted by both Feret's formula, and that developed by Kendall et al. Feret's formula however suggests that strength is dependent on the total volume of entrapped air, whereas the Kendall formula suggests that the strength depends on the largest void dimension.

1.3.3. Durability of Concrete.

A building is expected to have a life of many decades. Concrete used in its construction must have the durability to enable the expected life to be achieved without excessive maintenance. The achievement of adequate durability is therefore just as important as basic strength.

The strength of reinforced concrete can be degraded in two basic ways.

(i) The concrete can be damaged by physical or chemical attack,

and (ii) the concrete can be penetrated by chemicals which cause corrosion of the reinforcement

An additional effect in (i) is that if the concrete is damaged, access to the reinforcement will allow corrosion to take place, and in (ii), the products of corrosion have a greater volume than the steel from which they were produced, thus causing cracking of the concrete cover.

The most common physical attack is that caused by extremes of temperature. If there is significant difference in the thermal expansion or contraction between the aggregate and the mortar, then cracking can occur.

If the temperature falls to freezing point, and there is water in the pores near the surface of the concrete, this water will freeze and expand. After a number of freezing cycles, errosion of the surface material can be expected.

A chemical reaction can take place between the alkalis in cement, and active silica in some aggregates. The active forms of silica are opal, chalcedony, and tridymite. These are present in a number of rocks. The reaction, believed to be between the alkali hydroxides and the silaceous minerals, produces an alkali-silicate gel which absorbes water. Damage is then caused to the structure as a result of hydraulic pressure caused by osmosis [1].

Cement paste can be attacked by ground water from clay containing alkali, magnesium, or calcium sulphates. The sulphates react with calcium hydroxide and calcium aluminate hydrate to produce gypsum and calcium sulphoaluminate. The products of this reaction have much greater volume than the original compounds,

leading to expansion and disruption of the concrete [1].

Cement paste is attacked by CO_2 and SO_2 in the atmosphere in the presence of moisture. It is also attacked by acidic ground water. Part of the cement paste is dissolved and removed, leaving the cement in a soft porous condition [1]. When the attack is by CO_2, the process is called carbonation.

Concrete can be attacked by sea-water in a number of ways [1]. Sulphates in the water will cause sulphate attack, but the presence of chloride ions makes the products of the reaction more soluble, and they are leeched out by the sea-water. Expansion due to the products of the reaction is therefore prevented, and damage progresses at a much slower rate. Formation of salt crystals in the pores can cause disruption of the concrete. This form of attack normally occurs above the water level, where the sea-water is allowed to evaporate.

The conditions for corrosion of the reinforcement are discussed in detail by McArthur [7]. In general, corrosion requires the presence of moisture with a low pH value, and oxygen. Corrosion does not take place in an alkaline environment. Therefore, for corrosion to occur, the concrete cover must be either porous or damaged.

Carbonation of concrete causes a reduction in pH by the removal of calcium hydroxide. If carbonation takes place, the probability of corrosion is high.

Chloride ions present due to sea-water or de-icing materials, accelerate corrosion by the formation of anodic and cathodic regions in the material. Concrete which is covered and exposed by the tide

is most susceptible to corrosion due to sea-water [1].

In general poor durability can be attributed to high porosity or poorly compacted concrete with inadequate cover on the reinforcement.

1.4. High Alumina Cement.

The manufacture and properties of high alumina cement are described by Neville [1].

High alumina cement is manufactured by firing lumps of bauxite and limestone at a temperature such that the product is molten. This is then allowed to solidify and cool, and is then ground to a powder.

The main cementitious compounds are calcium aluminates. Calcium hydroxide is not present in the hydrated material. As a result, this cement has a high resistance to sulphate attack.

High alumina cement does not set rapidly. Initial set occurs after about 4 to 5 hours, with final set following after about 0.5 hours. The subsequent hardening and gain in strength is very rapid, with concrete reaching 80% of its ultimate strength after about 24 hours.

Concrete made from high alumina cement can deteriorate at higher temperatures in the presence of moisture. This is caused by conversion of calcium aluminate hydrates, present in the paste, to hydrates of a higher density. This increases the porosity of the cement paste substantially, and reduces strength.

2. QUALITY ASSURANCE.

As it might be possible to link the electrical properties of concrete with the mechanical properties, and so establish a basis for new quality assurance tests, it is important to define the problems of quality assurance in the Civil Engineering context

2.1. Quality Assurance in Building and Civil Engineering Projects.

2.1.1. Responsibilities for Quality Assurance.

The responsibilities for quality assurance in large projects depends on whether the project is concerned with building or civil engineering.

Consider first a building project such as a large office block. The client will employ an architect, and the building will be conceived by discussion between the client and the architect. Consulting engineers will usually be retained to undertake foundation and structural design. The client will also retain a consulting quantity surveyor, usually on the advice of the architect. A services engineer is also required. This might be the architect, or he may advise on choice. The client, architect, and consulting engineers, will then produce a final design and tender documents including specifications. Contractors will reply to these tenders, which will cover all aspects of the building, and a group of contractors will be selected to carry out the work. The

architect is frequently the team-leader or coordinator of the project.

Considering only the structural aspects of the building, the consulting structural engineers will have a resident engineer, who might not be on the site full time, a clerk of works, and a number of inspectors; the actual number depending on the size of the contract. The clerk of works and the inspectors will be on site full time. The contractor will have a contracts manager, who will generally only visit the site, a site agent who will normally be an ex-general foreman, and various foremen who direct operations. The overall responsibility lies with the architect, but monitoring of the work carried out by the contractors is the responsibility of the consulting engineer's team on site.

With regard to reinforced concrete, it is the responsibility of the resident engineer and his inspectors to check that the materials used in the concrete are of suitable quality for the job, or that the quality of ready-mix concrete delivered is adequate, and that the position where each batch of concrete is placed in the structure is recorded. He must ensure that the steelwork and shuttering are correctly placed, that the concrete is poured correctly with the required degree of compaction, that the curing conditions are correct under the weather conditions prevailing, and that when the shuttering is removed, the whole structure appears satisfactory. All of these operations must be monitored against the contract specifications or agreed modifications.

For civil engineering projects such as bridges, roads, etc., it is the civil engineering consultant who has overall

responsibility, and he will employ an architect as required. The responsibilities on site are very similar to those for building construction, except that the site agent will normally be a professional engineer.

2.1.2. Problems of Quality Assurance in Reinforced Concrete Structures.

The concrete mix used for structural concrete is a compromise between adequate strength and durability, and minimum cost. For a reinforced concrete beam, the tensile strength depends on the steel reinforcement, while the compressive strength depends on the concrete. The concrete mix must be such as to give adequate compressive strength, while at the same time having a workability that ensures that the reinforcement is properly coated with concrete, with a good bond between concrete and steel. It must also have a water content which is sufficiently low to give low porosity, and prevent oxygen and acidic compounds permeating the material and causing corrosion of the reinforcement.

The steel reinforcement must be correctly positioned, and the shuttering must be sufficiently accurate to ensure adequate cover.

If any of these requirements are not met, then a potentially hazardous situation can arise.

Tomsett [9] quotes A.W. Broomfield who summarised concrete construction in 1871 as having "the advantages of cheapness, strength and durability, rapidity of construction and economy of space, with chief disadvantages being its liability to failure from

the use of improper materials, or from the want of knowledge or proper care, or from the wilful misuse of proper materials."

Bate [10] discusses a number of failures in reinforced concrete construction. The cases quoted include:-

1973 University of Leicester reading room built in 1964. Sudden collapse of part of the roof after failure of the edge beam, caused by inadequate bearing and low strength high alumina cement concrete in edge beam, and poor control of cement content.

1973 Camden School assembly hall built in 1954. Sudden collapse of the whole roof due to inadequate bearing of roof beams on edge beams aggravated by corrosion of steel and conversion of high alumina cement concrete.

1974 Sir John Cass's Foundation and Red Coat C of E Secondary School, Stepney, swimming pool built 1965. Slight warning before collapse of one roof beam, with later collapse of a second beam, caused by conversion of high alumina cement concrete, subsequently attacked by sulphate.

1974 Warehouse roof built 1962.
Failure of one main beam due to corrosion of post-tensioned steel tendon caused by 2-4% calcium

chloride in the cement.

Bate lists among his conclusions the following:-

(i) Failures are very seldom due to any lack of basic scientific or technical knowledge, but rather to a failure to ensure that the knowledge was properly applied, or to an absence of enginering judgement.

(ii) Failures are usually due to human errors, which are likely to be the result of mismanagement, - the acceptance of the wrong priorities, misunderstanding or lack of communication between those with different responsibilities within the project.

Parsons & Melvin [11] give details of two cases of failure in concrete structures. The first concerned the failure of columns in Halls of Residence blocks completed in 1964, and which showed signs of failure in 1975. It was concluded that the failure in this case was due to inadequate cover of the reinforcement, and the presence of a superficial layer of concrete with enhanced porosity. The second case involved the ceiling of a cinema constructed about 1950, the failure being detected in 1982. The ceiling was constructed of precast panels, and there was evidence of bond failure as well as high concrete porosity.

It must be noted however that despite the failure cases described, there are many thousands of reinforced concrete structures which have given good performance over many years of

service.

While problems are generally associated with poor supervision and inspection, the use of quality assurance tests now available might reduce the extent of the problem. The number of these tests which can be used during construction is however limited.

2.2. Non-Electrical Quality Assurance Methods.

A wide range of tests for concrete are given in BS1881 [12] and have been described by various authors. There are also a number of tests which do not appear in BS1881.

The range of non-electrical tests of concrete include:-

- workability tests
- chemical and physical analysis
- bulk compressive strength tests
- in-situ mechanical tests
- ultrasonic tests
- radiation tests

2.2.1. Workability Tests.

Workability is the ease with which concrete can be placed, and the resistance of the constituents to segregation. The desired workability will however depend on the compaction equipment available, and the amount of reinforcement present.

Workability tests are usually concerned with some measure of the extent of the viscous forces available within a sample. A

number of such tests are described by Neville [1] and Tattersal & Bloomer [13].

The slump test is used extensively in site work all over the world with minor variations from country to country. Such a test is prescribed in BS1881. The test equipment consists of a mould in the shape of a fustrum of a cone 300 mm high with the top and bottom open. The mould is placed wide end downwards on a base, and is firmly pressed onto the base. The mould is filled with concrete from the top, the concrete being put down in layers with a prescribed compaction routine being carried out after the placement of each layer.

Immediately after filling, the mould is released from the base and slowly lifted. The unsupported concrete sample will slump. The decrease in height of the highest part of the slumped sample is defined as the amount of slump. Neville [1] gives a table relating the slump to the degree of workability, but warns that the slump test is not necessarily a measure of workability as defined earlier. It should also be noted that a given value of slump can be obtained with various proportions of constituents.

The behaviour of the sample during the slump test can give an experienced operator much information about the concrete mix, and allow corrections to be made for a defective mix. These assessments are obtained as a result of practical experience however, and are difficult to quantify.

The Vebe test, which is again prescribed in BS1881, is an attempt to quantify the effort required to remould a sample of fresh concrete. In this test, a sample of concrete is formed in a mould

similar to that for the slump test, but in this case the mould is positioned within a cylindrical container which in turn sits on a vibration table with given vibration characteristics.

The mould is withdrawn from the sample, and the sample vibrated until is has deformed to a specified degree within the cylindrical container. The figure obtained from the test is the vibration time necessary to achieve the required deformation.

This is regarded as a good laboratory test, and has the advantage that the treatment of the sample in the test is similar to that during placement.

Tattersal & Bloomer [13] have developed a workability test which is a measure of the relationship between the rate of shear, and the shear stress in fresh concrete. In this test a measured quantity of concrete is placed in a bowl, and an impeller is then rotated in the sample. A straight line relationship is found between the torque required and the angular velocity. The constants in this relationship are used to characterise a given mix. Only two sets of readings are required for this test, and it is therefore known as a two-point workability test. The repeatability of this test is reported to be good, but a calibration must be obtained for a known mix, if best results are to be achieved.

While figures can be assigned to all forms of workability test, a relationship between these values and the structural properties of the material is unlikely.

2.2.2. Chemical and Physical Analysis.

One approach to quality assurance is to analyse directly, the proportions of the constituents in the mix, from a sample of concrete.

Chemical testing procedures are detailed in BS1881 and are discussed by Bungey [14] and Neville [1]. These tests apply to hardened concrete.

Tests for cement content and cement/aggregate ratio depend on the fact that lime compounds and silicates in Portland cement are generally more readily decomposed and soluble in dilute hydrochloric acid than the corresponding materials in aggregate. The procedure involves the analytic determination of the proportions of calcium oxide and soluble silica. Values for the particular cement and aggregate used must be available for accurate results.

The original water content is determined by measuring the volume of capillary pores in a thin slice of concrete and adding to this the amount of combined water, which is determined by driving it off by heating to a high temperature, and absorbing it by a suitable chemical compound. The volume of the capillary pores is obtained by drying the sample, filling the pores with carbon tetrachloride in a vacuum desiccator, and measuring the gain in weight from the dry state. If the cement content is also measured, the water/cement ratio can be found.

The accuracy is limited by the fact that the chemicals used will attack the aggregate to some extent. The water content determination can be affected by the porosity of the aggregate, and

the extent of non-continuous capillary pores.

Bungey [14] also describes an analytical method based on X-ray fluorescence. In this technique, a sample is prepared by grinding and compressing a small quantity of concrete together with a binder under very high pressure. The sample is then bombarded by high-energy X-rays. The energies and intensities of the resulting X-ray fluorescence can be related to the elements present, and hence to the cement content. The results must be compared with samples of known cement content. This technique can also be used to determine chloride content.

Chemical tests are very expensive, and are normally only used in cases where there is a degree of uncertainty, or where disputes have to be resolved. They require specialist laboratory facilities and a high degree of skill and experience.

Physical testing methods for fresh concrete are given in BS1881, and are discussed by Neville [1]. Aggregate and cement content are found by weighing a sample, adding water to the sample to give a fixed volume, and weighing this in a container which is immersed in water. The coarse and fine aggregates are then separated out by washing and sieving, and similar weighings carried out on each of these. Knowing the density of the cement and the specific gravities of the fine and coarse aggregates, the water, cement, and aggregate proportions can be deduced.

A rapid analysis machine (RAM) developed by the Cement and Concrete Association for the determination of cement content is described by Dhir et al [15]. This machine produces a slurry of cement, silt, and fine aggregate from a known sample weight. From a

fixed proportion of this slurry, the fine aggregate is removed by filtering, and the cement and silt made to settle out using flocculating agents. The mass of this deposit along with sufficient water to give a fixed volume is then measured. Knowing the density of the concrete sample, the cement content can be deduced. A correction is required for the silt content. This equipment requires calibration using known mixes.

The performance of this machine is reported to be better than that of the procedure given in BS1881, but careful maintenance of the equipment is required.

2.2.3. Bulk Compressive Strength Tests.

In the United Kingdom, compressive strength testing of fresh concrete is normally carried out on sample cubes as detailed in BS1881, which also details compressive strength testing of cylindrical core samples taken from existing structures. Other countries require cylindrical samples of fresh concrete to be used.

Neville [1] discusses cube and cylinder testing for fresh concrete. For both kinds of samples, the sample geometry is obtained using cast steel moulds. The samples are poured in layers with prescribed compaction between layers. The samples are then kept at 20°C at at least 90% relative humidity for a day, and then demoulded and kept under water at 20°C until required for testing. Test are usually carried out at 7 days, 14 days, or 28 days after pouring.

For cube testing a number of different cube sizes can be used,

e.g. 150 mm, 100 mm, and 6 ins. For the smaller cubes the maximum aggregate size is restricted. Currently the tendency is to use 150 mm cubes. The platens of the testing machine are brought into contact with two opposite moulded surfaces of the cube. When the load is applied these platens will prevent lateral strain at the top and bottom surfaces of the sample. The strength of the sample in this test will therefore be greater than might be expected if only uniaxial compressive strain existed. Coefficients of variation of 3.5% are quoted for these tests.

The use of cylindrical samples is an attempt to overcome the problems associated with the cube test, and is recommended in a number of countries including the USA. The recommended ratio of height to diameter is 2/1, and the diameter is normally 150 mm. This should reduce the effect of clamping the ends of the sample. It is however common practice to use a cylindrical sample and then convert the result to an equivalent cube strength value. Neville [1] gives strength correction factors which correct measurements using different cylinder geometries to equivalent values for the 2/1 geometry, and then multiplies by a factor of 1.25 to give the equivalent cube strength.

Testing of core samples is very similar to that for fresh cylinders, and is described by Neville [1] and Bungey [14]. The recommended height to diameter ratio is again 2/1. Whether this is possible in a particular case will depend on from which part structure the core is taken. The core is cut to the required length, and the ends capped using high alumina cement. The samples are usually kept in water before testing, which produces a lower

crushing strength value, but gives more consistent results. The results for cores are generally lower than those for cylindrical samples of fresh concrete, because of the differences between site curing conditions and standard moist conditions.

Neville [1] describes accelerated curing techniques which allow a measurement of compressive strength within 7 hrs. of casting. In this procedure, the moulds are sealed after pouring, and the moulds placed in an oven in which the temperature is brought up to a temperature of 93°C over a period of about an hour. The samples are kept at this temperature for 5hrs. The samples are then removed, stripped from the moulds, cooled and tested.

The compressive strengths obtained are less than those for the normal 7 or 28 day tests by a factor of at least 2, but good correlation is obtained.

2.2.4. In-Situ Mechanical Tests.

A large number of in-situ mechanical tests have been developed for testing concrete in existing structures. These tests are described by Bungey [14,16], Keiller [17], Long [18], and Swamy & Ali [19]. The calibration of such tests is normally obtained by comparison with cube strength measurements.

The LOK test was developed in Denmark as part of a scheduled quality assurance programme for new structures. For this test, a steel disc 25 mm diameter and 8.5 mm thick is attached to the shuttering by a steel sleeve of length 25 mm such that when the concrete is poured, the disc will lie 25 mm below the surface of the

concrete. After the concrete is placed and has reached the required age, the sleeve is unscrewed from the disc and replaced by a rod connected to a hand operated tensioning jack. The system is tensioned against a 55 mm diameter reaction ring placed against the concrete surface, until failure occurs. This occurs symmetrically, in compression, in a narrow band between the cast-in disc and the reaction ring. Coefficients of variation of 8-10% can be obtained for this test [14], and the comparison with cube strength gives a straight line correlation of 0.96. The failure surface is conical, with an angle between the surface and the line of pull of 31°. Theoretical analysis indicates that this geometry is caused by failure in compression.

The CAPO test is a modification of the LOK test to allow application to existing structures. A hole is first drilled in the concrete. This is then under-reamed using an expanding tool. An expanding ring insert is then fitted giving an overall geometry similar to that of the LOK test. Application of the load is the same as that for the LOK test and similar failure conditions are obtained. There are problems associated with the accurate machining of the hole and fitting of the expanding ring. The coefficient of variation is not as good as that for the LOK test [16]. The test takes between 15 and 30 minutes to carry out at each point.

The internal fracture test was developed by the Building Research Establishment in the United Kingdom. In this test a 6 mm diameter hole is drilled to a depth of 30-35 mm in the concrete. A 6 mm wedge anchor bolt with an expanding sleeve is then fitted and tensioned using a hand operated torque-wrench. The system is

tensioned against a reaction ring until failure occurs, and the torque at failure is recorded. The torque meter reading is calibrated against compressive strength at failure. The failure surface is again conical, but the angle between the surface and the direction of pull is 78° indicating failure in tension. The accuracy is degraded with larger size aggregate particles. An uncertainty of ±30% is quoted for this test [16]. One major defect is that the torque wrench applies shearing forces as well as axial forces, and this affects the result. A modified system using a direct pull jack is reported to give an uncertainty of ±20% for 10 mm aggregate [16].

The pull-off test developed at Queen's University, Belfast, is a simplification of the internal fracture test. In this test a disc of 50 mm diameter is stuck to the surface by resin. An outer annulus may or may not be drilled into the concrete to define the fracture area. The disc is then pulled off by a tensioning device causing fracture of the concrete. It must be noted that failure occurs in tension in this test rather than compression. An uncertainty of about ±20% is quoted for this technique [18].

The Windsor probe test was developed in the USA. In this test a steel probe 3 mm in diameter and 79.5 mm length is fired into the concrete using a special gun with a standardized powder charge. The length of the probe remaining exposed is a measure of the strength of the concrete.

The failure mode of the concrete in this test is not well understood.

An uncertainty of ±20% is quoted for this test by Bungey [14],

but the system must be calibrated against known material, since differences in the hardness of aggregate affect the performance. Swamy & Ali [19] suggest that this test might underestimate the cube strength by as much as 40%.

The Schmidt Hammer test measures surface hardness rather than strength. A spring loaded mass is pressed against a plunger which is in contact with concrete surface. When a preset compression is obtained in the spring, the spring is released, causing forces to be exerted on the plunger and on the mass. The mass will rebound, and the maximum extension of the spring compared with the value before release is taken as a measure of the surface hardness. The accuracy is affected by the proximity of pieces of aggregate, and the kind of aggregate used. The equipment must therefore be calibrated for the mix being tested. An uncertainty of ±25% is suggested for this test [14].

Of the tests described, the most satisfactory are the LOK test, which must be planned at the time of construction, and the CAPO test, which requires careful operation. The internal fracture test and the pull off test depend on tensile strength, and can therefore be expected to give variable results when compared with compressive strength measurements. The Windsor probe test also gives variable results and the failure mechanism is not well understood. The Schmidt hammer test is very much dependent on the condition of the surface layer of the material.

All of these tests are affected by the the size of the aggregate, and some also on the hardness of the aggregate. Most require that the equipment be calibrated against mixes similar to

those under test, and that the average of a number of tests be taken. The tests must be carried out by skilled personnel.

Apart from the Schmidt hammer test, all of these tests are partially destructive.

2.2.5. Ultrasonic Tests.

Ultrasonic tests are described by Neville [1], Bungey [14,20], Tomsett [21], and Elvery & Ibrahim [22]. This is one of the few testing methods which are truly non-destructive.

Most ultrasonic testing involves the measurement of the ultrasonic pulse velocity of the material. This velocity depends on the density and the elastic moduli. The velocity measurement is normally carried out by fixing ultrasonic transducers on opposite parallel faces of the concrete structure. A sonic pulse generated at one transducer is received at the other transducer after passing through the workpiece. The time delay between the transmitted and received pulses is measured electronically. Knowing the physical distance between the two transducers, the velocity of propagation of the ultrasonic pulse can be determined.

The ultrasonic frequency within the pulse can be in the range 20-200 kHz, but most measurements are carried out at 54 kHz. The transducers are usually piezo-electric devices, and are designed to produce longitudinal propagation. In the United Kingdom the most commonly used equipment is the PUNDIT device manufactured by C.N.S. Electronics. This equipment is robust and can be used on site.

The equipment must be used by a skilled operator who is aware

of its limitations. The concrete surfaces must be sufficiently flat to allow the transducers to be positioned correctly, and an acoustic coupling medium must be used to ensure good transmission and reception.

The dimensions of the workpiece are important. The lateral dimensions should be at least one wavelength to prevent guided propagation and resonance effects, and the maximum aggregate size should be much less than one wavelength. At 54 kHz, a wavelength is in the region of 85 mm, depending on the velocity of propagation in the material. The thickness of the workpiece can be in the range 100 mm to 10 m, but the attenuation of the ultrasonic signal will be greater at the longer distances. The presence of reinforcement will also have an effect. The velocity of propagation is greater in steel than in concrete, and the variations in velocity are greater if the wave is propagated along the axis of the reinforcement rods rather than transversely to them. If however the diameter of the rods is less than 12 mm, they have little effect on practical results.

Velocity measurements between one set of test points can be measured to an accuracy of ±1% [14].

The interpretation of the results can be difficult. The velocity of propagation is greater for aggregate than for the cement matrix, the velocity is greater in saturated concrete than in dry concrete, and the velocity varies with the kind of cement used. It is generally accepted that ultrasonic tests are best used as comparative measuments rather than as direct measurements of potential strength of the material. It has been stated for example

that there is no direct correlation between variations in cube strength and variations in ultrasonic velocity [1]. It is also the case that while the ultrasonic velocity increases with increasing age of the concrete, the rate of increase of velocity slows more rapidly than the rate of increase in cube strength.

The usual procedures involve carrying out velocity tests on sample cubes which are subsequently crushed to determine the cube strength. A large number of tests are then carried out on the structure, and the results compared with the tests on the samples. Correlation would be expected between the two measurements, but variations in moisture content can be expected between the samples and the placed concrete, and this will cause a variation in velocity. Techniques have been developed which calibrate out the effects of variation in moisture content. Additional information is obtained by constructing a histogram of the velocity measurements. A narrow band of velocity measurements would tend to indicate good concrete with uniform compaction. A wide spread in velocities would indicate honeycombing, while distinct banding of velocities might indicate different concrete batches. It is suggested that a minimum number of velocity measurements on a particular section should be about 20. Figures of ±20% have been quoted for uncertainty in the measurement of strength at a 90% confidence level [14].

2.2.6. Radiation Tests.

Methods of testing using different forms of nuclear radiation are described by Jones [23] and Bungey [14].

X-ray and γ-ray photography techniques can be used to investigate the arrangement of aggregate particles in the concrete, the position and state of reinforcement, paste film thickness, air voids, segregation, and the presence of cracks. This is done by placing the X-ray or γ-ray source on one side of the workpiece, and a suitable photographic plate on the other. The advantage of γ-ray techniques is that the radiation can be produced by radioactive isotopes, without the need for complex high voltage equipment. γ-rays can be produced by a caesium 137 source for penetration depths of 50-300 mm, and by a cobalt 60 source for depths of 125-450 mm. The maximum depth which can be considered using this technique is about 450 mm.

γ-ray radiometry techniques can be used to assess the density of the material. With this technique, the γ source is placed at one side of the sample and a detector at the other side. Knowing the actual thickness of the material, an assessment of the density can be made. Backscattering measurements can also be carried out, but the extent of reflected radiation is very much affected by the heterogeneous nature of the material.

Neutron radiation can be used to assess the water content, since the hydrogen nuclei in water decrease the energy of fast neutrons. The numbers of slow neutrons obtained are counted and used as an indication of water content. One problem with this

technique is that a number of elements other than hydrogen will also reduce the energy of fast neutrons.

The main difficulty with radiation techniques is that safety requirements must be very strictly monitored. This problem, along with the cost of equipment, largely restricts their use to laboratories.

2.3. The Practical Application of Quality Assurance Tests.

In practice, the only tests which are likely to be carried out on concrete are, tests on the constituents of the concrete, a slump test, and cube tests; the crushing tests on the cubes being carried out normally at 28 days, unless there are special circumstances.

In the event of a poor result from the crushing test, a Schmidt Hammer test may be carried out, core samples may be taken, and perhaps an ultrasonic test will be carried out. In general it is only when problems occur, or where a dispute over responsibility must be resolved, that a wider range of tests will be applied.

Examination of the range of tests available explains why, in most cases, such a restricted range is used.

The slump test has been estabished as the test of workability for many years, and the equipment required is inexpensive. The equipment for the two point test is not however particularly expensive and gives a more meaningfull quantitative result. It might, through time, acquire greater favour.

Chemical and physical analysis in general, require laboratory

conditions and experienced personnel, and while the RAM test can be used on site, the maintenance of the equipment is crucial.

Bulk compressive test measurements are the main quality assurance test for concrete. However these tests are usually carried out in laboratories off site, and testing is not normally carried out before 28 days. By this time the concrete will have achieved most of its final strength, and even poor concrete will be very difficult and very expensive to remove. Tests using accelerated curing techniques would perhaps be more logical but would require compression testing equipment to be available on site, if best use is to be made of the technique. This equipment is usually large, heavy, and expensive, and since it is usually hydraulically operated, can present maintenance problems.

In-situ strength tests are generally semi-destructive, and require the concrete to have achieved resonable strength before they are applicable. Careful interpretation of the results is required.

Ultrasonic testing requires good surfaces, careful placement of the transducers, and a skilled operator. The main drawback preventing more general use of this equipment is the need for a skilled operator.

The hazards associated with radiation testing make these techniques unsuitable for routine use in the conditions which can be expected on a construction site.

On examination of the tests available, it appears that the industry has selected realistic tests, when expense and convenience are considered. The delay in establishing the quality of the concrete is perhaps the weak link in the system, since, if the

quality is found inadequate, there will be a tendency to leave the poor quality material in place unless it is absolutely crucial. A test which could be applied to concrete, on site, within 1 day of mixing, when it has only attained between 20-30% of its final strength [1], would therefore seem worthwhile, provided it can be carried out by personnel who are not specially skilled.

3. THE ELECTRICAL BEHAVIOUR OF THE CONSTITUENTS OF CONCRETE.

3.1. Lossy Dielectrics and Relaxation Processes.

A brief introduction to lossy dielectrics is given by Blythe [24], and an outline of the theory is given in Appendix A.

Loss in a dielectric results in the dielectric constant becoming complex, with both real and imaginary parts being functions of frequency.

From Appendix A:-

$$\varepsilon'(\omega) = \varepsilon_\infty + \frac{\varepsilon_s - \varepsilon_\infty}{1 + \omega^2\tau^2} \qquad (A.15)$$

$$\varepsilon''(\omega) = \frac{\varepsilon_s - \varepsilon_\infty}{1 + \omega^2\tau^2}\ \omega\tau \qquad (A.16)$$

where $\varepsilon'(\omega)$ = real part of dielectric constant

$\varepsilon''(\omega)$ = imaginary part of dielectric constant

ε_∞ = dielectric constant at infinite frequency

ε_s = static dielectric constant

τ = dielectric relaxation time (s)

ω = radian frequency (rad/s)

$= 2\pi f$

where f = frequency (Hz)

The behaviour of a lossy dielectric is frequently presented using a Cole-Cole diagram in which ε'' is plotted agains ε' as

ω is varied. Such a diagram is presented in Figure 3.1 for the simple relaxation process described in Appendix A.

From Expression A.16, it is possible to deduce that the conductivity will be

$$\sigma = \sigma_s + (\sigma_\infty - \sigma_s) \frac{\omega^2\tau^2}{1+\omega^2\tau^2} \qquad (A.21)$$

where σ_s = static conductivity (Sm^{-1})

σ_∞ = conductivity at infinite frequency (Sm^{-1})

The variations in ε', ε'', and σ, as functions of frequency are shown in Figure 3.2.

It is possible to define a phase lag δ given by

$$\frac{\varepsilon''}{\varepsilon'} = \tan \delta \qquad (A.2)$$

In cases where there is a static value of conductivity

$$\tan \delta = \frac{\sigma - \sigma_s}{\omega \varepsilon_o \varepsilon'} \qquad (A.12)$$

where ε_o = permittivity of free space

= 8.85×10^{-12} Fm^{-1}

Sometimes a relaxation frequency is defined rather than a relaxation time.

Thus

$$\omega_r = \frac{1}{\tau}$$

and

$$f_r = \frac{1}{2\pi\tau}$$

Alternatively a relaxation wavelength can be considered

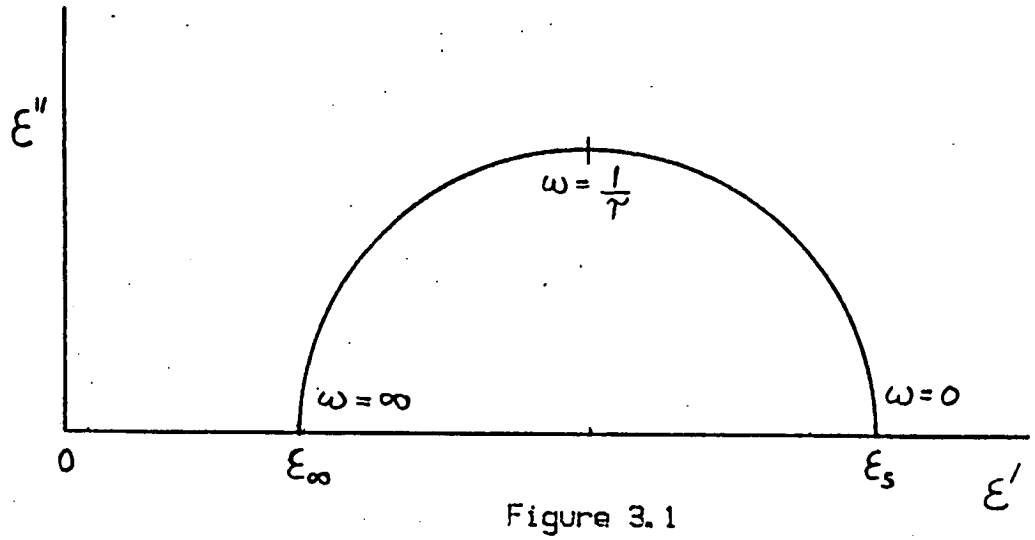

Figure 3.1
Cole-Cole Diagram

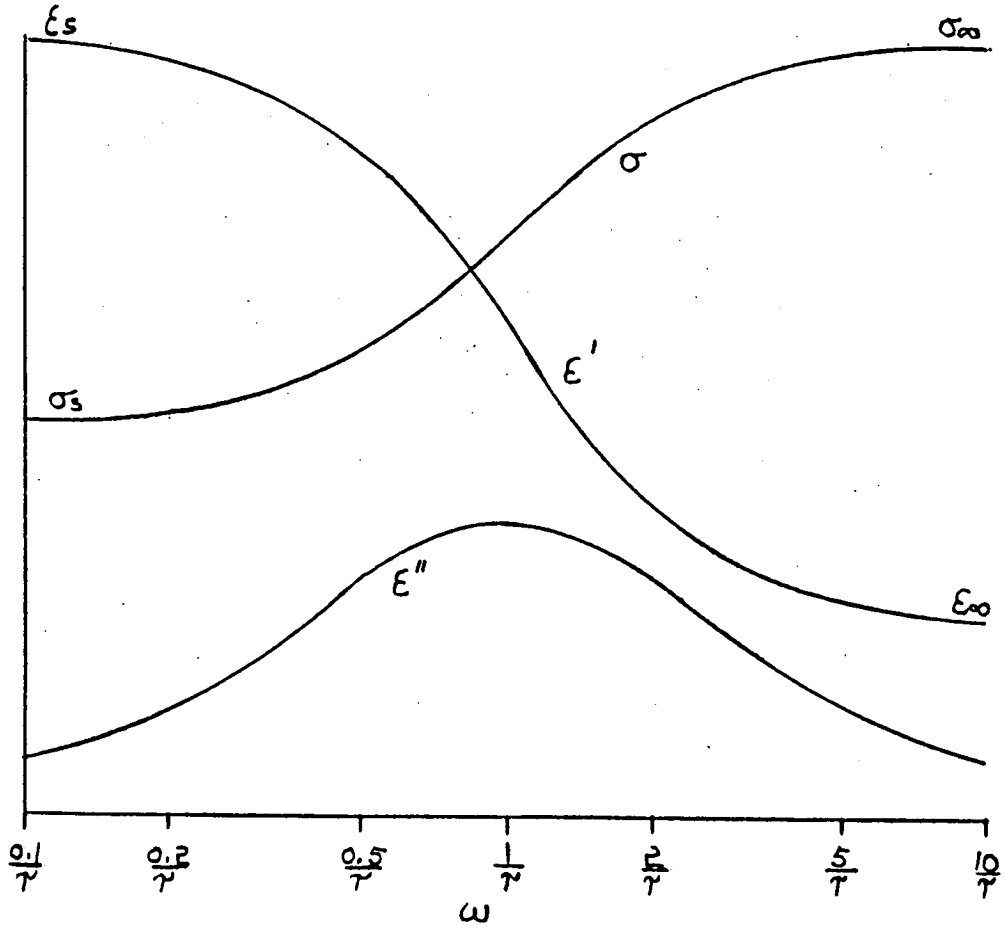

Figure 3.2
Relationships Between ε' ε'' and σ.

$$\lambda_r = 2\pi c\tau$$

where c = velocity of light

$= 3 \times 10^8$ ms^{-1}

3.2. The Dielectric Properties of Water.

3.2.1. Liquid Water.

The charge distribution within a water molecule is not symmetrical, and the molecule exhibits considerable dipole polarization, resulting in a high value for the dielectric constant.

Hasted [25] presents data on the dielectric properties of pure water deduced from the results of a number of workers, and gives expressions for the variation in the static dielectric constant with temperature as:-

$$\varepsilon_s = 87.740 - 0.4008T + 9.398 \times 10^{-4}T^2 - 1.410 \times 10^{-6}T^3 \quad (3.1)$$

after Malmberg & Maryott [26],

and:-

$$\log_{10}\varepsilon_s = 1.94404 - 1.991 \times 10^{-3}T \quad (3.2)$$

after Kay et al [27].

where T = temperature ^oC over the range 0 - 100 ^oC

Figure 3.3 after Hasted [25] is a Cole-Cole diagram showing experimental values for water for a wide frequency

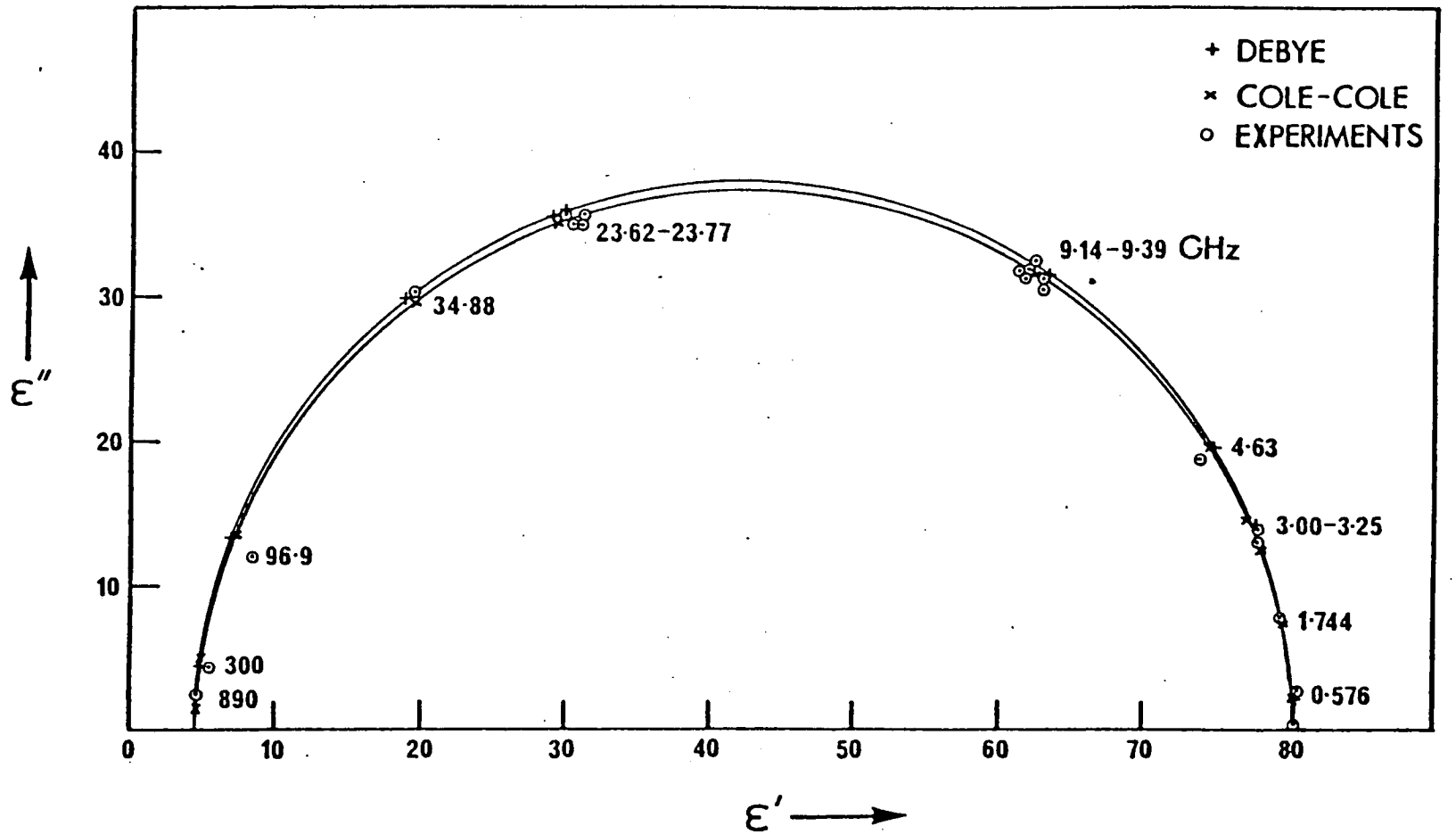

Figure 3.3
Experimental and Predicted Dielectric Properties of Water at 25 °C.
After Hasted.

range at 25 °C.

Table 3.1 shows relaxation parameters for water. α is a spread parameter on the relaxation time.

T_o(°C)	ε_∞	τ(x10^{-11} s)	α
0	4.46±0.17	1.79	0.014
10	4.10±0.15	1.26	0.014
20	4.23±0.16	0.93	0.013
30	4.20±0.16	0.72	0.012
40	4.16±0.15	0.58	0.009
50	4.13±0.15	0.48	0.013
60	4.21±0.16	0.39	0.011
75	4.49±0.17	0.32	-

Table 3.1
Relaxation Parameters for Water

Garside and Phillips [28] give the static conductivity of deionized water used for laboratory purposes as 0.8×10^{-4} Sm^{-1}.

3.2.2. Bound Water.

After setting, a large of proportion the original water content of a cement mix appears as chemically bound water. Neville [1] (Section 1.2.2) quotes 12% by volume at 50% hydration for 0.475 water/cement ratio, and 24% for 100% hydration.

Hasted [25] relates the dielectric relaxation effects of bound water to that of ice, and gives a value of 92 for the static dielectric constant for ice at 0 °C following Auty & Cole [29]. Results for dispersion by a number of workers using single crystals of ice are also given. Figure 3.4 shows results after Humbel et al [30] for different orientations of the crystal. The relaxation frequency is approximately 3 kHz.

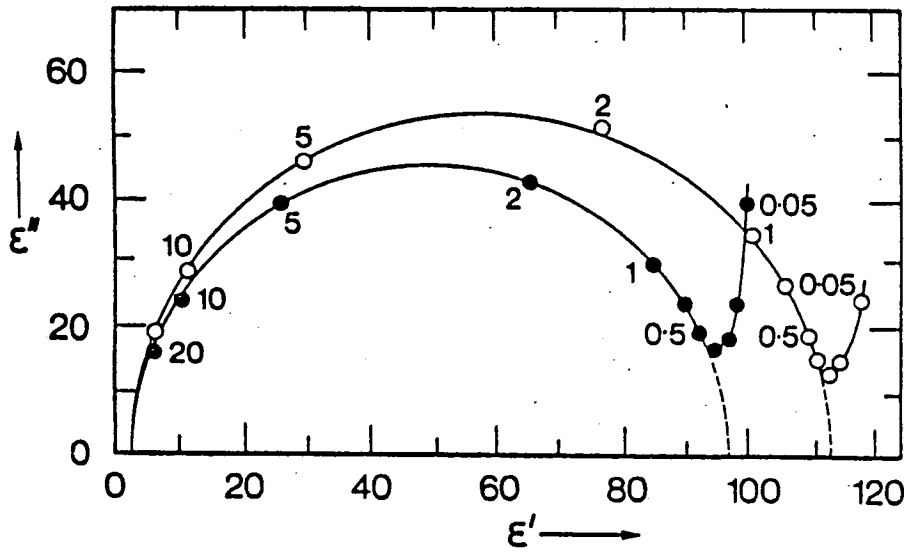

Figure 3.4
Dielectric Properties of a Single Crystal of Ice for Two Orientations. Frequencies in kHz.
Hasted after Humbel et al.

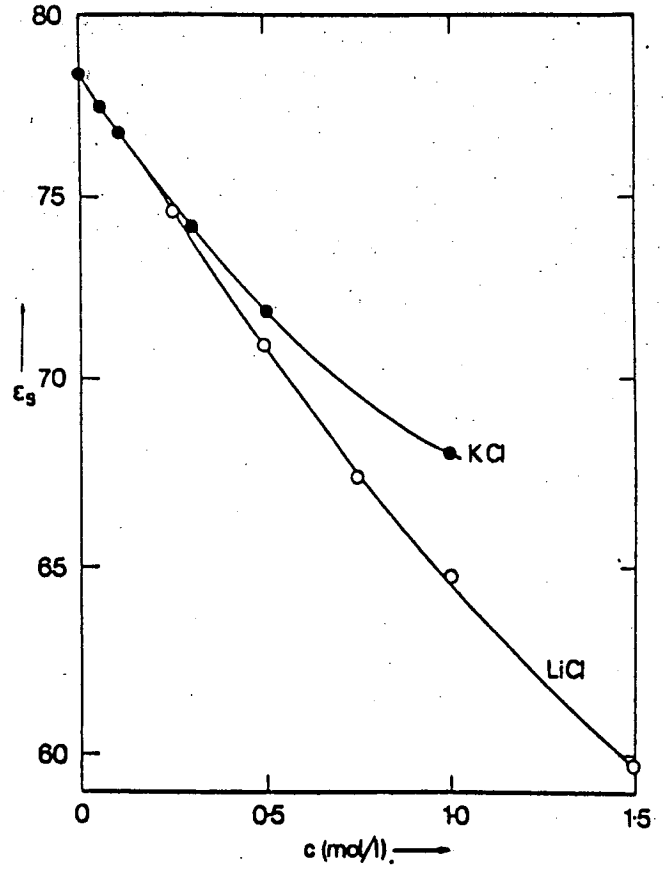

Figure 3.5
Dependence of Static Dielectric Constant on Concentration. Hasted after Collie et al.

Hasted [25] following Bjerrum [31] suggests that the relaxation process in ice is due to lattice defects caused by abnormal positioning of hydrogen atoms.

Hasted [32] gives values of conductivity following Auty & Cole [29] of $1-3\times10^{-4}$ Sm^{-1} for water and 1×10^{-7} Sm^{-1} for ice, both at the melting point.

De Loor [33] presents results obtained in the frequency ranges 0.1 - 10 MHz, and 3000 - 9375 MHz for variation in pore water content of cement paste. Some of the techniques used were poor; in particular, the control of pore water content. De Loor obtained Cole-Cole diagrams at the higher frequencies which were similar to those for water, and concluded that at microwave frequencies, conduction is due to free water in the pores.

De Loor's results also indicated a possible reduction in dielectric constant at low frequencies as the dry density increases due to hydration. It was therefore concluded that at low frequencies conduction becomes increasingly associated with bound water as hydration progresses.

Van Beek & Stein [34] investigated the relaxation frequency of cement paste over the frequency range 60 Hz - 300 kHz, with variation in temperature about the freezing point. No discontinuity was obtained in $\tan\delta$ at the freezing point, and it was concluded that conductivity was associated with water of crystallisation. The experimental technique used was not good, and relaxation effects could have been due to electrode polarization which is discussed in Section 3.3.1.

Lovell et al [35] investigated the behaviour of cement paste

at the freezing point at a wavelength of 0.033 m. No discontinuity was obtained in ε'' at the freezing point, and it was concluded that at these frequencies, conduction is associated with bound water.

3.3. Properties of Aqueous Ionic Solutions.

3.3.1. Low Frequency Effects.

The conductivity of an ionic solution depends on the species and concentration of ions, the solvent used, and the temperature.

The general theory of ionic conductivity is given by Glasstone [36].

The conductivities of ions can be given in terms of the equivalent conduction at infinite dilution in a particular solvent. The relationship between conductivity and equivalent conduction at infinite dilution is not linear. The actual equivalent conduction falls as the concentration increases. This can be compensated for, by using the conductance ratio, which is the ratio of the equivalent conduction at a particular concentration, to the equivalent conduction at infinite dilution.

Thus:-

$$\sigma = \sum_{n=1}^{N} c_n \alpha_n \Lambda_{on} \qquad (3.3)$$

where σ = conductivity of solution (Sm^{-1})

c_n = concentration of a particular ion (N)

α_n = conductance ratio at concentration c_n

Λ_{on} = equivalent conductance at infinite dilution (Sm^{-1}/N)

n = 1 -> N, the ionic species involved

Glasstone [36] suggests that the variation in equivalent conductance at infinite dilution varies according to:-

$$\Lambda_{oT} = \Lambda_{o25}(1 + \alpha[T - 25]) \qquad (3.4)$$

where Λ_{oT} = equivalent conductance at infinite dilution at temperature T °C (Sm^{-1})

Λ_{o25} = equivalent conductance at infinite dilution at 25 °C (Sm^{-1})

α = temperature coefficient of conductance (/°C)

and states that this is accurate for a temperature range 15 - 35 °C.

Glasstone gives values for relevant ions which are present. These are given in the following table:-

	Equiv. Cond. (Sm^{-1}/N)	Temp. Coeff. ($x10^{-2}$ /°C)
H^+	34.982	1.42
K^+	7.352	1.89
Na^+	5.011	2.09
$1/2Ca^{2+}$	5.950	2.11
OH^-	19.8	1.60
$1/2SO^{2-}_4$	7.98	1.96

Table 3.2.
Ionic Conduction Data at Infinite Dilution

Glasstone also suggests that the conductance ratios for strong electrolytes are largely independent of the particular salt used,

but depend on the valence type. Values are given in Table 3.3.

Valence Type	Concentration of Solution 0.10 N	0.01 N	0.001 N
uni-uni	0.83	0.93	0.98
uni-bi	0.75	0.87	0.95
bi-uni	0.75	0.87	0.95
bi-bi	0.40	0.65	0.85

Table 3.3
Conductance Ratio and Valence Type of Salt.

Monfore [37] gives a resistivity value of approximately 0.2 Ωm for a 0.2 N sodium hydroxide solution saturated with calcium hydroxide.

If current passes through an electrolyte, then chemical reactions must take place at the electrodes. Assuming the pore-water in cement to be the electrolyte, the electrode reaction will ultimately produce molecular oxygen and hydrogen at the electrodes. In normal aqueous electrolytes, bubbles of gas will be able to detach themselves from the electrodes, and float to the surface, but if the electrolyte is contained within cement paste, there is no mechanism for the removal of the gas once is has been generated. This gas will then form an insulating layer.

A method of preventing this build up of gas is to use electrodes which will act as a catalyst to recombine the hydrogen and oxygen to produce water. Glasstone [36] describes the use of platinum electrodes coated with platinum black for this purpose.

Even if a gas is produced, it is possible for the bulk properties of the material to be investigated using ac voltages, because an electric field will still be generated in the material and movement of ions will occur. The use of ac voltages will not

limit the generation of gas until the insulating layer is established. Blythe [24] discusses the effect of an insulating gas layer either due to imperfect contact between the electrodes and the surface of the material, or to the products of electrolysis, and states that this can cause an apparent increase in dielectric constant at low frequencies which is not in fact associated with the bulk properties of the material.

The analysis of the effect of a thin insulating layer is presented in Appendix B. Such a system behaves like a relaxation process with

$$\varepsilon_s = \frac{d}{d_1}\varepsilon_1 \qquad (B.8)$$

and

$$\varepsilon_\infty = \varepsilon_2 \qquad (B.9)$$

where d = thickness of the system (m)

d_1 = thickness of the insulating layer (m)

ε_1 = dielectric constant of the insulating layer

= 1 for a gas

ε_2 = dielectric constant of the bulk material

The relaxation time

$$\tau_1 = \varepsilon_o \frac{\varepsilon_1}{\sigma} \frac{d}{d_1} \qquad (B.10)$$

where σ = bulk conductivity of the material (Sm^{-1})

It is shown in Appendix B that an apparent low frequency dielectric constant of 10^5 can be expected in concrete samples due to this effect.

Johnson & Cole [38] carried out measurements on dielectric relaxation of formic acid, and devised a method of calibrating out electrode polarization effects using variable electrode spacing. This resulted in an apparent dielectric constant of 125.3 at 20 Hz being reduced to 13.6. Gillespie & Cole [39] describe experiments to measure the dielectric constant of sulphuric acid, using a similar calibration technique.

Schwan et al [40] describe an experiment to determine the dielectric constant of a colloid, and in particular, they describe the techniques used both to reduce, and to calibrate out, the effects of electrode polarization. In these experiments, the electrodes were covered with platinum black, and the spacing of the electrodes was variable to allow the electrode effects to be isolated.

The presence of ions in water reduces the static dielectric constant. The reason for this is complex. The presence of non-polar ions must reduce the dielectric constant, but each ion will, in addition, have a number of water molecules associated with it. These molecules will be orientated by the field of the ion, and will not therefore be able to respond to an applied electric field, thus reducing the polarizability of the solution, and further reducing the dielectric constant.

Hasted [25] presents data after Collie et al [41], which shows how the variation in dielectric constant is dependent on ion concentration. Figure 3.5 shows the non-linear characteristic at high concentrations, while Table 3.4 shows the effect of different ions. In Table 3.4 the ion concentration is assumed to have a

linear relationship such that:-

$$\varepsilon_s = \varepsilon_w + \delta c \qquad (3.5)$$

where ε_s = dielectric constant of solution

ε_w = dielectric constant of water

c = concentration (mole/litre)

δ = dielectric increment

The expression applies to low concentrations.

	$\delta(\pm 1)$
H^+	-17
Li^+	-11
Na^+	-8
K^+	-8
Rb^+	-7
Mg^{2+}	-24
Ba^{2+}	-22
La^{3+}	-35
F^-	-5
Cl^-	-3
I^-	-7
OH^-	-13
SO^{2-}_4	-7

Table 3.4
Dielectric Increments Due to Dissolved Ions.

Figure 3.6 by Hasted [25] after Pottel [42] shows the effect of very high concentrations.

3.3.2.. High Frequency Effects.

The presence of ions has an effect on the relaxation process which can be approximated by a shift in the relaxation frequency for water. Generally there is an increase in the relaxation frequency,

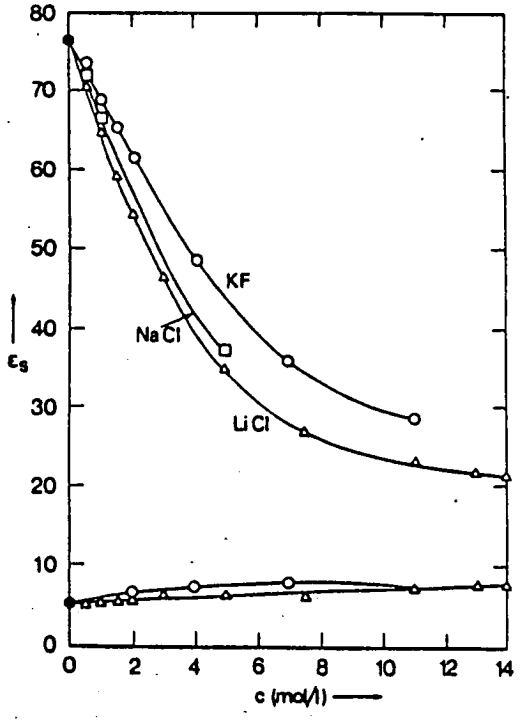

Figure 3.6
Effect of Very High Concentrations on Static Dielectric Constant. Hasted after Pottel.

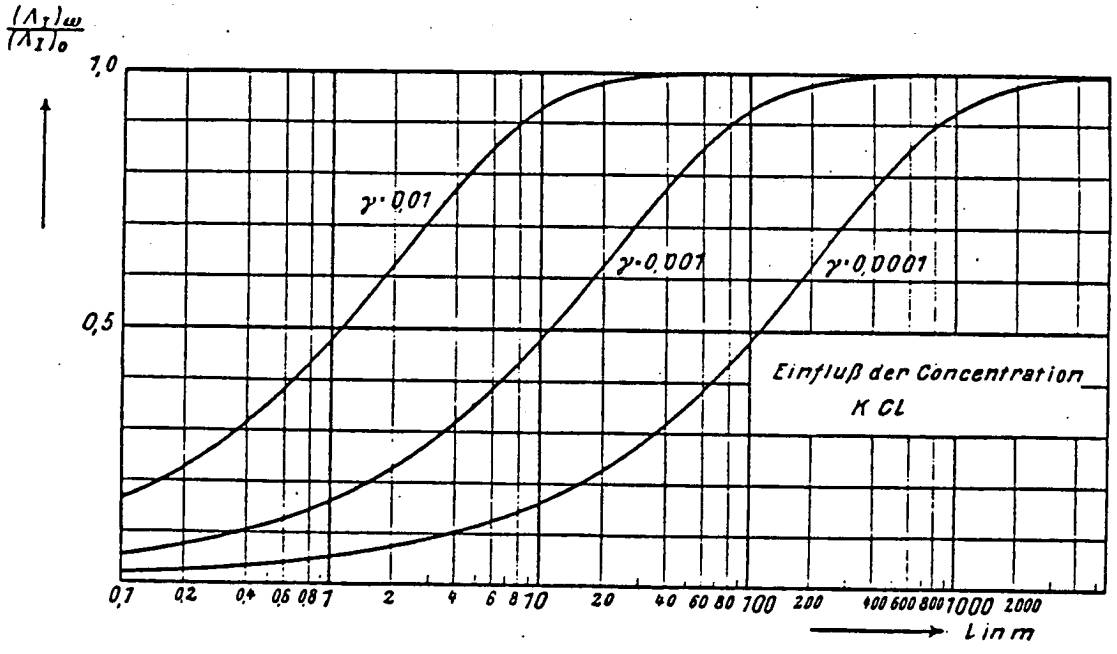

Figure 3.7
Theoretical Reduction in Conductivity with Wavelength due to Debye-Falkenhagen Relaxation after Debye & Falkenhagen.

but in the case of the hydrogen ion, a reduction is obtained. Hasted [25] presents the following table after Collie et al [41], which gives the variation in wavelength of the relaxation frequency with concentration.

	$\delta\lambda$ (± 2)$\times 10^{-4}$ m
H^+	+4
Li^+	-3
Na^+	-4
K^+	-4
Rb^+	-5
Mg^{2+}	-4
Ba^{2+}	-9
La^{3+}	-15
F^-	-4
Cl^-	-4
I^-	-15
OH^-	-2
SO^{2-}_4	-11

Table 3.5
Effect of Concentration on Relaxation Wavelength

The effect on the relaxation wavelength is given by:-

$$\lambda_s = \lambda_w + 2\delta\lambda c \qquad (3.6)$$

where λ_s = relaxation wavelength of solution (m)

λ_w = relaxation wavelength of water (m)

c = concentration (mole/litre)

$\delta\lambda$ = wavelength increment (m)

The effect of the ionic atmosphere surrounding an ion of a particular polarity was investigated by Debye & Falkenhagen [43]. They assumed that at some frequency the ionic atmosphere of opposite polarity surrounding an ion would no longer be able to follow the oscillatory motion of the ion. This should result in an increase in conductivity at high frequencies. Figure 3.7 shows values for the

reduction in conductivity based on this theory for potassium chloride solutions.

Confirmation of these theoretical figures is difficult because of the basic high conductivity of an ionic solution. Hasted [25] presents figures after Hasted & Roderick [44] which show the elevation of conductivity at a wavelength of 0.511 m. These are given in Table 3.6. The low accuracy of the measurements should be noted.

Solute	Concentration M	Δσ% (±9%)
NaCl	0.1	0
RbCl	0.05	9
	0.1	12.5
$BaCl_2$	0.05	37
	0.1	0
$MgCl_2$	0.05	0
	0.1	2.6
	0.2	3
$LaCl_3$	0.05	2.8
	0.1	0
NaBr	0.05	4
	0.1	9.5
LiI	0.1	5.4
KI	0.1	0
LiCl	0.1	0
KCl	0.1	10.3

Table 3.6.
Percentage Elevation in Conductivity.
λ = 0.511 m T = 5 °C

A further relaxation process which might be expected to give a fall in conductance rather than the increase predicted by the Debye-Falkenhagen effect, could be postulated because of the ionic mass and the viscosity of the surrounding medium. It might be expected that once the ion has broken free from its surrounding atmosphere, a further relaxation frequency would be reached at which

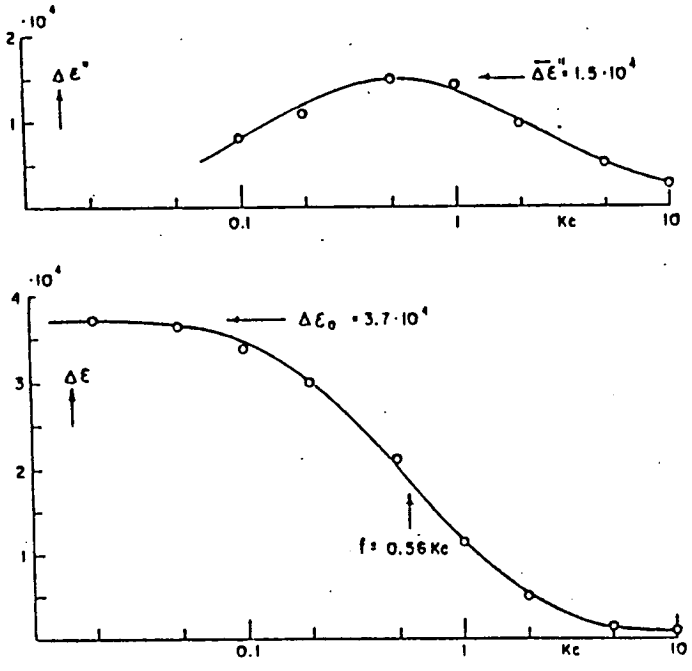

Figure 3.8
Low Frequency Dielectric Dispersion for a Suspension of Polystyrene Spheres after Schwarz.

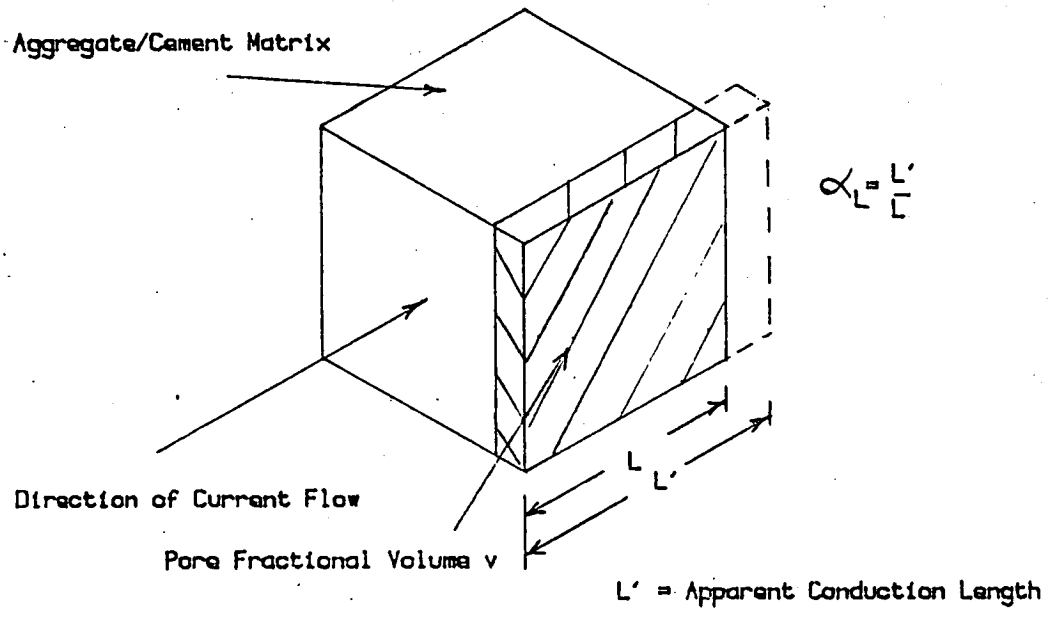

Figure 3.9
Monfore Low Frequency Model.

the ion is no longer able to respond to the electric field. It might even be expected that such an effect might occur at a lower frequency than the Debye-Falkenhagen effect because of the larger effective mass of the ionic atmosphere. No such effect has been described in the literature studied.

The possibility of dynamic lag effects in ionic motion are considered in Appendix C, and it is concluded that they are most likely to occur in the frequency range 40 - 4000 GHz.

3.4. Behaviour of Colloidal Suspensions.

A number of workers have shown that colloidal suspensions can produce a very high value of dielectric constant at low frequencies, along with low frequency dispersion effects. This is analysed by considering effects in the charged double layer round the particles. This could have relevance to cement grains in water before the paste structure is formed.

Schwarz [45] obtained a dielectric constant of 4×10^4 at low frequencies using a suspension of polystyrene spheres in an aqueous solution of potassium chloride. Figure 3.8. shows results for ε'' and ε'.

The technique used by Schwarz is described by Schwan et al [40]. Careful experimental procedures were used to prevent electrode polarization affecting the result. The polystyrene particles were of uniform size 1 μm, and had a surface coating to ensure dispersion. The volume fraction of polystyrene was in the region of 30%.

Arulanandan & Smith [46] suggest that effects in the double layer round colloidal particles of clay could affect the dielectric constant.

Springer et al [47] obtained a dielectric constant of the order of 10^3 using dispersions of polystyrene in aqueous solutions. Variable spacing of electrodes was coupled with a calibration technique to eliminate errors due to electrode polarization.

McCarter & Curran [48] report a dielectric constant of 10^6 at 1 kHz with cement paste which they attribute to colloidal effects.

3.5. Heterogeneous Media.

3.5.1. Low Frequencies.

Monfore [37] considered the relationship between the resistivity of concrete and that of cement paste with a corresponding water/cement ratio. He suggested that an increase in resistivity over that predicted by the simple model shown in Figure 3.9, could be due to an increase in effective length of the conduction path due to the obstruction caused by aggregate particles.

An effective length ratio can be defined as:-

$$\alpha_L = \frac{L'}{L} \qquad (3.7)$$

Monfore found that α_L increased with time, which indicates a difference in behaviour between cement paste on its own, and cement paste in conjunction with aggregate.

Applying Monfore's analysis to the problem of pore water in an aggregate/cement paste matrix, gives:-

$$\sigma = \frac{v\sigma_w}{\alpha_L} \qquad (3.8)$$

where σ = conductivity of concrete (Sm^{-1})

v = fractional volume of pore water

σ_w = conductivity of cement paste (Sm^{-1})

α_L = effective length ratio

Monfore obtained values of α_L in the range 0.81 - 1.37 for cement paste in concrete, and 1 - 1.46 for cement paste in mortar. Monfore considered the values of $\alpha_L < 1$ to be in error, and to be due to the absorption of water by aggregate.

Note that v and σ_w can also be expected to be functions of time.

Whittington et al [49] used a modified form of Archie's law, which is an empirical formula used to calculate the resistivities of porous rock, to relate the resistivity of cement paste to that of concrete. When applied to pore water in an aggregate/cement paste matrix, this gives an expression of the form:-

$$\sigma = \frac{v^m\sigma_w}{A} \qquad (3\cdot9)$$

where m and A are constants.

Whittington et al obtained values of m and A of 1.20 and 1.04. It is clear from the results presented however, that these quantities vary with time, again indicating a difference between

cement paste, and cement paste in conjunction with aggregate.

Whittington et al also considered various formulae by a number of workers to estimate the resistivity of concrete from that of cement paste. These formulae are dependent on the geometry of the imbedded aggregate particles, and are not thought to be directly applicable to the problem of pore water in an aggregate/cement paste matrix, where the geometry is different.

3.5.2. High Frequencies.

When particles of a medium with conductivity σ_2 and dielectric constant ε_2 are immersed in a medium with conductivity σ_1 and dielectric constant ε_1, dielectric relaxation effects take place because of the build-up of charge at the interfaces. This is known as the Maxwell-Wagner effect.

The work of many researchers has been surveyed by van Beek [50]. Van Beek presents the calculation for a two layer system consisting of a layer of material of conducticity σ_1, dielectric constant ε_1, and thickness d_1 in contact with another layer of a different material with conductivity σ_2, dielectric constant ε_2, and thickness d_2. This configuration is analysed as a series circuit consisting of two lossy capacitors. The results are in the form of the Debye relaxation equations with:-

$$\varepsilon_s = \frac{d(\varepsilon_1 d_1 \sigma_2^2 + \varepsilon_2 d_2 \sigma_1^2)}{(\sigma_1 d_2 + \sigma_2 d_1)^2} \qquad (3.10)$$

$$\varepsilon_\infty = \frac{d\varepsilon_1 \varepsilon_2}{\varepsilon_1 d_2 + \varepsilon_2 d_1} \qquad (3.11)$$

$$\tau = \varepsilon_o \frac{(\varepsilon_1 d_2 + \varepsilon_2 d_1)}{\sigma_1 d_2 + \sigma_2 d_1} \qquad (3.12)$$

$$\sigma_s = \frac{d\sigma_1 \sigma_2}{\sigma_1 d_2 + \sigma_2 d_1} \qquad (3.13)$$

where $d = d_1 + d_2$

From Expression A.19

$$\sigma_\infty = \sigma_s + \frac{(\varepsilon_s - \varepsilon_\infty)\varepsilon_o}{\tau} \qquad (3.14)$$

Considering the case where σ_1 is very small, i.e. medium 1 is a low loss dielectric, from Expression 3.10

$$\varepsilon_s = \frac{d}{d_1}\varepsilon_1 \qquad (3.15)$$

Thus a static dielectric constant much higher than that of medium 1 can be obtained depending on the relative thicknesses of

the media.

Van Beek [50] lists a large number of expressions developed by various workers to suit different geometries of imbedded particles.

The particular geometries of interest in this study are those for low concentrations of spheres immersed in a continuous medium, following Wagner [51] and later workers, those for prolate spheroids following Sillars [52], and those for randomly orientated ellipsoids developed by Fricke [53].

It must be noted that the expressions presented by Van Beek describing the equations developed by Fricke, are in error.

Fricke states that, because the conducting particles are randomly orientated, a spread in relaxation frequency will be obtained. An estimate of the relaxation time can be obtained from Expression A.20

The equations are:-

Spheres

$$\varepsilon_s = \varepsilon_1 \frac{2\sigma_1 + \sigma_2 + 2v(\sigma_2 - \sigma_1)}{2\sigma_1 + \sigma_2 - v(\sigma_2 - \sigma_1)} + 3v\sigma_1 \frac{(2\sigma_1 + \sigma_2)(\varepsilon_2 - \varepsilon_1) - (2\varepsilon_1 + \varepsilon_2)(\sigma_2 - \sigma_1)}{[2\sigma_1 + \sigma_2 - v(\sigma_2 - \sigma_1)]^2} \qquad (3.16)$$

$$\varepsilon_\infty = \varepsilon_1 \frac{2\varepsilon_1 + \varepsilon_2 + 2v(\varepsilon_2 - \varepsilon_1)}{2\varepsilon_1 + \varepsilon_2 - v(\varepsilon_2 - \varepsilon_1)} \qquad (3.17)$$

$$\tau = \varepsilon_o \frac{[2\varepsilon_1 + \varepsilon_2 - v(\varepsilon_2 - \varepsilon_1)]}{2\sigma_1 + \sigma_2 - v(\sigma_2 - \sigma_1)} \qquad (3.18)$$

Orientated spheroids

$$\varepsilon_s = \varepsilon_1 \frac{\sigma_1 + [A_a(1 - v) + v](\sigma_2 - \sigma_1)}{\sigma_1 + A_a(1 - v)(\sigma_2 - \sigma_1)}$$

$$+v\sigma_1 \frac{[\sigma_1 + A_a(\sigma_2 - \sigma_1)](\varepsilon_2 - \varepsilon_1) - [\varepsilon_1 + A_a(\varepsilon_2 - \varepsilon_1)](\sigma_2 - \sigma_1)}{[\sigma_1 + A_a(1 - v)(\sigma_2 - \sigma_1)]^2} \quad (3.19)$$

$$\varepsilon_\infty = \varepsilon_1 \frac{\varepsilon_1 + [A_a(1 - v) + v](\varepsilon_2 - \varepsilon_1)}{\varepsilon_1 + A(1 - v)(\varepsilon_2 - \varepsilon_1)} \quad (3.20)$$

$$\tau = \varepsilon_o \frac{\varepsilon_1 + A_a(1 - v)(\varepsilon_2 - \varepsilon_1)}{\sigma_1 + A_a(1 - v)(\sigma_2 - \sigma_1)} \quad (3.21)$$

Randomly orientated ellipsoids

$$\varepsilon_s = \varepsilon_1 + \frac{1}{3} v\varepsilon_1 (\sigma_2 - \sigma_1) \sum_{i=a,b,c} \frac{1}{\sigma_1 + A_i(\sigma_2 - \sigma_1)}$$

$$+ \frac{1}{3} v\sigma_1(\sigma_1\varepsilon_2 - \sigma_2\varepsilon_1) \sum_{i=a,b,c} \frac{1}{[\sigma_1 + A_i(\sigma_2 - \sigma_1)]^2} \quad (3.22)$$

$$\varepsilon_\infty = \varepsilon_1 + \frac{1}{3} v\varepsilon_1(\varepsilon_2 - \varepsilon_1) \sum_{i=a,b,c} \frac{1}{\varepsilon_1 + A_i(\varepsilon_2 - \varepsilon_1)} \quad (3.23)$$

$$\sigma_s = \sigma_1 + \frac{1}{3} v\sigma_1(\sigma_2 - \sigma_1) \sum_{i=a,b,c} \frac{1}{\sigma_1 + A_i(\sigma_2 - \sigma_1)} \quad (3.24)$$

$$\sigma_\infty = \sigma_1 + \frac{1}{3} v\sigma_1(\varepsilon_2 - \varepsilon_1) \sum_{i=a,b,c} \frac{1}{\varepsilon_1 + A_i(\varepsilon_2 - \varepsilon_1)}$$

$$+ \frac{1}{3} v\varepsilon_1(\varepsilon_1\sigma_2 - \varepsilon_2\sigma_1) \sum_{i=a,b,c} \frac{1}{[\varepsilon_1 + A_i(\varepsilon_2 - \varepsilon_1)]^2} \qquad (3.25)$$

where v is the fractional volume of imbedded particles and A_a, A_b, and A_c are depolarizing factors defined for prolate geometries as:-

$$A_a = \frac{-1}{(a/b)^2 - 1} + \frac{a/b}{[(a/b)^2 - 1]^{3/2}} \log_e \left\{ a/b + [(a/b)^2 - 1]^{\frac{1}{2}} \right\} \qquad (3.26)$$

$$A_b = A_c = \frac{1 - A_a}{2} \qquad (3.27)$$

where a is the length of the major axis, and b is the maximum diameter.

Van Beek [50] suggests that the fractional volume of particles in the continuous medium must be less than 0.1 for the equations to have validity.

Sachs & Spiegler [54] used a simplified dispersion model to describe measurements on calcium chloride solutions in a cation exchange resin. They assume that the system consists of two media A and B, each with its own values of dielectric constant and conductivity, and that the overall electrical behaviour can be described by the electrical characteristics of a number of parallel paths in these media.

The parallel paths are:-

(i) a path completely within medium A

(ii) a path completely within medium B

(iii) a path partially in medium A and partially in medium B.

By analysing these paths using normal circuit analysis techniques, Sachs & Spiegler obtain dispersive equations which provide a good model for their experimental measurements over the frequency range 20 - 90 MHz.

3.6. The Electrical Properties of Dry Aggregate and Dry Cement Paste.

Parkhomenko [55] has carried out an extensive survey of literature on the electrical properties of rocks and minerals; mainly from USSR sources, and has also carried out measurements.

Conduction processes in dry rocks, including metallic conduction, semiconductor conduction, and ionic conduction are considered. Any or all of these processes can occur in rocks, depending on the mineral content. Metallic and semiconductor conduction are associated with rocks having a high ore content. This is unlikely to be the case with most aggregates used for concrete in the United Kingdom. The predominant conduction mechanism in aggregate is therefore likely to be ionic, and aggregate will therefore behave like an insulator.

A number of points with regard to experimental technique are made, and it is suggested that some published data must be treated

with caution. The points particularly emphasised are the possibility of electrochemical processes at the electrodes resulting in the collection of charge in the dielectric close to the electrodes, and the need for accurate determination of the water content of the rocks.

The results presented show wide variations in dielectric constant and resistivity, depending on the water content. This is more pronounced for porous sedimentary rocks than for igneous and metamorphic rocks. Figure 3.10 shows the variation in dielectric constant of sandstone with moisture content after Keller & Licastro [56]. Figure 3.11 shows results for siltstone and sandstone with different electrode conditions and humidity levels. The resistivity graphs for dry rock are interesting in that the resistivity falls as the frequency increases. The effect of drying is to increase the low-frequency resistivity without affecting the high-frequency value significantly. The effect is therefore of a reduction in relaxation frequency. This might be due to the difficulty in drying out the pores in the bulk of the material.

Results are also presented for metamorphic and igneous rocks. Figures 3.12 and 3.13 show results for the dielectric constant, and Figures 3.14 and 3.15 show results for tanδ. The water content is not known, but Parkhomenko states that an increase in water content can cause dielectric constants of the order of 100 at 1 kHz for igneous rocks, but that this value is probably due to electrode polarization. The variation in tanδ for igneous rocks tends to reduce for frequencies in the range 10^6 - 10^7 Hz. This indicates an increase in conductivity and falling resistivity at these

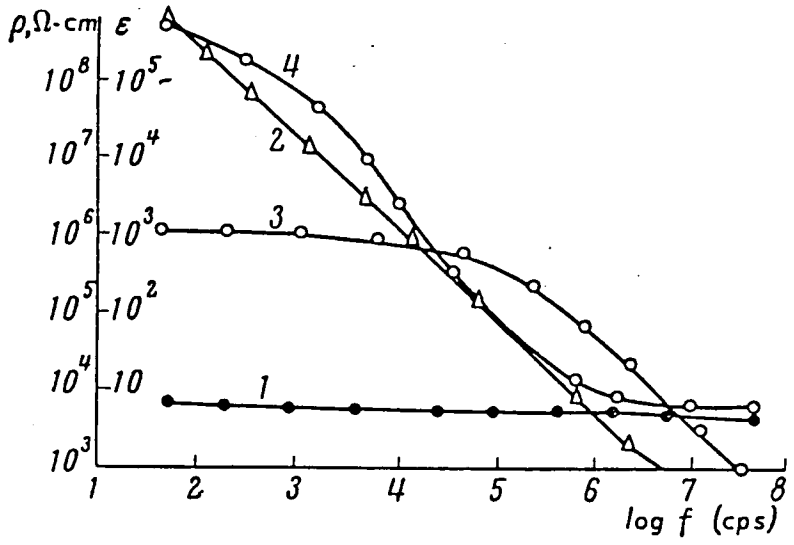

Figure 3.10

Dispersion of the Electrical Properties of Sandstone with Frequency and Moisture Content: (1) dielectric constant of a dry sample (2) resistivity of a dry sample (3) resistivity of a wet sample (4) dielectric constant of a wet sample. Parkhomenko after Keller & Licastro.

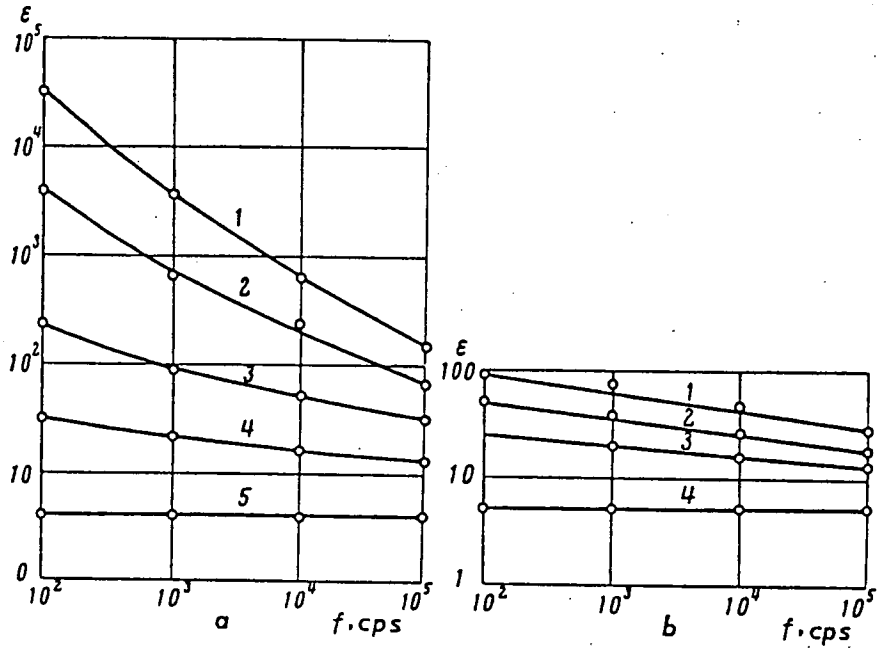

Figure 3.11

Relationship Between Dielectric Constant and Frequency: a - siltstone with incomplete contact between the electrodes and the sample: moisture content % (1) 15.7 (2) 12.0 (3) 5.1 (4) 2.1 (5) dry; b - sandstone with a mica separator between the electrodes and the sample: moisture content % (1) 0.71 (2) 0.15 (3) 0.05 (4) dry. After Parkhomenko.

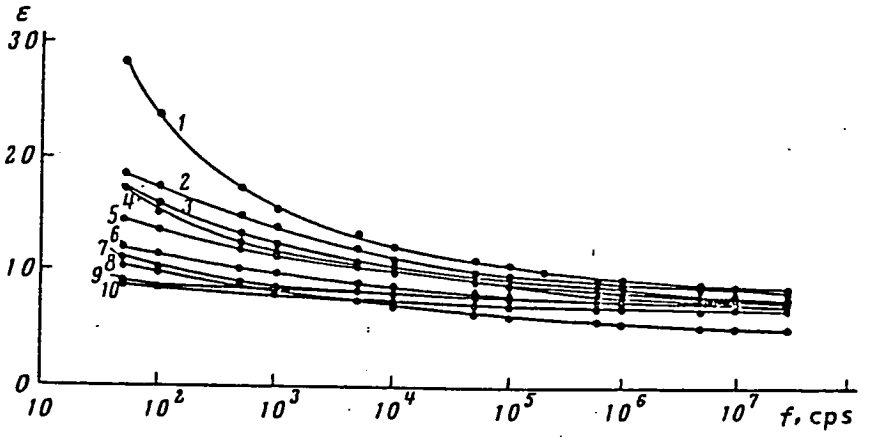

Figure 3.12

Relationship Between Dielectric Constant and Frequency: (1) diabase (2) diorite (3 4) gabbro (5) diabase (6) syenite (7) olivene (8 10) granite (9) obsidian. After Parkhomenko.

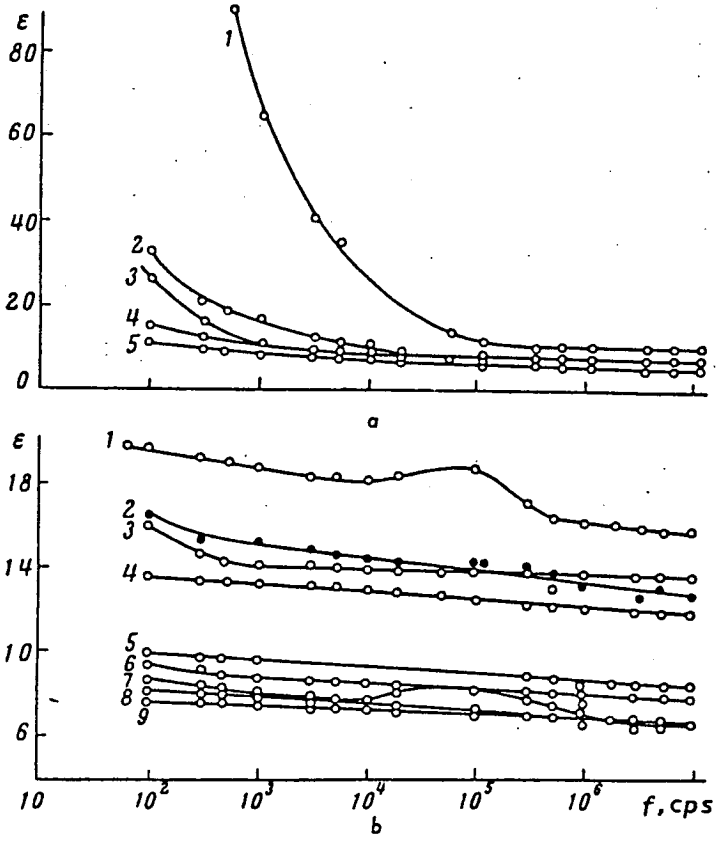

Figure 3.13

Relationship Between Dielectric Constant and Frequency for Acidic Intermediate and Basic Rocks: a - (1) leucophyre (2) vein-type malaphyre (3) monochrystalline nepheline (4) nepheline (under vacuum) (5) the same after heating at 900 oC; b - (1) plagioclase peridotite (2) serpentinite (3) olivene pyroxenite (4) peridotite (5) olivene pyroxenite (6) amphibolite (7) serpentinized dunite (8) weakly serpentinized dunite (9) pyroxenite. After Parkhomenko.

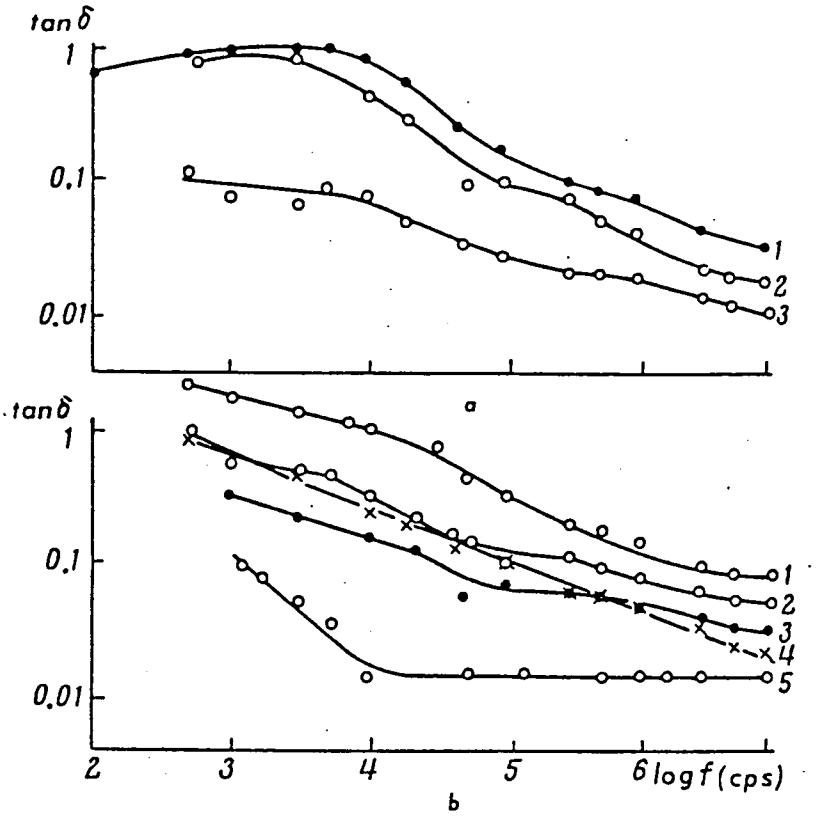

Figure 3.14

Frequency Dependence of Tanδ in Acidic Rocks: a - (1) leucophyre (2) vein-type melaphyre (3) urthyte: b - (1) uvite (2) trachyte fayalite (3) rischorrite (in vacuum) (4) aegarine (5) nepheline trachyte (after heating at 900 oC). After Parkhomenko.

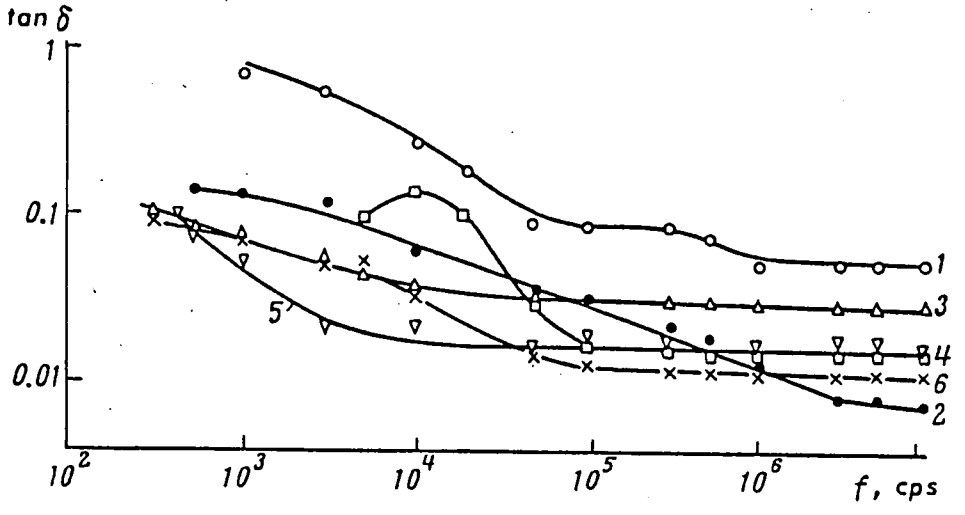

Figure 3.15

Frequency Dependence of Tanδ for Basic and Ultrabasic Rocks: (1) peridotite (2) weakly serpentinized peridotite (3) olivene pyroxenite (4) serpentinized dunite (5) olivene pyroxenite (6) amphibolite. After Parkhomenko.

frequencies, assuming a constant value of dielectric constant. This is similar to the behaviour of sedimentary rocks.

Parkhomenko gives the following data for dry rocks:-

Type of rock	Range of ε_r	Range of resist. (Ωm)
limestone	7.3 - 12.0	$1.2 - 2.3 \times 10^7$
sandstone	3.96 - 4.66	$3.1 \times 10^5 - 6.4 \times 10^8$
marble	8.22 - 9.0	$2.5 \times 10^8 - 1.8 \times 10^{18}$
slate	6.71 - 7.74	$1.6 \times 10^5 - 1.6 \times 10^7$
gneiss	8.0 - 15.0	3.2×10^6
quartzite	4.36 - 15.6	-
granite	4.5 - 5.42	$3 \times 10^{13} - 3.2 \times 10^{16}$
gabbro	8.8 - 12.8	-
diorite	5.9 - 11.5	-
basalt	10.3 - 15.6	1.3×10^7

Table 3.7
Properties of Dry Rocks.

Values for minerals are also given including the following:-

Mineral	Formula	Range of ε_r
rutile	TiO_2	89 - 173
chalcedony	SiO_2	5.6 - 7.5
gypsum	$CaSO_4.2H_2O$	6.3 - 7.9
vesuvianite	$Ca_3Al_2[SiO_4]_2[OH]_4$	7.2

Table 3.8
Dielectric Constant of Minerals.

The minerals containing titanium all have very high values of dielectric constant.

Monfore [37] gives the resistivity of rock which has been soaked in a saturated solution of calcium hydroxide. The measurements were carried out at 1 kHz, and are presented in the following table:-

Type	% Absorp	Resist. (Ωm)
sandstone	9.2	1.8×10^2
limestone	6.0	3.0×10^2
marble	0.9	2.9×10^3
granite	0.34	8.8×10^3

Table 3.9
Resistivities of Saturated Rocks.

The results for sandstone are an order of magnitude lower than the lowest values presented by Parkhomenko [55] after Keller & Licastro [56]. The Keller & Licastro result was however obtained with a water content of only 0.68%.

The properties of cement paste are very much dependent on the moisture content. Even after drying, the residual moisture might still be expected to have an effect, particularly at high frequencies. Hammond & Robson [57] quoting other workers, give resistivity values in the range 2.5 - 5.0×10^4 Ωm for air dried paste, and in excess of 10^8 Ωm for oven dried paste.

De Loor [33] deduced the dielectric constant of dry cement paste from measurements on pastes with various free water contents, and obtained values in the range 6 - 10 over the frequency range 0.1 - 9375 MHz. An approximate value of 7 is therefore a reasonable estimate when values presented for rocks and minerals are also considered.

From Parkhomenko [55], assuming ionic conduction is the predominant conduction mechanism in aggregate at normal temperatures, conductivity is of the form:-

$$\sigma = \sigma_o e^{-\frac{E}{KT}} \qquad (3.28)$$

where E = activation energy (J)

k = Boltzmann's constant (JK^{-1})

T = temperature (K)

σ_o = a constant (Sm^{-1})

Defining a temperature coefficient for conductivity at temperature To as:-

$$\frac{1}{\sigma} \left.\frac{d\sigma}{dT}\right|_{T=T_o} = \frac{E}{KT_o^2} \qquad (3.29)$$

and taking the range 0.1 - 1.3 eV given by Parkhomenko for activation energy for various rocks in the normal temperature range, gives temperature coefficients in the range 0.014 - 0.176 /°C at 20 °C.

In non-polar insulators, the dielectric constant is a result of electronic polarization. This process is not temperature dependent, and the temperature coefficient of the dielectric constant is related to the change in density with temperature.

From Neville [1], the coefficients of linear expansion of aggregate is in the range 0.9 - 16×10^{-6} /°C and for cement paste 11 - 16×10^{-6} /°C. Thus the temperature coefficients of the dielectric constant for both aggregate and cement paste can be expected to be in the range 4 - 7×10^{-15} /°C, which is negligible.

3.7. Deduced Electrical Properties of Concrete.

3.7.1 Behaviour of Pore Water.

Concrete can be regarded as a porous matrix of solid aggregate and cement paste which is permeated by water containing various compounds in solution. The cement paste has a much higher porosity than the aggregate. When water is initially added to the mix, the structure of the cement paste is not formed, and the concrete can be regarded as a suspension of cement grains and aggregate in an electrolytic solution. The paste structure is formed during hardening, and changes in the electrical properties can be expected at this time. As hydrolysis proceeds, the extent of the free water is reduced, and conductivity associated with the movement of ions in solution will fall.

From Double [2](Section 1.2.1.), values of the molarity of ions in pore water have been obtained for cement paste at 100 min. after the cement has been mixed. Values of equivalent conductance have been taken from Glasstone [36], and an estimate made of the conductivity of pore water.

Ions	Conc.(mM)	Conduct. at infinite dil. (Sm^{-1})
OH^-	72	1.426
Ca^{2+}	40	0.476
K^+	20	0.147
SO^{2+}_4	17	0.271
Na^+	5	0.025
H^+	1	0.035
	Total	2.380
For conductance ratio 0.75		1.79

Table 3.10.
Estimate of Pore Water Conductivity.

A concentration of hydrogen ions was chosen to give zero net charge.

The above value compares with 0.2 Ωm for resistivity or 5.0 Sm^{-1} for conductivity given by Monfore [37] for an 0.2 N sodium hydroxide solution saturated with calcium hydroxide, and a value of 1.45 Sm^{-1} by Morelli [58] for cement powder in water.

This value is at least 4 orders of magnitude greater than the conductivity of deionized water quoted by Garside & Phillips [28].

Assuming that the effects of concentration of ions are cumulative, and that the concentrations are relatively low, the effects of dissolved ions on the static dielectric constant and the relaxation wavelength are calculated after Hasted [25] (Expressions 3.5 and 3.6).

Ion	Conc. (mM)	$\Delta\varepsilon$	$\Delta\lambda x10^{-5}$ (m)
OH^-	72	-0.936	-2.88
Ca^{2+}	40	-0.88	-4.8
K^+	20	-0.16	-1.6
SO^{2+}_4	17	-0.119	-3.74
Na^+	5	-0.04	-0.4
H^+	1	-0.017	+0.08
	Totals	-2.152	-13.34

Table 3.11.
Increments in Dielectric Constant and Relaxation Wavelength.

The static dielectric constant of water at 20 °C using the expression of Malmberg & Maryott [26](3.1) is 80.063. From Table 3.11, the dielectric constant of pore water is then 77.9.

From Table 3.1, ε_∞ for water is 4.23, and the relaxation time is $0.93x10^{-11}$ s. This gives a relaxation wavelength of $1.753x10^{-2}$ m. From Table 3.11 the increment in relaxation wavelength is -0.013x10-2 m, giving a wavelength of 1.74x10-2 m, and a relaxation time of 0.923x10-11 s.

From Chapter 7, the maximum frequency of interest is 1 GHz. Assuming that the presence of ions has no effect on ε_∞, the dielectric constant can be calculated from Expression A.15, giving a value of 77.7. The change in conductivity can be calculated (Expressions A.19 and A.21), giving a change of 0.24 Sm^{-1} and a maximum conductivity of 2.03 Sm^{-1}.

From the above values, assuming that Debye-Falkenhagen and dynamic lag effects (Section 3.3.2) are not significant, the characteristics of pore water do not change by more than 10% over the frequency range of interest. A conductivity of 1.79 Sm^{-1}, and a dielectric constant of 77.9 will be assumed.

These values will have temperature coefficients associated with them. For conductivity, from Table 3.10, the most significant ions for conduction are OH^- and Ca^{2+}. From Table 3.2, assuming a temperature coefficient somewhere between those for the two ions, a value of about 1.8×10^{-2} /°C might be expected. From Expression 3.1, a temperature coefficient of -0.47×10^{-2} /°C at 20 °C can be expected for dielectric constant.

3.7.2. Low Frequency Characteristics.

It will be assumed that the conductivity of pore water is 1.79 Sm^{-1} (Section 3.7.1), and that the value for the resistivity of rock and the cement matrix is 1.6×10^5 Ωm (Table 3.7), which corresponds to a conductivity of 6.25×10^{-6} Sm^{-1}.

Assuming a geometry of combined aggregate/cement matrix, and pore water, as shown in Figure 3.9, the total conductivity is given by:-

$$\sigma = v\sigma_w + (1 - v)\sigma_m \qquad (3.30)$$

where v = fractional volume of pore water

σ_w = conductivity of pore water (Sm^{-1})

σ_m = conductivity of aggregate/cement matrix (Sm^{-1})

For v = 0.1%

$$v\sigma_w = 1.79 \times 10^{-3} Sm^{-1}$$

$$(1 - v)\sigma_m = 6.24 \times 10^{-6} Sm^{-1}$$

Thus for practical purposes, the aggregate/cement matrix can

be regarded as an insulator, and the total conductivity will be related to the pore water, when the geometry of Figure 3.9 is considered, by:-

$$\sigma = v\sigma_w \qquad (3.31)$$

Using the extension of Monfore's [37] analysis gives:-

$$\sigma = \frac{v\sigma_m}{\alpha_L} \qquad (3.32)$$

where α_L = effective length ratio

Note that v, σ_w, and α_L, can all be expected to be functions of time.

Taking a value of 1.4 for α_L, assuming the fractional volume of pore water to be 12%, corresponding to the value given by Neville [1] (Section 1.2.2) for 50% hydration at water/cement ratio 0.475, and taking the fractional volume of cement matrix in the concrete to be given by:-

$$v_{cm} = \frac{1 + S_c r_w}{1 + S_c r_w + \frac{S_c}{S_a} r_a} \qquad (3.33)$$

where r_w = water cement ratio

= 0.475

s_a = specific gravity of aggregate

= 2.584

s_c = specific gravity of dry cement powder

= 2.99

r_a = cement aggregate ratio

= 4.5

(The data on specific gravities was obtained from Morelli [58].) gives a value of fractional volume of cement paste as 0.314, and therefore gives a fractional volume of pore water in concrete of 3.77×10^{-2}, giving in turn a total conductivity of 4.809×10^{-2} Sm^{-1} and a resistivity of 20.8 Ωm. When the water is first added to the concrete mix, the effective pore water fraction is 100%, giving a volume fraction of pore water in concrete of 0.314, a conductivity of 0.4 Sm^{-1}, and a resistivity of 2.5 Ωm.

Using Expression 3.9 derived from Whittington et al [49] where:-

$$\sigma = \frac{v^m \sigma_w}{A}$$

and taking A = 1.04, and m = 1.20, gives for a pore water conductivity of 1.79, and a pore water volume fraction of 3.77×10^{-2}, a conductivity for concrete of 3.36×10^{-2} Sm^{-1}, or a resistivity of 29.8 Ωm, and for a pore water fractional volume of 0.314, a conductivity for concrete of 0.427 Sm^{-1} or a resistivity of 2.34 Ωm.

Thus for the concrete mix specified, with 50% hydration, the low frequency conductivity can be expected to be in the range 3.0×10^{-2} - 5×10^{-2} Sm^{-1}, and resistivity 20 - 30 Ωm, and when water is initially added to the mix, the conductivity can be expected to be in the range 0.400 - 0.427 Sm^{-1}, and the resistivity in the range 2.3 - 2.5 Ωm.

Thus the conductivity can be expected to fall by a factor of at least 0.1 between the time at which the concrete is mixed and the time at which hydration reaches 50%. The final conductivity will depend on the extent to which the pores have become sectionalised. There will however be a probability distribution associated with this process, and a direct conduction path is likely under all circumstance. The continuous pores must however remain full of water, and if the concrete is allowed to dry out so that the pores are emptied, the conductivity can become very low.

The measured value of the dielectric constant at low frequencies is uncertain, and will depend on the degree of electrode polarization which occurs (Section 3.3.1), the amount of water which is chemically combined (Section 3.2.2), and the colloidal effects of the cement powder at an early stage (Section 3.4). These effects can all combine to give dielectric relaxation effects in the kHz region.

Taking the change in conductivity due to these processes from Expression A.8:-

$$\sigma_D = \omega\varepsilon_o\varepsilon'\tan\delta$$

and taking $\varepsilon' = 10^6$

$\tan\delta = 4$

$\omega = 2\pi \times 10^3$ rad/s

from McCarter & Curran [48], gives for cement paste, $\sigma_D = 0.222$ Sm^{-1}. This compares with a value for conductivity of 0.5 Sm^{-1} quoted by McCarter & Curran at this stage. Dispersion effects will therefore affect the result of the bulk conductivity measurements

and will therefore have to be taken into account in such measurements.

The effects of electrode polarization and colloidal charges can be expected to reduce as the area of conduction paths is reduced and the cement grains undergo hydrolysis. The relaxation effects of bound water will however increase as hydrolysis progresses, resulting in a further fall in the dielectric constant at frequencies greater than the relaxation frequency for bound water.

Because of the difficulty in predicting the extent of these various effects, measurement of the low frequency dielectric constant will have limited use in the characterisation of concrete.

Assuming that the temperature is not raised sufficiently for the conductivity of the aggregate and cement matrix to become significant, then for both the Monfore [37] model, and the model by Whittington et al [49] (Section 3.5), the conductivity of concrete depends directly on the conductivity of pore water. The temperature coefficient for conductivity will therefore be directly related to that for pore water, and will be in the region of 1.8×10^{-2} /°C (Section 3.7.1).

3.7.3. High Frequency Characteristics.

The components of concrete do not appear to exhibit inherent dielectric relaxation effects until frequencies above 10 GHz, although there might be doubt about the Debye-Falkenhagen effect and dynamic lag effects (Section 3.3.2). Relaxation effects at high frequencies are therefore due to concrete being a heterogeneous material. The equations presented by Van Beek [50] (Section 3.5.2) have therefore been used as models.

From Section 3.6, considering the dielectric constants of rocks and cement paste, a value of 7 for the aggregate/cement paste matrix has been chosen.

The conductivity of the matrix is taken as that for the highest dry conductivity of rock given in Section 3.6. This is 6.25×10^{-6} Sm^{-1}, corresponding to a resistivity of 1.6×10^{5} Ωm.

The dielectric constant of the pore water is taken as 77.9, and the conductivity as 1.79 Sm^{-1} (Section 3.7.1).

The fractional volume of pore water has been taken as 0.0377 (Section 3.7.2), the diameter of the pores as 1.3 μm (Section 1.2.2), and an initial value of 40 mm has been taken for the length of the pores. The results for the computations for the various models are given in Table 3.12.

	Conductivity of Matrix $\sigma = 6.25\times10^{-6}$ Sm^{-1}	$\sigma = 0$ Sm^{-1}
Two layer model		
ε_s	7.27	7.27
ε_∞	7.25	7.25
f_r(Hz)	4.12×10^{8}	4.12×10^{8}
Spheres		
ε_s	7.82	7.82
ε_∞	7.63	7.63
f_r(Hz)	3.47×10^{8}	3.47×10^{8}
Orientated spheroids		
ε_s	229	2.59×10^{7}
ε_∞	9.67	9.67
f_r(Hz)	1.61×10^{4}	46.9
Randomly orientated ellipsoids		
ε_s	84.2	8.31×10^{6}
ε_∞	8.19	8.19
f_r(Hz)	3.06×10^{5}	51.4

Table 3.12
Mawell-Wagner Computation

where ε_s = dielectric constant below the relaxation region

ε_∞ = dielectric constant above the relaxation region

f_r = relaxation frequency (Hz)

As the complexity of the model increases, the value of ε_s increases and the value of f_r falls. There is however a reduction in ε_s and an increase in f_r between the oriented spheroid model and the randomly orientated ellipsoid model. The randomly orientated ellipsoid model is closest geometrically to the matrix/pore water model of concrete.

The results of calculations made on the basis that the aggregate/cement matrix is a perfect insulator are also presented.

It can be seen that, while the conductivity of the aggregate/cement matrix does not affect ε_∞, there are major differences in ε_s and f_r for the more complex models. The conductivity of the matrix is therefore an important parameter with regard to ε_s and f_r.

Variation in the pore length has no effect on ε_∞ for either orientated spheroids or randomly orientated ellipsoids, but it does have a major effect on ε_s and f_r. Figure 3.16 shows the effect of variation in pore length on ε_s, and Figure 3.17 shows the effect on f_r, for the randomly orientated ellipsoid model in each case.

The changes in the matrix conductivity, dielectric constant of pore water, and conductivity of pore water, have been calculated for a temperature rise of 10 ^oC, from the expressions given in Sections 3.6 and 3.7.1. The change in dielectric constant of the matrix is assumed to be negligible.

The modified values are:-

conductivity of matrix	1.72×10^{-5} Sm^{-1}
dielectric constant of pore water	74.2
conductivity of pore water	2.11 Sm^{-1}

The results are given in Table 3.13 in comparison with the results for 20 ^oC, for the randomly orientated ellipsoid model.

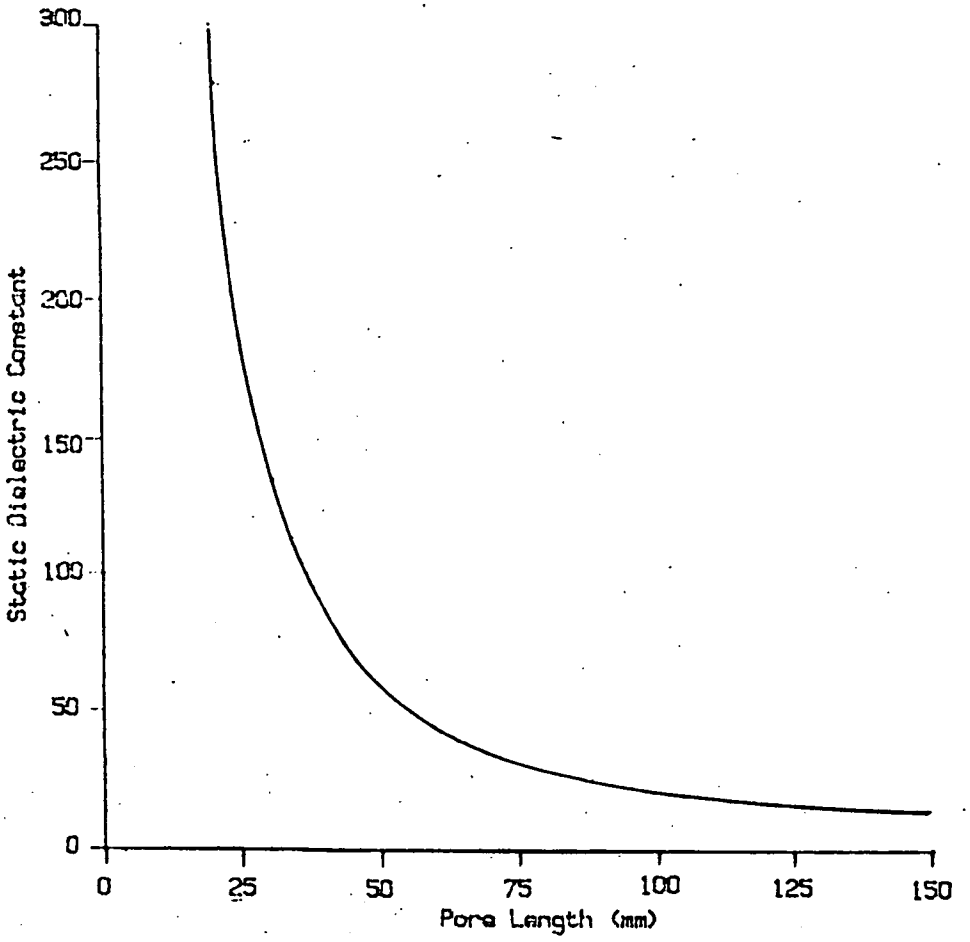

Figure 3.16
Effect of Pore Length on Static Dielectric Constant.

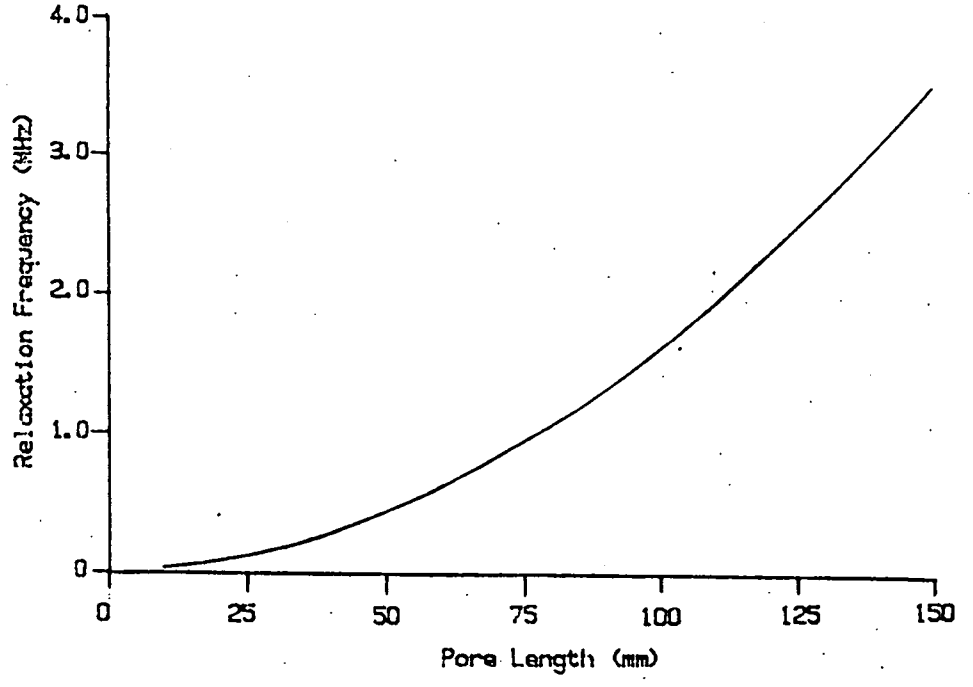

Figure 3.17
Effect of Pore Length on Relaxation Frequency.

	Temperature (°C) 20	30
ε_s	84.2	22.1
ε_∞	8.16	8.11
f_r(Hz)	3.06×10^5	2.08×10^6

Table 3.13
Effect of Temperature on the High Frequency Model.

Thus variation in temperature causes large changes in ε_s and f_r. These changes are largely accounted for by an increase in the conductivity of the aggregate/cement matrix, because of the high temperature coefficient assumed.

As hydration progresses, the fractional volume of pore water will be reduced. The effect of a 50% fall in pore water for the randomly orientated ellipsoid model is given in Table 3.14.

	Fractional Vol. of Pore Water 0.0377	0.0198
ε_s	84.2	45.7
ε_∞	8.16	7.58
f_r(Hz)	3.06×10^5	3.06×10^5

Table 3.14
Effect of Variation in the Fractional Volume of Pore Water.

There is a large fall in ε_s, a much smaller fall in ε_∞, and very little change in f_r.

From the form of the Maxwell-Wagner equations (Section 3.5.2), the dielectric constant at high frequencies is related to the fractional volume of pore water and the dielectric constants of the pore water and of the aggregate/cement matrix, while at lower frequencies, the conductivity is related to the fractional volume of

pore water and the conductivities of the pore water and the aggregate/cement matrix. The low frequency dielectric constant and the high frequency conductivity depend on all parameters, with the low frequency dielectric constant known to be sensitive to the conductivity of the aggregate/cement matrix.

As hydration progresses, and the fractional volume of pore water is reduced, a large reduction in ε_s can be expected, and probably also in σ_∞, although the relaxation frequency might be unaltered.

Variation in temperature could have a significant effect on behaviour, largely due to variations in conductivity of the aggregate/cement matrix.

While computations have been carried out for constant values of length and diameter of capillary pores, there will in fact be a statistical distribution of these dimensions, which will result in a statistical distribution of relaxation effects. Pores which have lengths equal to the sample length will contribute to a static value of conductivity.

3.7.4. Electrical Model of Concrete.

At low frequencies, relaxation effects can be expected due to electrode polarization, the characteristics of bound water, and colloidal effects due to cement grains. These effects will cause a distribution of relaxation frequencies which can be represented by the equivalent circuit of Figure 3.18. The parameter which is most likely to characterise the concrete at these frequencies is the bulk

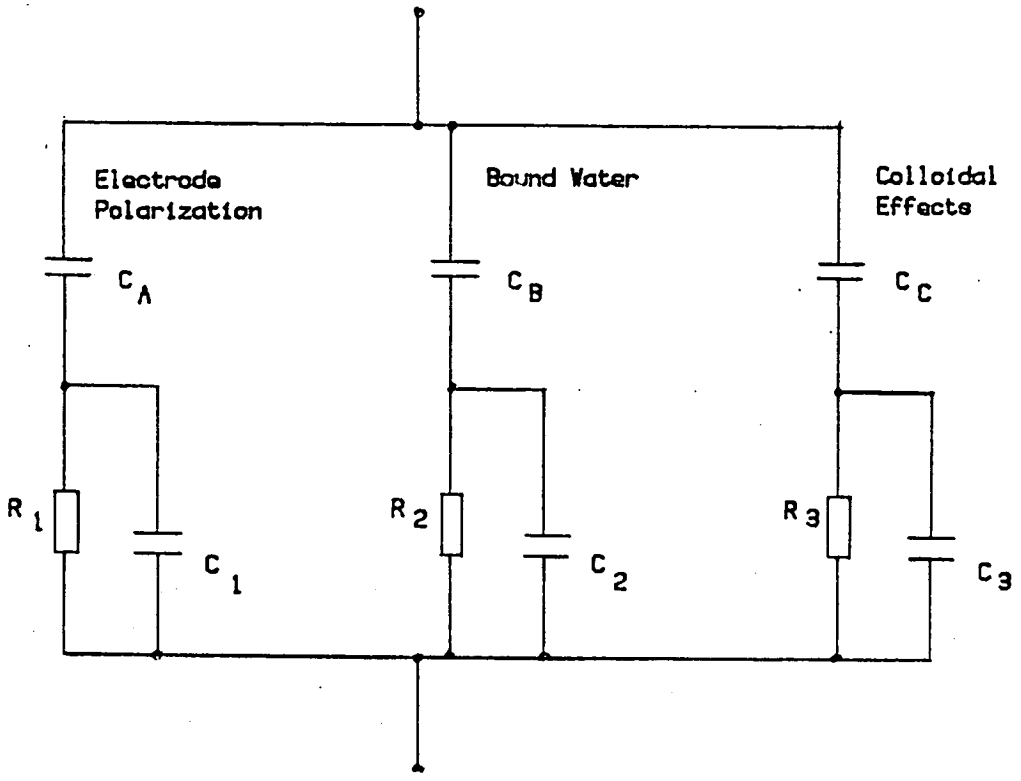

$$\frac{1}{R} = \frac{1}{R_1} + \frac{1}{R_2} + \frac{1}{R_3}$$

R_1; R_2; R_3 due to bulk conductivity

C_1; C_2; C_3 due to bulk dielectric constant

$$\tau_A = C_A R_1 \quad \tau_B = C_B R_2 \quad \tau_C = C_C R_3$$

$$\tau_1 = C_1 R_1 \quad \tau_2 = C_2 R_2 \quad \tau_3 = C_3 R_3$$

Figure 3.18
Low Frequency Equivalent Circuit

conductivity (or resistivity) which is related to:-

$$\frac{1}{R} = \frac{1}{R_1} + \frac{1}{R_2} + \frac{1}{R_3} \qquad (3.34)$$

If time constants τ_1, τ_2, and τ_3, due to the bulk dielectric constants, are much less than τ_A, τ_B, and τ_C, due to low frequency effects, then R can be measured with suitable choice of frequency and measuring technique, and the conductivity can then be calculated.

The bulk conductivity will be related to that for the pore water, and the fractional volume of pore water, but will include an effect due to the more difficult conduction paths through the aggregate/cement matrix, which will cause a reduction in conductivity. This effect can be expected to vary with the age of the concrete, as will the conductivity and fractional volume of the pore water. The aggregate/cement matrix can be regarded as an insulator. A suitable model would be that presented by Monfore [37], and shown in Figure 3.9.

The temperature coefficient of conductivity for concrete will be similar to that for pore water, and will be approximately 1.8×10^{-2} /°C.

At high frequencies the electrical behaviour of concrete is controlled by Maxwell-Wagner effects due to the heterogeneous nature of the material. There will be a distribution of Debye equations describing the variations in dielectric constant and conductivity with frequency, because of the statistical distribution of capillary pore geometry.

At frequencies above the range of relaxation frequencies, the dielectric constant is related to the dielectric constants of the components, and to the fractional volume of pore water. At frequencies below the relaxation range, a similar condition will arise with conductivities. The low frequency dielectric constant and the relaxation frequencies are sensitive to the conductivity of the aggregate/cement matrix.

Relaxation frequencies in the range 50 kHz to 3 MHz can be expected.

The effects of temperature on the high frequency behaviour will be complex. It might be that the high temperature coefficient of conductivity of the aggregate/cement matrix will cause major changes in the relaxation frequency, and in the dielectric constant below the relaxation frequency range, as the temperature is varied.

4. PREVIOUS INVESTIGATIONS INTO THE ELECTRICAL PROPERTIES OF CONCRETE.

4.1. Low Frequencies.

4.1.1 Spencer.

Spencer [59] carried out measurements of electrical resistance to determine the water content of structural concrete. Stainless steel electrodes were used, since copper and mild steel electrodes gave less accurate results.

An a.c. oscillator and bridge were used because of the electrolytic nature of the conduction process, but the frequency of the oscillator is not reported.

A calibration chart to allow compensation of readings with temperature is presented. On this chart, a change of 22.2 ^{o}C produces a fractional change in conductivity of 0.53, giving a temperature coefficient of 0.024 $/^{o}C$.

Measurements were carried out on test slabs in the Colorado River Desert, on the lining of an aqueduct tunnel, and on a dam, with the electrodes buried in the structures.

Spencer's conclusions were that, for a tunnel lining in dry rock, problems can occur because of drying out just as for a structure in the open air, and that thick structures such as dams do not show moisture loss more than about 0.6 m from the surface. It was also found that concrete gains moisture in the presence of surface water very much faster than it loses it when left to dry

out.

4.1.2. Calleja.

Calleja [60] used steel electrodes to measure the electrical resistance of cement paste as a means of investigating the end of the setting process and the onset of hardening. Calculations of resistivity and conductivity were not carried out, but the variation in resistance with time was measured, along with the variation in temperature due to the exothermic nature of the hydrolysis reaction. A 1 kHz system was used to avoid electrolytic and polarization effects. No details of the mix used were given.

In further work [61], measurements of resistance were carried out over the frequency range 40 Hz to 20 kHz. For frequencies in the range 5 - 20 kHz, little variation in resistance was found, but as the frequency was reduced below 5 kHz, the resistance values increased. Problems were encountered in obtaining measurements below 100 Hz.

4.1.3. Hammond & Robson.

Hammond & Robson's [57,62] experiments were concerned with measurements on cement paste using ordinary Portland cement, high alumina cement, and concretes made using these cements.

The water/cement ratio used for cement pastes was 0.235, and that for concretes 0.49, the cement/sand/aggregate ratios being 1:2:4. The samples were moulded in the form of 102 mm cubes, with

brass plate electrodes moulded on two opposite faces. Initial measurements were made with the samples still in the moulds which were made of insulating material. When the samples were demoulded, electrical contact between the electrodes and the sample was ensured by coating the electrodes with a thin layer of colloidal graphite paste. Initial experiments carried out using d.c. show significant electrode polarization effects up to 12 hrs after mixing [57]. Comparative measurements of resistivities for the mixes used, are presented for periods of up to 150 days after mixing. For concrete made using Portland cement, the resistivity remains at about 10 Ωm until approximately 8 hrs after mixing. The resistivity then increases until, after 1 day, it has reached approximately 24 Ωm. High alumina cement gives higher resistivities than Portland cement by approximately a factor of 10. The increase in resistivity from the initial value starts earlier, and takes place over a much shorter time, reaching an approximately constant value after 1 day. The repeatability of results is good with a maximum variation between samples using the same mix proportions of approximately 10%.

Further measurements [62] were carried out using an a.c. bridge over a range of frequencies on samples which were at least 5 days old. There was little variation in the resistance measured using ordinary Portland cement over the range 50 Hz - 25 kHz, although there was a significant fall in resistance with increasing frequency for high alumina cement. The bridge also allowed equivalent shunt capacitance to be measured. In all cases the equivalent shunt capacitance fell with increasing frequency. The equivalent shunt capacitance also falls with increasing age of the

sample.

The ratios of the resistivity of concretes to those of the corresponding cement pastes were found to vary over the first 24 hrs from 5:1 to 3:1.

Using a resitivity/temperature relationship of the form:-

$$\rho = \rho_o e^{a(\frac{1}{T} - \frac{1}{To})}$$

where ρ = resistivity at temperature T (Ωm)

ρ_o = resistivity at temperature To (Ωm)

a = a constant (K^{-1})

T = temperature (K)

To = reference temperature (K)

gives a temperature coefficient of resistivity:-

$$\frac{1}{\rho}\frac{d\rho}{dT} = \frac{-a}{T^2}$$

Hammond & Robson [62] gave a as 5500 K^{-1}, which corresponds to a temperature coefficient of -0.064 /^oC at 20 ^oC. This is a very high value, which might be due to the sample drying out. This paper is quoted in most later work in this field.

4.1.4. Van Beek & Stein.

Van Beek & Stein [34] investigated the relative proportions of free water and bound water in cement pastes over the frequency range 60 Hz - 300 kHz. Measurements of ε' and tanδ (Section 3.1) were

carried out on cement pastes which were still hydrating, and on pastes which were more than 60 days old, and thus considered to be completely hardened. Measurements were also carried out over the temperature range -22 °C to 18 °C.

The water/cement ratio used was 0.285, and the samples were in the form of discs of diameter 4.5 mm and thickness 2 mm, or diameter 32.2 mm and thickness 3.1 mm. Samples to be used for measurements on hardened material were stored in their moulds for 2 days, demoulded and stored in water for 41 days, and then dried in a desiccator for 17 days. The opposite faces of the small samples which were used to determine the variation in measured parameters with time, were polished, and discs of aluminium foil, which were used as electrodes, were stuck on with a small amount of pure vaseline. For the larger samples, the faces were not polished, but a similar method of placing electrodes was used.

Measurements of electrical impedance were made using an a.c. bridge, and values of the dielectric parameters calculated. For hydrating samples, initially tanδ increased at very low frequencies, and also at very high frequencies. After 20 days a maximum was obtained at approximately 300 kHz. By 54 days this had fallen to 50 kHz. Low frequency values of ε' in the region of 700 were reported initially, but the measurements had poor reproducability. Consistent results were obtained with the hardened samples with a low frequency value of ε' of about 200, and a maximum for tanδ at about 10 kHz. Variation in the humidity of the atmosphere had very little effect on the results. As the temperature was reduced from 18 °C to -22 °C, there was a gradual reduction in the relaxation

frequency from about 10 kHz to 1 kHz. There did not appear to be any discontinuity near freezing point.

Van Beek & Stein concluded that for hydrating cement paste, conduction is initially due to pore water, and that the gradual reduction in relaxation frequency is due to the water molecules becoming locked in the lattice, although the reduction in conductivity with time is mentioned. In the fully hardened samples, conduction was thought not to be due to pore water because of the negligible effects of atmospheric humidity, and the lack of discontinuity as the temperature is reduced through the freezing point.

The method of fixing the electrodes to the samples might well result in a capacitance, caused by the vaseline layer, being placed in series with the sample. This capacitance, in conjunction with charge polarization, will give rise to low frequency relaxation effects. No attempt appears to have been made to take these effects into account. As the resistance of the sample increases as a result of hydration, the relaxation frequency will fall. The results for fully hardened samples would indicate that, under the conditions applying for the experiment, the static conductivity is not related to pore water. It could be that for the low water/cement ratio used, the pores have become highly segmented.

4.1.5. Bell et al.

Bell et al [63] investigated both the capacitive and conductive effects in mortar and concrete for use as a measure of water content. It was thought that measurements of capacitance might be more suitable because of the effects of variation in the salt content of the pore water on conductivity.

The mix parameters used for mortars were, water/cement ratio 0.67 and cement/fine aggregate ratio 1:2.5, and for concrete, water/cement ratio 0.67 and cement/fine aggregate/coarse aggregate 1:2:1.75. Samples were in the form of discs of diameter 76 mm and thickness 4 mm and 7 mm, and prisms 10 mm x 25 mm x 51 mm. Only the discs were used for capacitance measurements, and these were placed between electrode plates which were insulated by a thin layer of PTFE. The prisms were used only for conductivity measurements, and had electrodes painted on the ends using silver conducting paint.

The samples were cured under water for a period of 28 days, and then progressively dried while a range of measurements were taken with different water contents. The water content was then progressively increased by exposure to water vapour, or by brief immersion in water, and further measurements taken. Several cycles of wetting and drying were carried out on the samples, and a correction was made for increase in dry weight due to continued hydration. Measurements were made using a.c. bridges. Capacitance measurements were carried out at 60 Hz, 600 kHz, and 1 MHz, although the measurements at 60 Hz and 600 kHz were of relative capacitance only. Conductivity measurements were carried out at 10 Hz and 1

MHz. Measurements were also carried out on samples which were dried and then soaked in a 1.0 N sodium chloride solution.

The required measurement accuracy for water content was taken by Bell et al as 0.25%. The capacitance measurements at 60 Hz were able to achieve this only at very low water contents, but the measurements at 600 kHz and 1 MHz were able to give this accuracy for water contents up to 6%. The variation in accuracy with frequency was attributed to electrode capacitance effects which dominated the low frequency measurements. It was also concluded that conductivity might also be considered as an indicator of water content within the accuracy limits considered. Non-reversible effects and hysteresis were noted in both capacitance and conductivity measurements during the drying and wetting cycles. This was more pronounced with thinner samples dried at 105 ^{o}C than with thicker samples dried at 60 ^{o}C. The effect of soaking in a sodium chloride solution is to increase both capacitance and conductivity at 1 MHz. This was found to reduce the water content over which the required accuracy can be achieved. Conductivities measured at 10 Hz and 1 MHz with a disc sample and a prism sample of the same material gave very similar values.

The non-reversible and hysteresis effects which were more pronounced with samples dried at 105 ^{o}C would indicate that bound water is being driven off at this temperature. The effects of thickness are probably due to a distribution of moisture content within the thicker samples. The small variation in conductivity between measurements at 10 Hz and 1 MHz when an increase might have been expected at the higher frequency might indicate a problem in

the experimental technique, perhaps related to the sample geometry. It must be noted that the water/cement ratio used in these experiments is higher than that normally used for structural concrete.

4.1.6. Monfore.

Monfore [37], investigated resistivity of concrete with regard to the insulating properties of concrete railway sleepers, which is of importance if the rails are to be used as conductors in a signalling system. He suggests a conduction model of insulating particles imbedded in a conducting matrix in which the conducting matrix runs the full length of the sample and has a cross-sectional area proportional to its fractional volume. From conductivity measurements, an effective length can be deduced which is greater than the physical length. This takes into account the convoluted conduction paths in the concrete (Section 3.1.5.).

The samples used were in the form of cubes with brass electrodes which made contact with the material using a graphite/water paste. Some samples were cast with imbedded stainless steel electrodes. A number of different cements were used, and some samples had part of the cement content replaced by fly ash. Water/cement ratio was 0.41. The cement/aggregate ratios are not given explicitly, but have been estimated to be 1:5.6.

Measurements were carried out on cement pastes, mortars, and concrete. Specimens were demoulded after 24 hrs curing in a moist atmosphere at 23 ^{o}C, and then stored in lime water at 23 ^{o}C.

Measurements were carried out on the effects of polarization using d.c., and a.c. impedance measurements were made using a bridge at 100 Hz, 1 kHz, and 10 kHz. A 4% fall in resistance was observed between 100 Hz and 10 kHz, and a fall by a factor about 200 in the effective parallel capacitance over the same frequency range. The temperature coefficient of resistivity was found to be approximately 0.018 /^{o}C for cement paste.

The ratio of resistances of samples with external plate electrodes to those with imbedded electrodes did not remain constant with time.

The resistivity increased with time of continuous moist storage, which was believed to be due to either a decrease in evaporable water, or to leaching. After 7 days the resistivity of a cement paste was found to be 10 Ωm, and for concrete with the same water/cement ratio 50 Ωm. After 100 days the corresponding values had increased to 15 Ωm and 80 Ωm.

The effects of ammonium phosphate, hydroxyacetic acid, hydroethyl cellulose, and calcium chloride admixtures were investigated. Generally all gave reduced resistivity after 7 days. However, by 90 days, the first three produced a higher resistivity; hydroxyacetic acid by as much as a factor of 2. Calcium chloride always gave a reduced resistivity. These effects were more variable if a cement with a high alkali content was used.

Measurements on mortars with different aggregate contents, and pastes with water/cement ratio 0.5, gave values of effective length for conduction throught the cement paste in the mortar which varied by less than 6% between 3 days and 28 days, although a definite

variation with time was noted. The corresponding variation in effective length ratio for concrete was in the region of 20%, with a low value of 0.81 which was thought to be due to conduction in the coarse aggregate. It was also suggested that only 10% of evaporable water significantly contributed to electrical conductivity.

Although this is an important paper on the low frequency electrical properties of concrete, information given about the aggregate content of the concrete samples used is limited.

4.1.7. Efimenko & Ivanov.

Efimenko & Ivanov [64] briefly describe a servo-controlled 5 kHz a.c. bridge which allows rapid measurement of the conductivity of concrete. The paper infers that in the Soviet Union, electrical conductivity measurement is frequently used for the investigation of the properties of concrete.

4.1.8. Whittington et al.

Whittington et al [49] investigated the variations in the resistivity/time characteristics of cement pastes and concretes with changes in the mix parameters.

It is suggested that the electrical properties of a sample might not be uniformly distributed because of stratification and differential drying, as well as the basic heterogenity of the material. Expressions developed by various workers which will allow the resistivity of concrete to be calculated, knowing the

resistivity of the corresponding cement paste, are discussed.

Measurements carried out on cement paste, mortar, and concretes, with water/cement ratios in the range 0.4 - 0.8, cement/aggregate ratios between 1:1 and 1:2 for mortars, and 1:3 and 1:6 for concretes. Specimens were 100 mm cubes moulded with brass plate electrodes. For the first 24 hours, the specimens were kept in steel moulds which were lined with polythene to provide electrical insulation. After 24 hrs. the samples were demoulded, the electrodes removed, and the samples stored under water at 23 ^{o}C. For measurements, the specimens were removed from the water, surface dried, and electrodes connected by using a thin layer of fresh cement paste of water/cement ratio 0.5. Some samples were stored outdoors under 200 mm of sand following normal curing for 13 days.

A low frequency square voltage waveform was applied to the samples to overcome the polarization effects which would have been encountered using d.c. Graphs of resistivity against time were produced for times between 10 min and 128 days after placing. For concrete of water/cement ratio 0.6, and cement/aggregate ratio 1:6, the resistivity increased from an initial value of 8.2 Ωm to 17.5 Ωm after 1 day. In general the results show that initial variations in resistivity are relatively small, but after about 6 hrs, with the onset of hardening, a rapid increase in resistivity takes place, which continues until about 14 days. Beyond 14 days the increase in resistivity is relatively small. There is little variation in the resistivities of cement pastes of differing water/cement ratio before hardening commences.

The samples in outdoor storage showed variations in resistivity which correlated with variations in temperature. Assessment of these variations gave a temperature coefficient of resistivity of -0.022 /°C. The resistivities of concretes and mortars were related to that of cement paste with the same water/cement ratio. The mathematical relationship chosen was a modified form of Archie's Law given by:-

$$\rho = \rho_p A v^{-m}$$

where ρ = resistivity of concrete

ρ_p = resistivity of the corresponding cement paste

v = fractional volume of cement paste

A, m = constants

From an assessment of all the results obtained, A was found to be 1.04, and m 1.20. It was found however that these values were not constant with time, the values presented being average values.

The similarity between graphs of resistivity against time and those of crushing strength against time were noted, and since both are related to the hydration process, it was suggested that this technique could be developed as a quality control test for structural concrete.

This paper gives detailed results for the variations in resistivities of cement pastes, mortars, and concretes, with time. This information is not readily available elsewhere. However the problems associated with electrode polarization have not been investigated. Depending on the frequency of operation, this could

give rise to errors in the resistivity measurements, particularly when the material is fresh.

4.1.9. McCarter & Curran.

McCarter & Curran [65] investigated the variations in electrical resistivity and dielectric constant for cement pastes and mortars as a method of studying the structural changes which occur during hydration.

The electrode system used had a coaxial geometry with inner radius 2.5 mm and outer radius 50 mm. The height of the test cell was 80 mm. The space between the inner and outer electrodes was filled with the material being tested. Water/cement ratios were in the range 0.3 to 0.5 for cement paste, and 0.6 to 0.8 for mortars, the cement/aggregate ratio being 1:2. The electrode material is not given. Impedance measurements were carried out using an a.c. bridge operating at 1 kHz. Measurements were taken automatically every 5 min., and the data, in the form of resistance and capacitance values, outputted on a printer. The samples were held in a cabinet in which the temperature was 20 ^{o}C, and the relative humidity 50%. Temperature was measured by a thermistor imbedded in a 100 mm cube.

The resistivity characteristics of cement pastes all start with resistivities approximately 4 Ωm after about 1 hr. This value remains fairly constant for a time depending on the water/cement ratio, and then increases. At 1 day, the resistivities are in the range 10 - 80 Ωm, with the low resistivity values associated with high water/cement ratios. A discontinuity occurs near the point

where the resistivity starts to rise. A value of dielectric constant calculated from the capitance measurement gives values as high as 10^6. The graphs of variation in calculated dielectric constant with time show a reciprocal characteristic to the resistivity graphs. The variations in resistivity for mortars show similar tendencies to those for cement pastes, although none of the mortar samples has the same water/cement ratio as the cement pastes. The resistivities of the mortar samples are generally greater than those for the cement pastes, with higher water/cement ratios giving lower resistivities after 1 day. Values of dielectric constant for mortars are quoted as being greater than 4×10^5, and the graphs of dielectric constant again show a reciprocal characteristic to those for resistivity.

The dielectric constant calculated from the capacitance measurement is inferred to be due to the bulk properties of the material, although no assessment of the effect of electrode polarization has been made, and measurements might be in the frequency range where a higher resistance than that due to the bulk properties is obtained because of relaxation processes.

More detailed comments on this paper are given by Wilson & Whittington [66] and are presented in Appendix D.

4.1.10. Buenfeld & Newman.

Buenfeld and Newman [67] used a resistivity technique to investigate the permeability of mortars and concrete to sea water.

The water/cement ratios used were 0.4 and 0.6. The aggregate

content is not given. In some of the samples, part of the cement was replaced by pulverized fuel ash, and blast furnace slag. Tests were also carried out using sulphate-resisting Portland cement. The samples were in the form of discs of diameter 100 mm, and thickness 25 and 45 mm. The specimens were cured in lime water at 20 °C for 28 days prior to testing, and then mounted in a test cell which allowed one face of the disc to be immersed in lime water to simulate bulk pore water, while the other face was immersed in sea water. Stainless steel electrodes were placed in the sea water and lime water reservoirs. Details of the method of calibrating out the resistances of the electrolytes in the reservoirs are not given. Measurements were made in comparison with samples with lime water in each reservoir, allowing the effects of continuing hydration to be calibrated out. Resistance measurements were made between the electrodes using an a.c. bridge operating at 1 kHz, which avoided the problems associated with electrode polarization. The resistance was corrected to 21 °C using a temperature coefficient of 0.025 /°C following Spencer [59]. Measurements on mortar samples were continued for more than 130 days, and for concrete samples, more then 230 days.

All samples initially showed an increase in resistance with time up to about 2 months. In some mortar samples, the resistance then reduced slightly, but in others the resistance continued to rise. Examination of the surface of the sample exposed to sea water, using a low magnification scanning electron microscope, showed the formation of surface layers where the surface has been exposed to sea water. Two surface layers were observed in most

cases. The layer closest to the sample was found to be brucite [$Mg(OH)_2$] and the outer layer was found to be largely aragonite [$CaCO_3$]. The growth of these layers is believed to be due to the presence of magnesium ions in sea water. The presence of the layers is believed to cause a decrease in the permeability of mortar and concrete which might help to retard the ingress of chloride ions, and reduce corrosion of the reinforcement.

The effects of electrode polarization might not be negligible in these experiments. This will however only affect the accuracy of the resistance measurements, and will not affect the general trends observed. These experiments are an example of the practical application of electrical measurements to the investigation of a civil engineering problem.

4.2 High Frequencies.

4.2.1. De Loor.

De Loor [33] measured the dielectric constant of hardened cement pastes at spot frequencies in the range 0.1 - 9375 MHz in an investigation into the distribution of pore water and absorbed water.

The water/cement ratios used were 0.26, 0.31, and 0.36 for measurements between 0.1 and 3750 MHz, and 0.24 for measurements at 7450 and 9375 MHz. The sample geometry for measurements between 0.1 and 3750 MHz consisted of a disc of diameter approximately 36 mm and thickness 6.5 mm, with a hole in the centre for use with coaxial

transmission line equipment. The sample used at 7450 and 9375 MHz consisted of a rectangular prism with volume approximately 1.4×10^3 mm^3, for use with waveguide equipment. The disc samples were demoulded after a day, and cured under water for 1 month or longer. The prism sample was cured in the laboratory atmosphere.

After curing, the samples were dried for 10 days at 100 °C and then placed in a dessicator for a further 7 days. During a measurement sequence, the samples were left in the laboratory atmosphere at relative humidity 50 - 70%, and the density obtained by weighing before each measurement. For high water contents the samples were wetted with distilled water. Following the measurement sequence, the samples were redried to allow further measurements at a greater age.

Measurements of dielectric constant between 0.1 and 10 MHz were obtained using the sample as the dielectric in a capacitor with secondary electrodes painted on the specimen with silver paint, although the method of measurement is not described. Measurements at 3000 and 3750 MHz were carried out using normal dielectric measurement techniques in coaxial lines, and at 7450 and 9375 MHz, rectangular waveguide techniques were used.

Measurements between 0.1 and 5 MHz show a progressive increase in dielectric constant as the free water content is increased, with the possibility of a maximum occuring at high values. The dielectric constant falls progressively as the frequency is increased. On a graph showing dielectric constant against density for various frequencies, the curves can be extrapolated to meet at a point in the low density and low dielectric constant region. It is

deduced that this density corresponds to the condition of no free water. The dielectric constant at this point is approximately 6.3. Measurements at different ages show that this density and the corresponding dielectric constant increase with age.

The variations in dielectric constant with moisture content are similar at 3000, 3750, 7450 and 9375 MHz, although the graphs used at 7450 and 9375 MHz have logarithmic scales, while the other results are on a linear scale, which makes interpretation difficult. The variations in dielectric constant with moisture constant are significantly less, compared with the lower frequencies, although they still change by a factor greater than 2 over the range of water contents used. Calculations of tanδ show a progressive increase as the water content is increased. As the frequency is increased, for a given water content, tanδ falls between low frequencies and 3000 MHz, and then increases to an intermediate value at 7450 and 9375 MHz. Problems were reported with measurements in the 3000 MHz region however. By assuming that the measurements at microwave frequencies lie on an arc on a Cole-Cole diagram (Section 3.1), an assessment of the relaxation time was obtained. This was close to the value for free water.

De Loor concludes from the measurements at low frequencies that conduction must be due to both pore water and adsorbed water, but at microwave frequencies, conduction is due only to pore water, because of the relaxation time obtained.

There might well have been problems in the distribution of water within the samples, since an equilibrium condition was never reached. Drying at 100 ^{o}C might have driven off some of the bound

water. The extent of the data presented at microwave frequencies might be inadequate to determine the relationships affecting dielectric dispersion, considering that there were measurement problems in the 3000 MHz region.

4.2.2. Lovell et al.

Lovell et al [35] investigated the dielectric properties of water loaded brick and hardened cement paste, to determine whether conduction is due to bound water or pore water. Measurements were carried out at a wavelength of 33.3 mm.

Rectangular samples of Leicester red brick and Portland cement paste, with a water/cement ratio 0.28, which had been allowed to harden for 3 months, were loaded with weighed amounts of water, and inserted into a rectangular waveguide. The measurement section of the waveguide had external temperature control. The temperature within the waveguide was assumed to be the same as the external temperature. Measurements of ε' and ε'' were made at 33.3 mm wavelength, using standard microwave techniques. Measurements were carried out over the temperature range -20 to +15 ^{o}C.

A large discontinuity in the graphs of ε' and ε'' against temperature is obtained for brick at about 3 ^{o}C. There are no similar discontinuities in the results for cement paste. The value of ε'' for brick falls at the discontinuity as the temperature is increased. The dielectric constant obtained for cement paste is approximately 20.

Lovell et al conclude that, because of the lack of

discontinuity at the freezing point, the dielectric behaviour of cement paste at 33.3 mm is not associated with free water.

The dielectric constant obtained for cement paste in this experiment is surprisingly high, and the fall in the value of ε'' for brick at temperatures above the point of discontinuity is unexpected. It could be that, while the discontinuity undoubtedly exists in the measurements on brick, the mechanism producing the discontinuity is not perhaps that suggested. The water/cement ratio is very low in this experiment, and is less than that necessary for complete hydration of the cement paste to take place [1]. The fractional volume of capillary pores in the samples can therefore be expected to be small.

4.2.3. Rzepecka et al.

Rzepecka et al [68] carried out measurements of dielectric constant of mortars and concretes with the aim of establishing a relationship with mechanical strength, and therefore establishing a quality assurance test for concretes. Measurements of reflection coefficients from concrete surfaces were also made.

Measurements were carried out on mortars with water/cement ratios in the range 0.580 - 0.595, and cement/aggregate ratio 1:3.62. A very fine grained sand was used as aggregate for these experiments. The concretes investigated were made using both ordinary and rapid hardening Portland cement. The water/cement ratio was 0.77, and the cement/sand/aggregate ratio 1:3.7:3.77. The samples for dielectric measurements were in the form of rectangular

prisms to fit rectangular waveguide. Large blocks of concrete were used for reflection coefficient measurements. Crushing strength measurements were carried out on the waveguide samples, and on cylindrical samples.

Values of dielectric constant and tanδ were obtained from waveguide standing wave measurements at 2450 MHz using both long samples in open circuited waveguide, and short samples in waveguide terminated by a sliding short circuit. Measurements of the modulus of the reflection coefficient were obtained with the waveguide terminated in a horn of gain 15 dB, with the end of the horn against the concrete surface, and also at a distance of 0.31 wavelengths away from the surface.

For mortars, the dielectric constant initially falls rapidly with curing time, but the rate of change then reduces after approximately 250 hrs, although the dielectric constant continues to fall. At 20 hrs. after mixing, the dielectric constant is approximately 7, and after approximately 250 hrs., it has fallen to approximately 5.2. Increase in water/cement ratio in the range 0.580 - 0.595 causes a significant increase in the dielectric constant at all curing times in the range 20 - 700 hrs. Tanδ starts at approximately 0.3 after 20 hrs curing, and falls slowly at first. The rate of fall increases, reaching a maximum after approximately 250 hrs, and then reduces. After 700 hrs tanδ is approximately 0.4. Larger water/cement ratios give larger values of tanδ.

For concretes made from ordinary Portland cement, the dielectric behaviour is similar to that for the mortars. Dielectric constant starts at approximately 7.5 after 20 hrs curing, and falls

to approximately 5.3 after 600 hrs. Tanδ starts at approximately 0.33 and falls to 0.04 after 600 hrs. Using rapid hardening Portland cement, the dielectric constant was 7.8 after 20 hrs, and fell rapidly to 5.9 after 180 hrs. No measurements are given beyond this time for rapid hardening cement. Tanδ starts at 0.17 after 20 hrs, and falls to 0.08 after 180 hrs, the initial fall being very rapid. Graphs of crushing strength against dielectric constant are similar for both kinds of cement, with a fall in crushing strength being related to an increase in dielectric constant. The relationship being approximately linear. The crushing strength is 15.9 MPa for dielectric constant 6, falling to 7.6 MPa for dielectric constant 7.

Graphs of crushing strength against modulus of reflection coefficient are also presented. The measurements give curves with low values of reflection coefficient giving high values of crushing strength. For concrete made with ordinary Portland cement, a crushing strength of 17.3 MPa gives a reflection coefficient of 0.28, and for a crushing strength of 6.9 MPa, a reflection coefficient of 0.37, with the horn on the surface of the concrete, and corresponding values of reflection coefficient of 0.33 and 0.42 with the horn separated from the concrete by distance 0.31 wavelengths. The curves for rapid hardening cement are similar, but with higher values of reflection coefficient for the higher strength region.

Further experiments were carried out to find the effect of drying concrete by microwave radiation at 2450 MHz at an intensity of 1.2 kWm^{-2}. If curing is carried out under microwave radiation

for long periods, the strength of concrete after 28 days might only be about 50% of that which has been cured normally.

It is concluded that a relationship between the strength of concrete and its microwave properties has been established, but that much more work is required before it can be considered a feasible quality assurance technique. It is stated from other work that the penetration of radiation at 2450 MHz into concrete varies between 38 and 100 mm during the aging process, and that the use of lower frequencies would give greater penetration.

This paper gives useful data on the behaviour of concrete at 2450 MHz. The water/cement ratio of 0.77 used for concrete is high for structural applications. The fact that similar values are obtained for dielectric constant against curing time for both mortar and concrete using ordinary Portland cement is surprising, since a calculation of fractional volume of water in the mix in each case, based on the values of specific gravity used in Section 3.7.2. gives:-

specific gravity of cement 2.99

specific gravity of aggregate 2.584

mortar:- water/cement ratio 0.59

cement/aggregate ratio 1:3.62

fractional volume of water in the mix 0.25

concrete:- water/cement ratio 0.77

cement/aggregate ratio 1:7.47

fractional volume of water in the mix 0.19

Thus the mortar with a significantly lower initial fractional volume of water gives similar values of dielectric constant. In the practical case, it is the long term strength of concrete which is important. It might therefore have been more useful to find a relationship between early values of dielectric parameters and the strength at 28 days.

4.2.4 Taylor & Arulanandan.

Taylor & Arulanandan [69] carried out dielectric measurements on cement pastes over the frequency range 10 - 50 MHz, and using a simple electrical model, attempted to relate these properties to the physical properties of the material.

The paper discusses the advantages of a possible electrical method of testing compared with traditional methods of testing cement and concrete, and also the problems of investigating cement hydration.

The cement paste samples used were cylindrical of diameter 12.7 mm and approximate length 38 mm. The cement used was ordinary Portland cement. A full range of tests was carried out up to an age of 1 week for samples with water/cement ratios 0.3 and 0.35. Measurements were also carried out on other samples with water/cement ratios 0.3, 0.35, and 0.4, when approximately 24 hrs old. No information is given about the curing procedure used. Values of dielectric constant and conductivity are calculated from impedance data obtained using an a.c. bridge over the frequency

range 10 - 50 MHz. The method of measurement follows that of Sachs & Spiegler [54].

Graphs of dielectric constant and conductivity against frequency are presented. These give values of dielectric constant in the region of 110 at 10 MHz, falling to 75 at 50 MHz, and values of conductivity of approximately 0.19 Sm^{-1} at 10 MHz increasing to 0.26 Sm^{-1} at 50 MHz. Graphs are given for ages 23, 35, and 52 hrs. There is an increase in apparent dielectric constant, and a reduction in conductivity with age.

A three component electrical model of the cement paste is then developed in which three conduction paths are considered. These are, a path completely within the cement matrix, a path partially within the cement matrix and partially within the pore water, and a conduction path completely within the pore water. Expressions for the effective dielectric constant and conductivity for this model are obtained, assuming that each component can be represented by values of dielectric constant and conductivity along with geometrical factors, including the relative volumes involved in the three paths. The parameters of the model are then determined by obtaining the best fit to the measured data using non-linear programming techniques. The relative volumes of the three conduction paths are then plotted against age of the cement paste.

From the graphs, Taylor & Arulanandan conclude that the relative volume of the cement matrix path increases with time. The rate of increase is greatest during the first day, and then continues at a slower but steady rate throughout the first week. The relative volume of cement matrix is higher for lower

water/cement ratios. The relative volume of the pore water path decreases with time. By comparison between samples of different water/cement ratio at age 25 hrs, the fractional volume of cement matrix is sensitive to water/cement ratio in the range 0.35 - 0.4, but is less sensitive below 0.35. This might be related to the volume of water required for complete hydration, which is known to be in the range of water/cement ratios 0.3 to 0.35.

This paper describes a technique which could be developed into a useful tool for the analysis of dielectric dispersion data in relation to the basic parameters of a cement or concrete mix. The restricted frequency range of the data must limit the accuracy of the model, since, for example, neither the dielectric constant or conductivity has reached limiting values at either the high or the low frequency extremes. The model used has definite geometrical dimensions, while capillary pore lengths can be expected to have a statistical distribution, which will result in a statistical distribution of relaxation frequencies, and a deviation of the dispersion graphs from the values of the simple model. Systematic variations are noticeable between the measured and model values on the dispersion graphs. The graphs of volume proportions against time have been extrapolated for ages less than those at which measurements have been carried out, giving a misleading impression. Over the period between about 4 hrs and 10 - 20 hrs, the calculated results indicate a fall in the fractional volume of the cement matrix. Similar systematic variations also occur after about 60 hrs. This might indicate a defect in the model.

4.2.5. Misra.

Misra [70] describes measurements of complex dielectric constant at 9.375 GHz for a number of substances including cement.

The measurements were made using a rectangular waveguide 4 port directional coupler and sliding short circuit. Values obtained for dry cement powder are ε' 2.23, ε'' 1.77, and for water ε' 59.74, and ε'' 31.11 which correspond to values for water given in Section 3.2.1. at this frequency. As the water content of the cement is increased up to 15% by mass, ε' increases to 13 and ε'' to 17. The accuracy of the measurement is estimated to fall as $\tan\delta$ increases.

The details of the arrangement of the microwave coupler system are not given, although reference is made to other papers describing this system and other methods of microwave dielectric measurements.

5. PROTOTYPE LOW FREQUENCY RESISTIVITY MEASUREMENT SYSTEM.

5.1. General Requirements.

The general requirement is for equipment to carry out automatic resistivity measurements on a significant number of samples of concrete for a period of up to 100 days after mixing. This follows the work reported by Whittington et al [49] where manual measurement techniques were used.

The samples must be in a form such that curing, and subsequent crushing strength tests, can be carried out according to BS1881 [12], and must be sufficiently large so that maximum size aggregate does not affect the variability excessively. The number of samples must be such that the variability of resistivity due to the heterogeneous nature of concrete can be assessed.

The range of resistivities to be measured should correspond to those of Whittington et al [49], with suitable extension to cover contingencies. This range is from 1.1 Ωm for a cement paste 100 min after mixing, to 50 Ωm for concrete of water/cement ratio 0.6, and cement/sand/aggregate ratios 1:2:4, held in outdoor storage.

Allowing for experiments in which limited drying out occurs, by increasing the upper resistivity limit by a factor of 2, gives an extended range of 1.1 - 100 Ωm.

Assuming that measurements can be carried out over a temperature range 0 - 50 °C, that the above resistivity range applies at 23 °C, and taking a coefficient of resistivity of

-0.022 /°C [49], gives a required resistivity range of 0.447 - 150.6 Ωm. A range of 0.4 - 150 Ωm is assumed.

Consideration of equipment required for control and calculation suggested the use of a Rockwell AIM65 microcomputer, which is based on the R6502 microprocessor. This computer allows operation in both machine code and BASIC, has adequate interfacing ports and control lines, and prints output on a paper roll.

These considerations give a general specification:-

1. Resistivity range 0.4 - 150 Ωm.
2. Temperature range 0 - 50 °C. The output resistivity data is to be corrected to 20 °C.
3. Sample number 15, with a possible extension to 60.
4. Samples to be in the form of 150 mm cubes, excluding the thickness of electrodes.
5. On demoulding after 1 day, the samples to be stored under water at 20 °C, and withdrawn automatically for measurement [12].
6. Control, calculation, and output of data to be by means of a Rockwell AIM65 microcomputer.

Accuracy of measurement is not considered at this stage (see Section 5.3).

5.2. Measurement System.

5.2.1. Resistivity Measurements.

Because of the ease with which both amplitude and frequency can be controlled, it was decided that a square test waveform should be used for energising the resistivity tests rather than a sinusoidal waveform.

Assuming that the electrical behaviour of concrete at low frequencies can be represented by a capacitance and resistance in series (Section 3.7.4), the test circuit can be represented by the equivalent circuit of Figure 5.1. This circuit is analysed using Laplace transforms in Appendix E.

From Appendix E, the output amplitude in the absence of the series capacitance would have been:-

$$v_o = V_r \frac{R_s}{R_r + R_s} \qquad (E.2)$$

and the voltage of the positive half cycle of the waveform is:-

$$v_o = \frac{V_r R_s}{R_r + R_s} \left\{ 1 + \frac{R_r}{R_s} \frac{(t_o - T/4)}{\tau} \right\} \qquad (E.6)$$

where t_o = time from start of half cycle (s)

T = period of waveform (s)

$\tau = C_s(R_r+R_s)$ (s)

Thus when $t_o = T/4$, the effect of the capacitance is eliminated.

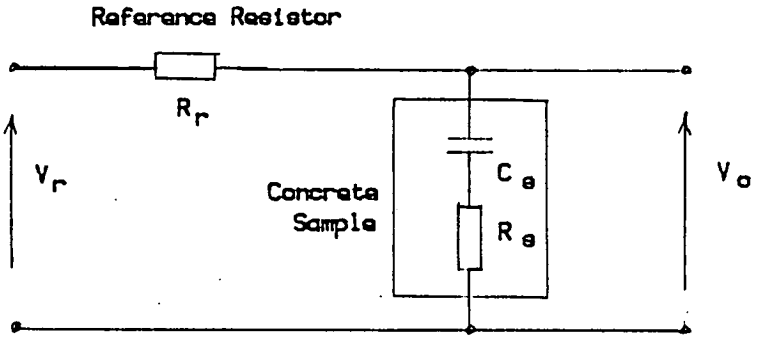

Figure 5.1
Equivalent Circuit

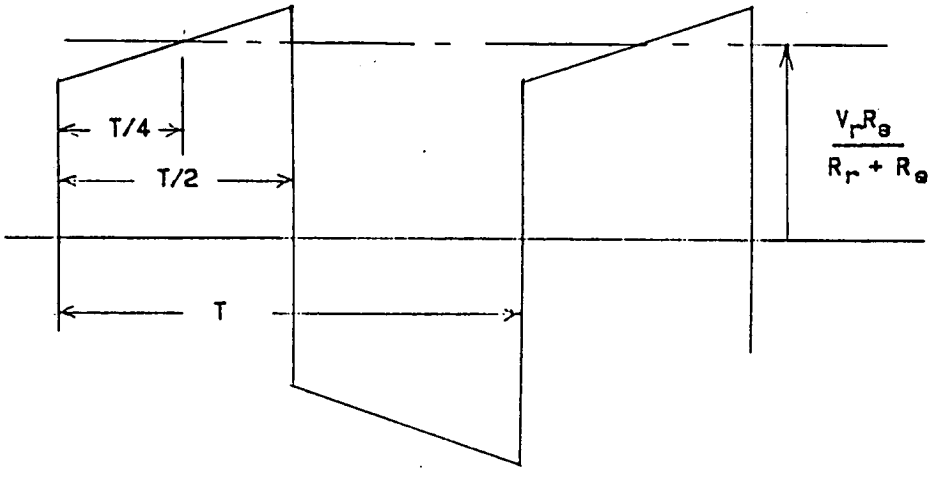

Figure 5.2
Theoretical Output Waveform

Therefore, if the measurement is carried out at the mid-point of the positive half cycle, the output voltage depends only on R_s, and not on C_s. R_s, the effective series resistance of the sample, can then be obtained.

The maximum fractional deviation in v_o due to C_s is:-

$$|\alpha|_{MAX} = \frac{1}{4} \frac{R_r}{R_s} \frac{T}{\tau} \qquad (E.5)$$

Thus by reducing T (i.e. increasing frequency), the extent of this deviation can be reduced.

Figure 5.2 shows the form of the output waveform given by Expressions E.6 and E.7.

Tests were carried out on a concrete sample, using the circuit of Figure 5.1, to determine the shape of the output waveform. The results are shown in Figure 5.3. It can be seen that the higher the frequency, the more rectangular the waveform becomes. For the sample used (water/cement ratio 0.5, cement/sand/aggregate ratios 1:1.5:3, and age 12 days) a frequency of 2 kHz gives a good waveform shape.

By applying Expression E.4 to the measurements carried out on the sample, the value of the time constant was found to be approximately 1 s.

Having obtained a value for the series resistance R_s, the resistivity of the sample cube is:-

$$\rho = R_s l \qquad (5.1)$$

where l is the length of a face of the cube (m).

Frequency 2.5 Hz

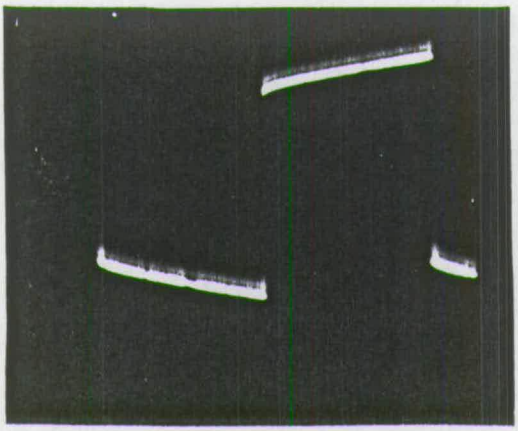

Frequency 100 Hz

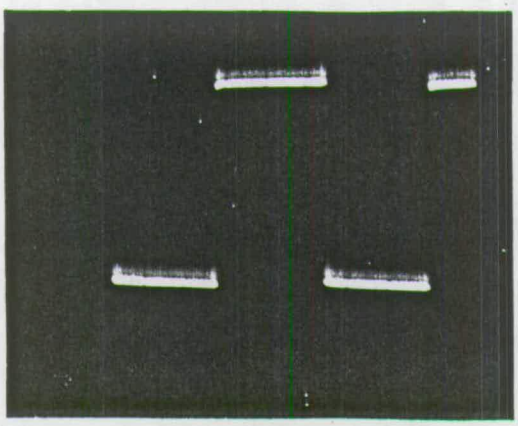

Frequency 2 kHz

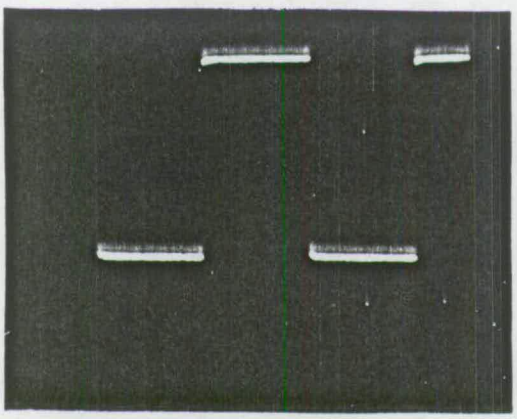

Figure 5.3
Output Waveform for Concrete Sample

The electrodes completely cover two opposite faces of the sample cubes, and stainless steel electrodes 2 mm thick (14 s.w.g.) are used. The resistivity range 0.4 - 150 Ωm therefore gives a resistance range for 150 mm cubes of 2.67 Ω to 1 kΩ. Fringing effects over this resistance range will be negligible.

5.2.2. Temperature Measurements.

The temperature coefficient of cement paste and concrete is relatively high (0.022 /°C [49]), and must be taken into account during measurements unless the environment is closely controlled. The hydration reaction is exothermic, and will result in a temperature distribution throughout the sample cubes. Inserting a temperature sensor into the sample will affect the resistivity measurement. It was therefore decided to fix a sensor to one of the electrodes, and to take this temperature as the temperature of the sample. The height of the electrodes was increased to allow the sensor to be mounted, and to allow sockets to be fitted for resistivity and temperature cables.

Platinum film resistance elements were used as sensing elements because of their linearity and good stability. These were fixed to the 0V electrode by a thin film of Araldite.

The sensitivity of metal film temperature sensors is low compared with thermistors, for example, and it was decided to fit the amplifiers associated with the sensors as close to the sensors as possible to reduce possible pick-up problems. The form of the transducer and amplifier circuit used is shown in Figure 5.4. To

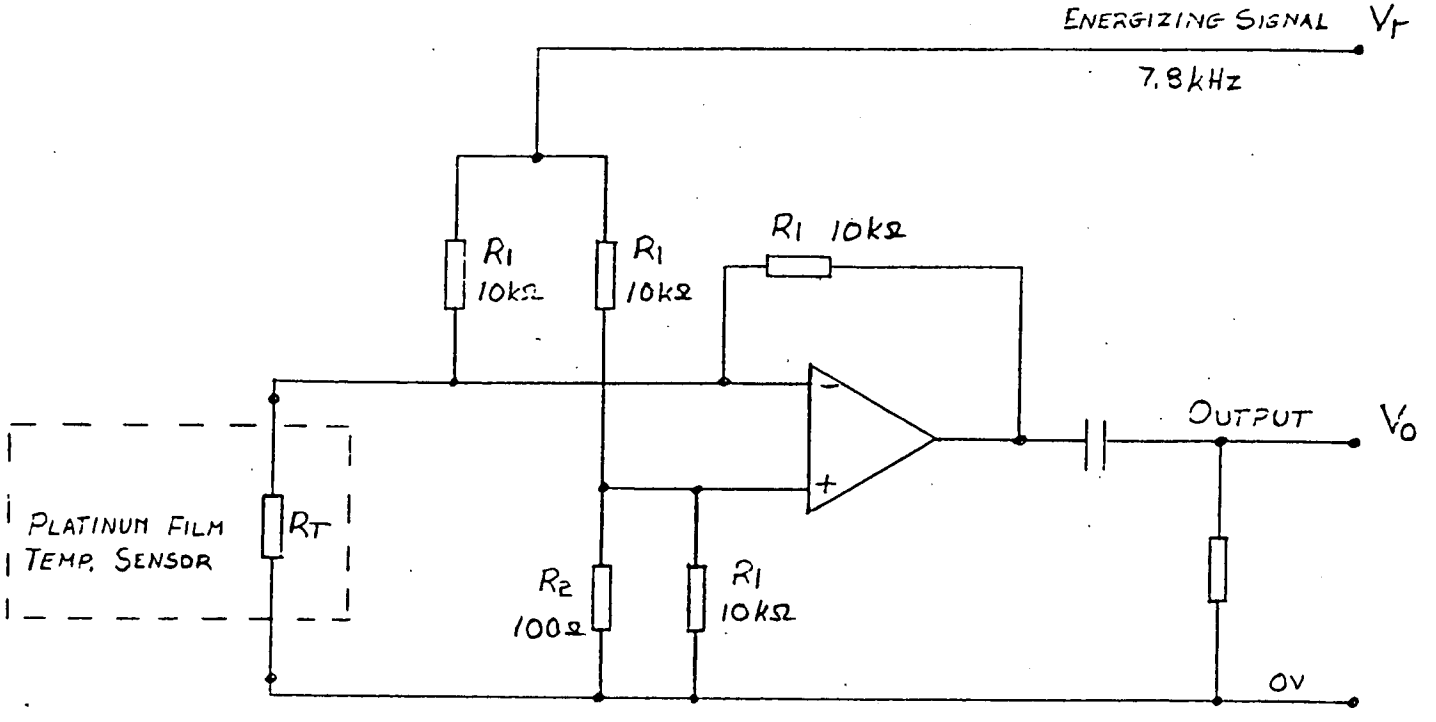

Figure 5.4
Temperature Transducer and Amplifier Circuit

eliminate possible problems with d.c. offsets in the high gain amplifier, a square wave energising signal at 7.8 kHz was used. The output of the transducer amplifier was then a.c. coupled to the processing system. The output voltage from the amplifier is:-

$$V_o = \frac{V_r}{1 + \frac{2R_2}{R_1}} \left(\frac{R_2}{R_T} - 1\right) \qquad (5.2)$$

Thus:-

$$R_T = \frac{R_2}{1 + \left(1 + \frac{2R_2}{R_1}\right)\frac{V_o}{V_r}} \qquad (5.3)$$

For the platinum film element:-

$$R_T = R_o(1 + \alpha T) \qquad (5.4)$$

where R_T = resistance at temperature T (Ω)

R_o = resistance at 0 ^oC (Ω)

α = coefficient of resistivity

= 3.85×10^{-3} /^oC

T = temperature (^oC)

Thus:-

$$T = \frac{1}{\alpha}\left(\frac{R_T}{R_o} - 1\right) \qquad (5.5)$$

5.2.3. Sample Moulds.

Initial work was carried out using cast steel 152 mm (6 ins) moulds, suitably shimmed to give 150 mm sample cubes between 2 mm (14 s.w.g.) stainless steel electrodes. Insulation was provided by a thin continuous PVC wall liner and separate base. These were placed in the mould before the electrodes were positioned. Additional insulation was provided at joins and edges by pieces of "cling film".

Considerable time was spent in ensuring that the insulation was complete before resistivity tests were carried out. This was a particular problem in experiments with a high fractional volume of water.

Figure 5.5 shows a sample in a cast steel mould with additional insulation. Figure 5.6 shows a sample on demoulding, with the temperature sensor visible on one of the electrodes.

Eventually, to eliminate any insulation problem, moulds fabricated from industrial grade PVC were obtained. While the tolerances on these moulds are not sufficiently tight to comply with the requirements of BS1881 [12], they are adequate to ensure a negligible effect on the accuracy of resistivity measurements

5.3. Description of the System.

A brief description of the system is given by Wilson et al [71]. This is presented in Appendix F.

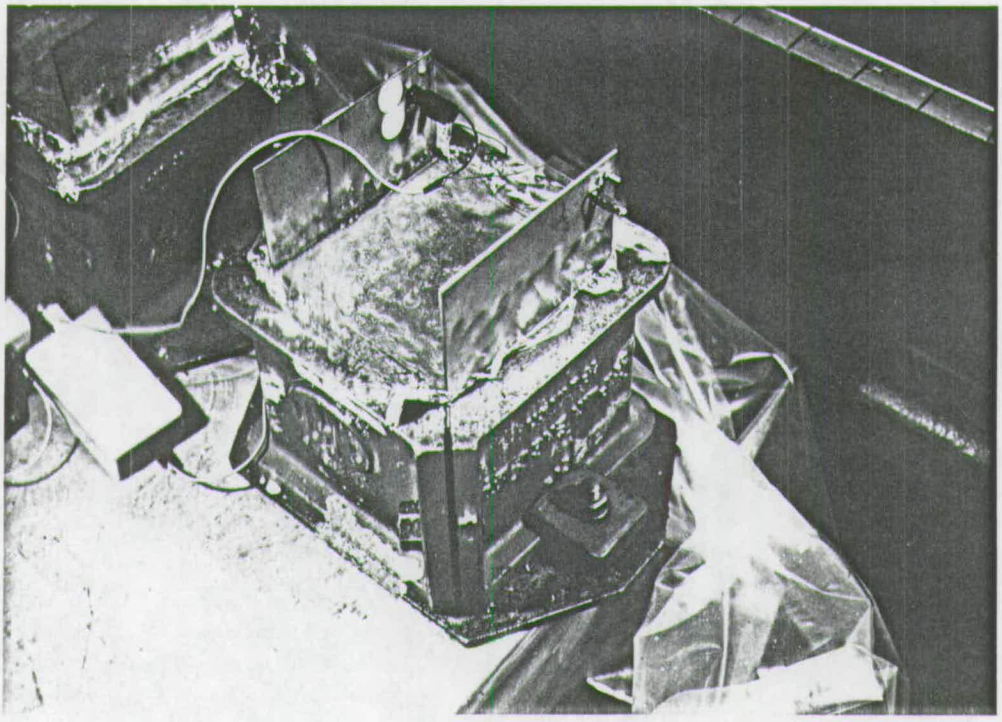

Figure 5.5
Sample in Mould with Additional Insulation

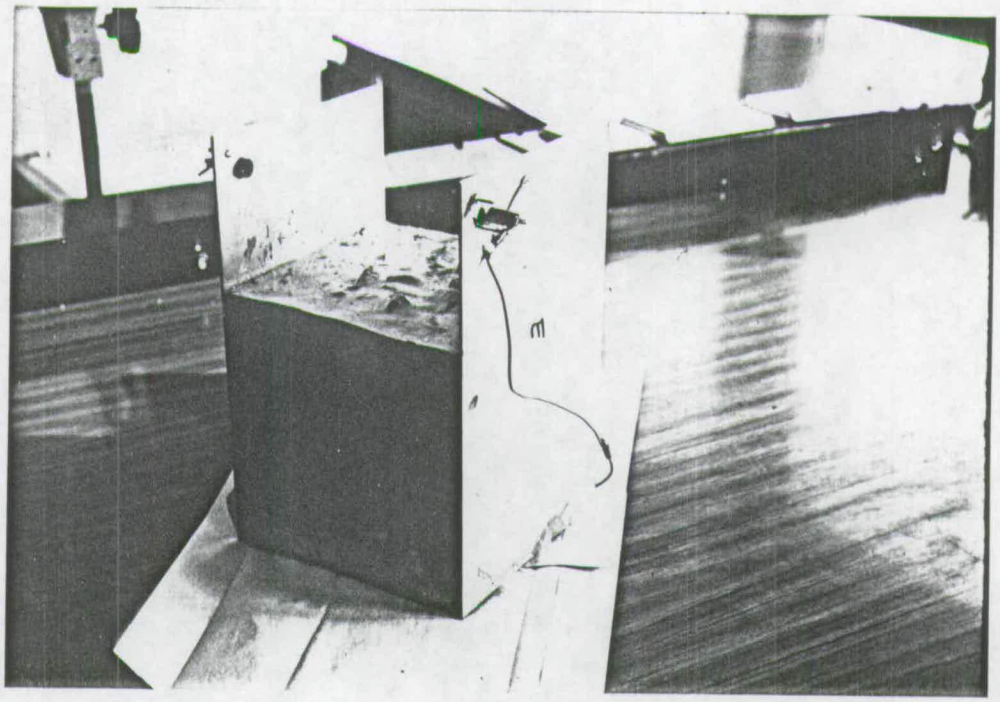

Figure 5.6
Sample on Demoulding

5.3.1. Hardware.

The complete system comprises the following units:-

(i) samples with electrodes and temperature sensors

(ii) temperature amplifiers which are positioned fairly close to the samples

(iii) electronics unit

(iv) hoist and hoist control unit

(v) AIM65 computer system

(vi) power supplies.

Figure 5.7 shows the complete system in operation.

The electronics unit, shown in Figure 5.8, contains the following circuits:-

(i) timing circuit

(ii) multiplexer

(iii) temperature rectifier

(iv) A/D converter

(v) memory expansion

(vi) control circuit

Circuit diagrams of the electronics and the hoist control unit are presented in Appendix G.

Figure 5.9 is a hardware system diagram which will be used to describe the operation of the system.

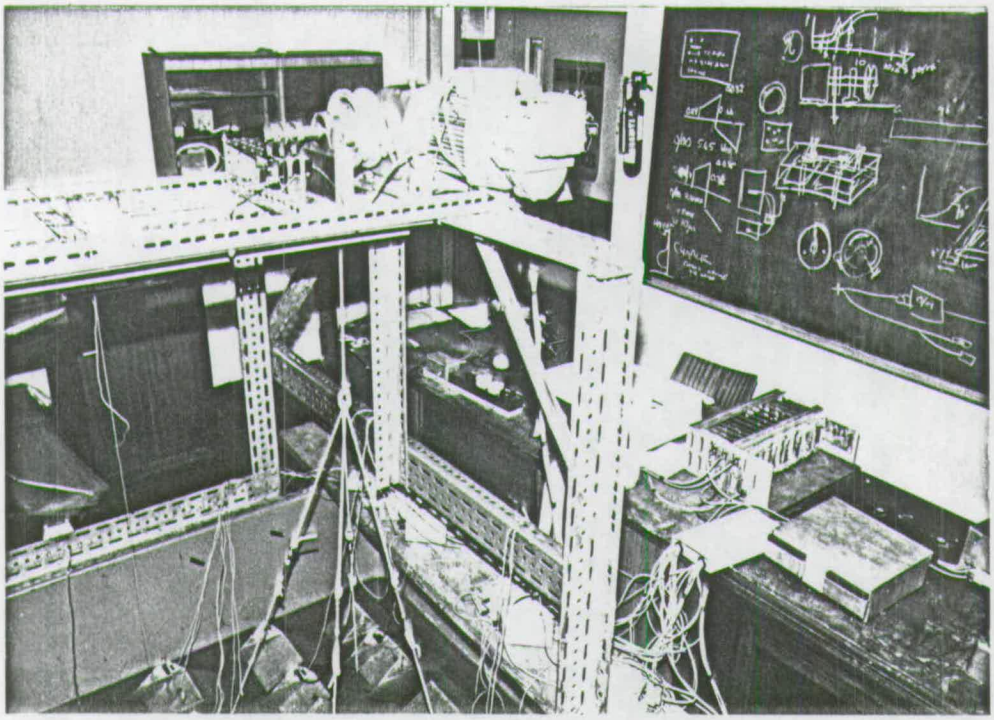

Figure 5.7
Complete System

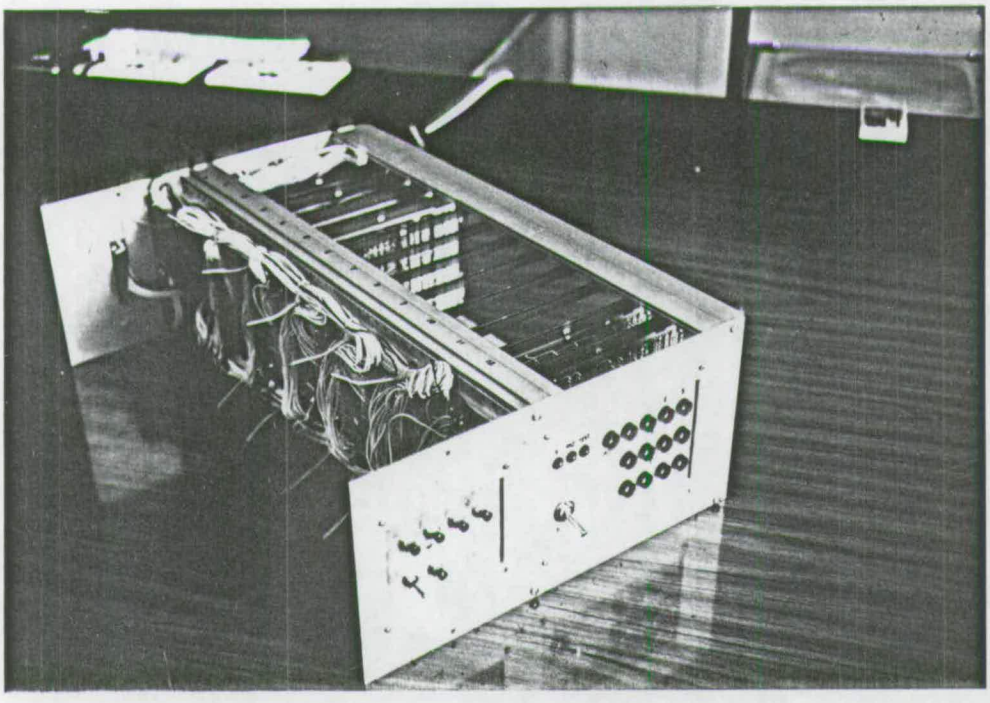

Figure 5.8
Electronics Unit

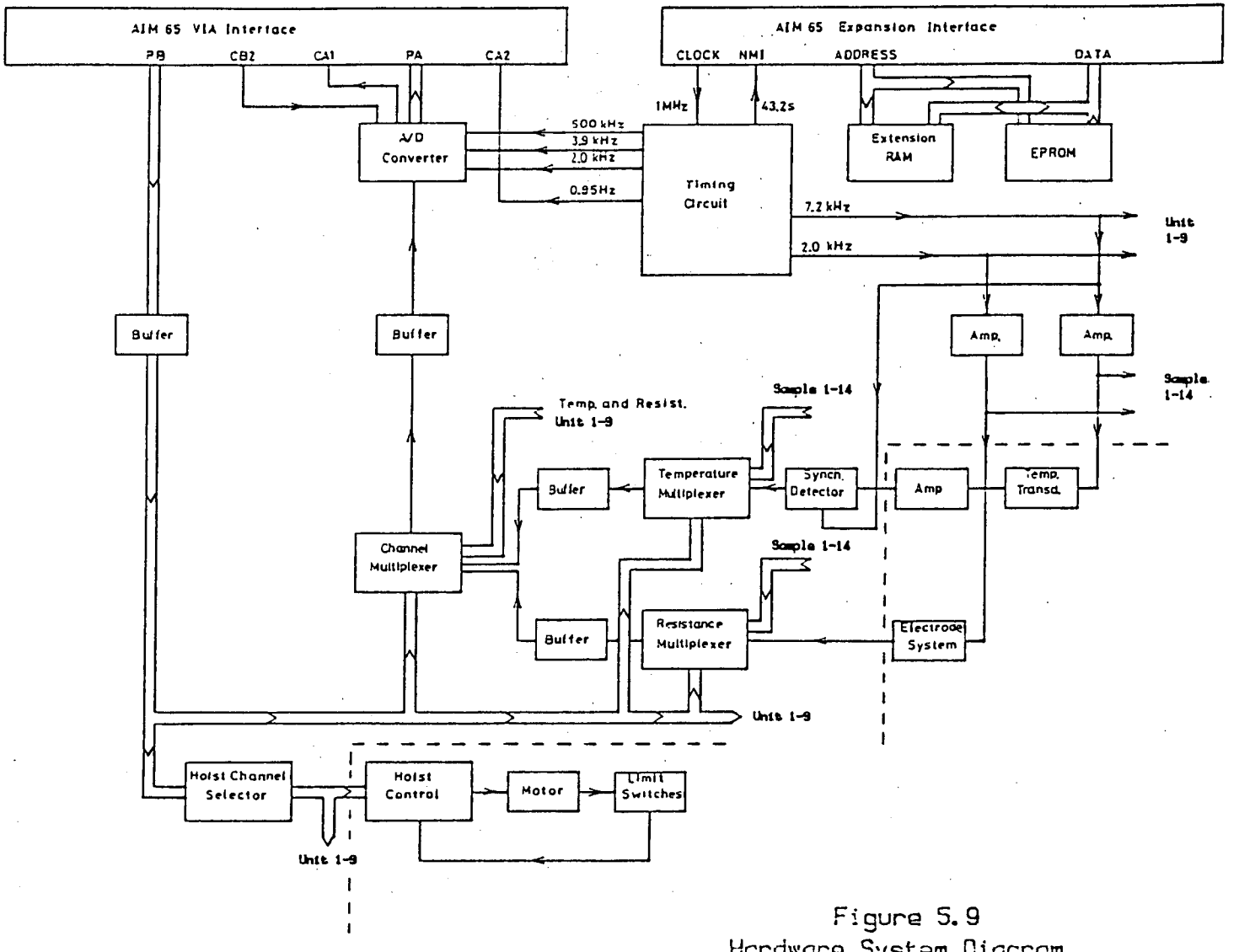

Figure 5.9
Hardware System Diagram

Timing Circuit. (Figure G.1)

The master timing signal for the system is the 1 MHz square wave signal derived from the crystal controlled clock signal for the AIM65. This signal is obtained at the AIM65 expansion interface. The 1 MHz signal is frequency divided in the timing circuit by a series of 4 bit binary counters. The first three counters are free running, and generate the following TTL signals:-

(i) 500kHz:- clock signal for the A/D converter

(ii) 7.81 kHz:- temperature energising signal

(iii) 3.91 kHz:- intermediate signal used in initiating A/D conversion

(iv) 1.95 kHz:- (2 kHz) resistivity energising signal

(v) 244 Hz:- intermediate output signal.

The intermediate output signal is fed to a further group of four 4 bit binary counters, only the first two stages of the last counter being used. These counters are gated to produce an output pulse from a JK flip flop every 43.2 s, with an accuracy of 1 in 10^4. The signal from the JK flip flop resets the counters. A NAND circuit is inserted in the output line to allow the output signal to be controlled by a voltage from a toggle switch. The output signal has a pulse width of 4.1 ms, and its period of 43.2 s corresponds to 0.0005 day. This is the basic timing interval for experiments. The 43.2 s signal is applied to the Non-Maskable Interrupt (NMI) terminal on the AIM65 expansion interface. This ensures that an interrupt will take place under all circumstances.

A signal at approximately 0.95 Hz is obtained from the second counter chain for use in calibration procedures. This signal is fed

to the AIM65 as the CA2 signal on the VIA interface.

The operation of the gating circuits controlling the second group of counters can be modified by the presence of a test control voltage. This reduces the period of the system timing signal to 0.432 s, and is useful for maintenance purposes.

Multiplexer. (Figure G.2)

The 2 kHz signal from the timing circuit is amplified and applied to one end of 16 reference resistors, corresponding to the series resistor in Figure 5.1. The other end of each of these resistors is connected to one of the sample electrodes, the other electrodes being connected to the 0V line. The amplitude of the 2 kHz square wave fed to the reference resistors is controlled by the collector voltages of two transistors connected as a complementary emitter follower. These voltages are controlled by an adjustable voltage stabiliser which gives complementary positive and negative output voltages. One of the reference resistors is not connected to a sample. Rather it is connected to a calibration resistor. Measurement of resistivity is carried out by comparing the voltage across each sample with the voltage across the calibration resistor. This makes the resistivity measurement independent of the voltage applied to the reference resistors.

The output voltage is symmetrical about 0 V to reduce possible polarization effects in the samples.

The voltages obtained at the junction of the reference resistors and the electrodes (or calibration resistor) are the output voltages. These are fed to a 16 way analogue multiplexer.

The required output is selected by the binary code on 4 address lines. These address lines originate at the AIM65 VIA interface PB output port, and are buffered. The output from the multiplexer is buffered by a non-inverting amplifier with approximately unity gain. The d.c. offset at the output of this amplifier can be adjusted by a potentiometer.

The 7.81 kHz energising signal for the temperature measurement is also generated in this circuit. The amplitude of the 7.81 kHz temperature energising square wave signal is controlled in the same way as the 2 kHz signal.

The outputs from the temperature rectifier unit are fed to another 16 way analogue multiplexer on this circuit, with the output selected by the same address lines as the resistivity multiplexer. The output of the multiplexer is buffered by a non-inverting amplifier with a gain of approximately two with an output d.c. offset adjustment.

This circuit has facilities to allow d.c. signals to be injected to allow setting of amplifier offsets.

High stability resistors with selection tolerance 0.1% are used where the component tolerance can affect system accuracy.

Figures 5.10 and 5.11 show the multiplexer circuit, and illustrate the form of construction of circuits in the electronics unit.

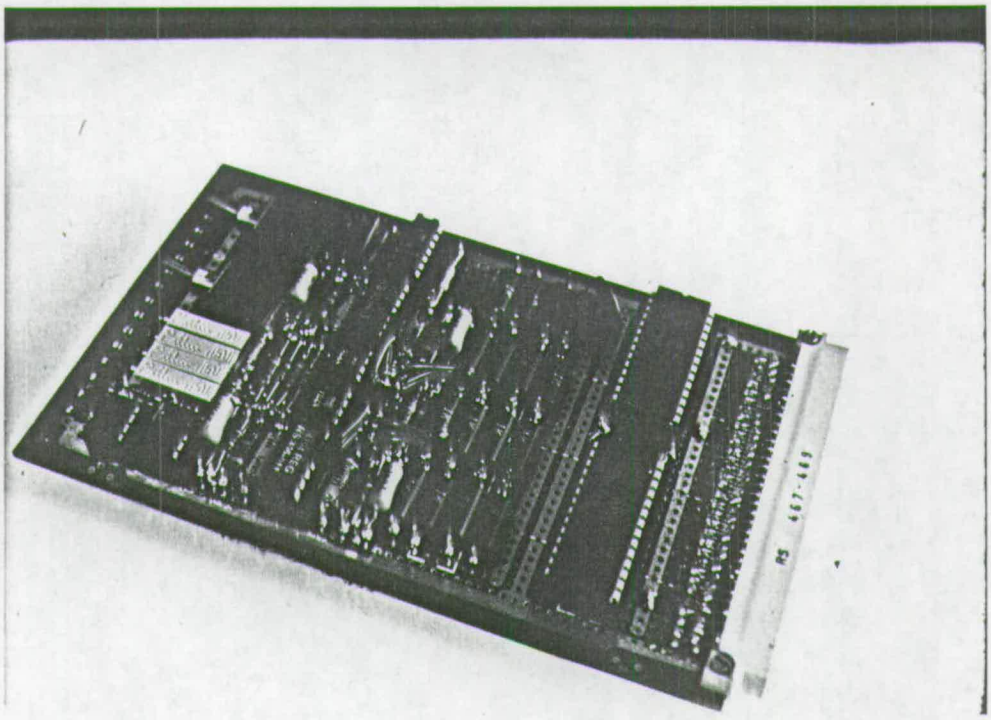

Figure 5.10
Multiplexer Circuit - Top

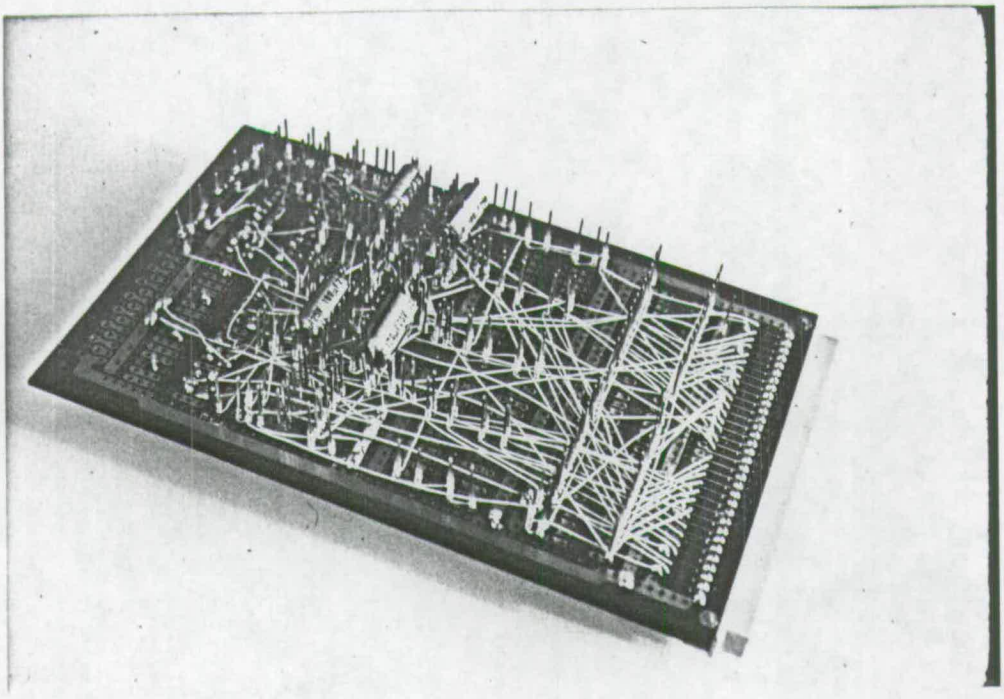

Figure 5.11
Multiplexer Circuit - Underside

Temperature Amplifiers. (Figure G.3)

Each sample has an associated platinum film temperature sensor and amplifier, which is of the form shown in Figure 5.4, and is energised by a controlled amplitude 7.81 kHz signal.

The amplifiers are mounted separately, as close to the samples as possible to reduce the possibility of pick-up.

Figure 5.12 shows a temperature amplifier unit.

Temperature Rectifiers. (Figure G.4)

The outputs of the temperature amplifiers are fed to synchronous detectors located in the electronics unit. These detectors consist of FET switches feeding storage capacitors. The switches are operated by a 7.81 kHz logic signal from the timing circuit.

Measurement of temperature is by comparison of the output due to a transducer with the output due to the calibration resistor, to ensure that the measurements are independent of the amplitude of the 7.81 kHz energising signal.

The signals are then fed to a multiplexer circuit.

A/D Converter. (Figure G.5)

The resistivity and temperature output signals from the multiplexer circuit are further multiplexed in the A/D converter circuit by means of an 8 way analogue multiplexer. The required output is selected by 3 digital address lines which originate from the AIM65 VIA interface PB output port. The other 6 analogue input lines to the multiplexer are available to allow an expansion of the

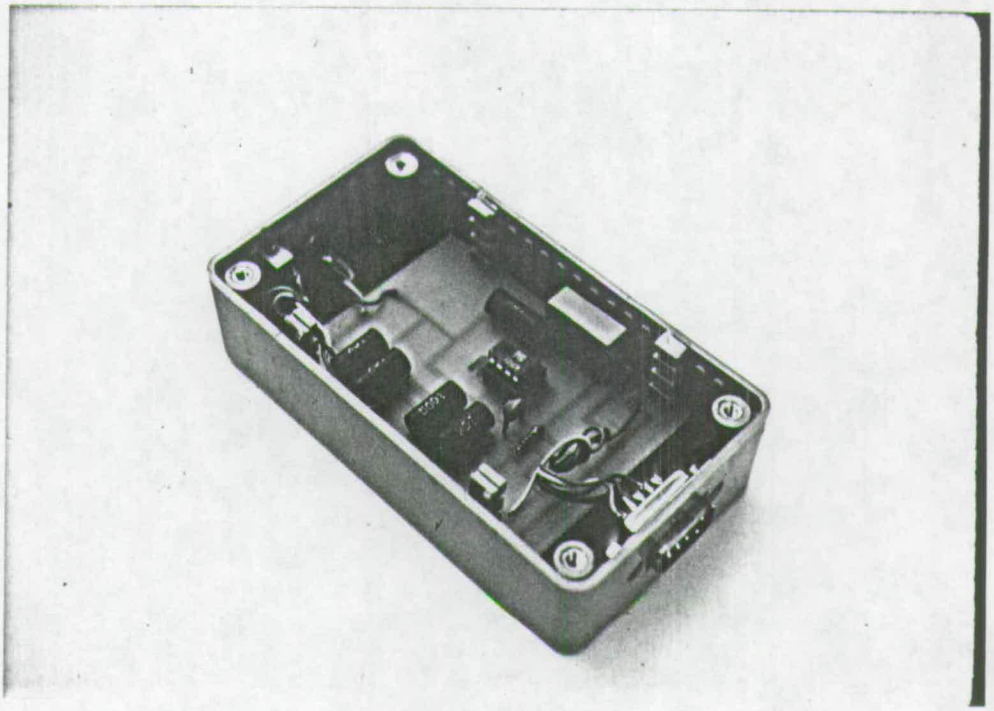

Figure 5.12
Temperature Amplifier Unit

number of samples from 15 to 60. The output of the multiplexer is buffered by a non-inverting amplifier which has a gain of approximately unity with adjustments for gain and d.c. output offset.

The output from the buffer amplifier is fed to a successive approximation 8 bit A/D converter with a conversion time of 15 us. The input to the A/D converter is limited to prevent damage. Since the input voltage is stable over the conversion time, a sample and hold circuit is not required.

A logic circuit with inputs from the timing circuit along with a control signal from the CB2 terminal of the AIM65 VIA interface unit controls the operation of the A/D converter, and ensures that measurements of resistivity are taken at the mid-point of the positive half cycle of the energising waveform as described in Appendix E.

The A/D converter generates a logic signal when conversion is complete. This signal is fed to the CA1 terminal of the AIM65 VIA interface unit. The 8 bit digital output of the converter is fed to the PA input port of the VIA.

Memory Extension. (Figure G.6)

This unit includes two 4k byte EPROMS which contain the operating program for the system. There are also facilities for two sections of 2k byte static RAM, used when developing the system program. These memory units are connected to the AIM65 through the expansion interface using the normal computer address and data lines.

Control Circuit. (Figure G.7)

The control circuit gives indication that power supplies are on, and an indication that 43.2 s timing signals are being transmitted to the computer, indication of test sequences being demanded on circuit boards, manual control of four hoists required for 60 samples, provision for injecting signals onto tests points for setting up amplifiers, including additional boards required to extend the number of samples from 15 to 60.

The 43.2 s timing signal is controlled by a toggle switch.

Control of the hoists is by multiple two channel digital multiplexers which allow control of the hoists for each group of 15 samples, by outputs from the PB port of the VIA interface of the AIM65, or by signals from push button switches supplying operate and stop signals, and by a toggle switch which controls hoist up/down movement. When an operate signal is demanded, the corresponding logic output changes from 1 to 0, a stop signal causes a change in the stop output from 0 to 1. The directional demand is 1 for up and 0 for down. Control of the multiplexer is by a +5 V signal from a toggle switch for normal operation, and 0 V for manual control. The switch also provides an input to the test monitor, giving a test indication when manual control is selected.

Hoist and Hoist Control Circuits. (Figures G.8, G.9)

The hoist consists of a NERCO Type DRD71 240 V a.c. two phase induction motor with capacitor start. The direction of rotation depends on the phase of the voltage to the start winding. The start winding is open circuited by an inertia switch when the motor has run up to speed. The motor is fitted with a disc brake which is released when the RUN winding is activated, ensuring that the motor will not run back when stopped under load. The normal running speed of 1425 r.p.m. is reduced by a worm gearing system to 1.06 r.p.m.

The motor drives a drum of diameter 127 mm, giving a rate of rise of the samples from the water bath of 7 mms^{-1}. The shaft is fitted with upper and lower limit cams which operate heavy duty microswitches at the upper and lower limits. Logic 1 (+5 V) signals are produced by the microswitches when the the limits are reached. The total lift of the hoist is 330 mm, which takes 0.8 min. A third microswitch is connected in series with the RUN winding of the motor. Should the hoist overrun the limit switches, this microswitch will switch off the motor, and prevent any damage. A toggle switch is connected in parallel with this microswitch to allow power to be reapplied, so that the motor can be driven back under manual control.

The hoist lifts a wooden tray carrying up to 15 samples, giving a combined mass of approximately 130 kg. Supports on the tray allow the samples to be inclined at 45°. This allows surface water to run off the samples before a measurement is taken. The samples are removed from the water bath approximately 5 min. before readings are taken, and are returned immediately afterwards.

The hoist control circuit controls power to the hoist in response to signals from the control unit in the electronics unit. Control of a.c. power is by an OPERATE relay which controls the RUN and BRAKE windings of the motor, and by an UP/DOWN relay which controls the START winding.

AIM65 Microcomputer.

The Rockwell AIM65 microcomputer is a low cost computer based on the 8-bit R6502 microprocessor. It has an accumulator, two index registers, uses 16 address lines, and is clocked at 1 MHz.

The microcomputer is fitted with 4k bytes of RAM and a versatile interface adapter (VIA) which has two 8 bit input/output ports. Port PA is used for input in this application, and port PB for output. The VIA also has 4 control lines, line CB2 is the output command line for A/D conversion, line CA1 is the conversion complete input signal, and line CA2 carries a 0.95 Hz signal used in setting up procedures. Line CB1 is not used.

The microcomputer has a keyboard, and electronic display, a dot matrix using a narrow paper roll, and facilities for loading and storing programs using an audio cassette recorder.

The software includes a monitor, editor, assembler, and BASIC interpreter.

Interfacing is by the VIA already described, however the computer address and data buses, and control signals, are available on an expansion interface. This is used for expansion RAM, the system EPROMs, to provide a 1 MHz clock pulse to the electronics unit, and also to initiate non-maskable interrupts (NMI).

The microcomputer has its own internal power supplies.

Power Supplies.

The power supply unit produces d.c. voltages of +5 V, ±15 V, and +12 V, for the electronics unit, hoist control unit, and temperature amplifiers.

5.3.2. Software.

The system software is designed to control the experiments and to print output data when required. For experiments lasting more than 1 day, after which the samples must be stored under water, the software controls the hoist which removes the samples from the water bath.

For the initial system with the capability of measuring up to 15 samples, the samples can be arranged as 15 separate experiments, or as one experiment with 15 samples, or any intermediate arrangement. An experiment can be started or stopped in the presence of other experiments.

Once hardening has started, initial changes in resistivity are rapid, but the rate of change slows as the experiment progresses. The measurement sequence used is therefore a logarithmic sequence based on decades measured in days. 5 measurements are carried out in each decade, the sequence being 1.5, 2.5, 4, 6.5, and 10. The first decade starts at 0.0015 days, and the last measurement is at 100 days.

Information regarding individual experiments is held in a timetable which is arranged in the order in which measurements are

to be carried out, the next measurement to be taken having the lowest position in the timetable, and the latest measurement the highest position. As measurements are carried out, experiments are reinserted into the timetable in the correct position for the next measurement.

Data regarding each experiment is held as 6 bytes of information within the table. These bytes contain the following information:-

byte 1 - next measurement time; two most significant decimal digits

byte 2 - next measurement time; two median decimal digits

byte 3 - next measurement time; two least significant decimal digits

byte 4 - position of first sample of the experiment

byte 5 - number of samples in experiment

byte 6 - time code for next measurement

Control of the timetable, addressing the multiplexers, transfer of data from the A/D converter, and control of the hoist, are carried out by machine code programs. System control, calculation of results, and control of the printer and electronic display, are by BASIC programs. Both forms of program are stored on 2 4 kbyte EPROMs.

The software provides the following facilities:-

(i) initiation of new experiments and removal of old

(ii) measurement of an experiment sample set, on demand, to supplement automatic measurements

(iii) monitoring of any output available from the A/D converter on the electronic display

(iv) monitoring of the calculated temperature of any sample on the electronic display

(v) operation of the hoist on demand from the computer keyboard

(vi) print out of the list of experiments in the system, and the number of samples in each

(vii) print out of the current system time

(viii) correction of system time

Figure 5.13 is a program system diagram. The different functions indicated can include both BASIC and machine code segments.

Most of the running time is concerned with the Control program. When experiments are being fed into the system, the route is Control, Keyboard, Input, Measurement Indicator, Hoist, Display, and return to Control. When the system is running normally, a timing pulse resulting in a non-maskable interrupt (NMI), will cause the system to take the path Control, Clock, Measurement Indicator, Hoist, Display, and return to Control. If at that time a measurement is required on any particular experiment, then the path also includes the Output program.

In general the system will eventually return to the Control program following a branch into another routine. In the case of interrupt routines, the system will return to the next instruction in the routine in which the system was running prior to the interrupt.

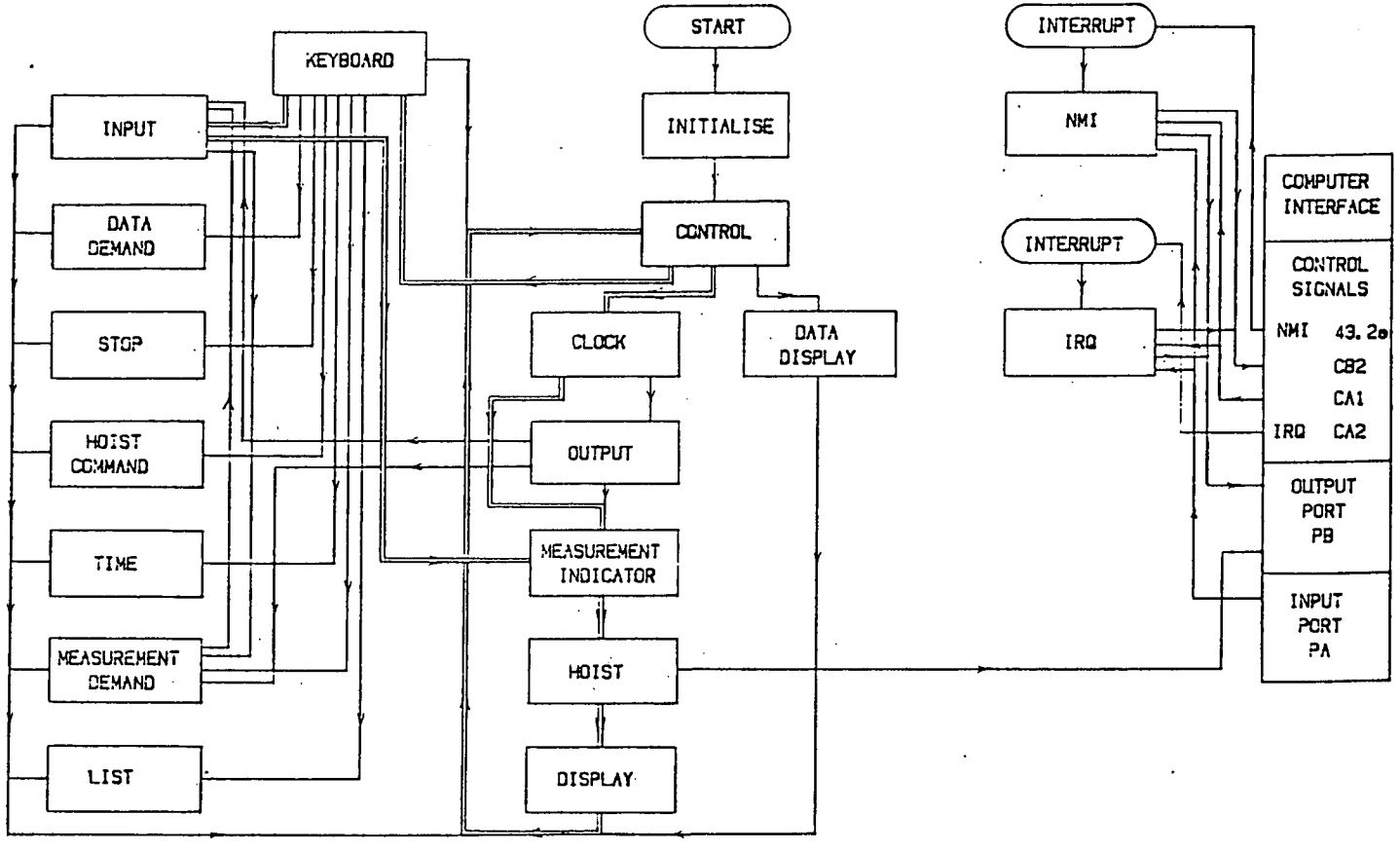

Figure 5.13
Program System Diagram

The system is brought into operation by typing the START sequence on the computer keyboard. This results in the Initialization program being entered.

Initialization.

Counters are initialized in both BASIC and machine code programs, and constants are set. The time of day (hrs. min. sec.) at which the system is to be started is fed into the system, and the operator instructed to close the switch which enables timing impulses with period 43.2 s at the correct time.

The system then jumps to the Control program.

Control.

This forms a loop in which 3 indicators are monitored. These indicators are:-

(i) the NMI indicator which shows that a 43.2 s timing pulse has been received, and causes a jump to the Clock program,

(ii) the keyboard indicator which shows that the space bar on the computer keyboard has been depressed, and causes a jump to the Keyboard program,

(iii) the data indicator which indicates that a 0.95 Hz impulse has been received when the system is in the the data demand mode, and causes the system to jump to the Data Display program.

Clock.

The system time is updated as a result of the NMI condition and the NMI indicator is reset. The measurement indicator is monitored. If this gives a positive indication then measurement data must be outputted and the system jumps to the Output program. If no output is required, the system jumps to the Measurement Indicator program.

Output.

The system time is printed out. The resistivity, temperature, and corrected resistivity for all samples in the experiment undergoing measurement are calculated and printed out. The data required for these calculation has already been obtained by the NMI program if the measurement indicator has been set. The measurement indicator is then reset. The output data is in the form shown in Table 5.1:-

```
00.0200
UNIT TIME 00.0015

0/00
127.8 45.6 199.8

0/01
127.8 45.6 199.8

0/02
127.8 45.6 199.8

0/03
127.8 45.6 199.8
```

Table 5.1
Output Format

UNIT TIME indicates the time in days for which the experiment

has been running. 0/00 indicates that the following three numbers refer to sample 00 in unit 0. For this sample, the resistivity is 127.8 Ωm, the temperature is 45.6 °C, and the corrected resistivity is 199.8 Ωm. 0/01 indicated that the next three numbers refer to sample 01 in unit 0.

If the measurement has been carried out because of the Measurement Demand program, then a jump is made to this program. If the measurement is a routine measurement on an experiment, then the next measurement point for that experiment is set. If all measurement points have been completed then a jump is made to the Input program so that the experiment can be deleted. If further measurements have to be made, the next measurement time is calculated, and is then placed in the entry for this experiment on the timetable; this will be the first experiment in the timetable, the timetable is then reshuffled so that the experiment appears in its correct position for the new measurement time.

The system then jumps to the Measurement Indicator program.

Measurement Indicator.

If there are no experiments on the timetable, the system jumps to the Hoist program.

The measurement time of the first experiment on the timetable is monitored. If this corresponds to the time when the next system timing pulse is received, then the measurement indicator is set.

The system jumps to the Hoist program.

Hoist.

The normal condition for the hoist is in the down (sample immersed) condition.

The hoist demand commands set up by the Hoist Command program are set, and if there are no experiments on the timetable, the system jumps to the machine code sequence which operates the hoist.

If there are experiments on the timetable, then the measurement times of all experiment which require measurement within the next five timing intervals are monitored. If the experiment time for any experiment is less than one day, or if a hoist disable indication is given for the experiment on the timetable, then no action is taken. If the measurement time for an experiment is less than five timing intervals, then an up demand is set. The machine code segment which controls the hoist according to the demand condition set is then entered, operating the hoist if required.

The system jumps to the Display program.

Display.

If the system is in the data monitor mode, the system returns to Control.

If the system is not in data monitor mode, then the system time, the start sample of the next experiment to be measured, and the time of that measurement are displayed on the electronic display with the format:-

00.0195 0/00 00.0200

where 00.0195 is the system time in days, 0/00 indicates that the next experiment to be measured is in unit 0, and starts at sample 00, and 00.0200 is the system time at which this measurement will take place.

If there are no experiments on the timetable, then the format is:-

00.0195 0

where 00.0195 is the system time.

The system returns to Control.

Keyboard.

The Keyboard program is entered if the keyboard monitor indicator is set in the Control program showing that the spacebar on the computer keyboard has been depressed.

The system time is printed out and the operator indicates which program is required by typing in a single letter:-

I - Input
D - Data Demand
S - Stop
H - Hoist Demand
T - Time
M - Measurement Demand
L - List

The system jumps to the program selected. If a key which does not correspond to one of these letters is depressed, then the system returns to the Control program.

Input.

The operator indicates whether a new experiment is being inputted, or if an existing experiment is to be deleted. If an experiment is to be deleted, then the system jumps to the delete section of the program.

For a new experiment, the operator supplies the following data:-

(i) sample start position for experiment

(ii) number of samples in the experiment

(iii) whether or not the hoist is to be disabled

(iv) the time elapsed since water was added to the mix

The first measurement point for the experiment is calculated. If a point cannot be found the system assumes an error and returns to Control. If there is no error, then the time at which the first measurement is to take place is calculated, the timetable is altered to leave a blank position at the first position, and the data for the experiment is entered at that position. The timetable is then reshuffled to place the experiment in its correct position on the timetable.

The system jumps to the Measurement Indicator program.

If the delete section of the Input program is entered, the operator provides the start location of the experiment, and indicates the number of samples to be deleted; all the samples can be deleted.

The timetable is searched until the experiment is found, and if not all samples are to be deleted, the number of remaining

samples is set on the timetable, and the system returns to Control.

If the experiment is to be deleted completely, then the data for the experiment is removed from the timetable, and the timetable adjusted to remove the space.

If the delete operation is due to a measurement demand sequence, then the system jumps to the Measurement Demand program, if the delete operation is because the last measurement in the sequence has been completed, then the system jumps to the Measurement Indicator program, otherwise the system returns to Control.

Data Demand.

The operator indicates whether an existing data demand sequence is to be deleted, or if a new sequence is to be initiated. If a sequence is to be deleted, then the data demand indicator is reset, and the interrupts generated by the CA2 control line are disabled. The system then returns to Control.

If a new sequence is to be initiated, the operator indicates what data is to be displayed. The command is of the form OR04, ORR, OT04, OTR, indicating resistitivity in unit 0 sample 04, unit 0 resistivity reference, temperature in unit 0 sample 04, and unit 0 temperature reference respectively.

If temperature data is demanded, the operator requests either A/D output or calculated temperature output.

A data demand indicator is set with a value which depends on whether unmodified A/D converter data has been requested, or calculated temperature data. Interrupts are enabled in the computer

system using the normal interrupt request signal (IRQ). The IRQ is activated by a transition on the CA2 control line at the VIA. This is fed by a 0.95 Hz signal from the timing circuit.

The system returns to Control.

Stop.

The system is brought to a halt in an orderly fashion by a BASIC PAUSE statement. The system can be restarted by depressing the CONTINUE key on the computer keyboard. The system then returns to Control.

Hoist Command.

The operator directs which hoist is to be affected, and then indicates whether the hoist is to be raised or lowered. A lower command returns the system to the normal operating mode where the position of the hoist depends on the measurements which are to be made. The program sets the correct demand indicator for raise or lower.

The system returns to Control.

Time.

The operator feeds in the correct current time in hrs. min. and secs. The computer then calculates the correct system time from old system time, old start time, and current time, and resets to the correct system time.

The system returns to Control.

Measurement Demand.

If there are no experiments on the timetable, the system returns to Control.

If there are experiments present, the operator feeds the unit and the position of the first sample of the experiment. The program then locates the experiment on the timetable, and stores all the data on the experiment from the timetable. The experiment is then deleted, and then reinserted with the earliest possible measurement time depending on whether or not the hoist must be operated, and the measurement time of the first experiment on the timetable. The measurement demand indicator is set, and the system jumps to the Input program where the reinsertion of the experiment is carried out.

Once a demanded measurement has been made, the system returns to the Measurement Demand program from the Output program. The measurement demand indicator is incremented, and a command is set to delete the experiment from the timetable. The system then jumps to the delete section of the Input program.

The experiment having been deleted, a return is made to the Measurement Demand program. The measurement time for the experiment is reset to the original value which was stored. The measurement demand indicator is reset.

The system jumps to the Input program to reinsert the experiment in the timetable with the original information.

List.

The system checks the number of experiments, and returns to Control if there are none.

If there are experiments, the start location and number of samples for each experiment are obtained from the timetable, and printed out according to the format:-

0/00 4

This indicates that there is an experiment in unit 0 which starts at sample 00, and consists of four samples, i.e. 00, 01, 02, and 03.

The system returns to Control.

Data Display.

If the data state indicator is 1, the system outputs data from the A/D converter which has already been obtained by the IRQ program. The data is outputted on the electronic display using the format:-

00.0505 D OR00 240.

where the first number is the system time in days, D indicates that a data demand sequence is in operation, OR00 indicates that the data presented is in unit 0, is resistivity data, and refers to sample 00. 240 is the value of the A/D converter output. For a temperature value, R would be replaced by T, and if the sample

number 00 is replace by R, this indicates a reference output.

The data monitor indicator is reset, and the system returns to Control.

If the data state indicator is 2, a temperature calculation has been demanded, and the temperature output for the sample has been obtained. This value is stored, the data state indicator set to 3, the data monitor indicator reset, and the system returned to Control.

If the data state indicator is 3, a temperature reference measurement has just been made. This data is combined with the temperature data obtained previously from the required sample to calculate temperature. The data state indicator is set to 2.

The calculated temperature data is outputted on the electronic display using the format:-

00.0080 D 0T00 45.6

where 00.0080 is the system time in days, D indicates a data demand sequence is in operation, 0T00 indicates a temperature measurement on sample 00 in unit 0. 45.6 is the calculated temperature in ^{o}C. The digit following the decimal point indicates that this is a calculated temperature.

The data monitor indicator is reset, and the system returns to Control.

NMI Interrupt.

Accumulator and registers are saved. A memory location containing the number of unserviced timing pulses is incremented. If the measurement indicator is not set, the accumulator and registers are restored, and the system returns from the interrupt.

If the measurement indicator is set, address data on the particular sample to be measured is fed to the electronics unit by the VIA, and the A/D converter activated. Data is supplied by the A/D converter to the VIA for resistivity and temperature of each sample in the particular experiment, and also for the resistivity and temperature references. The accumulator and registers are restored, and the system returns from the interrupt.

IRQ Interrupt.

The accumulator and registers are saved. Address information for the data to be obtained is passed to the electronics unit by the VIA, and the A/D converter activated. Data from the A/D converter is fed to the computer by the VIA. The data measurement indicator is set, and the accumulator and registers are restored.

The system returns from the interrupt.

5.3.3. Environmental Control.

Long-term storage of samples is under water. The bath used consists of a large fibreglass tank which can accommodate two trays each with fifteen samples, and which is linked to a small subsidiary tank by inlet and exit pipes. This tank is fitted with a 3 kW

electric heater. A pump is fitted in the inlet pipe which is of small diameter. The exit pipe is of large diameter. Both pump and heater are operated by a mains contactor, which is in turn controlled by a thermostat with an immersed temperature sensor in the main tank. If the water temperature in the main tank falls below 20°C, the contactor closes, causing warmer water to be circulated through the main tank. The temperature differential between the operate and release points for the thermostat is a fraction of a degree.

5.3.4. Data Output and Graph Plotting.

The data output from the AIM65 is printed on a paper roll of width 57 mm by a dot matrix printer, as the measurements are taken. Thus, if there are a number of experiments on the system, the data for the different experiments will be interlaced on the print-out.

A set of programs has been developed for the Hewlett-Packard HP85 computer system which allows the output data on the print out to be transcribed manually from the paper roll, into the HP85. The data is inputted in time sequence, including interlacing of readings for different experiments. The HP85 programs then give a print-out of complete results experiment by experiment. These programs also allow the data for individual experiments to be recorded on a magnetic tape cassette, and the automatic plotting of graphs of resistivity against time for completed experiments.

The graphs are plotted on a logarithmic time scale with two decades from 0.01 to 1 day, or with four decades from 0.01 to 100

days. Results can be plotted for a single sample in an experiment, or for the average values of all the samples in an experiment. In this case, the symbol I is used to indicate the average value. The average values is indicated by the position of the mid-point of the vertical line, and the length of this line indicates the 95% confidence limits on the average value. If the required height is less than the width of the horizontal bars, the symbol is replaced by +. If there are three or less samples in the experiment, the average indication is replaced by individual points, each sample being indicated by an identifying symbol.

Figure 5.14 is an example of tabulated data output from the HP85, and Figure 5.15 is an example of a resistivity graph.

5.4. Calibration and Accuracy.

Measurements of output for both the active channel and a reference channel are carried out for resistivity and temperature measurements. The calculated values of resistivity and temperature depend on the ratio of the two measurements. This will result in good long term stability of the system.

```
DATE 3-2-82
START 0:00          NUM 5
WATER:CEMENT 0.5:1
CEMENT:SAND:AGGREGATE 1:1.5:3
TEMP COEFFICIENT 0.022

SAMPLE NUMBER  1
    TIME      RES    TEMP    C RES
 0.0400       6.6    16.7      6.1
 0.0650       6.3    17.6      6.0
 0.1000       6.6    18.4      6.4
 0.1500       6.9    18.5      6.8
 0.2500       7.5    19.4      7.4
 0.4000       9.5    19.3      9.4
 0.6500      15.0    19.5     14.8
 1.0000      22.0    20.2     22.1
 1.0315      32.2    20.7     32.7
 1.5000      28.0    18.4     27.0
 1.9995      32.8    19.5     32.4
 4.0000      42.5    14.5     37.4
 5.0015      43.9    16.8     40.8
 6.5000      43.9    17.3     41.3
 7.2290      41.8    22.2     43.0
 9.2330      37.9    23.4     40.7
12.0035      49.8    17.4     47.0
13.2165      45.7    20.2     45.9
14.2250      49.8    19.9     49.7
15.0000       0.0     0.0      0.0
16.3475       0.0     0.0      0.0
20.2905       0.0     0.0      0.0
23.1055       0.0     0.0      0.0
25.0000       0.0     0.0      0.0
28.1005       0.0     0.0      0.0
```

Figure 5.14
Tabulated Data Output

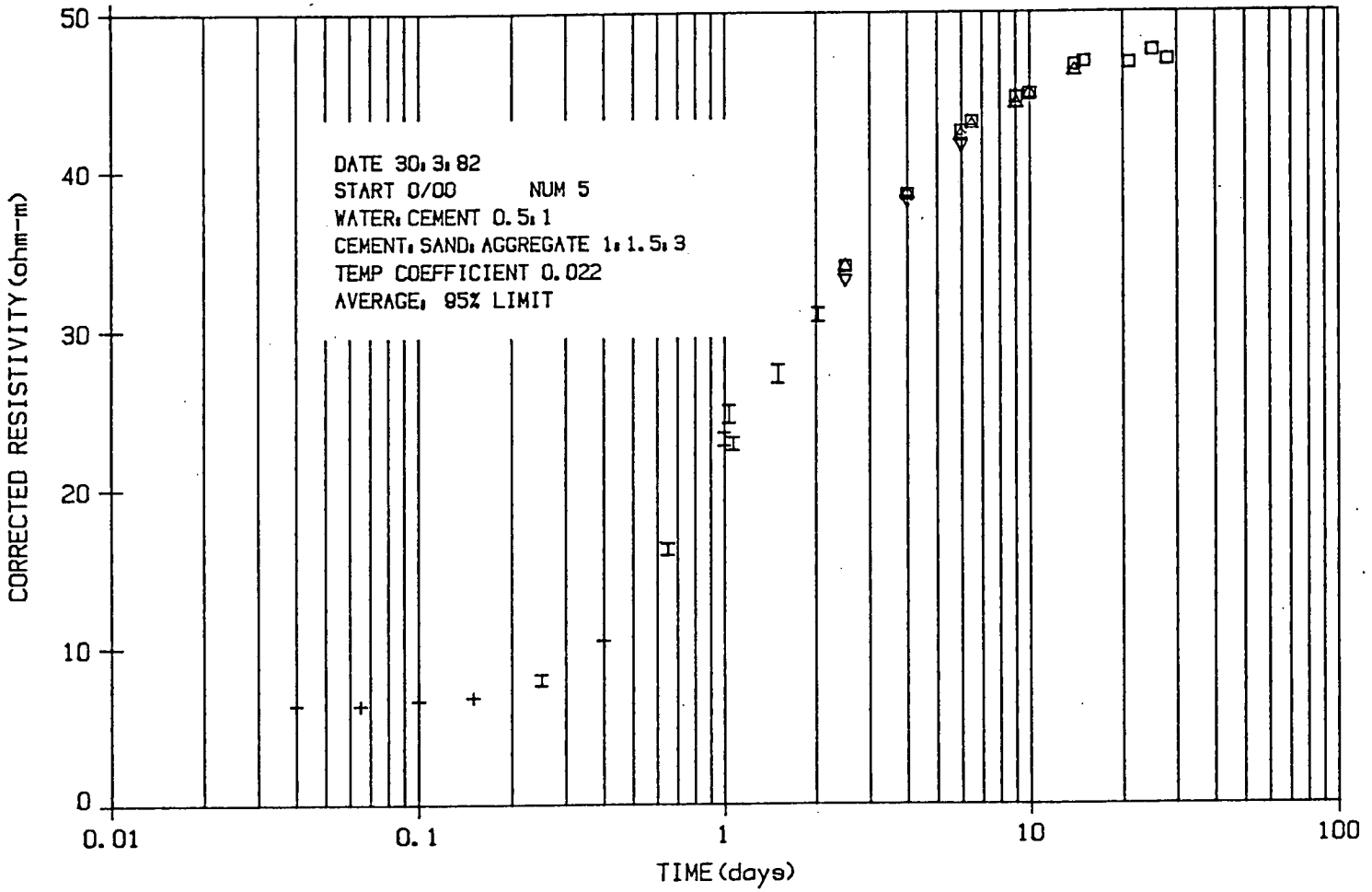

Figure 5.15
Resistivity Graph

5.4.1. System Parameters.

A/D Converter.

The A/D converter has an operating voltage range 0 - 2.5 V, and has 256 levels. One level therefore corresponds to 9.7656×10^{-3} V. Least error is obtained if the digital output is assumed to correspond to the mid-point of a given output level range. The input voltage to the A/D converter due to a digital output N where $0 < N < 255$ is therefore given by:-

$$V_o = 9.7656 \times 10^{-3}(N+0.5)$$

The reference voltages required in both the resistivity and temperature measurement systems are assumed to give digital outputs N = 235. Thus:-

$$V_{or} = 2.2998 \text{ V}$$

Resistivity System.

The input to the A/D converter from the resistivity measurement system is from Expression E.2 :-

$$V_o = \frac{R_s}{R_r + R_s} V_r G \qquad \text{(E.6)}$$

where R_s = Resistance of sample (Ω)

R_r = Resistance of reference resistor (Ω)

= 1 kΩ

V_r = Reference voltage applied to reference resistor (V)

G = Voltage gain through resistivity multiplexer

= 1

The maximum value of resistivity to be measured is 150 Ωm, which corresponds to a resistance of 1 kΩ for a 150 mm cube. This must produce an input of 2.5 V to the A/D converter. Thus:-

$$V_r = \frac{R_r + R_s}{R_s} \quad \frac{V_o}{G}$$

= 5V

Thus V_r must be 5 V peak or 10 v peak to peak.

Also from Expression 5.6

$$V_{or} = \frac{R_c}{R_r + R_c} \; V_r G \qquad (5.7)$$

where R_c = calibration resistance (Ω)

From Expressions 5.6 and 5.7

$$V_o = V_{or} \frac{R_s}{R_r + R_s} \cdot \frac{R_r + R_c}{R_c}$$

giving

$$R_s = \frac{R_r}{\frac{R_r + R_c}{R_c} \; \frac{V_{or}}{V_o} - 1}$$

From Expression 5.7

$$R_c = \frac{R_r}{\frac{V_r}{V_{or}} - 1}$$

$$= 851.72\ \Omega$$

Thus from Expression 5.8

$$R_s = \frac{10^3}{\frac{10^3 + 851.72}{851.72}\ \frac{V_{or}}{V_o} - 1}$$

$$= \frac{10^3}{2.1741\ \frac{V_{or}}{V_o} - 1} \qquad (5.9)$$

and from Expression 5.1

$$\rho = R_s l$$

where ρ resistivity (Ωm)

l = length of side of cube (m)

= 0.15 m

Thus

$$\rho = \frac{150}{2.1741\ \frac{V_{or}}{V_o} - 1} \qquad (5.10)$$

Temperature System.

The input to the A/D converter from the temperature measurement system is from Expression 5.2 :-

$$V_o = \frac{V_r}{1 + \frac{2R_2}{R_1}} \left(\frac{R_2}{R_T} - 1\right) \qquad (5.11)$$

where R_T = Resistance of temperature sensor (Ω)

R_1 = 10 kΩ

R_2 = 100 Ω

V_r = Reference voltage applied to temperature amplifiers (V)

G = Voltage gain through temperature multiplexer = 2

Thus

$$V_o = \frac{V_r}{0.51} \left(\frac{100}{R_T} - 1\right) \qquad (5.12)$$

For the temperature sensor (RS type 158-283 [72]), when the temperature is 0 °C, R_T = 100 Ω and V_o = 0 V. The maximum temperature to be measured is 50°C. The resistance of the sensor at this temperature is 119.39 Ω. The voltage input to the A/D converter at this temperature must be +2.5 V.

Thus

$$V_r = \frac{0.51\ V_o}{\frac{100}{R_T} - 1}$$

$$= -7.851\ V$$

The negative sign occurs because of a 180° phase difference between the reference voltage and the output voltage. V_r must be 7.851 V peak, or 15.702 V peak to peak.

Also from Expression 5.12 :-

$$V_{or} = \frac{V_r}{0.51}\left(\frac{100}{R_c} - 1\right) \qquad (5.13)$$

where R_c = calibration resistance (Ω)

From Expressions 5.12 and 5.13

$$V_o = V_{or}\frac{\left(\frac{100}{R_T} - 1\right)}{\left(\frac{100}{R_c} - 1\right)}$$

giving

$$R_T = \frac{100}{\left(\frac{100}{R_c} - 1\right)\frac{V_o}{V_{or}} + 1} \qquad (5.14)$$

From Expression 5.13

$$R_c = \frac{100}{0.51 \frac{V_{or}}{V_r} + 1}$$

$$= 117.56\ \Omega$$

remembering that V_r is negative.

Thus from Expression 5.14

$$R_T = \frac{100}{1 - 0.1494 \frac{V_o}{V_{or}}} \qquad (5.15)$$

From Expression 5.5 :-

$$T = \frac{1}{\alpha}\left(\frac{R_T}{100} - 1\right)$$

Substituting from Expression 5.15 gives

$$T = \frac{1}{\alpha} \frac{0.1494 \frac{V_o}{V_{or}}}{1 - 0.1494 \frac{V_o}{V_{or}}}$$

$$= \frac{38.81 \frac{V_o}{V_{or}}}{1 - 0.1494 \frac{V_o}{V_{or}}} \qquad (5.16)$$

since $\alpha = 3.85 \times 10^{-3}\ /^oC$.

Corrected Resistivity.

The resistivity corrected to 20 ^{o}C is given by :-

$$\rho_{20} = \rho_T(1 + \alpha_c[T - 20]) \qquad (5.17)$$

where ρ_T = resistivity at temperature T ^{o}C (Ωm)

α_c = temperature coefficient of resistivity of concrete ($/^{o}C$)

= 0.022 $/^{o}C$

Thus

$$\rho_{20} = \rho_T\ (1 + 0.022[T - 20]) \qquad (5.18)$$

5.4.2. Calibration Procedures.

Calibration procedures require the following equipment:-

(i) Noise free variable d.c. source e.g. Time Electronics D.C. Voltage Potentiometer 2003N

(ii) High accuracy d.c. digital voltmeter e.g. Data Precision Type 2540A1

(iii) Digital thermometer e.g. Technoterm 5500 with immersion probe

(iv) A container of cold water into which the electrodes with temperature sensors can be placed without the sensors being immersed

The data demand program allows the output of the A/D converter to be monitored on the electronic display, and also allows the calculated temperature obtained from any temperature transducer to

be displayed.

A/D Converter.

1. Put the test switch for the A/D converter to the TEST state.
2. Monitor A/D converter output using the D program to monitor OR00.
3. Inject +9.766 mV at the input test point.
4. Adjust offset potentiometer RV_1 to give equal times at 000 and 001 on the display
5. Inject +2.490 V at the input test point.
6. Adjust gain potentiometer RV_2 to give equal times at 254 and 255 on the display.
7. Repeat 3 - 6 until satisfactory.
8. Return the A/D test switch to NORMAL.

Multiplexer - Resistivity.

9. Monitor A/D converter output using the D program to monitor ORR.
10. Adjust RV_1 on the multiplexer to give equal time between 234 and 235 on the electronic display.
11. Note the position of the potentiometer control, and adjust RV_1 to give equal times between 235 and 236, noting the increment required in the control position.
12. Reverse the position of the control on RV_1 by half the total increment.
13. Monitor the A/D converter output using the D program to

monitor OR00.

14. Short circuit the resistivity banana plug connectors on the lead for sample OR00.

15. Adjust RV_3 on the multiplexer to give equal time between 000 and 001.

16. Put the resistivity test switch to the TEST state.

17. Inject a d.c. voltage at the resistivity multiplexer test point such that the indication has equal time at 001 and 002.

18. Adjust RV_3 to give equal time between 000 and 001.

19. Return the resistivity test switch to the NORMAL state.

Multiplexer - Temperature.

20. Monitor A/D converter output using the D program to monitor OTR.

21. Adjust potentiometer RV_2 on the multiplexer to give equal times at 234 and 235 on the electronic display.

22. Note the position of the control, and adjust RV_2 to give equal times at 235 and 236, noting the increment in the control position required.

23. Reverse the position of the control on RV_2 by half the increment.

24. Monitor the A/D converter output using the D program to monitor OT00.

25. Put the temperature test switch on the multiplexer to the TEST position.

26. Inject a d.c. signal of +9.766 mV at the temperature test point.

27. Adjust RV_4 on the multiplexer to give equal times at 000 and 001.

29. Return the test switch to the NORMAL position.

Temperature Amplifiers.

30. Place all 0 V electrodes in a draught free water bath at a temperature of approximately 20 ^{o}C. (water must not cover the temperature transducers and sockets).

30. Connect all transducer temperature output sockets to the corresponding temperature amplifiers.

31. Measure the temperature of the water in the water bath using the digital thermometer.

31. Monitor the temperature outputs using the D program for values OT00 to OT14 in turn, using the CALCULATE mode.

33. Adjust RV_1 on the temperature amplifier for the corresponding transducer (OT00 to OT14) until the indicated temperature on the electronic display is as near the measured temperature as possible.

5.4.3 Accuracy.

General.

All uncertainties will have a statistical distribution about the required value, and the form of the distribution will depend on the nature of the uncertainty. Only two forms of distribution will be considered; the uniform distribution, and the normal distribution.

For a uniform distribution over the interval ±I, the standard deviation is

$$\sigma = 0.577I$$

Using the method followed by Hermach [73], for accuracy limits ±I, and assuming a normal distribution, the standard deviation will be approximately

$$\sigma = 0.333I$$

When a process involves the sum of a number of quantities each having an uncertainty, the standard deviation of the overall uncertainty is given by

$$\sigma = \sqrt{\sum_{K=1}^{N} \sigma_K^2}$$

where σ_k = individual standard deviations

N = the number of uncertainties being summed

assuming that the variables are uncorrelated.

Having obtained the standard deviation of the overall uncertainty, it is neccessary to know the distribution of the

overall uncertainty before the limits of uncertainty can be obtained. The central limit theorem states that as the number of random processes added increases, the overall distribution tends to the normal distribution no matter what the distribution of the individual components are. Assuming in this case that there are always sufficient individual processes to give a normal distribution, the limits of uncertainty due to overall standard deviation σ_T will be approximately

$$I = \pm 3\sigma$$

A number of factors which might contribute to the overall uncertainty of the system have been considered, and have been found to be negligible. These factors are:-

(i) multiplexer ON resistance

(ii) amplifier open loop gain

(iii) amplifier common mode rejection ratio

(iv) effect of temperature variations on resistance values

(v) slew rates of amplifiers

(vi) settling times of multiplexers

(vii) input offset voltage and current drifts of amplifiers

Note:- This would not have been the case for temperature amplifiers if d.c. excitation had been used for the transducers.

Resistivity

A/D Converter

Since the gain of the buffer amplifier used in the A/D converter circuit is set during setting up procedures, the tolerance on components in the circuit will have no effect on the system.

There will be an error due to quantisation which will apply to both measured voltages and the reference voltage. An error will occur both due to zeroing and to gain setting. The uncertainty limits will be ±0.5 LSB (least significant bit) of the A/D converter. Assuming a uniform distribution, and allowing for two measurements during setting up gives:-

standard deviation of uncertainty in output voltage

$$\sigma_o = 3.985 \times 10^{-3} \text{ V}$$

standard deviation of uncertainty in output reference voltage

$$\sigma_{or} = 3.985 \times 10^{-3} \text{ V}$$

The accuracy of the digital voltmeter specified in Section 5.4.2 is sufficiently high not to affect the accuracy of the system.

Multiplexer.

The resistivity multiplexer has an amplifier circuit of the form shown in Figure 5.16. The gain of this amplifier is nominally unity, but will depend on resistors R_1 and R_2 , and tolerances on these resistors will cause an uncertainty in the output voltage. Differentiating the gain expression for this circuit with respect to R_1 and R_2 gives for infinitely small changes:-

$$\Delta V_o = \left\{ - \frac{R_2}{R_1} \frac{\Delta R_1}{R_1} + \frac{R_2}{R_1} \frac{\Delta R_2}{R_2} \right\} V_o$$

Assuming that the tolerance on the resistors is +10%, and that this is normally distributed, the standard deviation in output voltage due to these uncertainties will be

$$\sigma_o = 6.925 \times 10^{-4} V_o$$

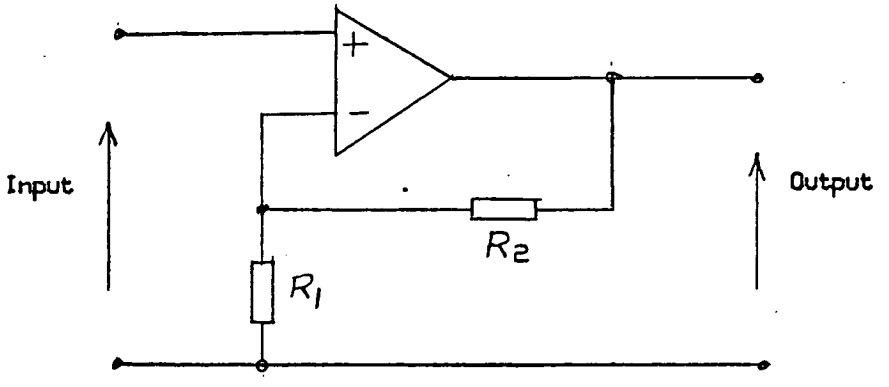

Figure 5.16
Non-Inverting Amplifier

The crosstalk between inputs to the multiplexer is 75 dB. Assuming that the input voltages are uniformly distributed over the range 0 - 2.5 V, gives a standard deviation due to 15 inputs of 9.94×10^{-4} V.

The setting up procedure again requires that certain outputs be obtained from the A/D converter, resulting in an error of ±0.5 LSB, producing a standard deviation at the output of 2.817×10^{-3} V.

Combining these uncertainties gives an overall standard deviation for the output voltage of

$$\sigma_o = \sqrt{(6.925 \times 10^{-4} V_o)^2 + 8.923 \times 10^{-6}}$$

The standard deviation in the reference voltage where $V_{or} = 2.2998$ V will therefore be 3.385×10^{-3} V.

Reference Resistor.

The reference resistor in the circuit shown in Figure 5.1 has a tolerance of 0.1%. Differentiating the output voltage with respect to R_r gives

$$\Delta V_o = \frac{-V_r R_r R_s}{(R_r + R_s)^2} \quad \frac{\Delta R_r}{R_r}$$

Assuming that the resistance is normally distributed, gives for the standard deviation in output voltage:-

$$\sigma_o = \frac{1.665\ R_s}{(R_s + 1000)^2}$$

Reference Channel.

The reference channel has both a reference resistor, and a calibration resistor R_c in series, both of which have a tolerance of 0.1%. Differentiating the output reference voltage with respect to both of these resistances gives

$$V_{or} = \frac{V_r R_r R_c}{(R_r + R_c)^2} \frac{\Delta R_c}{R_c} - \frac{V_r R_r R_c}{(R_r + R_c)^2} \frac{\Delta R_r}{R_r}$$

Inserting the appropriate values gives the standard deviation in reference output voltage of 5.859x10-4 V.

Resistivity Measurement.

By differentiating Expression 5.8, the variation in estimated resistance of the sample due to variations in output voltage and output reference voltage is

$$\Delta R_s = \frac{5 \times 10^3}{(5 - V_o)^2} \Delta V_o - \frac{2.174 \times 10^3 V_o}{(5 - V_o)^2} \Delta V_{or}$$

Inserting the appropriate values gives for the standard deviation in resistance

$$\sigma = \frac{1}{(5 - V_o)^2} \sqrt{(5 \times 10^3 \sigma_o)^2 + (2.174 \times 10^3 V_o \sigma_{or})^2}$$

The standard deviation in resistivity is then

$$\sigma_R = \sigma l$$

the expected variation in the length l of the faces of the sample cubes having a negligible effect.

Truncation of the printed resistivity output data will result in a further uncertainty with standard deviation 0.0289 Ωm.

Values of R_S and V_O have been calculated for resistivities in the range 0.4 - 150 Ωm. The standard deviations in output voltage and output reference voltage due to the individual contributions listed were then used to calculate the standard deviation of resistivity

Graphs of standard deviation σ and also of 3σ against resistivity are given in Figure 5.17. For a normally distributed variable, the probability of the 3σ limit being exceeded is small. This can be taken as the approximate tolerance on resistivity measurement.

From the computations carried out, the quantisation error of the A/D converter is the most significant factor affecting accuracy. The increase in standard deviation at high values of resistivity is due to the reduction in measurement sensitivity as the resistance of the sample approaches that of the corresponding reference resistance.

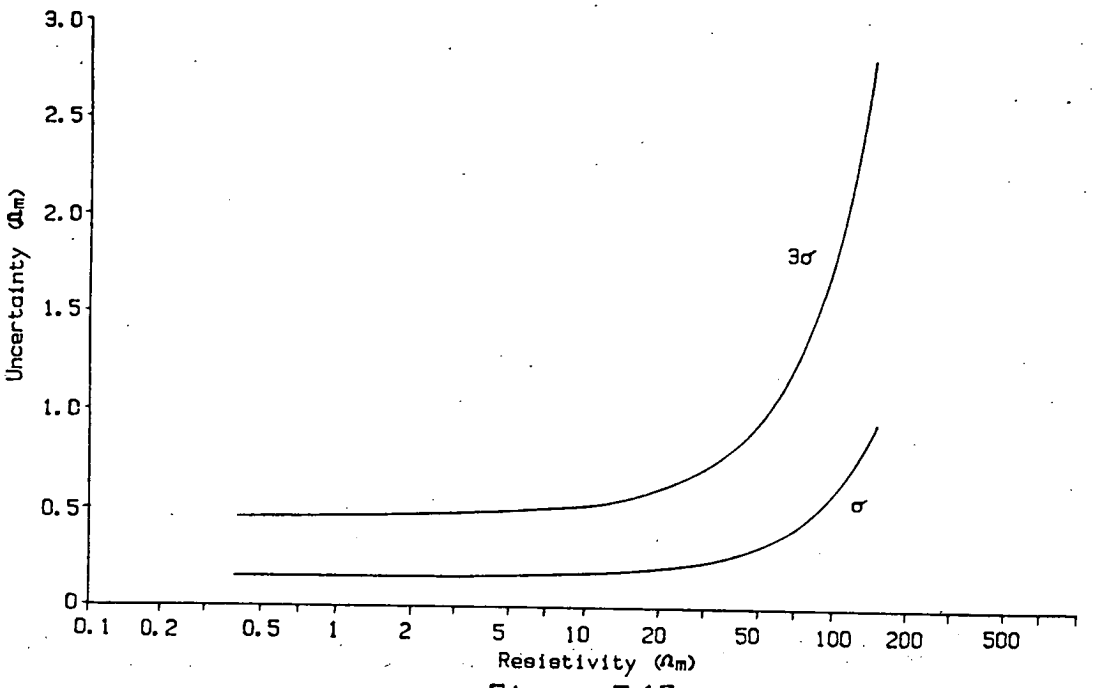

Figure 5.17
Uncertainty in Measured Resistivity

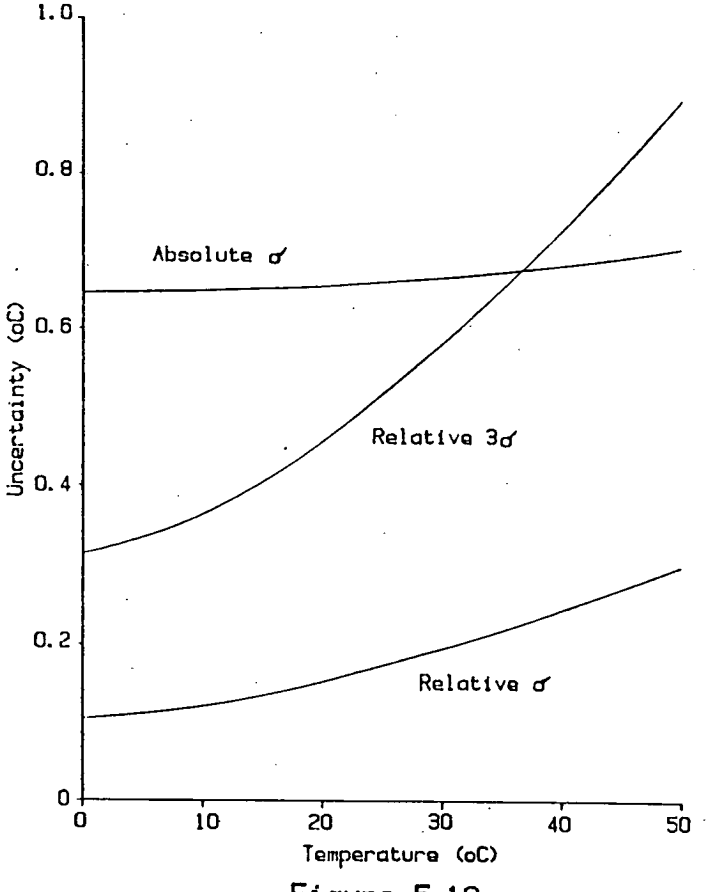

Figure 5.18
Uncertainty in Measured Temperature

Temperature.

A/D Converter.

The behaviour of the A/D converter circuit is exactly the same for the temperature measurement as for resistivity measurement, giving standard deviations in the measurement of output voltage and output reference voltage of 3.985x10-3 V.

Multiplexer.

The behaviour of the temperature multiplexer is again similar to that of the resistivity multiplexer, but because of different values used in the amplifier circuit, the values of standard deviation are different, being, for output voltage:-

$$\sigma_o = \sqrt{(2.355 \times 10^{-4} V_o)^2 + 8.923 \times 10^{-6}}$$

and for output reference voltage 3.036x10-3 V.

Temperature Rectifier.

The performance of the temperature rectifier is dependent on the behaviour of the synchronous switch. The characteristics of the switch used are such that the accuracy of the system is not degraded.

Temperature Amplifier.

The uncertainty analysis of the temperature amplifier is complex because of the adjustment made to give the correct temperature indication. The circuit is analysed in Appendix H, and gives for the standard deviation in output voltage to the A/D converter:-

$$\sigma_o = 0.9056 \left| \frac{1}{R_T} - \frac{1}{R_{To}} \right|$$

where R_T = resistance of transducer at temperature T ^oC (Ω)

R_{To} = resistance of transducer at temperature of calibration (Ω)

and for the output reference voltage, 9.936×10^{-3} V.

Temperature Measurement.

Differentiating Expression 5.15 with respect to the output voltage and output reference voltage gives:-

$$\Delta R_T = 1.494 \times 10^{-3} R_T^2 \left(\frac{\Delta V_o}{V_{or}} - \frac{V_o}{V_{or}^2} \Delta V_{or} \right)$$

This gives for the overall standard deviation in calculated resistance of transducer :-

$$\sigma = 6.497 \times 10^{-4} R_T^2 \sqrt{\sigma_o^2 + 0.189\, V_o^2 \sigma_{or}}$$

Values of R_T and V_o have been calculated over the temperature

range 0 - 50 °C, and used to calculate the standard deviation in calculated resistance. From Expression 5.5, the standard deviation in measured temperature is then:-

$$\sigma_T = \frac{1}{100\ \alpha}\ \sigma$$

$$= \frac{\sigma}{0.388}$$

The temperature system is calibrated against a digital thermometer, and for the thermometer listed in Section 5.4.2, the absolute accuracy is ±2.0 °C, and the stability ±0.05 °C. These values must be included in the assessment of temperature uncertainties. Assuming the accuracy on absolute measurement is normally distributed, and that for stability is uniformly distributed, gives a standard deviation for absolute accuracy of calibration reference of 0.633 °C, and that for stability 0.029 °C. The accuracy of the system as a whole will depend on the absolute value, but if comparative measurements are made between the calibration source and the system the stability value should be used.

Figure 5.18 shows graphs of absolute temperature standard deviation and also of relative standard deviation, taking into account all the sources of uncertainty listed, including the calibration reference. It can be seen that, at all temperatures, the limiting factor for absolute accuracy is the accuracy of the calibration reference thermometer.

Corrected Resistivity.

Differentiating Expression 5.18 with regard to measured resistivity, measured temperature, and assumed value of temperature coefficient for concrete gives:-

$$\Delta\rho = (1 + 0.022[T - 20])\Delta\rho_T - 0.022\rho_T\Delta T$$

Using standard deviations, and accumulating in the usual way, allows the standard deviation in corrected resistivity to be calculated for different temperatures. Figure 5.19 shows the effect of temperature on corrected resistivity. This should be compared with Figure 5.17 which shows uncertainty in measured resistivity. The effect of temperature uncertainty becomes significant above resistivities of approximately 5 Ωm.

Consider the temperature range 15 - 25 °C. The accuracy at maximum corrected resistivity corresponds to a standard deviation of 0.17%, or a tolerance of ±5%, assuming a normal distribution. At low values of resistivity; for example at 20 °C and corrected resistivity 0.4 Ωm, the standard deviation is 0.15 Ωm, and the tolerance ±0.45 Ωm. The uncertainty for measurements on low resistivity cement pastes will therefore be very significant.

The overall performance could be improved by using an A/D converter with a greater number of binary digits for output, and by using a more accurate calibration thermometer for temperature measurement.

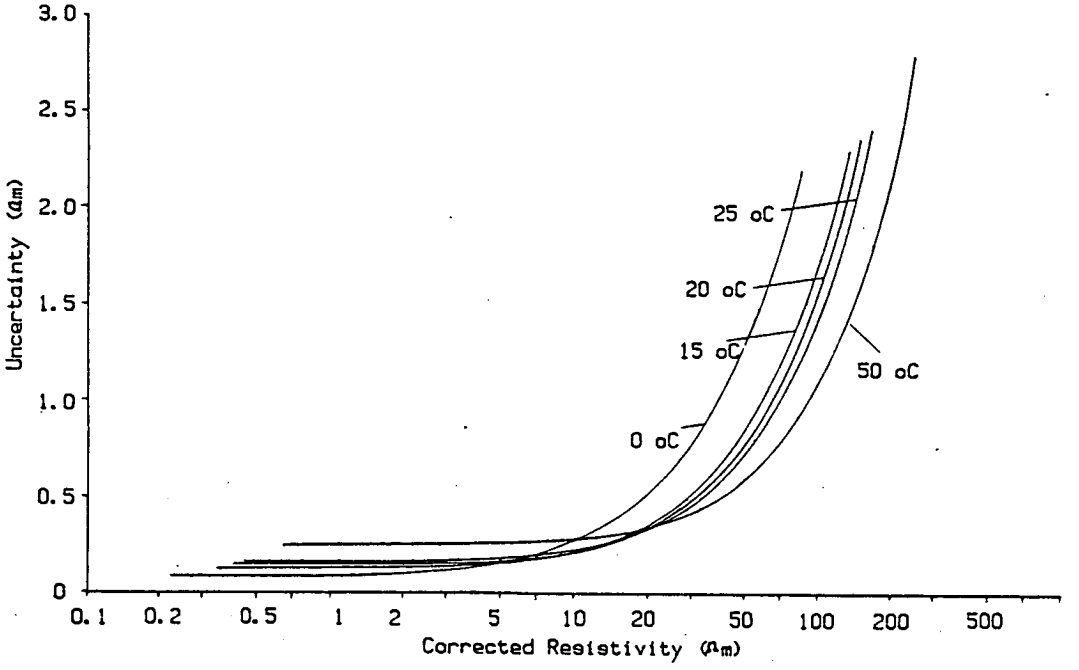

Figure 5.19
Uncertainty in Corrected Resistivity

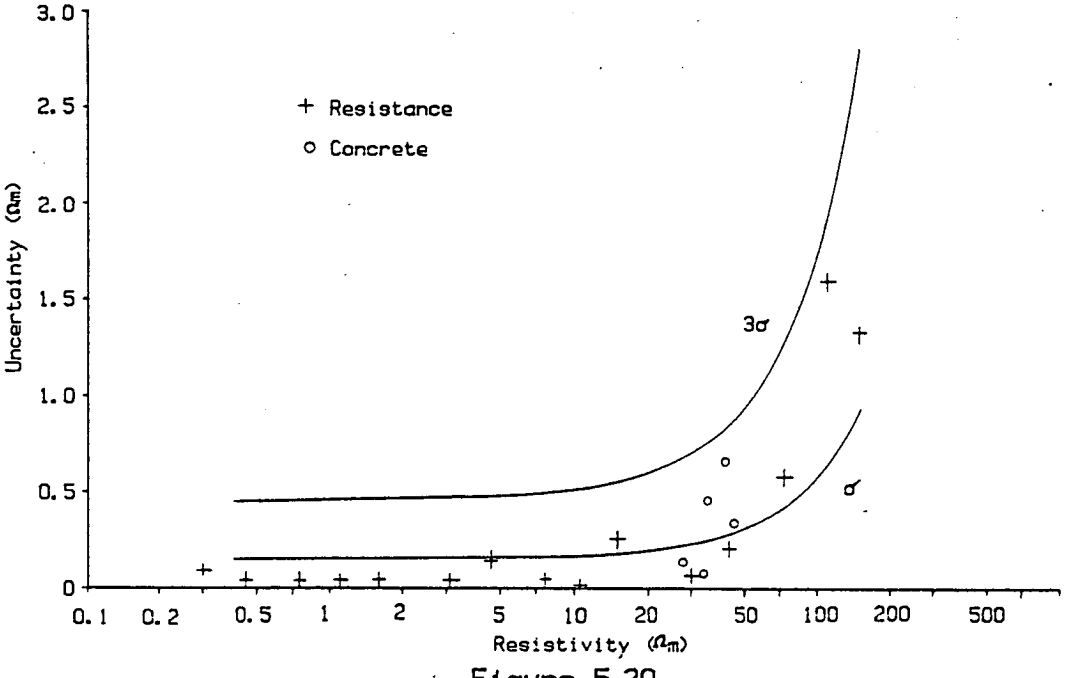

Figure 5.20
Measured Error in Resistivity

5.5. Results.

Figure 5.20 shows measurements of the error between resistivity as measured by the system, and as measured by a Wayne-Kerr Universal Bridge Type B221 which has an accuracy of 0.1%. The measurements are of uncorrected resistivity, so that temperature accuracy has not been taken into account.

Most of the measurements are using resistors in place of samples, but some are taken on concrete. The measurements are within the predicted accuracy of the equipment.

The possibility of the electrode material affecting the result by differences in electrolytic action was considered. Figure 5.21 shows results for similar brass and stainless steel electrodes using the same concrete mix. (water/cement ratio 0.5, cement/sand/aggregate ratios 1:1.5:3) The differences are negligible. The brass electrodes were found to have a tendency to spring off the samples, and were more expensive. Stainless steel electrodes were therefore used.

Initial problems of insulation using cast steel moulds were severe, and resulted in a significant spread in measured values using the same mix. Figure 5.22 shows results obtained during an insulation trial (water/cement ratio 0.5, cement/sand/aggregate ratios 1:1.5:3). The discontinuity after 1 day giving an increase in resistance when demoulding took place, is significant. Figure 5.23 shows the results of a further trial using the same concrete mix where cast steel moulds were also used, but the insulation was improved. The reduction in spread of the results was partly due to

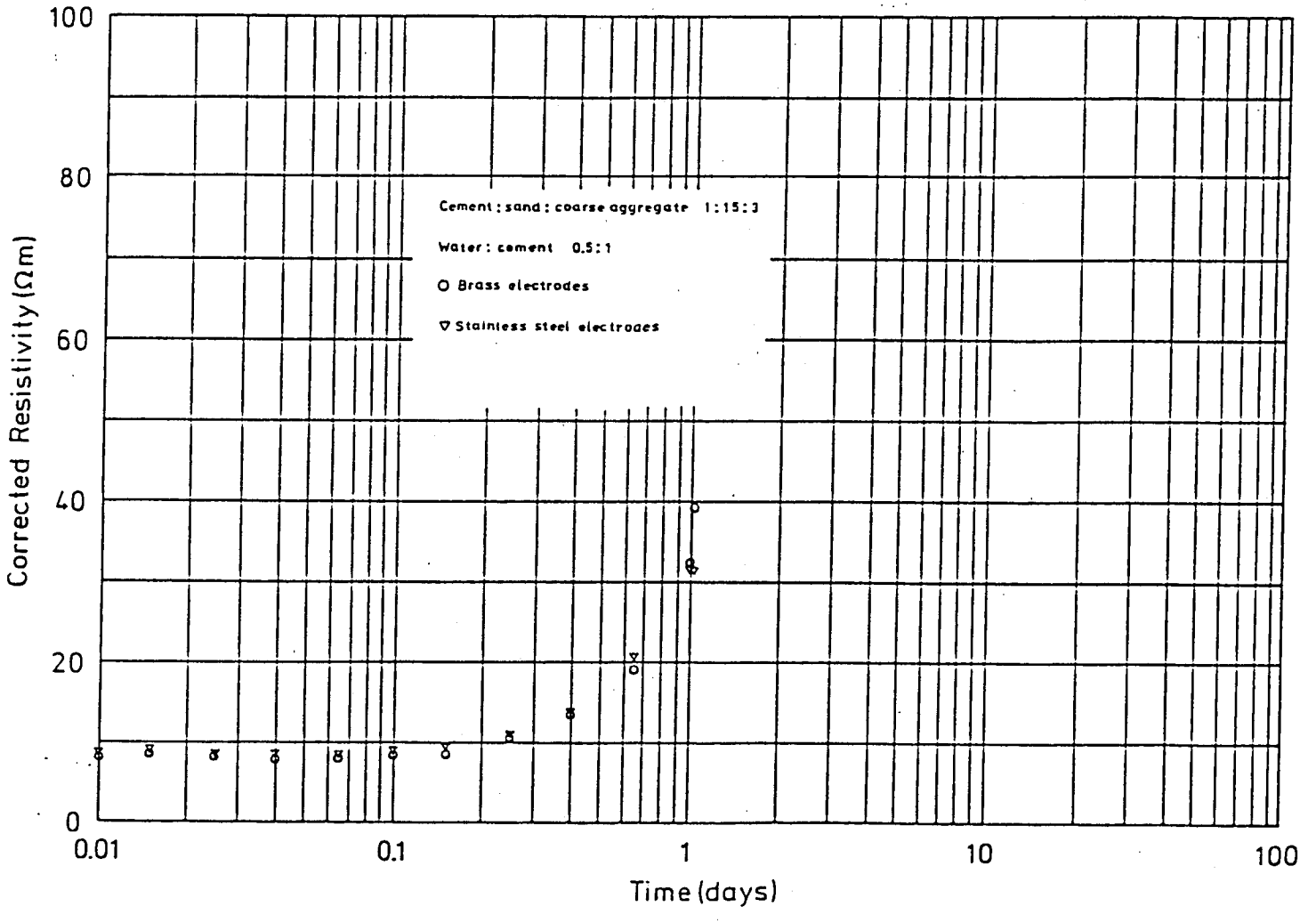

Figure 5.21
Electrode Trial

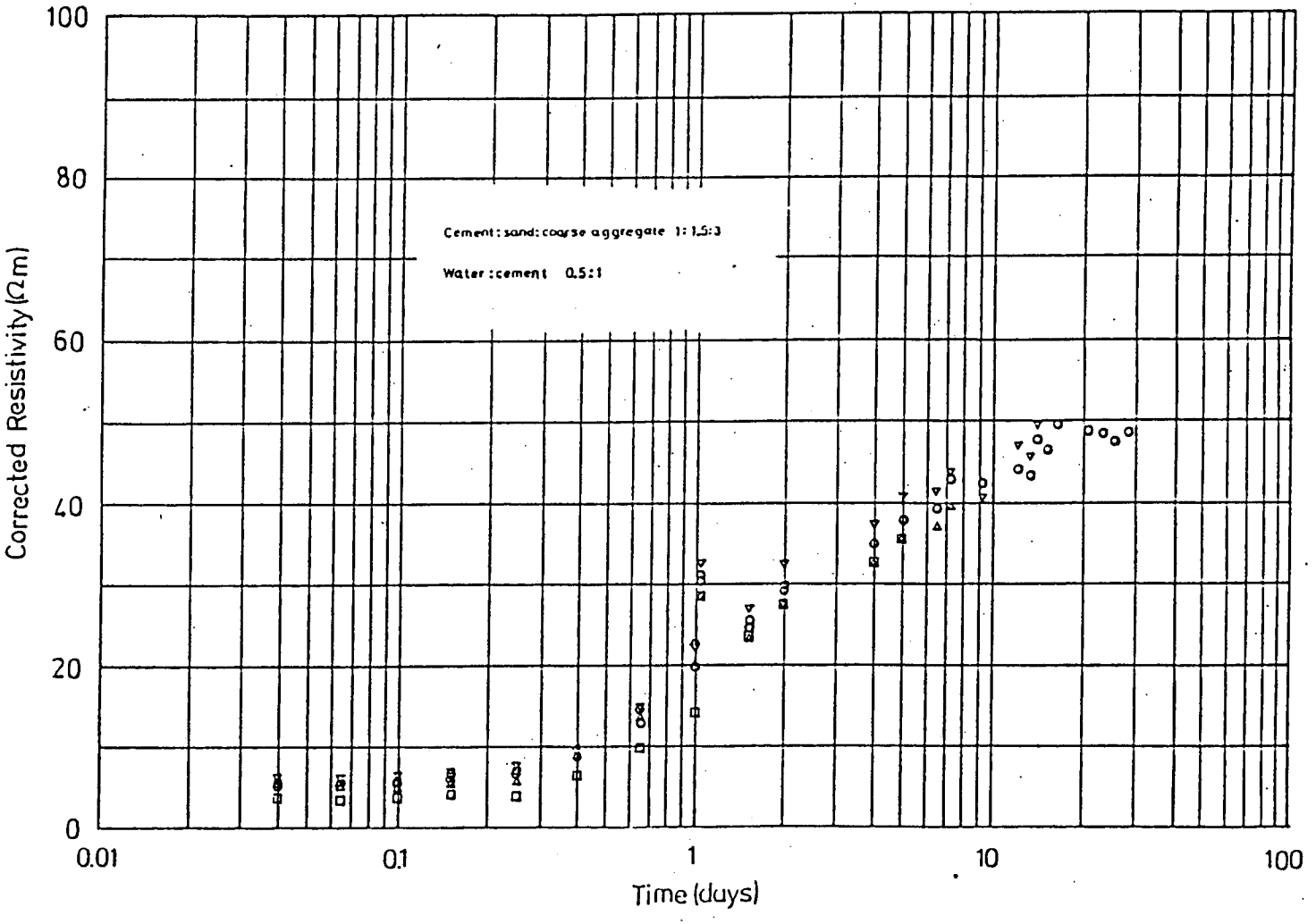

Figure 5.22
Insulation Trial

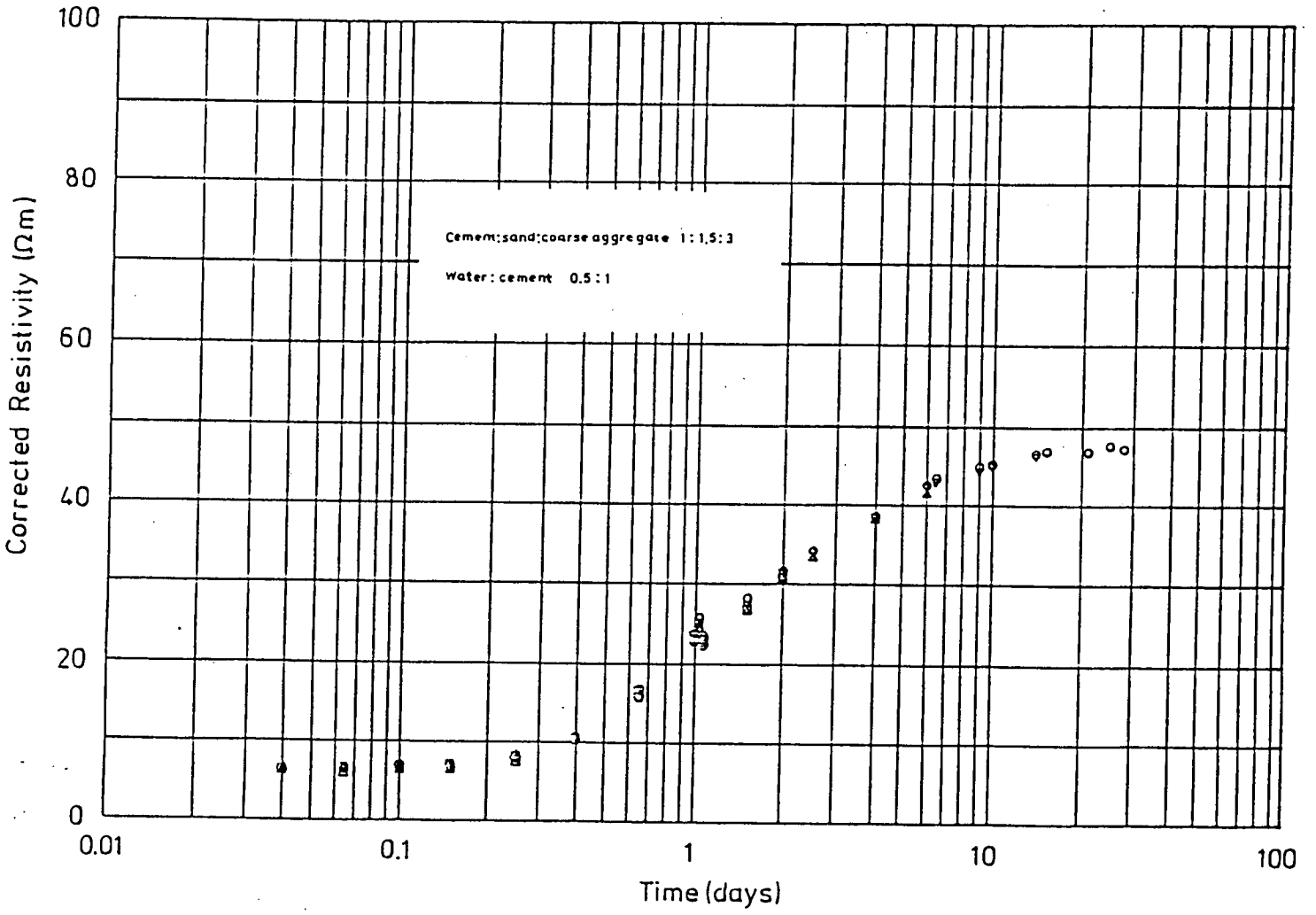

Figure 5.23
Final Proving Trial

improved sampling techniques of the batch of concrete used, and partly due to improved insulation.

The equipment was subsequently handed over to the Department of Civil Engineering and Building Science at the University of Edinburgh for use in a research programme. Because of the urgency of this programme, extensive measurements to establish the accuracy of resistivity measurements on concrete, or of the accuracy of the temperature measurements were not carried out. The results of this research programme are reported by Morelli [74]. This work was largely carried out using PVC moulds.

5.6. Improvements to the System.

The main shortcoming of this system was the need to transcribe output data from the printer of the AIM65 system into the HP85 system for subsequent analysis and graph plotting, a lengthy and error-prone process.

Another major problem was associated with the number of individual units in the system with the problems of reliability of plugs, sockets, and leads, in a civil engineering environment.

There were also a number of problems with programming. Before the programs were transcribed to EPROM, the RAM available was found to be very marginal. The BASIC program was therefore written in such a way as to minimise the amount of mememory required. This resulted in as many operations as possible being carried out within a single program line. While this results in efficient programming, it makes understanding and modification of the program difficult

because of the complexity of the program listings.

The original intention was that the equipment would run for a maximum time of 100 days. However after considerable programming work had been carried out, it was decided that the system should be modified to allow it to run continuously, with experiments being fed in and deleted as required. This requires that the system time be reset to 0 when 100 days is reached, with subsequent adjustment to measurement times in the time-table. The method used to confirm that this boundary had been crossed when carrying out measurements is ponderous, and could be much simplified.

A redesign of the system was therefore undertaken to remove the defects encountered, and to incorporate other minor improvements. This system is described in Chapter 6.

6. DEVELOPED LOW FREQUENCY MEASUREMENT SYSTEM.

6.1. Changes to the Prototype System.

6.1.1. Introduction.

Once the original equipment became operational in a Civil Engineering environment, a number of possible improvements became apparent (Section 5.6). It was therefore decided to produce an upgraded version. The changes include:-

(i) replacement of the Rockwell AIM65 microcomputer by a Hewlett-Packard HP85 desktop computer

(ii) repackaging of the system in a form more suitable for a Civil Engineering environment

(iii) incorporation of custom designed microcircuits in certain areas of the system.

6.1.2. Controlling Computer System.

The controlling computer was changed from the Rockwell AIM65 to a Hewlett-Packard HP85 to allow data both to be printed out immediately and to be recorded on disc for subsequent processing without transcription.

The HP85 computer has a total storage capacity of 32 kbytes as compared with 8 k for the AIM65. This allows techniques to be used, which produce more readable, simpler, and more easily modified

programs.

Interfacing to the HP85 was carried out using an IEEE bus structure, which requires the incorporation of an R6502 microprocessor with EPROM, RAM, and VIA electronics interface units, along with an MC68488 IEEE bus interface unit. The R6502 microprocessor was chosen because of familiarity with the coding, operation, and software compatibility.

6.1.3. Repackaging.

Once the prototype equipment had been operated by Civil Engineers, it was decided that the packaging was inadequate for such duty. The following improvements were therefore implemented:-

(i) grouping of temperature amplifiers into three groups of five packaged together

(ii) the integration of all other units apart from the hoist into a single electronics unit

(iii) the use of more robust connectors.

6.1.4. Temperature Rectifiers.

Synchronous detection of the temperature signal can be effectively carried out using the sampling capability of the A/D converter system, obviating the need for the temperature rectifier circuit (Section 5.3.1). The frequency of the temperature energizing signal was therefore made the same as that of the resistivity monitoring system (2 kHz) to simplify the logical

operation of the system.

6.1.5. Incorporation of Microcircuits.

Advantage was taken of a cell library for LSI design developed in the Department of Electrical Engineering at the University of Edinburgh [75]. The cells have broadly similar characteristics to TTL logic components which were used in the prototype equipment.

It was agreed that the new equipment would be a suitable vehicle for a trial of the cell library by an engineer not associated with the development team. The timing circuit and the hoist control circuit were identified as two circuits to which the cell library could be applied.

A description of the development of the microcircuits is given in Appendix I.

6.1.6. Resistivity Multiplexer.

To eliminate any error due to d.c. offset in the output of the resistivity energising amplifier charging the capacitance of the concrete test sample, a blocking capacitor was inserted in the line between the junction of the sample and the reference resistor and the input to the multiplexer.

6.2. General Requirements.

The general specification and accuracies for the new equipment are as for the prototype (Section 5.1). Although each electronic unit has a capacity of 15 samples, system extension is possible by fitting other identical units to the IEEE bus system.

The principle of operation is largely the same as for the prototype system (Section 5.2).

6.3. Description of the System.

A description of the principle of operation and details of the changes in the developed system are given by Wilson et al [76] which is presented in Appendix J.

The measurement system is generally similar to that of the prototype system, but with some redistribution of functions and improvement to circuits. A complete description of hardware is given here only if there is a major difference from the prototype system.

Two levels of software are required. These are:-

(i) the system software for control, initiation of measurements calculation of results, and presentation of outputs; this program is in BASIC.

(ii) the microprocessor software which is written in machine code and is stored in an EPROM in the electronics unit; this controls communication with the system software, communication with the system software, and carries out

measurements and other operations as required.

6.3.1. Hardware.

The measurement system comprises the following units:-

(i) samples with electrodes, temperature sensors and associated amplifiers

(ii) electronics unit

(iii) hoist

(iv) Hewlett-Packard HP85 computer and HP9121 disc drive unit.

Figure 6.1 shows the complete system.

The electronics unit shown in Figure 6.2 contains the following circuits:-

(i) timing circuit

(ii) resistivity multiplexer

(iii) temperature multiplexer

(iv) A/D converter

(v) microprocessor

(vi) memory and interface

(vii) IEEE bus interface

(viii) control unit

(ix) power supplies.

Circuit diagrams for the system are given in Appendix K.

A hardware system diagram is presented in Figure 6.3 and will be used to describe the operation of the system.

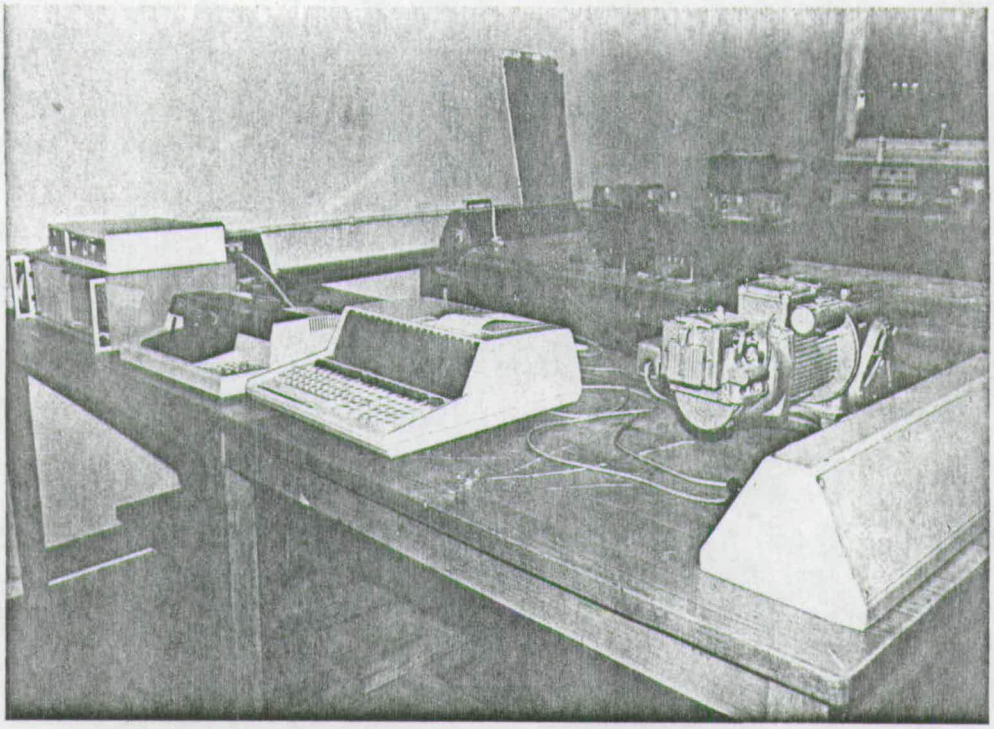

Figure 6.1.
Developed System

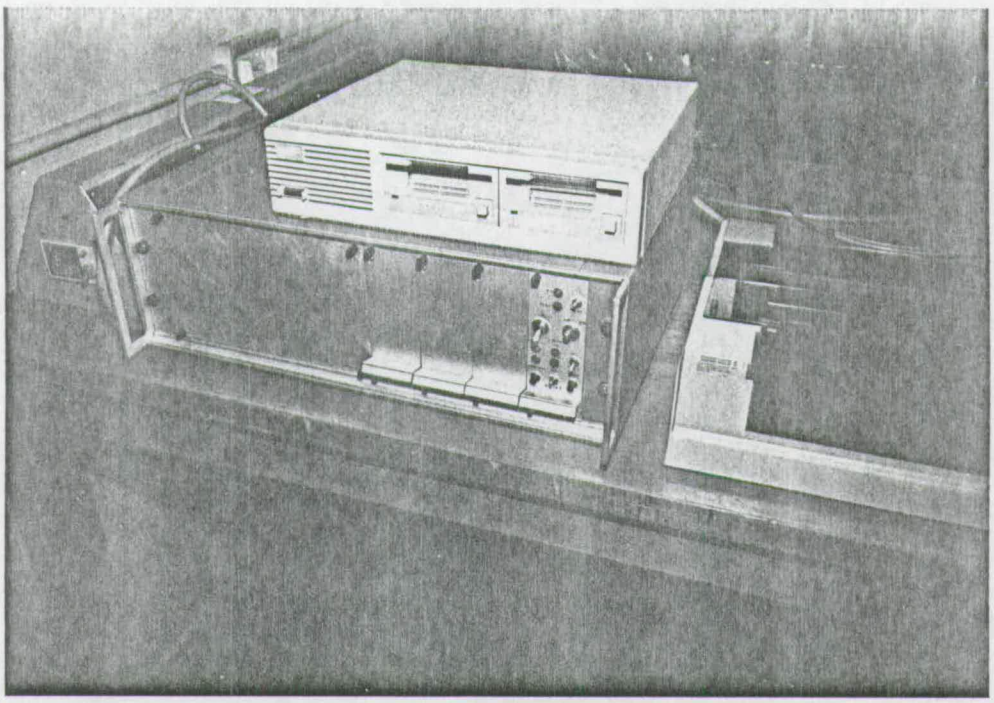

Figure 6.2.
Electronics Unit

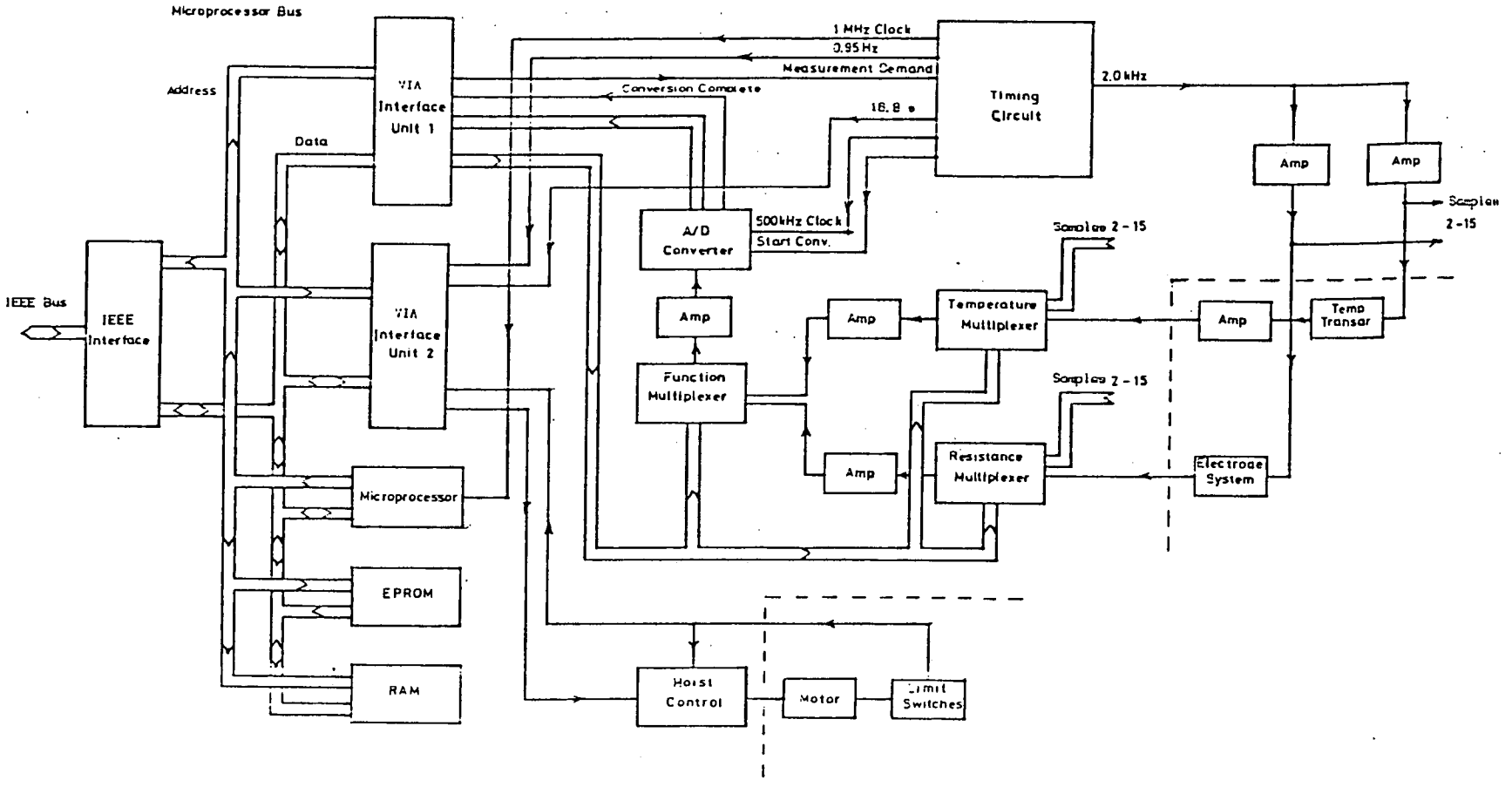

Figure 6.3.
Hardware System Diagram

Timing Circuit. (Figure K.1)

The main element of the timing circuit is the custom microcircuit type JW07 which is discussed in Appendix I, and which carries out the functions of the timing circuit of the prototype system (Section 5.3.1). In addition, this circuit generates the measurement demand signal which was part of the function of the A/D converter circuit in the prototype system, and the 1 MHz clock signal for the microprocessor, using a quartz crystal which is mounted in the timing circuit. The following TTL signals are generated:-

(i) 1 MHz:- microprocessor clock

(ii) 500 kHz:- A/D converter clock

(iii) 1.95 kHz:- (2 kHz) resistivity and temperature energising signal

(iii) start conversion:- for control of the A/D converter

(iv) 0.95 Hz:- a control signal used during calibration procedures

(v) 16.784 s:-the basic system timing signal.

The 16.784 s signal should have had a period of 43.2 s corresponding to 0.0005 days. 16.784 s is the result of a design defect which was not possible to correct in the time available (Appendix I), correction being made in software. The system timing signal is activated by a TIMING ON signal from the control unit.

The generation of a start conversion pulse is controlled by a measurement demand signal from the memory and interface unit.

The timing circuit includes amplifiers to generate the

resistivity and temperature energising signals from the 2 kHz output from the microcircuit. The output voltages are symmetrical about zero to ensure that for the resistivity energising signal applied to the concrete samples, polarisation effects are minimised.

Concrete Samples.

Each measurement unit can accommodate 15 samples, each with 14 s.w.g. stainless steel electrodes, and held in PVC moulds (Figure 6.4). The connector for the platinum film temperature transducer has been changed from the prototype system to a more robust miniature BNC connector.

Resistivity Multiplexer. (Figure K.2)

The resistivity energising signal from the timing circuit is applied to each of the samples via one of 16 reference resistors, the other electrode being earthed. Sample voltages are multiplexed through series capacitors.

One of the reference resistors is connected to a calibration resistor of 851.72 Ω instead of a sample.

D.c. test voltages may be injected into the multiplexer to allow d.c. offsets to be trimmed out.

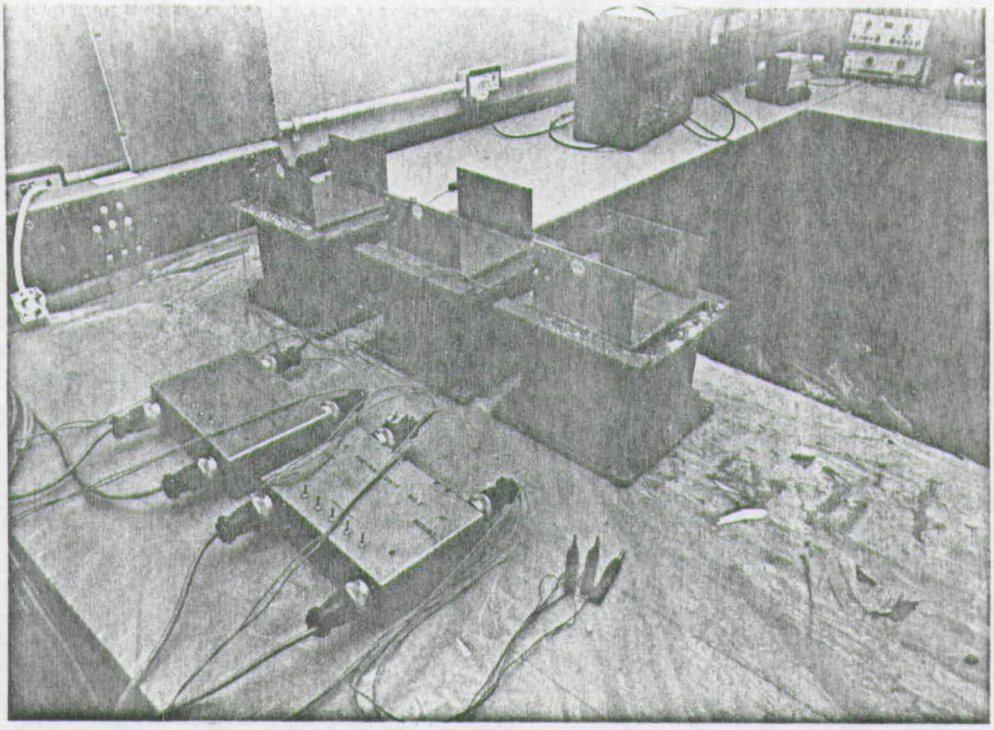

Figure 6.4.
Samples with Electrodes and PVC Moulds

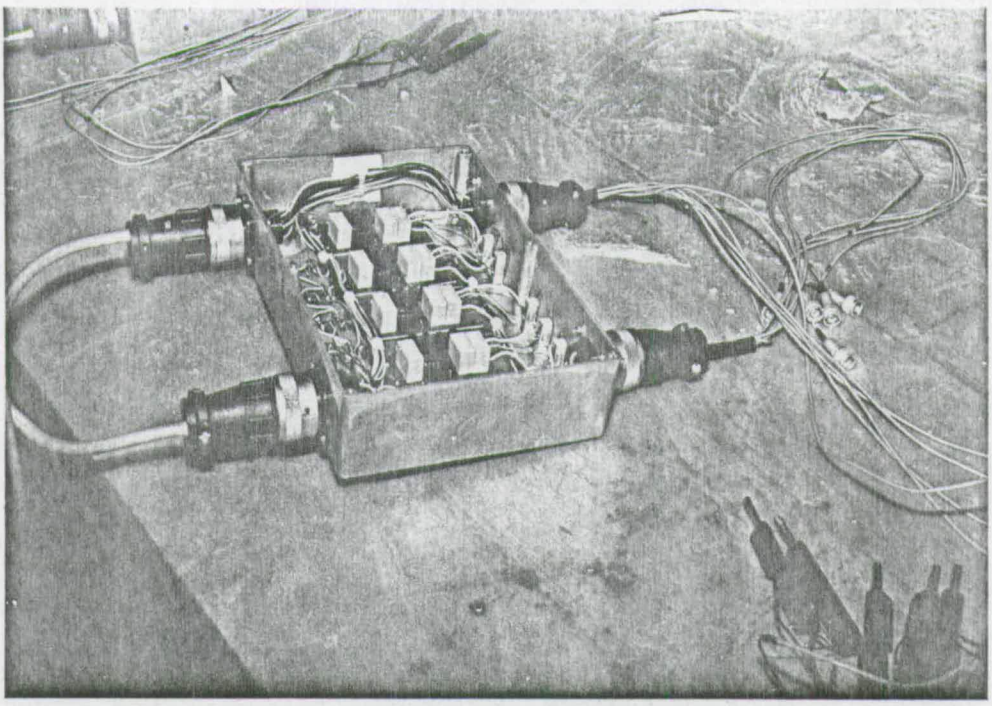

Figure 6.5.
Temperature Amplifiers

Temperature Amplifier. (Figure K.3)

The signals from the temperature transducers are fed to amplifiers packaged in groups of five in diecast boxes. Connections to the boxes are by robust multiway connectors with a positive locking action. A group of amplifiers, which are similar to those of the prototype equipment (Section 5.3.1), is shown in Figure 6.5.

Temperature Multiplexer. (Figure K.4)

The arrangement for temperature multiplexing is similar to resistivity multiplexing already described. A calibration resistance of 117.56 Ω replaces one temperature sensor.

A/D Converter. (Figure K.5)

The outputs form the resistivity and temperature multiplexers are fed to a further multiplexer in the A/D converter unit. Either resistivity or temperature signals are selected by one address line which originates in the memory and interface unit.

The output from the multiplexer is fed via an amplifier with adjustable gain of approximately unity, to an eight bit successive approximation A/D converter. When conversion is complete, data on the eight logic output lines is read by the microprocessor system. These lines are also connected to the memory and interface unit.

The amplifier is fitted with a diode output limiter to prevent damage to the A/D converter.

Microprocessor. (Figure K.6)

A reset signal is applied to the microprocesor on switch ON through a timing circuit that ensures that a reset condition still exists when the power supply reaches full voltage. The reset circuit can also be activated by a push switch on the unit.

Memory and Interface. (Figure K.7)

The memory and interface unit contains a 2 kbyte RAM working space, and a 4 kbyte EPROM containing the program for the microprocessor. The unit also includes two versatile interface adaptors (VIA) providing a total of 32 data input/output lines and 8 control lines, for communication between the microprocessor and the electronic circuits.

IEEE Bus Interface. (Figure K.8)

The MC68488 microcircuit is the basis of this unit which provides communications between the microprocessor and the HP85 computer.

The IEEE bus used is an instrumentation bus with 8 data lines and 8 control lines. A strict protocol, which is signalled by the control lines, is used to transmit data in both directions. The MC68488 microcircuit, which is isolated from the main IEEE bus lines by bi-directional buffers, ensures that the protocol is implemented automatically during the transmission and reception of data.

The unit also includes a selector circuit which places an identifying code on the data lines when demanded by the interface microcircuit. The identifying code is set by a 6 pole sub-miniature

switch on the unit.

The IEEE instrumentation bus allows up to 14 units to be interconnected. Some of these positions are taken up by the HP85 computer and peripherals, but it is still possible to interconnect a total of 10 measurement units to the system, giving a total capability of 150 samples.

Control Unit. (Figure K.9)

The 240 V a.c. mains supply to the power units and the hoist is routed through the control unit. The MAINS ON switch controls the supply to power units, and if this switch is closed, the HOIST ON switch controls the power to the hoist motor.

The custom microcircuit JW12 (Appendix I) used to operate the hoist is located in the control unit, and replaces the hoist control unit of the prototype system. This microcircuit generates control signals for relays controlling the RUN and START windings of the hoist motor. The normal control of the hoist is by OPERATE, UP, and STOP signals generated by the microprocessor, and fed to the hoist microcircuit from the memory and interface unit. When a TEST toggle switch is depressed on the control unit, generation of these signals is transferred from the microprocessor system to OPERATE, UP, and STOP switches on the control unit. This allows complete manual control of the hoist.

A master timer logic signal is transmitted by the memory and interface circuit to the control unit, and is then fed to the

timing circuit by way of a toggle switch as a TIMING ON signal. The switch allows control of the time when system timing pulses are initiated.

Power Units.

The power supplies are packaged units compatible with the equipment rack. The three units provide:-

(i) +5 v at 3 A

(ii) ±15 V at 500 mA

and (iii) +12.7 V at 500 mA

for mains switching relays which control the hoist.

Hoist. (Figure K.10)

A separate hoist is required for each measurement set of 15 samples. The hoist assembly is identical to the prototype system except that positive locking multiway connectors have been used.

Power Distribution and Control. (Figure K.11)

Mains power lines go direct to the MAINS ON switch in the control unit. Following this switch, the lines split into power supply lines and hoist lines. A HOIST ON switch in the control unit acivates the hoist. Both the power supply and hoist lines are fused and have radio frequency interference filters fitted to prevent noise carried on the mains interfering with the microprocessor circuits. The fuses and filters are mounted on the equipment rack.

The power supply lines then go direct to the power units, while the hoist lines go to the hoist control OPERATE and REVERSE

relays, also fitted to the equipment rack. The operation of these relays is identical to the prototype system.

Hewlett-Packard HP85 Computer.

This is a desktop computer fitted with an IEEE bus interface system for communication between peripherals, which in this case includes measurement units.

Hewlett-Packard HP9121 Double Disc Drive.

This unit can accommodate two 89 mm, 287 kbyte, storage discs, one to load the system program and data processing programmes once experiments are completed, the second to record data during experiments.

6.3.2. System Software.

The system software controls the running of an experiment, initiates measurements, and outputs data as required. The program is stored on magnetic disc, and must be loaded into the HP85 computer before experiments commence.

The software can control up to 10 measurement units, each with a capability of 15 samples. Within any measurement unit, the samples can be arranged as one experiment with 15 samples, or as 15 separate experiments, or any intermediate arrangement. An experiment can be started or stopped in the presence of other experiments.

The measurement sequence used in the prototype equipment

giving 5 measurements per temporal decade up to 100 days (Section 5.3.2) is available. An additional sequence giving 10 measurements per decade up to 1 day has also been incorporated. The system includes control of the hoist for experiments which exceed 1 day and where the samples are stored under water.

The timetable holding the information on individual experiments is in the form of a matrix with the rows giving data on particular experiments, and the columns corresponding to different experiments in order of measurement times. The row elements contain the information given in Table 6.1.

Element	Function
1	next measurement time
2	measurement indicator which indicates that the next measurement occurs as the result of a measurement demand sequence
3	stored measurement time; used to store original measurement time during a measurement demand sequence
4	experiment time; time for which the experiment has been running
5	unit number; number of the measurement unit in which the experiment is running
6	start number; location of the first sample in the experiment
7	number of samples in the experiment
8	hoist disabled; indicates that the hoist is is not required for this particular experiment
9	measurement sequence
10	measurement position; the position of the experiment in the measurement sequence selected.

Table 6.1.
Timetable Matrix Functions.

The software provides the following facilities:-

(i) initiation of new experiments and removal of old

(ii) measurement of an experiment sample set, on demand, to supplement automatic measurement

(iii) monitoring of any output available from the A/D converter on the CRT

(iv) monitoring of measured resistivity, temperature, or corrected resistivity of a sample, on the CRT

(v) operation of the hoist on demand from the computer keyboard

(vi) print out of a list of all experiments in the system with unit, start location, and number of samples

(vii) print out of all the data held in the timetable for each experiment

(viii) a sequence which allows the magnetic disc to be changed while experiments are running

(ix) print out of real time and date when the computer time was initialized, and the capability of correcting computer time

(x) provision to allow the measurement unit selected to provide master timing signals, to be changed

(xi) print out of program options available and their calling codes

(xii) the ability to bring the program to a halt with the possibility of a restart.

Figure 6.6 is a system program diagram.

Most of the running time is in the Control program. When experiments are being fed into the system, the route is Control, Keyboard, Input, and return to Control. When the system is running

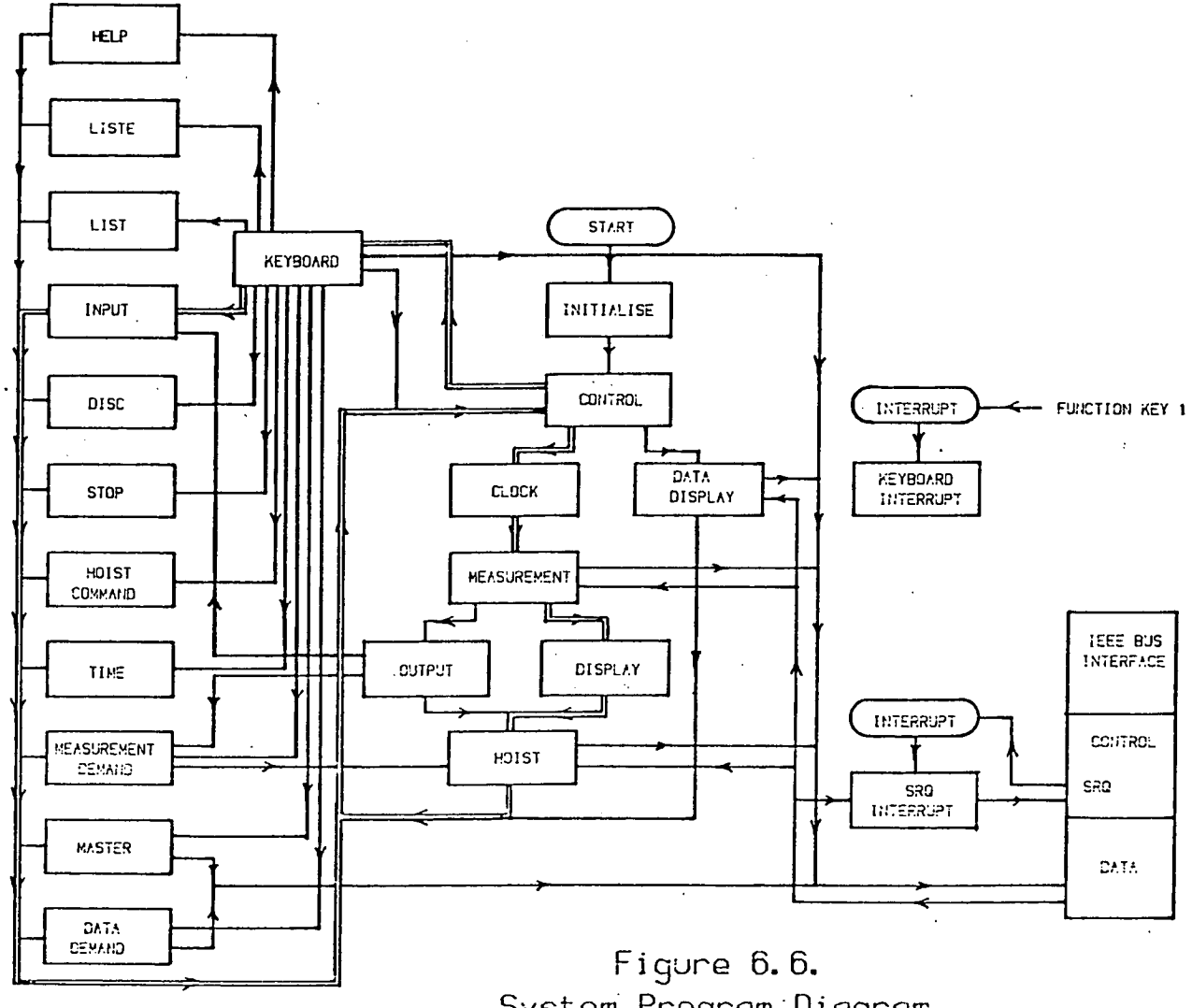

Figure 6.6.
System Program Diagram

normally, a system timing pulse generates a service request (SRQ) on the IEEE bus control line. This causes the system to take the path Control, Clock, Measurement, Display, Hoist, and Control. If, at the time calculated by the Clock program, a measurement must be taken, then the route includes Output instead of Display.

In general, the system will eventually return to the Control program following a branch to another routine. If interrupts are generated as a result of SRQ commands, or by function key 1 on the keyboard being depressed, then the program will return to the next instruction in the routine in which the system was running prior to the interrupt.

The system is brought into operation by generating a reset in each of the measurement units on the bus, either by switching on, or by depressing the RESET button on the unit. The system program is then loaded from the magnetic disc, and a RUN command initiated from the keyboard, causing the Initialization program to be entered.

Initialization.

Counters are initialized and constants set, the data disc is intialized, and the time of day (hrs, min, secs) at which the system is to be started is fed into the system. A measurement unit is selected to generate the system timing pulses, and the operator is instructed to close the TIMING ON switch on that particular unit, at the correct time. The system then implements the Control Program.

Control.

This forms a loop in which 2 indicators are monitored. These indicators are:-

(i)(a) the timing indicator which, when set to 1, shows that a system timing pulse has been received, and causes a jump to the Clock program

(b) and, when set to 2, shows that a 0.95 Hz impulse has been received when the system is in the data demand mode, and causes a jump to the Data Display program

(ii) the keyboard indicator which shows that function key 1 on the keyboard has been depressed, and causes a jump to the Keyboard program

An interrrupt enable command for the SRQ signal is also included in this loop. The interrupt is disabled when any of the program options are requested, or when data is being transferred on the IEEE bus. This ensures that the interrupt is reset on return to the Control program.

Clock.

The timing indicator is reset, and the system time is updated by the number of system timing pulses received since the last update. The pulse counter is then reset. If the system time exceeds 100 days, then 100 days is subtracted from system time, and from all measurement times held in the timetable.

If there are no experiments the system jumps to the Measurement program, otherwise the experiment time held in the

timetable for each experiment is updated, and the system then jumps to the Measurement program.

The clock program carries out the correction necessary because of the sytem timing period being 16.785 s instead of 43.2 s (Section 6.3.1).

Measurement.

If there are no experiments on the system, or if the system time does not correspond to the measurement time for the first experiment on the timetable, the system jumps to the Display program.

If measurements are required, a measurement code is sent to the measurement unit in which the first experiment on the timetable resides, giving the start location of the experiment, and the number of samples. The unit carries out the measurements and transmits the data to the HP85 computer. The last byte transmitted is a unit status byte.

The system jumps to the Output program.

Display.

The CRT display is cleared, and if there are no experiments in the system, the system time and a zero are displayed according to the format

```
11.4567  0
```

and the program jumps to display warning messages.

If there are experiments in the system, the system time, unit number, start position, number of samples, and the measurement time of the next experiment to be measured are displayed on the CRT using the format

```
11.4567   1  12   3  15.9495
```

If the hoist has not reached the correct upper or lower limit during the last four timing intervals, the following warning message with appropriate unit number are displayed.

```
** HOIST CHECK ERROR   3
```

If a test switch is in the TEST position on any unit, the following warning message and the unit number are displayed

```
** TEST ROUTINE ON    4
```

The number of data bytes stored on the magnetic disc is displayed according to the format

```
DATA BYTES 390
```

If the number of data bytes stored equals or exceeds 9000, the following warning message is displayed.

```
** CHANGE DISC
```

The system then jumps to the Hoist routine.

Hoist.

The presence of a hoist UP demand is monitored. This can be due to a hoist command, or to a measurement being required within 0.0035 day, for an experiment in which the samples are currently stored under water.

Hoist control codes are transmitted to all measurement units indicating whether particular hoist should be up or down. A unit status byte is then returned to the HP85 from each unit.

The status byte includes data on whether the upper or lower hoist end stop has been reached. This is compared with the hoist demand, and if they do not correspond, a counter is incremented. If the count reaches 4 a warning is displayed by the Display program. If a correct result is obtained, the counter is reset to zero. The unit status byte also contains information regarding the state of the test switches on the unit. If a test switch has been operated, a warning is displayed by the Display program.

The system returns to Control.

Output.

Note that after any output to the magnetic disc unit, the counter, which indicates the number of data bytes stored on disc is incremented by the appropriate amount.

The system time is printed out. If the hoist monitor counter indicates any error, the warning message

** HOIST CHECK ERROR

is printed, and also sent to the magnetic disc unit.

The unit status byte is checked, and if the end stop position is not correct for the experiment being measured, the error message

**HOIST OPERATION ERROR

is printed, and also sent to the disc unit.

If the status byte indicates that a test switch has been operated on the unit, the warning message

** TEST ROUTINE ON

is printed and sent to the disc unit.

The experiment time is printed according to the format

EXPERIMENT TIME 1.4956

and the time is transmitted to the disc unit.

The resistivity, temperature, and corrected resistivity, are calculated, and the unit number, sample number, resistivity, temperature, and corrected resistivity, are printed out for all the samples in the experiment according to the format of Table 6.1, and are also transmitted to the disc unit.

The data for the experiment is removed from the timetable and

stored. If the measurement resulted from a measurement demand sequence, a jump is made to the Measurement Demand program.

The next point on the measurement sequence is calculated, and if the last point on the sequence has been taken, a jump is made to the Input program to allow the experiment to be deleted.

The next measurement time is calculated and the experiment data reinserted in the timetable at the correct point according to the next measurement time.

The system then jumps to the Hoist program.

Data is outputted by the Output program in the order in which measurements are carried out. If there are a number of experiments in the system, the output data for these experiments will therefore be interlaced.

Keyboard.

The Keyboard program is entered if the keyboard indicator in the Control program is set, indicating that function key 1 on the keyboard has been depressed.

Interrupts due to an SRQ on the IEEE bus are disabled, and if a Data Demand sequence is in operation, this is deleted by resetting the data demand indicator and transmitting a code to the current master timer measurement unit inhibiting data demand pulses.

The operator types in the code for the program option required:-

INPUT	Input
MEAS	Measurement Demand
DATA	Data Demand
HOIST	Hoist Command
LIST	List
LISTE	List Experiments
DISC	Disc
TIME	Time
STOP	Stop
HELP	Help
MASTER	Master Timer

If the information typed in does not correspond to one of these codes, the computer displays an error message, the keyboard indicator is reset, and the system returns to control, otherwise the system jumps to the program selected.

Input.

The keyboard indicator is reset. The system time and INPUT are printed, the operator indicates whether a new experiment is being inputted, or if an existing experiment is to be deleted. If a delete operation is required, the system jumps to the delete section of the Input program.

If a new experiment is inputted, code I is transmitted to the disc unit, and the operator then provides the following information:-

(i) the date

(ii) the measurement unit in which the experiment is located

(iii) the location of the first sample in the experiment

(iv) the number of samples in the experiment

(v) the water/cement ratio

(vi) the cement/sand/aggregate ratio

(vii) the time elapsed since water was added to the mix

(viii) the measurement sequence required, or HELP

(ix) whether or not the hoist is to be disabled

This data is also printed out along with the temperature coefficent of resistivity currently used by the program. Parts of this information are also transmitted to the disc unit. The HELP routine causes a description of the measurement sequences available to be printed out.

The counter which stores the total number of experiments is then incremented, and the measurement point in the sequence selected, and the experiment time at the first measurement, are calculated.

If the sequence selected is not recognised, an error message is displayed, the experiment counter is decremented, and the system returns to Control.

The system time for the first measurement is calculated, and the experiment data inserted into the timetable matrix in the correct measurement time position.

The system then returns to Control.

If a delete operation is required, DELETE is printed, and code D is transmitted to the disc unit. The operator inputs the following information:-

(i) measurement unit

(ii) start sample number for the experiment

(iii) the number of samples to be deleted from the experiment or A.

If code A is used, then all of the samples are to be deleted. This information along with code A if applicable is transmitted to the disc unit.

Note that samples are deleted starting from the highest numbered sample in the experiment.

If not all of the samples in the experiment are to be deleted, the number of samples on the experiment held in the timetable is decremented as required, and the system returns to control.

If all the samples are to be deleted, the experiment counter is decremented, the data for the experiment is eliminated from the timetable, and the timetable is reset as required. The system returns to Control.

Measurement Demand.

The keyboard indicator is reset, and the system time and MEASUREMENT are printed out. If no experiments are present, a warning statement is displayed, and the system returns to Control.

If experiments are present, the operator inputs the measurement unit, and the position of the first sample in the experiment. This information is printed out, and the position of

the experiment in the timetable is found. If the experiment is not found, a warning message is displayed, and the system returns to Control. If the experiment is found, the matrix row containing the experiment data is removed from the timetable, the current measurement time for the experiment is stored in row element 3, and the measasurement demand indicator; element 2, is set.

If the experiment time is not greater than 1 day, or if the hoist disable indicator (row element 8) is set, the measurement time (element 1) is set at the current time plus 0.0005 days, but if the hoist is to be used, the measurement time is set at the current time plus 0.004 days to allow time for the hoist to operate, and the water to run off the samples.

The experimental data is then replaced in the timetable in the correct order of measurement time, and the system returns to Control.

If a jump is made to the Measurement Demand program from the Output program, following measurements initiated by Measurement Demand, the stored measurement time (row matrix element 3) is restored (matrix element 1), and the measurement demand indicator (element 2) reset. The experiment data is then replaced in the timetable in the correct measurement time position, and the system jumps to Hoist.

Data Demand.

The keyboard indicator is reset, and the system time and DATA printed out. The operator indicates whether a Data routine is to be deleted. If so DELETE is printed out and the system returns to Control, the necessary delete action having been taken when the Keyboard program was entered. The delete action includes resetting the data demand indicator.

If the routine is not to be deleted, the data demand indicator is set, and the operator indicates whether the data is to come directly from the A/D converter, or if calculated values of resistivity or temperature are required. These are indicated by modes D and C respectively. If A/D converter data is required, a mode indicator is set.

The operator inputs the unit and sample number to be monitored. If mode C has been demanded, the following selection data is displayed:-

RESISTIVITY 1

TEMPERATURE 2

CORRECTED RES 5

and if mode D has been demanded, the selection data displayed is:-

RESISTIVITY 1

TEMPERATURE 2

RES REFERENCE 3

TEMP REFERENCE 4

The operator then types in the required code number, and the system sends a code to the measurement unit, which is currently the master timer which causes the unit to generate 0.95 Hz data timing pulses, thus producing SRQ signals on the IEEE bus.

The system then returns to Control.

Hoist Command.

The keyboard indicator is reset, and the system time and HOIST are printed out.

The operator indicates which unit is to be affected, and whether the hoist is to be raised or lowered. The demand indicator for that hoist is set by the program for the condition required. The unit number and the hoist demand are printed out.

The system returns to control.

List.

The keyboard indicator is reset, and the system time and LIST are printed out. The program prints out all the data held in the timetable, experiment by experiment, starting with the experiment with the earliest measurement time, and returns to Control.

List Experiments.

The keyboard indicator is reset, and the system time and LISTE are printed out. The program prints out the unit, number of the first sample, and the number of samples, for all experiments, starting with the experiment with the earliest measurement time, and

then returns to Control.

Disc.

The keyboard indicator is reset, and the system time and DISC are printed out. A code E is transmitted to the disc unit, and the ouput buffer closed.

The operator is instructed to remove the old disc and insert a new one. The new disc is initialized, a new data file is created, and the output buffer opened. Should an error occur during this sequence, a warning message is displayed. The operator is then instructed to re-insert the disc.

The disc byte counter is then reset, and the system returns to Control.

Time.

The keyboard indicator is reset, and the system time and TIME are printed out. The date and time when the system was initialized are also printed out, and the operator indicates whether those have to be modified. If not, the system returns to Control.

If the date or time have to be modified, the new start date and time are entered from the keyboard and are printed out. The operator types in a new system time which is printed out. The operator is then instructed to close the timing switch on the unit selected as a master timer, at the correct instant, and the system returns to Control.

If the system is being initialized, the operator is instructed to close the timing switch on the unit selected as master timer, at

the correct instant, and the system returns to Control.

Stop.

The keyboard monitor is reset, and the system time and STOP are printed out. The system is brought to a halt in an orderly fashion by a BASIC PAUSE statement.

The system can be restarted by depressing the CONTINUE key on the keyboard, which causes the system to return to Control.

Help.

The keyboard monitor is reset and the system time and HELP are printed out. A list of program selector codes is printed out together with a short explanation.

The system then returns to Control.

Master Timer.

The keyboard indicator is reset, and the system time and MASTER are printed out. The operator types in the unit number for the new master timer. If this is not recognised, a warning message is displayed, and the process repeated.

The operator is directed to close the timing switch on the new master timer unit, and a code is sent to the old master timer unit cancelling the master timer function. A code is then sent to the new master timer unit enabling the master timer function, and the system returns to Control.

Data Display.

This program is entered as a result of the timing indicator being set to 2 in the Control program. The timing indicator is reset to 0, and a code is sent to the unit selected in the Data Demand program instructing it to carry out measurements on the selected sample. This information is then transmitted back to the HP85 computer.

The value of the A/D converter output for resistivity, resistivity reference, temperature, and temperature reference, for the sample, are isolated, and the values of resistivity, temperature, and corrected resistivity are calculated, and the display is cleared.

If data demand mode D has been selected, then the required A/D output from those above will be displayed with 0.5 added. System time, unit number, sample number, and A/D converter output, are displayed according to the format:-

10.5955 1 14 114.5

If resistivity, temperature, or corrected resistivity, has been selected, then system time, unit, sample number, and the required value are displayed using the format:-

10.5955 1 14 124.42

for resistivity values, and

for temperature values.

The system returns to Control.

Service Request (SRQ) Interrupt.

Serice requests cause the current program line to be completed, and then a jump to the Service Request Interrupt routine.

Service requests can only be generated by the master timer measurement unit. When a service request occurs, further SRQ interrupts are disabled, and a serial poll is carried out on the master timer unit. This causes the unit to transmit an SRQ status byte to the HP85 computer.

If bit 0 of the status byte is set, then a system timing pulse has occurred. The timing pulse counter is incremented, and the timing indicator set to 1. The SRQ is then cleared, interrupts are enabled, and the system returns from interrupt.

If an SRQ has occurred without bit 0 of the status byte being set, and the data demand is not set, the program jumps to the return sequence. If the data demand indicator is set, the timing indicator is set to 2, and the program then jumps to the return sequence.

The return sequence causes the interrupt to be cleared, enables further SRQ interrupts, and returns to the next program line prior to the interrupt.

Keyboard Interrupt.

A keyboard interrupt is generated when the function key 1 on the computer keyboard is depressed. This causes the current program line to be completed, and then a jump to the Keyboard Interrupt routine.

The keyboard indicator is set and the program jumps to the next program line prior to the interrupt.

6.3.3. Microprocessor Software.

This program is held on an EPROM in the memory and interface unit (Figure K.7) of the measurement unit, and is written in R6502 machine code. Figure 6.7 is a software system diagram which will be used to describe its operation.

The program is entered by causing a reset on the microprocessor. This takes place when the power supplies are switched ON in the electronics unit, or if the RESET button is pressed on the microprocessor circuit (Figure K.6). This causes the system to enter the Initialization program.

Initialization.

This program resets variables, and sets up the conditions of operation for the IEEE bus interface unit and the two VIA interface units.

The system enters the Control program.

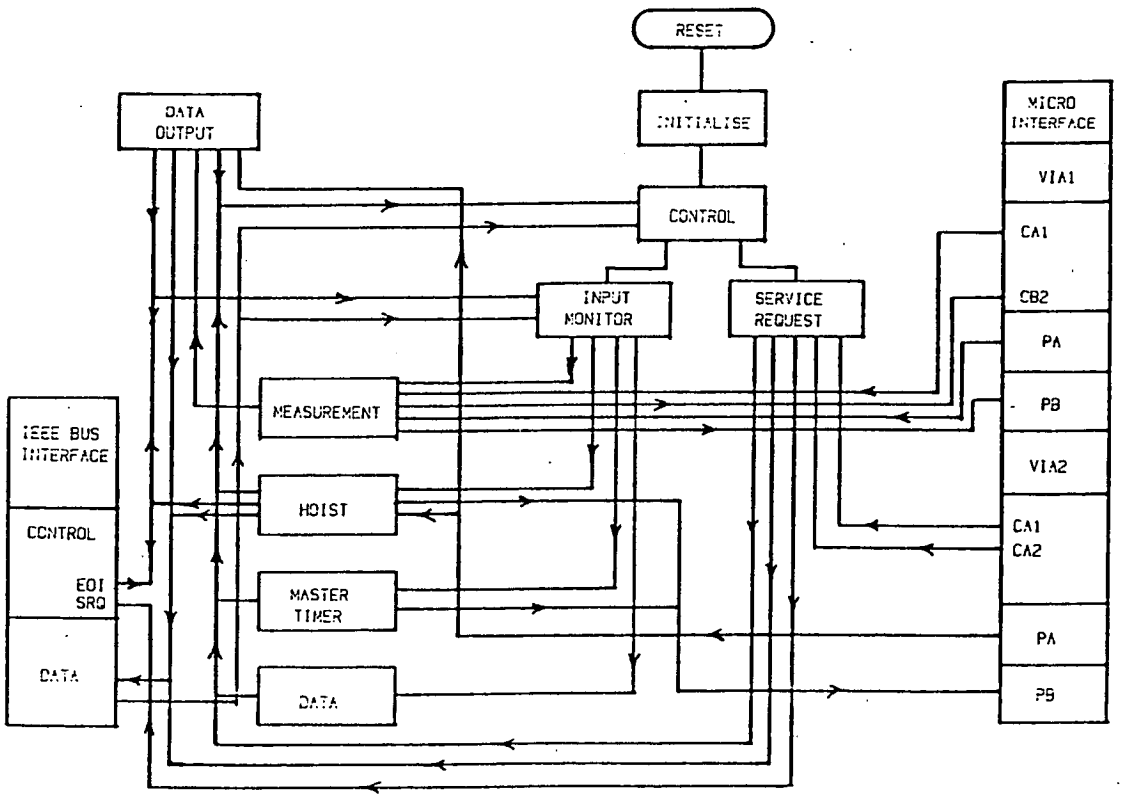

Figure 6.7.
Microprocessor Program Diagram

Control.

The control program is a loop in which two units are monitored. The IEEE bus interface unit is monitored to check whether the measurement unit has been addressed as a listener by the HP85 computer, and VIA2 is monitored to check whether a timing pulse requires service action.

The Control program loop also includes a reset and clear routine for the IEEE bus interface unit.

If the unit is addressed as a listener, the program jumps to the Input Monitor program and, if timing pulses are received, the system jumps to the Service Request program.

Input Monitor.

The Input Monitor checks if a byte of information has been received from the HP85 computer, and if so the byte is stored. This process continues until an END OR IDENTIFY (EOI) signal is received on the IEEE bus control lines, showing that the last byte has been transmitted.

the first byte of information is a program code, which causes a jump to the following programs:-

M	Measurement
H	Hoist
T	Master Timer
D	Data

Measurement.

Of the two bytes of information following the program code, the first is the location of the first sample in the experiment, the second is the number of samples in the experiment.

A logic measurement demand signal is generated and fed to the timing circuit by VIA1 control line CB2. The program then supplies the multiplexer address information on VIA1 output port PB, for the measurement of resistivity, resistivity reference, temperature, and temperature reference, for each sample in turn, and on receipt of a logic 1 CONVERSION COMPLETE signal on control line CA1 of VIA1, stores the digital data from the A/D converter presented on VIA1 input port PA.

When all measurements are completed, the measurement demand signal is cancelled, and the program jumps to the Data Output program.

It proved necessary to include a delay in this program following the storage of each byte of information, to ensure stable operation. This is believed to be due to the characteristics of the VIA units.

Data Output.

The system waits until it is addressed as a talker by the HP85 computer, and then transmits all the stored data to the HP85 computer, obtaining a confirmation signal that the data has been accepted by the HP85 after each byte is transmitted.

The last byte to be transmitted is a measurement unit status byte which is the data at the VIA2 PA port. This byte contains the

following information:-

bit 0 test function selected - logic 1

bit 1 upper hoist end stop reached - logic1

bit 3 lower hoist end stop reached - logic 1

An EOI signal is generated on the IEEE bus control lines when the status byte is transmitted, indicating to the HP85 computer that data transfer is complete.

The system then returns to Control.

Hoist.

The second byte of the data received on the IEEE bus indicates the hoist demand. An OPERATE and UP/DOWN signal is generated, and fed to the control unit by VIA2 output port PB. A delay of approximately 1 s is allowed before the control signal is removed, ensuring that the hoist control circuits are unaffected by transients caused by the starting of the hoist motor.

The system waits until it is addressed as a talker, transmits the measurement unit status byte along with an EOI control signal, and then returns to Control.

Master Timer.

If the second byte of data received on the IEEE bus is a zero, the routine to inhibit the master timer function is entered. The master timer signal fed to the control unit from VIA2, is cancelled, and VIA2 is inhibited from indicating master timer pulses on control line CA1. The system returns to Control.

If the second byte of data received from the IEEE bus has

value 1, a master timer signal is sent to the control unit VIA2 output port PB. VIA2 is instructed to recognise master timer pulses received from the timing circuit on VIA2 control line CA1.

The system returns to Control.

Data.

If the second byte of data received from the IEEE bus has value 1, VIA2 is instructed to recognise 0.95 Hz data timing pulses on control line CA2.

If the second byte is zero, VIA2 is disabled from recognising data pulses.

The system then returns to Control.

Service Request SRQ.

This routine is entered as a result of the VIA2 indicator being monitored in the Control program.

The IEEE bus SRQ function is reset.

If VIA2 indicates that a master timing pulse has been received on control line CA1, a data byte with bit 0 set to logic 1 is stored. If VIA2 indicates that a data timing pulse has been received on control line CA2 a data byte with bit 1 set to logic 1 is stored.

VIA2 is cleared, and the stored data byte transferred to the serial poll register of the IEEE bus interface unit. This automatically generates an SRQ signal on the IEEE bus control lines. The program then waits until the HP85 computer carries out a serial poll which transfers the data byte to the HP85. It has then been

found necessary to insert a delay before normal operation continues to ensure stability.

The system returns to Control.

6.3.4. Environmental Control.

A water bath with controlled temperature and a tray to allow the samples to be withdrawn from the bath by the hoist, are not available. Current experiments do not require that the samples be stored underwater.

6.3.5. Data Output and Graph Plotting.

The data output from the developed equipment is, in principle, similar to that of the prototype equipment (Section 5.3.4). The data is however available on magnetic disc, and can be loaded into the data processing program without having to be transcribed using the computer keyboard.

The method of graph plotting is similar to that for the prototype equipment. However, in the averaging mode, averages are presented if there are three or more samples. Temperature is also plotted on the graph. Figure 6.8 is an example of a resistivity and temperature graph. Figure 6.9 shows the format of tabulated data output.

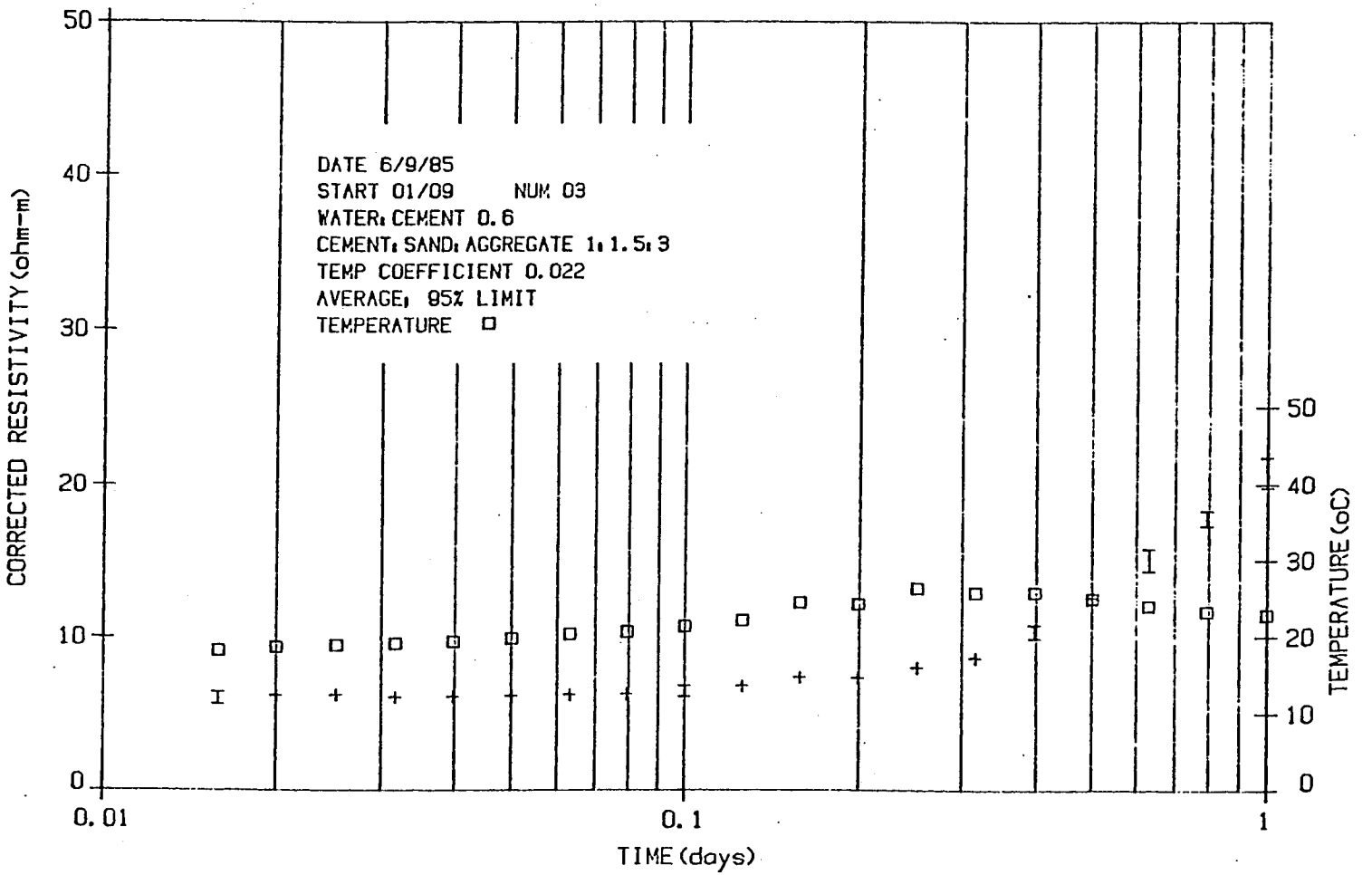

Figure 6.8.
Resistivity and Temperature Graph

DATE 19/9/85
START 01/09 NUM 03
WATER:CEMENT 0.4
CEMENT:SAND:AGGREGATE 1:1.5:3
TEMP COEFFICIENT 0.022

SAMPLE NUMBER 1

TIME	RES	TEMP	C RES
0.0127	7.57	19.2	7.43
0.0160	7.86	19.3	7.75
0.0200	7.90	19.4	7.80
0.0253	7.90	19.8	7.86
0.0317	7.90	19.7	7.85
0.0398	7.90	19.9	7.83
0.0501	7.86	20.1	7.88
0.0632	7.86	20.8	8.00
0.0795	7.90	21.0	8.06
0.1001	8.22	21.1	8.42
0.1259	8.22	21.4	8.49
0.1585	8.51	22.0	8.89
0.1995	9.17	22.8	9.74
0.2512	10.17	27.8	11.90
0.3163	11.85	28.9	14.18
0.3983	16.85	27.2	19.51
0.5012	22.89	25.6	25.69
0.6310	30.49	23.0	32.50
0.7944	39.61	20.1	39.70
1.0001	45.67	20.5	46.15

SAMPLE NUMBER 2

TIME	RES	TEMP	C RES
0.0127	7.57	19.2	7.43
0.0160	7.57	19.3	7.46
0.0200	7.57	19.2	7.43
0.0253	7.57	19.3	7.46
0.0317	7.90	19.7	7.85
0.0398	7.54	19.6	7.48
0.0501	7.90	20.1	7.92
0.0632	7.57	20.4	7.64
0.0795	7.57	20.7	7.68
0.1001	7.90	20.9	8.05
0.1259	7.90	21.3	8.11
0.1585	8.55	21.8	8.90
0.1995	8.88	22.2	9.31
0.2512	9.88	26.5	11.28
0.3163	11.23	28.1	13.22
0.3983	15.34	26.4	17.48
0.5012	20.86	24.6	22.95
0.6310	28.54	22.4	30.85
0.7944	36.18	19.4	35.74
1.0001	42.72	20.3	43.60

SAMPLE NUMBER 3

TIME	RES	TEMP	C RES
0.0127	7.25	18.6	7.02
0.0160	7.22	19.2	7.08
0.0200	7.57	19.3	7.45
0.0253	7.57	19.3	7.45
0.0317	7.57	19.7	7.53
0.0398	7.90	19.7	7.85
0.0501	7.57	20.0	7.57
0.0632	7.57	20.7	7.68
0.0795	7.57	20.7	7.68
0.1001	7.86	21.1	8.05
0.1259	8.19	21.4	8.45
0.1585	8.55	22.0	8.93
0.1995	8.88	22.6	9.39
0.2512	9.88	27.8	11.56
0.3163	11.85	27.3	13.75
0.3983	16.85	26.0	19.06
0.5012	22.89	24.3	25.05
0.6310	30.65	21.9	31.95
0.7944	39.14	19.3	38.49
1.0001	45.42	20.1	45.52

Figure 6.9.
Tabulated Data Output

6.4. Calibration and Accuracy.

6.4.1. System Parameters and Predicted Accuracy.

System accuracy has not been changed by the removal of the temperature rectifier circuit, and is slightly improved by the inclusion of a second decimal place in calculated data. The theoretical uncertainty graphs for the prototype equipment are therefore assumed to apply to the developed system (Figures 5.17 - 5.20).

6.4.2. Calibration Procedures.

Calibration procedures require the equipment described in Section 5.4.2. Calibration temperature is monitored by touching a contact probe onto the electrode, close to the temperature transducer, to avoid possible inaccuracies because of the thermal inertia of the components.

The detailed calibration procedures are similar in form to those for the prototype equipment, and are presented in Appendix L.

6.5. Results.

6.5.1. Accuracies.

Figure 6.10 shows measurements of error between resistivity as measured by the system, and as measured by a Wayne-Kerr Universal

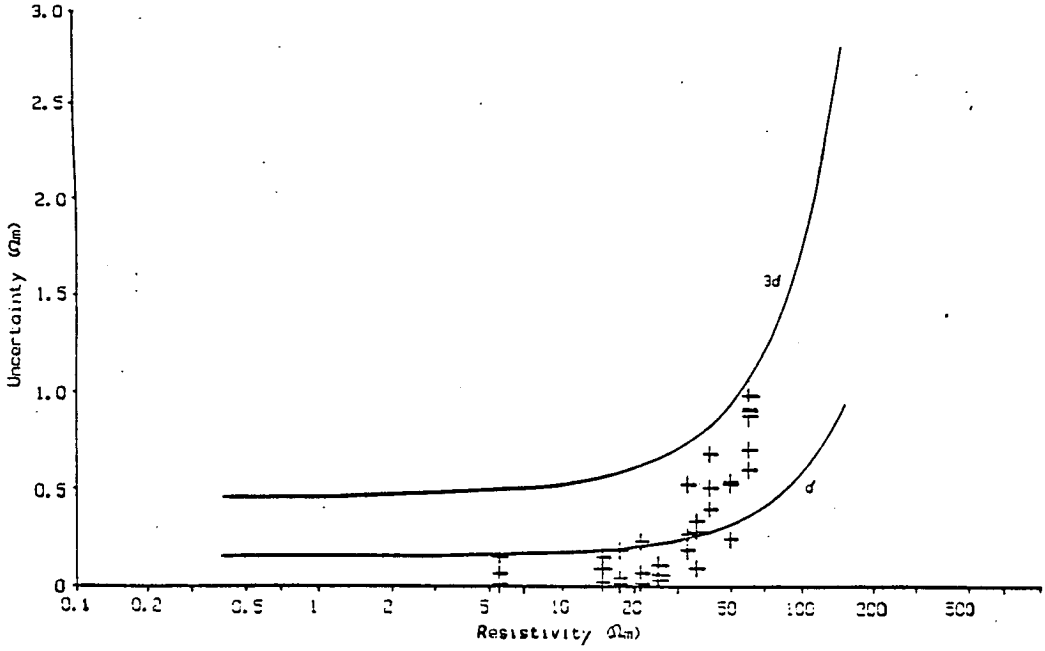

Figure 6.10.
Resistivity Accuracy

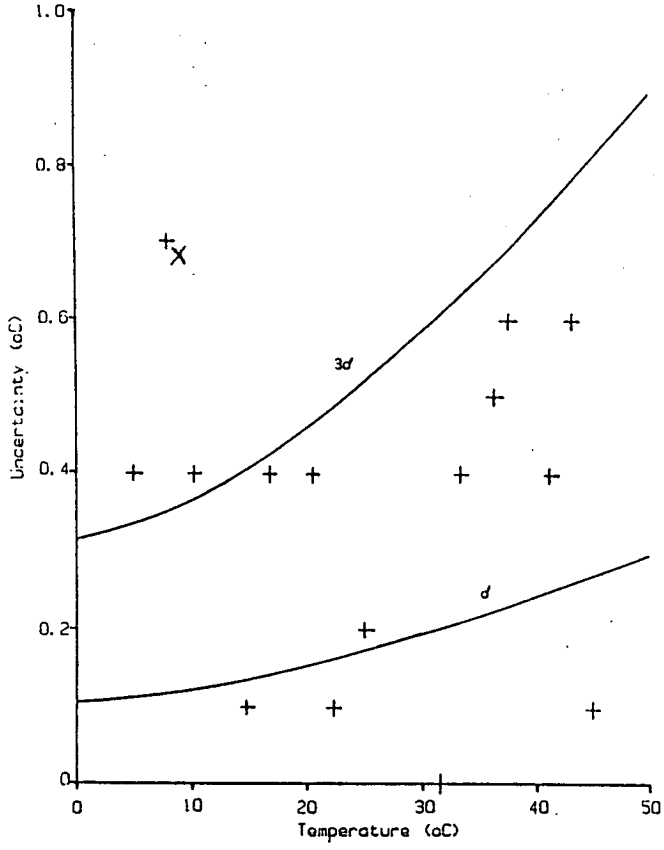

Figure 6.11.
Temperature Accuracy

Bridge Type B221, which has an accuracy of 0.1% and operates at 1.592 kHz. The measurements are for uncorrected resistivity so that the results are not dependent on temperature. The estimated uncertainty (Section 5.4.3) is also shown. The measurements, carried out on on concrete samples, give results similar to the prototype system with uncertainty in the region of 0.2 Ωm at low resistivities, and 1% at high resistivities.

Figure 6.11 shows measurements of error between temperature as measured by the system and that measured by a Technoterm 5500 digital thermometer using a contact probe, which is the equipment used for calibration. The results presented are therefore of relative accuracy, and take no account of uncertainties in the calibration equipment. The estimated uncertainties (Section 5.4.3) are also presented.

The results correspond to the predicted values, except for point X which assumed to be due to a reading error. The discrete nature of the temperature output is illustrated by the measurement errors.

6.5.2. Measurements on Concrete.

The following measurements on concrete were carried out before the incorporation of blocking capacitors described in Section 6.1.6. There is an error of approximately +1 Ωm at low values of resistivity, rising to +2 Ωm at high values, because of asymmetry in the energising voltage waveform.

Figures 6.12 - 6.22 show the initial series of results for

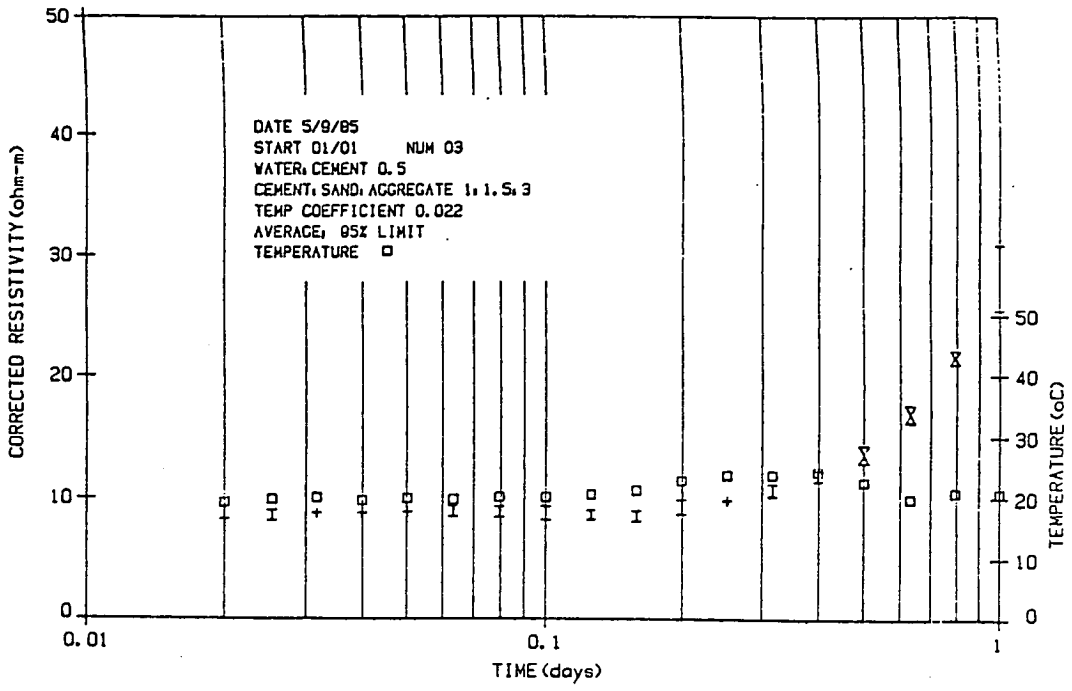

Figure 6.12.
Test 1

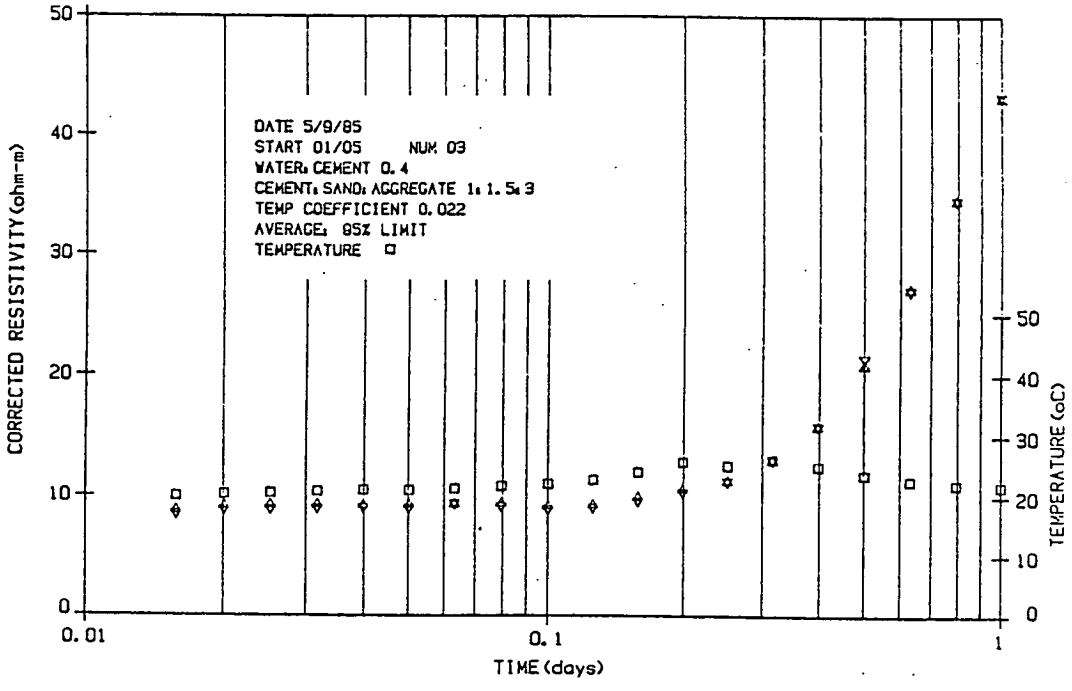

Figure 6.13.
Test 2

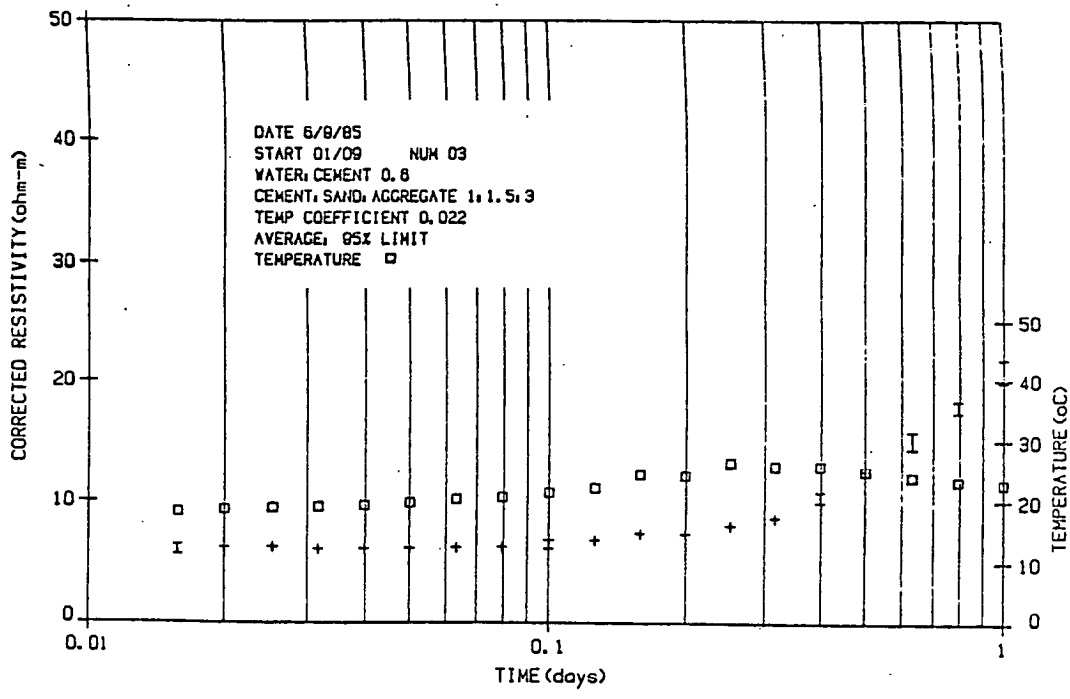

Figure 6.14.
Test 3

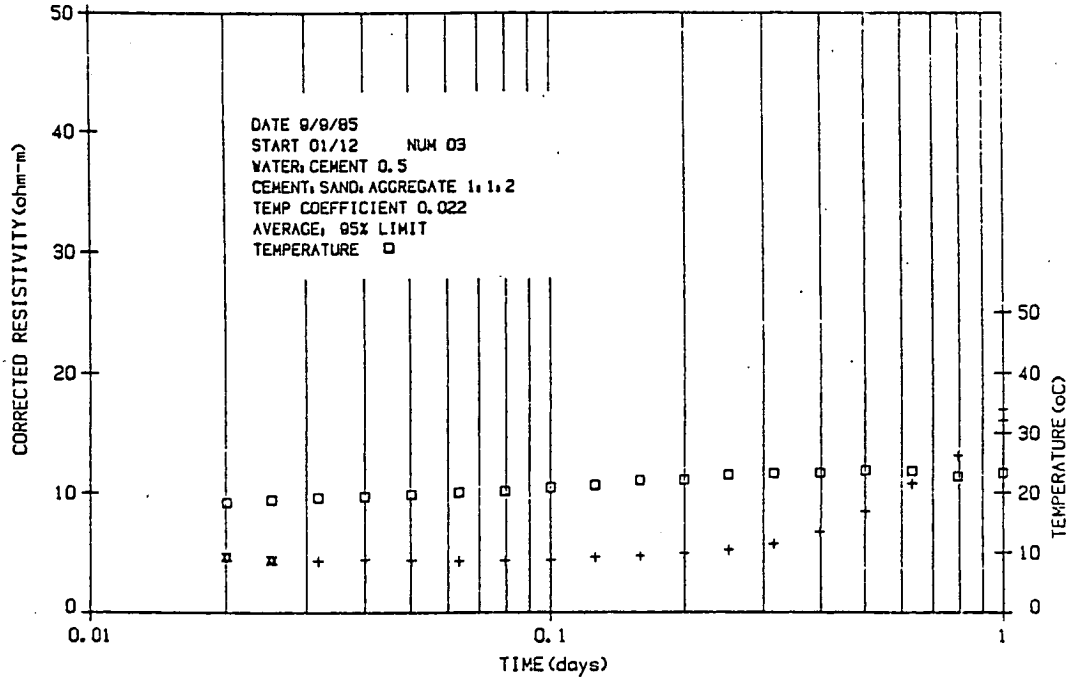

Figure 6.15.
Test 4

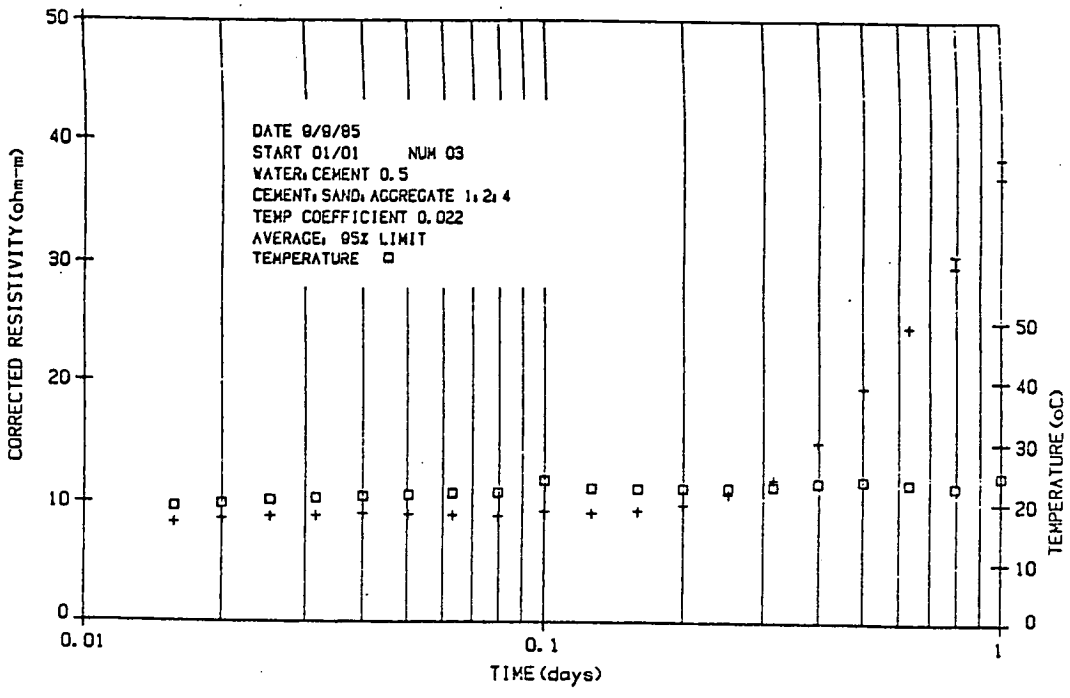

Figure 6.16.
Test 5

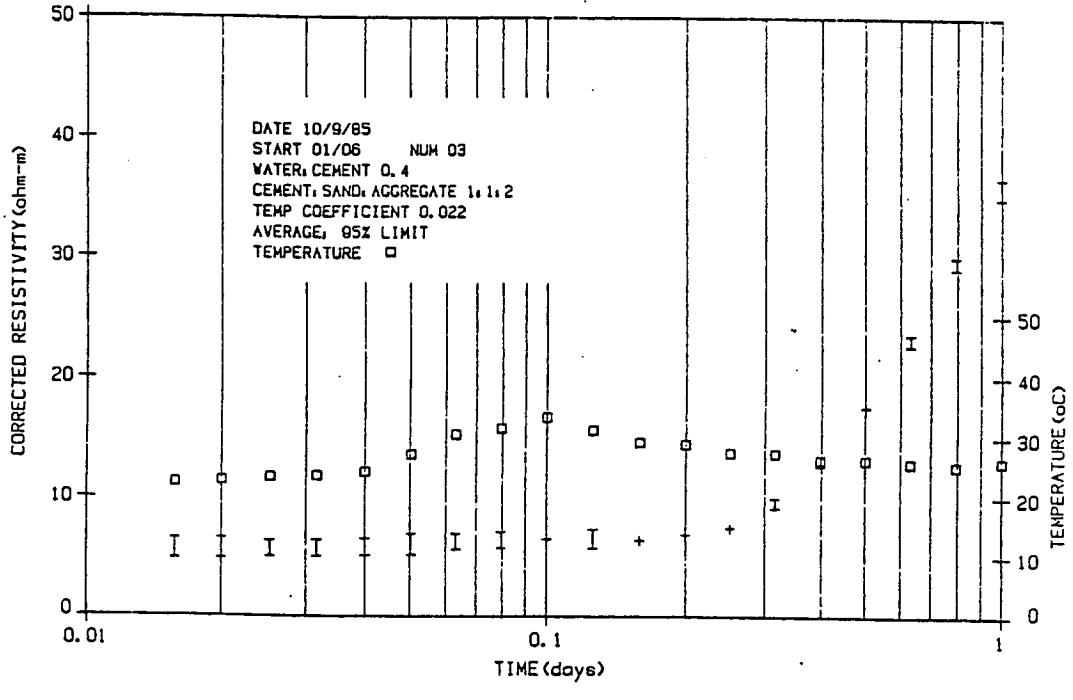

Figure 6.17.
Test 6

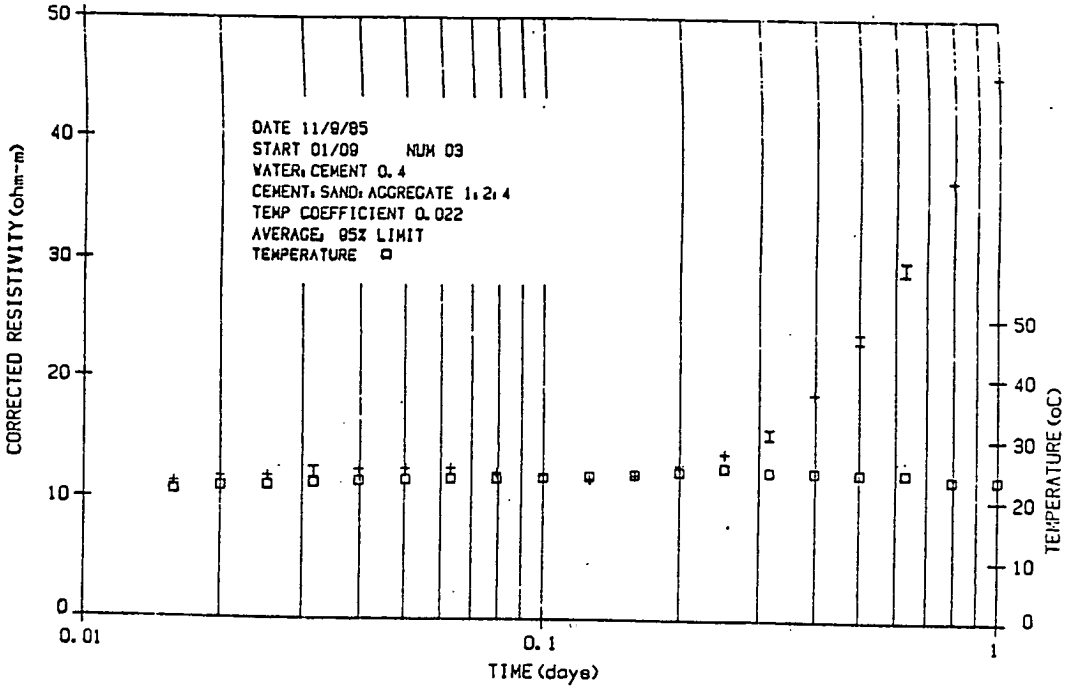

Figure 6.18.
Test 7

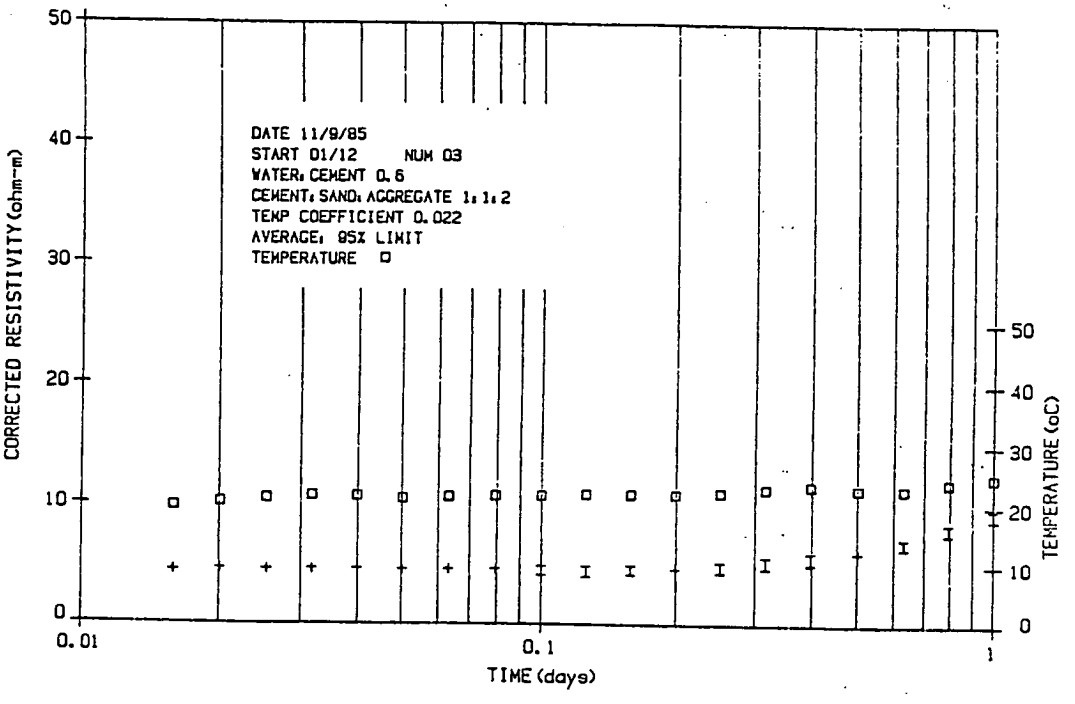

Figure 6.19.
Test 8

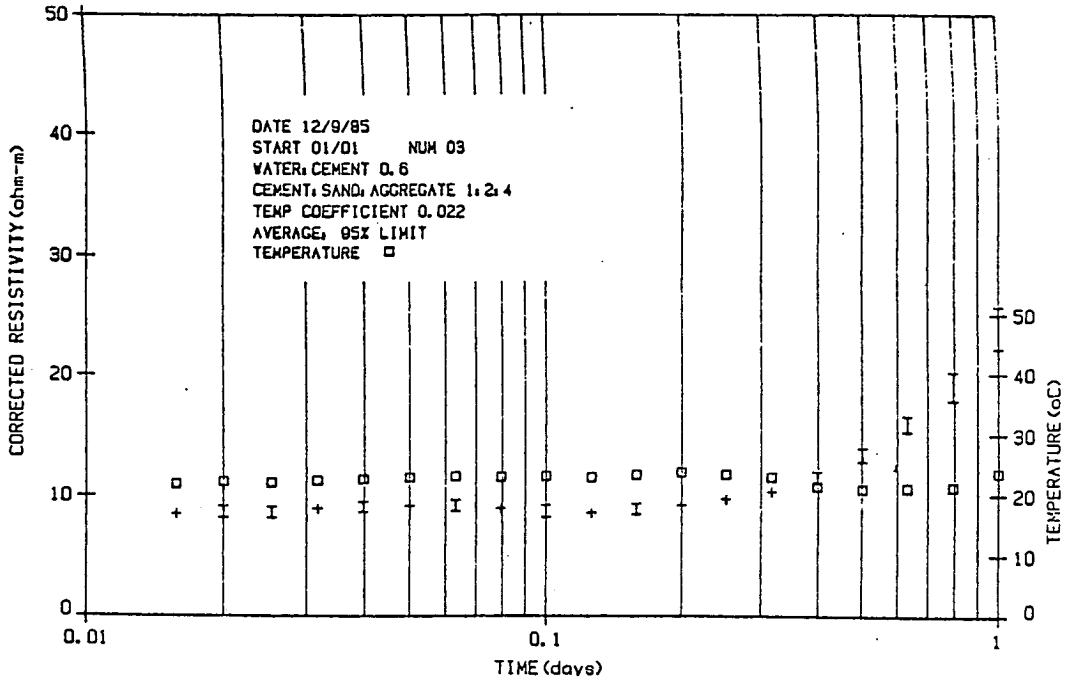

Figure 6.20.
Test 9

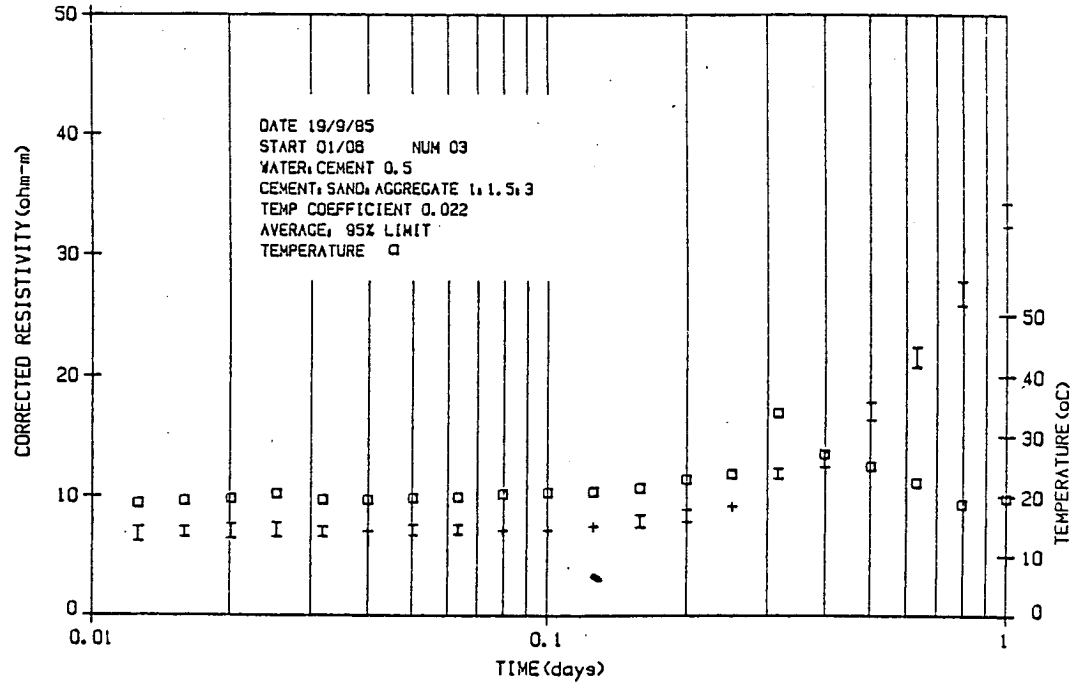

Figure 6.21.
Test 10

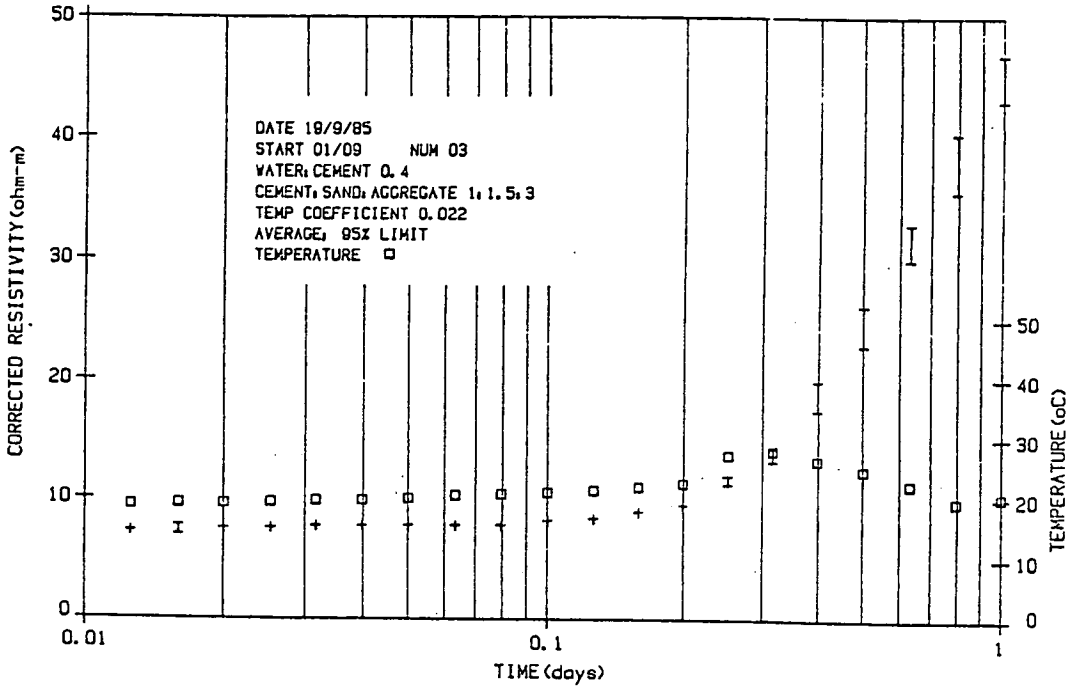

Figure 6.22.
Test 11

corrected resistivities of different concrete mixes. The materials used were:-

(i) cement - Ordinary Portland Cement supplied by Blue Circle, Dunbar

(ii) sand - Tay sand

(iii) aggregate - crushed whinstone, 20 mm nominal

The sand and coarse aggregate were both supplied by D.Fisher, Balerno, Edinburgh.

Because neither sand nor aggregate was dried beforehand, there is uncertainty in the water/cement ratios used. Table 6.2 presents statistical data from the tabulated output:-

			Resistivity at 0.1 day		Resistivity at 1 day	
Test	W/C	C/S/A	Av. (Ωm)	S.D. (Ωm)	Av. (Ωm)	S.D. (Ωm)
1	0.5	1:1.5:3	8.76	0.39	28.22	1.94
2	0.4	1:1.5:3	9.09	0.14	43.27	0.09
3	0.6	1:1.5:3	6.46	0.25	20.76	0.69
4	0.5	1:1:2	4.37	0.17	16.53	0.33
5	0.5	1:2:4	9.26	0.10	37.83	0.54
6	0.4	1:1:2	6.49	0.12	35.72	0.59
7	0.4	1:2:4	12.01	0.18	45.22	0.00
8	0.6	1:1:2	4.54	0.26	9.35	0.32
9	0.6	1:2:4	8.69	0.34	23.90	1.26
10	0.5	1:1.5:3	7.13	0.17	33.28	0.68
11	0.4	1:1.5:3	8.17	0.17	44.89	1.36

Table 6.2.
Statistics of Resistivity Measurements

Note that for all tests except for test 2, there were 3 samples, while for test 2 there were 2 samples.

Figure 6.23 shows graphs for cement/sand/aggregate ratio 1:1.5:3, and various values of water/cement ratio, superimposed, while Figure 6.24 shows graphs for water/cement ratio 0.5, and various values of cement/sand/aggregate ratio, superimposed.

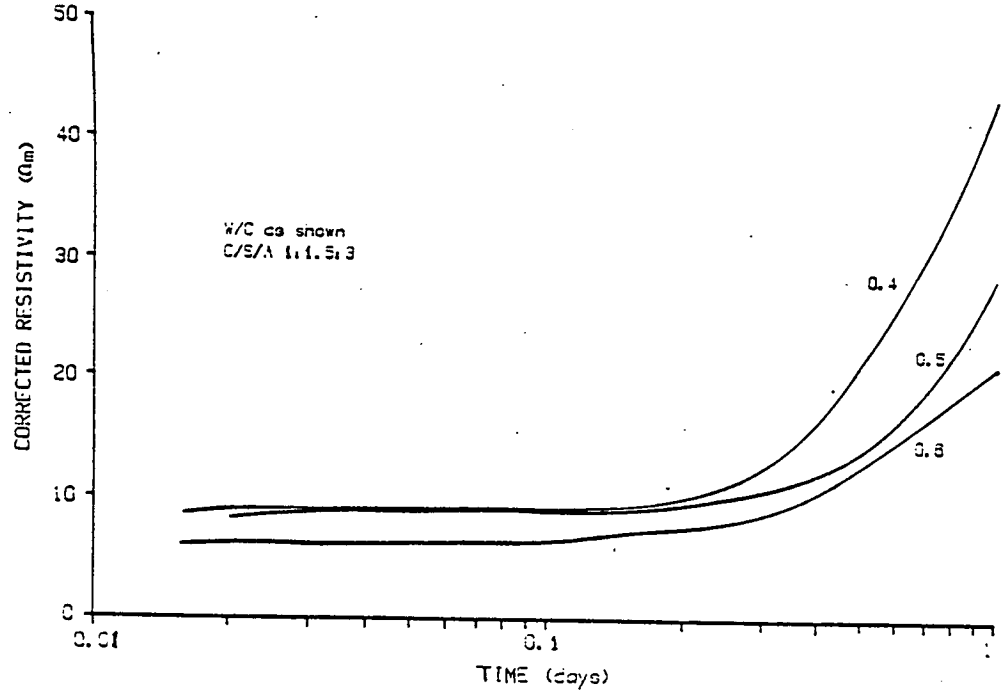

Figure 6.23.
Constant C/S/A Ratios

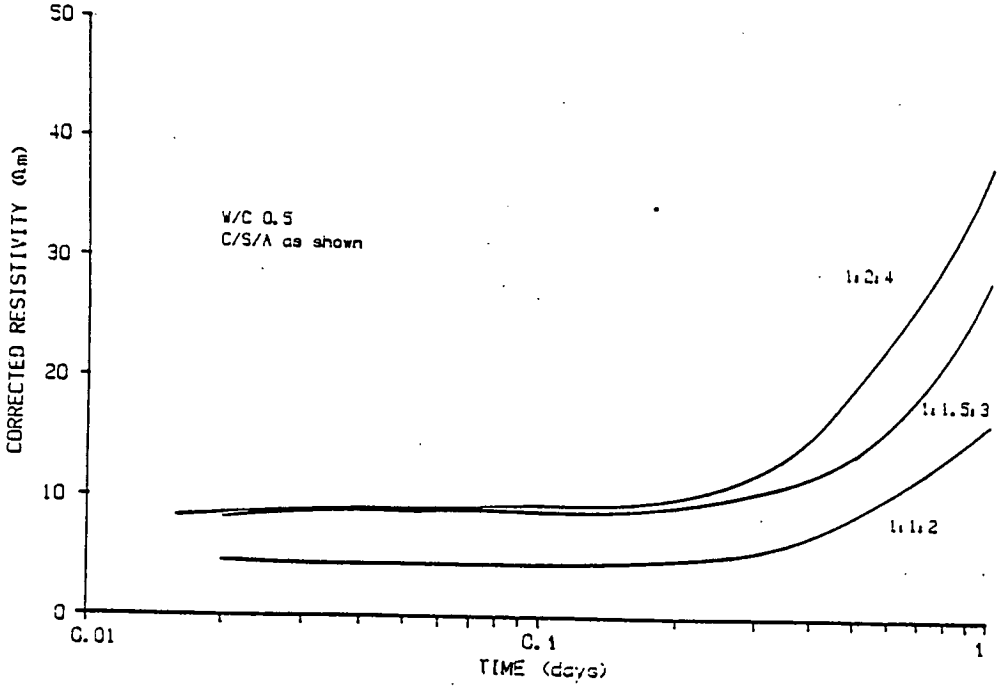

Figure 6.24.
Constant W/C Ratio

Figure 6.25 shows the resistivity values of Table 6.1 plotted, with the water/cement ratio and cement/sand/aggregate ratio also indicated.

6.5.3. Low Frequency Relaxation.

When comparative resistivity measurements were carried out for assessment of accuracy, the a.c. bridge was also used to measure the capacitance of the samples. The capacitance measured was the equivalent shunt capacitance. The series capacitance was calculated from this value [66](Appendix D), and the relaxation time

$$\tau_r = CR$$

and hence the relaxation frequency

$$f_r = \frac{1}{2\pi\tau_r}$$

was calculated. Figure 6.26 shows relaxation frequency plotted against resistivity.

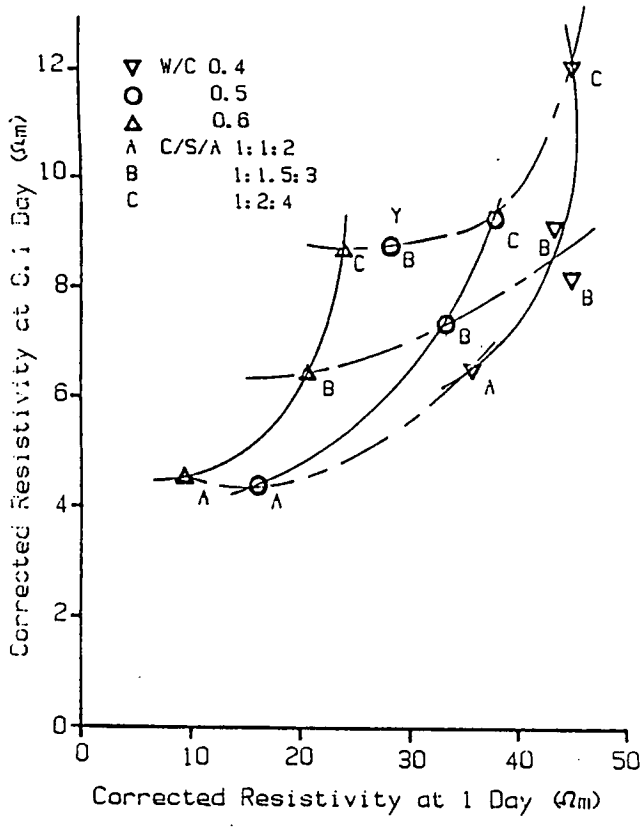

Figure 6.25.
Combined Resistivity Graph

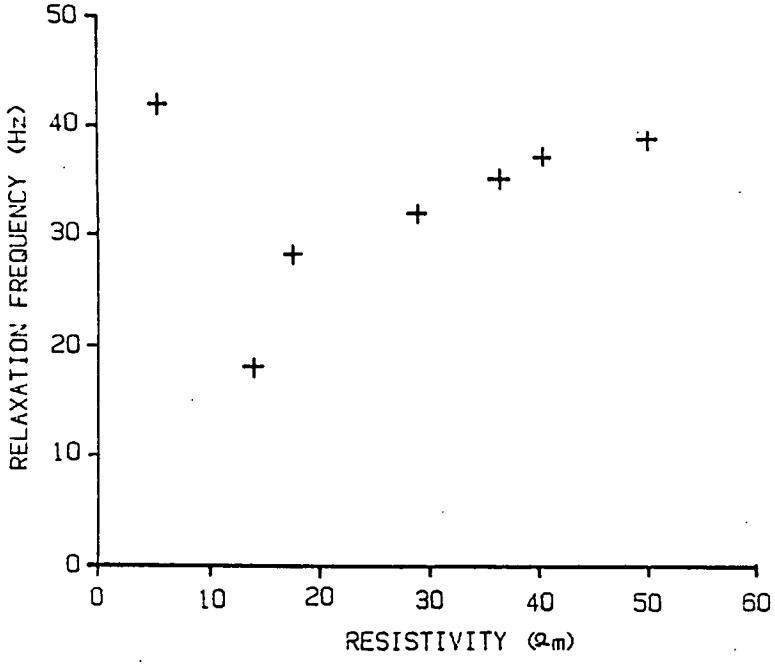

Figure 6.26.
Relaxation Frequency

6.6. Discussion and Conclusions.

6.6.1. Equipment

The equipment in general operates within the predicted uncertainty limits. The accuracy can be improved over the temperature range by calibrating the thermometer used to set up the temperature monitoring system (Section 6.4.2). The equipment would then be working within the relative temperature uncertainty limits presented in Figure 6.11. Further improvement in accuracy would require that the 8 bit A/D converter be replaced by a 12 or 16 bit converter. While the system is currently acceptable for the measurement of the resistivity of concrete with resistivities generally greater than 5 Ωm, it is less appropriate for the accurate measurement of the resistivity of cement paste with resistivities less then 5 Ωm. Accurate measurements on such material will require the replacement of the A/D converter.

The equipment has been shown to be a reliable and convenient system for the measurement of the low frequency resistivity of concrete.

6.6.2. Low Frequency Resistivity of Concrete.

The general shape of the resistivity/time graphs agrees with that predicted in Section 3.7.2 for a similar mix. In Section 3.7.2 the initial resistivity is expected to be in the range 2.3 to 2.5 Ωm, rising to 20 to 30 Ωm at 50% hydration. The mix is assumed to

have water/cement ratio 0.475, and cement/total aggregate ratio 1:4.5. It has not been possible to predict when 50% hydration will occur, but resistivities in the range 20 to 30 Ωm are obtained after 0.8 day for similar mixes (Figures 6.12 and 6.21). The initial resistivity for these results is in the range 7 - 9 Ωm, or in the range 6 - 8 Ωm allowing for the systematic error which was present when the results were taken.

The initial resistivity is considerably higher than the predicted values, which assumed that only a small fraction of the water in the mix was effectively removed from the conduction process. The values obtained would suggest that that approximately 60% of the water is not available for conduction at this stage. It would be expected that the amount of water removed from the conduction process in the initial stage is dependent on the amount of cement available.

It should be noted that for test 2 and test 11, both with similar mixes, there are differences in the values for initial resistivity. This is believed to be due to the water content of the sand and aggregate, which has not been taken into account in these experiments.

Figures 6.23 and 6.24, showing superimposed graphs, could be used as a method of quality control by defining limits for the resistivity of the required mix. From these graphs, it would seem that the supposed mix of test 1, water/cement ratio 0.5 and cement/sand/aggregate ratios 1:1.5:3, is in error. The possibility of obtaining similar resistivity graphs with different mixes must be considered.

Figure 6.25, which is a plot of resistivity data at 0.1 and 1 day, suggests that such data defines a particular mix uniquely, and that such a graph could be used to assess the mix for a given sample. For example, point Y, which corresponds to test 1, appears to be in error, and has too much water and aggregate, indicating too little cement.

To obtain a usable calibration graph, the water content of the sand and coarse aggregate would have to be closely controlled. This suggests however that resistivity measurements could be used on-site to obtain a mix with a specific water content, which had been designed under controlled conditions in the laboratory.

6.6.3. Low Frequency Relaxation Effects.

While Figure 6.26 shows considerable variation in the relaxation frequency, the value is fairly constant over a wide range of resistivity values, indicating that the relaxation time is also fairly constant over this range of resistivities.

The argument presented in Appendix D [66], suggests that the relaxation time is given by the product of the bulk resistance of the concrete and the capacitance due to an insulating layer, and that this value should remain constant as the resistivity of the sample increases with time. The results shown in Figure 6.26 therefore support the theory that low frequency relaxation effects in concrete are due predominately to electrolytic effects. This is also supported by the waveforms of Figure 5.3.

7. HIGH FREQUENCY MEASUREMENTS.

7.1. Introduction.

It became clear early in the development of the low frequency measuring equipment that there were certain conditions that the equipment could not detect. For example the presence of entrapped air in concrete cannot be differentiated from the presence of additional aggregate, since in general, aggregate has a very high value of resistivity. (Section 3.6.)

Taylor and Arulanandan [69] measured the electrical impedance of cement pastes over the frequency range 1-100 MHz and derived values for conductivity and dielectric constant. They attempted to assess the proportion of free water in their samples as the hydration of the cement progressed. In the experiments described here, similar techniques have been applied to concrete with the initial aim of distinguishing between entrapped air and additional aggregate. Since the dielectric constant of air is 1, and that for aggregate is in the range 3.5 - 15, variations in impedance should be detectable.

These experiments have been described in a paper by Wilson et al [77], which is presented as Appendix M.

7.2. Experimental Method.

7.2.1. Measurement System.

The experimental work has been directed to establishing that entrapped air can be detected by high-frequency impedance measurements, assuming that a low-frequency resistivity test has first been carried out and has indicated a higher than normal value of resistivity.

The basis of the measuring system is the Hewlett-Packard RF Impedance Analyser Type HP4191A, which covers the frequency range 1 to 1000 MHz. The analyser is controlled by a Hewlett-Packard HP85 computer, and data is stored on a magnetic disc. Data is outputted either on the printer of the HP85 computer, or on a graph plotter. The units are interconnected on an IEEE-488 bus system.

The sample geometry used is a 150 mm cube, which is an industry standard for crushing strength measurements [12], and is also that used for low frequency measurements (Section 5.1). Stainless steel plate electrodes are placed on two opposite faces of the cube to form a parallel plate transmission line with the concrete as dielectric. At one end of the electrode system there is a transition to 50 ohm coaxial line which is the form of connection required by the analyser.

The sample arrangement is shown in Figure 7.1., and the complete system is shown in Figure 7.2.

The concrete samples are produced by pouring the mix into PVC moulds in which the electrodes have been positioned. The components

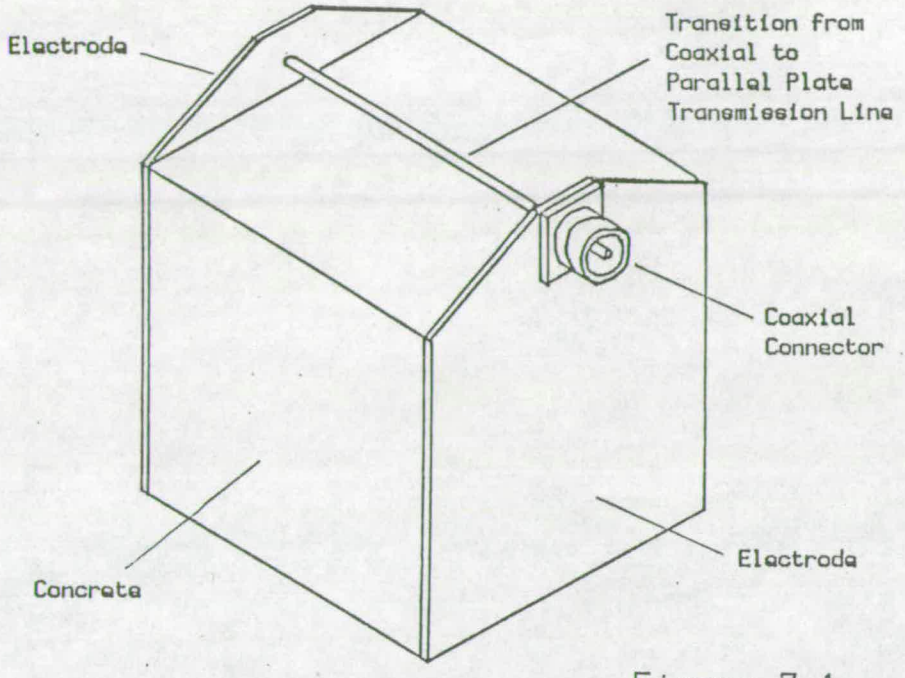

Figure 7.1.
Sample Arrangement

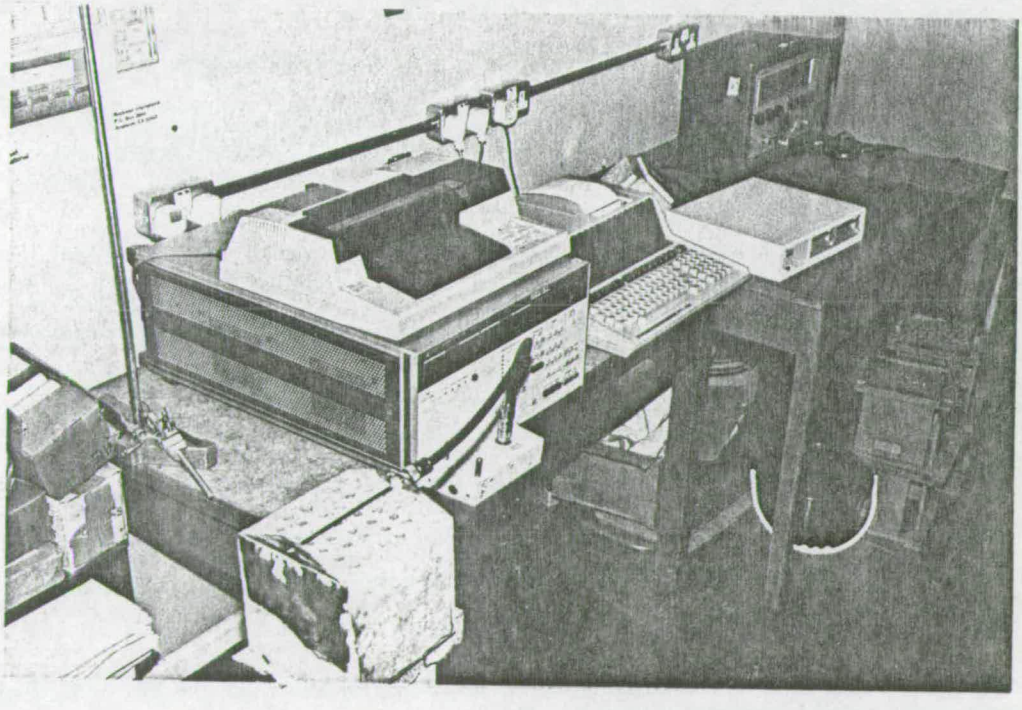

Figure 7.2.
High Frequency Measurement System

for the transition to coaxial line are assembled after the concrete had been poured. It has been found that there is generally a good bond between the concrete and the electrodes, although occasionally problems occur, largely due the handling required to carry out the tests.

After demoulding, the samples were stored in a water bath and withdrawn when measurements were required.

Impedance measurements were carried out over the frequency range 1 - 100 MHz, and also in the range 500 - 700 MHz, where half wave resonance causes an impedance maximum.

In addition to impedance measurements, measurements were taken of the low frequency resistance using an a.c. component bridge which operates at 2 kHz. The temperature of one of the electrodes on each sample was also measured prior to impedance measurements, using an electronic thermometer.

7.2.2. Concrete Samples.

Early trials were largely concerned with establishing the experimental technique, and the development of computer programs for controlling the measurement system and for processing and plotting results.

In initial experiments, the presence of air voids was simulated by adding expanded polystyrene packing chips to the mix. There were difficulties when the samples were vibrated, in that the polystyrene chips rose to the surface. The possibility that the polystyrene was absorbing water had also to be considered.

A more controllable technique was developed which allows a large number of full depth holes to be cast in the concrete. Two moulds were modified to allow 9.5 mm diameter mild steel rods to be passed through the bases. The pattern of rods was arranged in a semi-random manner. One pattern of rods was arranged to give a 5% volume of air in the cube, and the other pattern to give 10%. The rods were enclosed in plastic sleeving to allow withdrawal. The ends of the rods pass through the base of the mould into a thick wooden block, which supports the rods vertically. This system operated satisfactorally, all the rods being successfully withdrawn before demoulding, and the plastic sleeving removed.

Figure 7.3. shows a mould ready for pouring, Figure 7.4. a filled mould, Figure 7.5. the sample with rods and sleeving withdrawn, and Figure 7.6. the sample on demoulding.

Four samples were used to obtain the data presented. These were:-

(i) a normal sample of concrete with water/cement ratio 0.5:1 and cement/sand/coarse aggregate ratio 1:1.5:3

(ii) a sample using the same basic mix, but with additional aggregate added to give an additional aggregate volume of 5%

(iii) a sample using the same basic mix, but with holes moulded in the sample to give an air volume of 5%

(iv) a sample using the same basic mix, but with

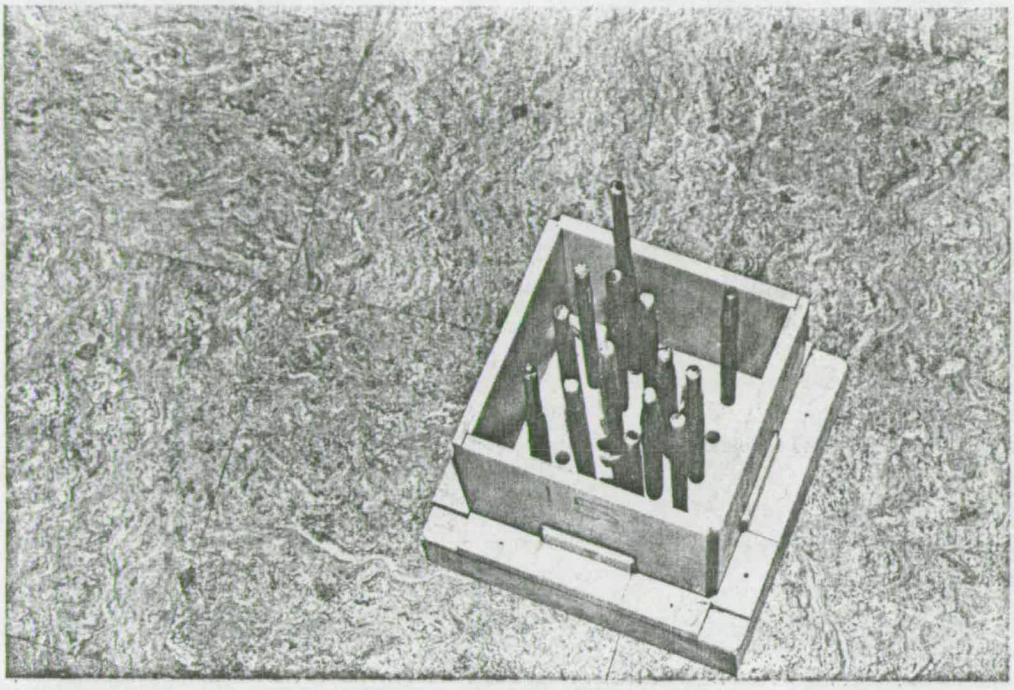

Figure 7.3.
Mould Ready for Pouring

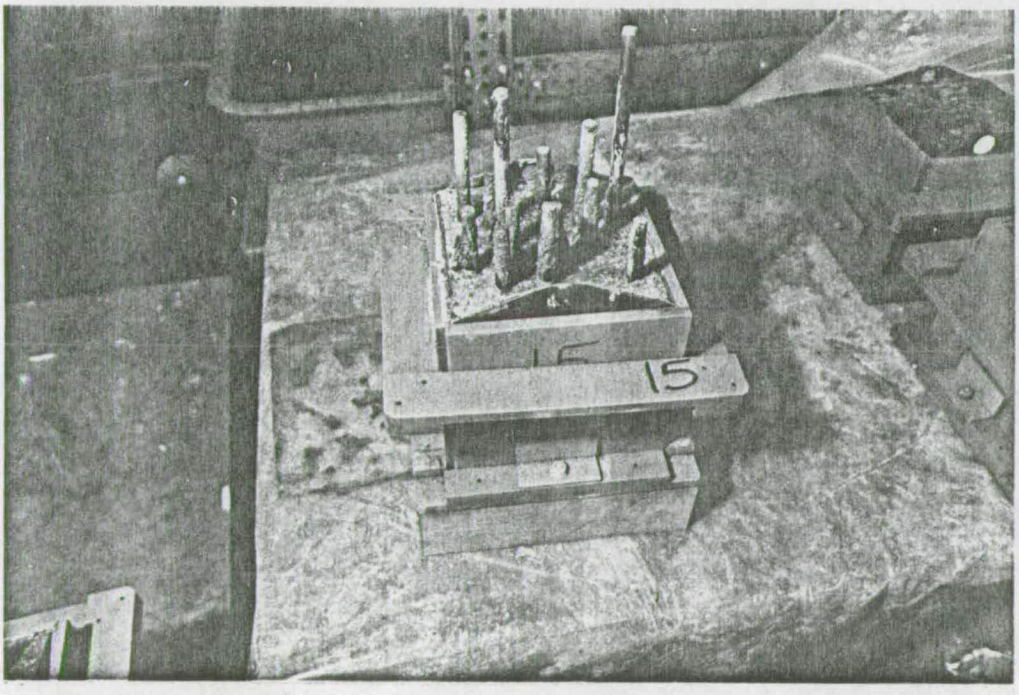

Figure 7.4.
Filled Mould

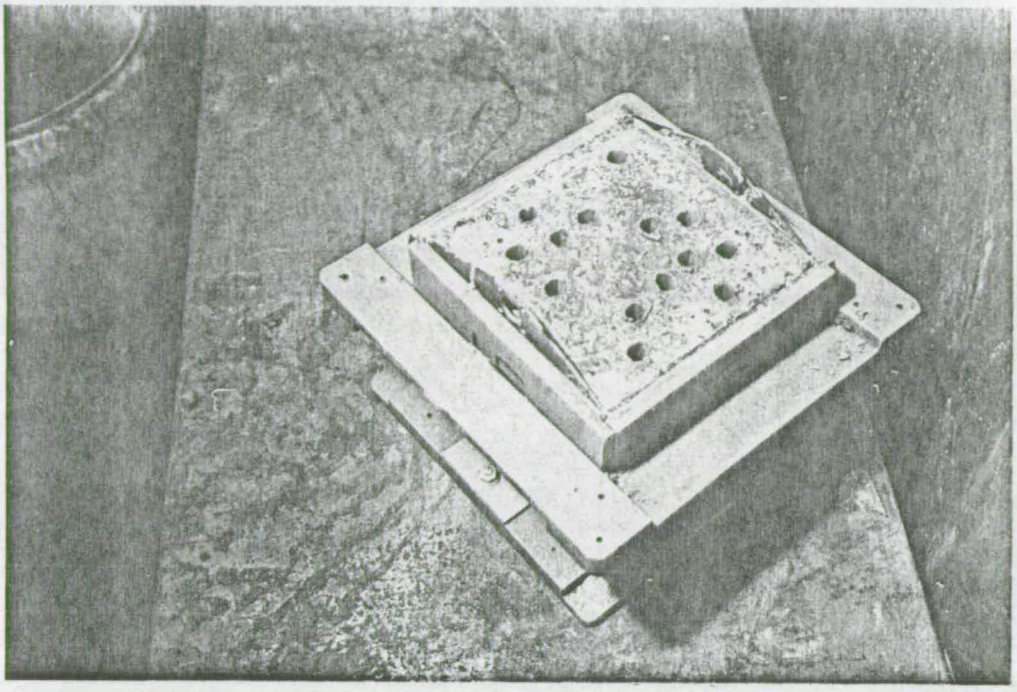

Figure 7.5.
Rods and Sleeving Withdrawn

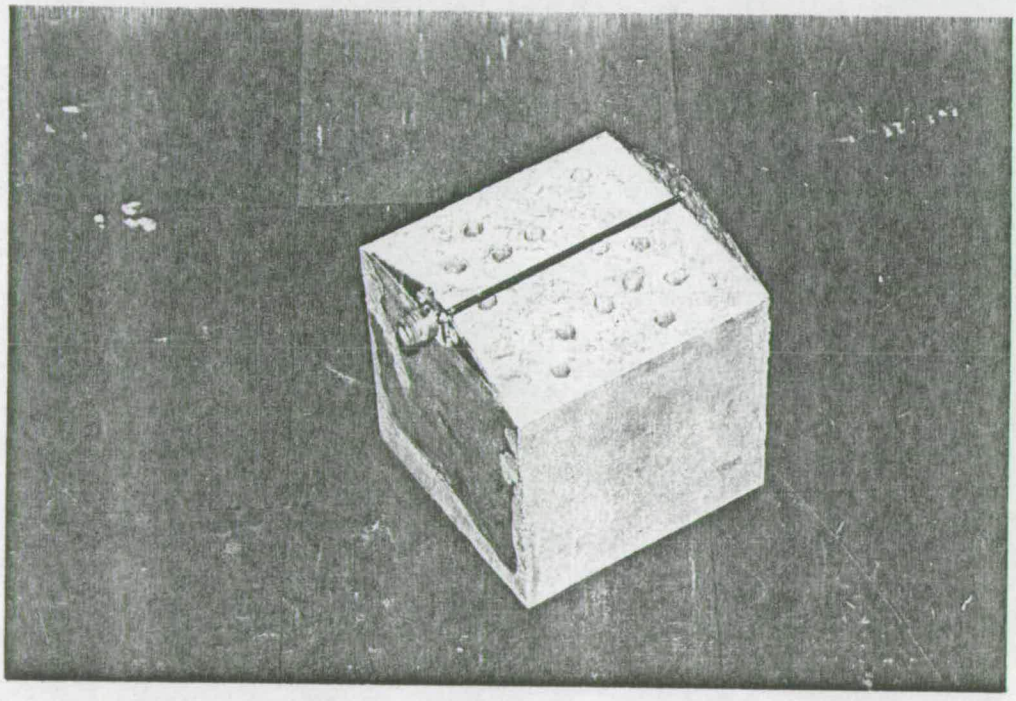

Figure 7.6.
Demoulded Sample

holes moulded in the sample to give an air volume of 10%.

7.2.3. Data Processing.

Programs were developed for the HP85 computer for controlling the impedance analyser, storing the impedance data, tabulating the impedance data in polar form as a function of frequency, and plotting graphs of impedance against frequency, either in polar or cartesian form.

Readings over the frequency range 1 - 100 MHz are taken for 51 points logarithmically spaced, and for the frequency range 500 - 700 MHz, there are 51 linearly spaced points.

7.3. Trial Results.

7.3.1. Lower Frequency Band.

Results of impedance measurements carried out over the frequency range 1 - 100 MHz are shown in Figures 7.7 - 7.10. The times of these measurements following addition of water to the concrete mix are:-

Figure 7.7; 1.05 days; just after demoulding.

Figure 7.8; 1.07 days; after the samples had been stored in water.

Figure 7.9; 6.02 days.

Figure 7.10; 12.85 days.

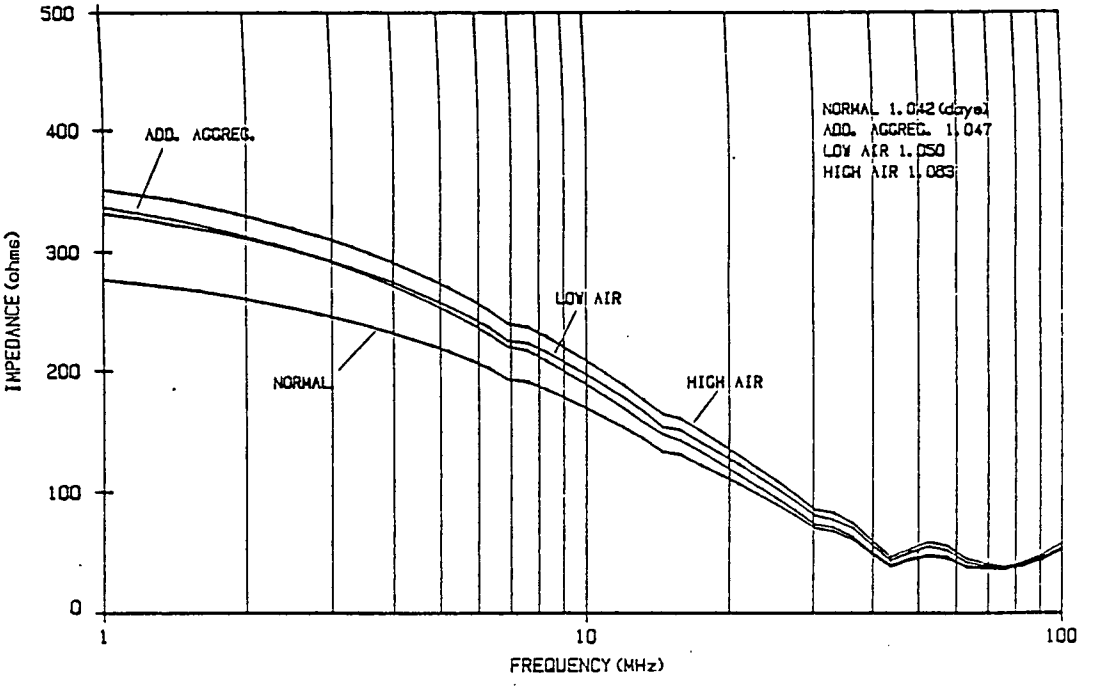

Figure 7.7.
Low Freq. 1.05 Days

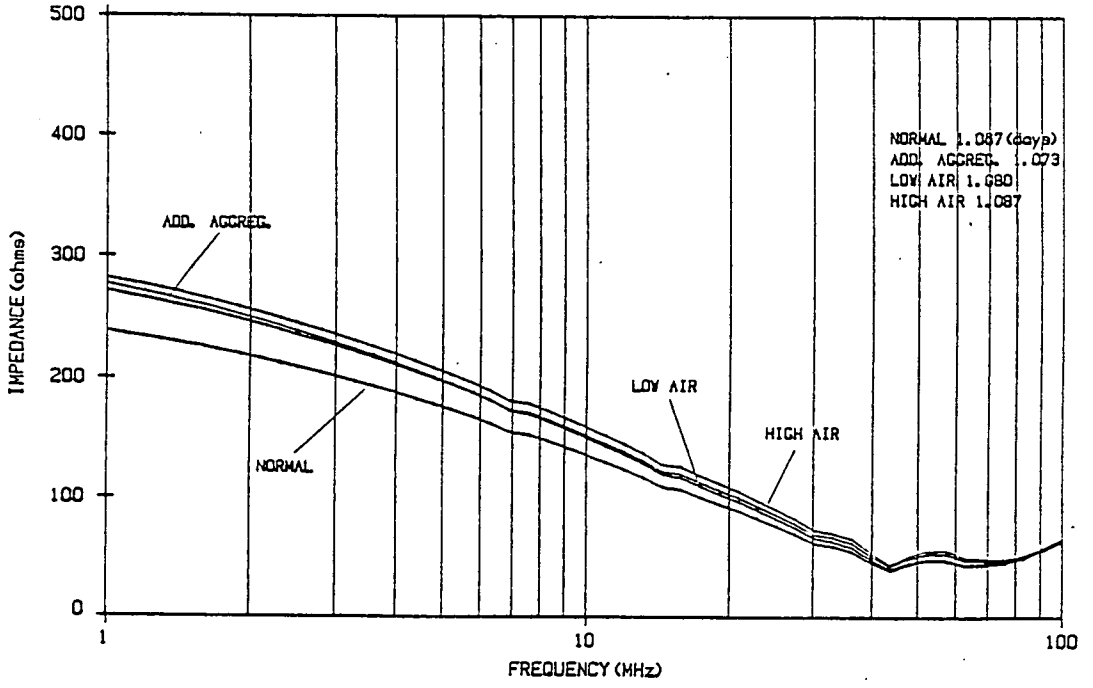

Figure 7.8.
Low Freq. 1.07 Days

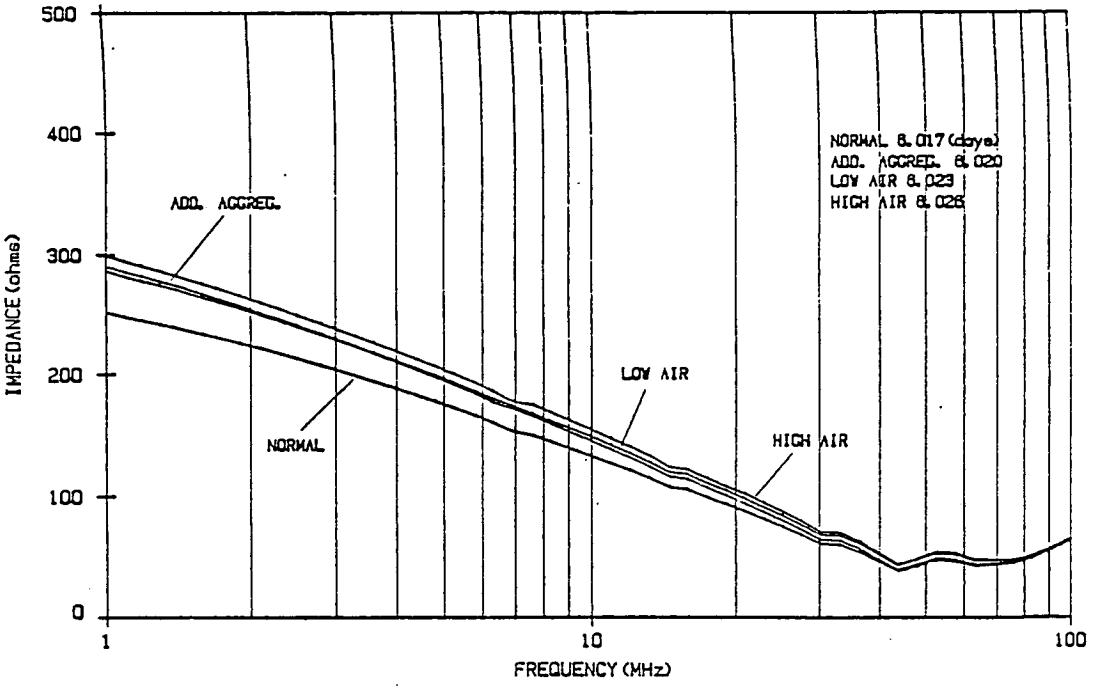

Figure 7.9.
Low Freq. 6.02 Days

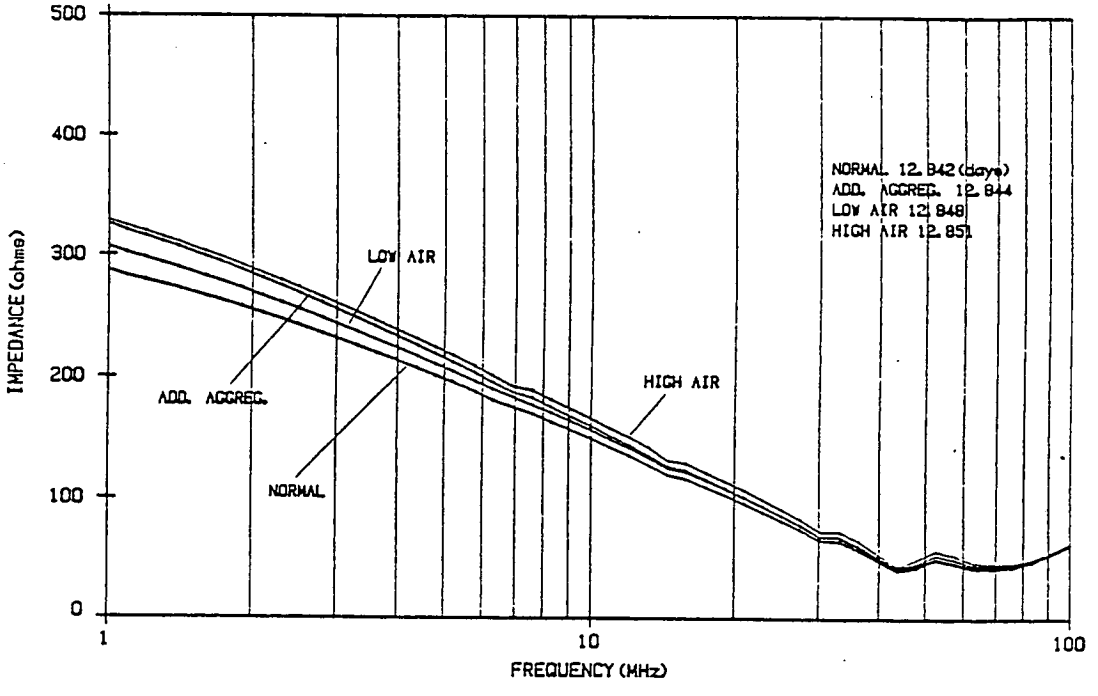

Figure 7.10.
Low Freq. 12.85 Days

The graphs show a progressive fall in impedance up to a frequency of 40 MHz. Above 40 MHz, minor resonances occur which are due to the coaxial to parallel plate transition. While the shape of the impedance/frequency graph for additional aggregate is similar to that for the normal mix, the slope is different from that for the low air content. This might be a basic difference in response for samples with additional aggregate compared with those containing air.

7.3.2. Higher Frequency Band.

The results for meaurements in the higher frequency range are given in Figures 7.11 - 7.14, and have the following measurement times:-

Figure 7.11; 1.05 days; just after demoulding.

Figure 7.12; 1.10 days; after the sample had been stored in water.

Figure 7.13; 6.01 days;

Figure 7.14; 12.82 days.

The graph for the normal sample has a relatively broad maximum, with a relatively high resonant frequency at which the peak occurs. Additional aggregate causes the resonant frequency to be reduced, but still with a relatively broad response. A small amount of air causes a reduction in resonant frequency and narrowing of the response. A greater amount of air causes a higher resonant frequency with an even narrower response. It should be noted in

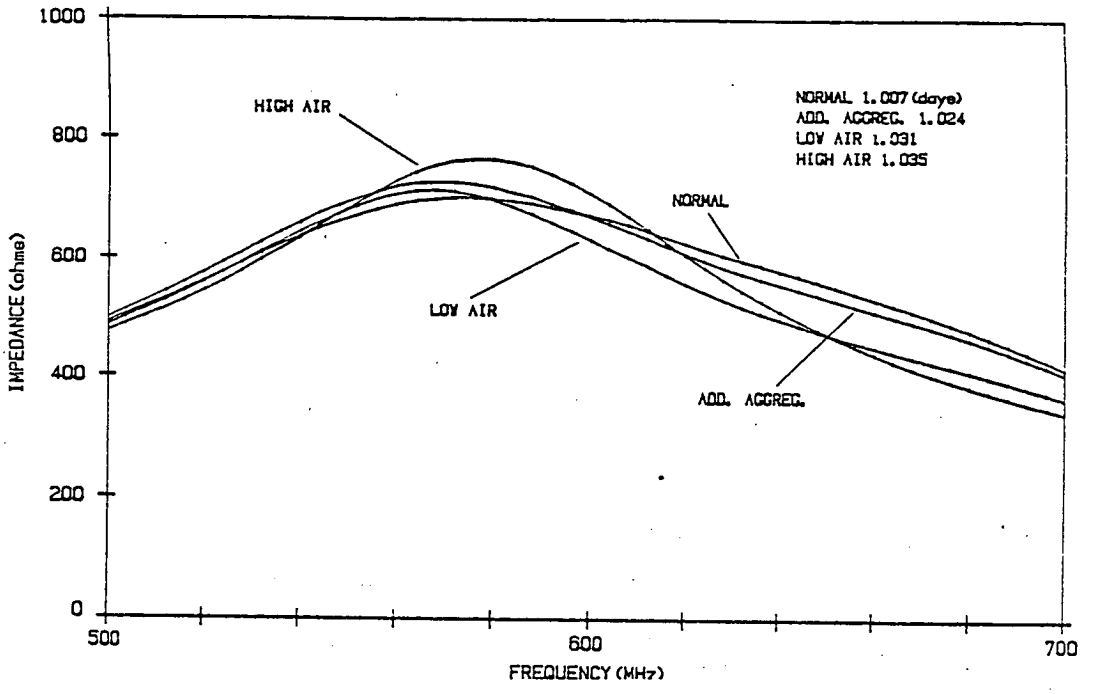

Figure 7.11.
High Freq. 1.05 Days

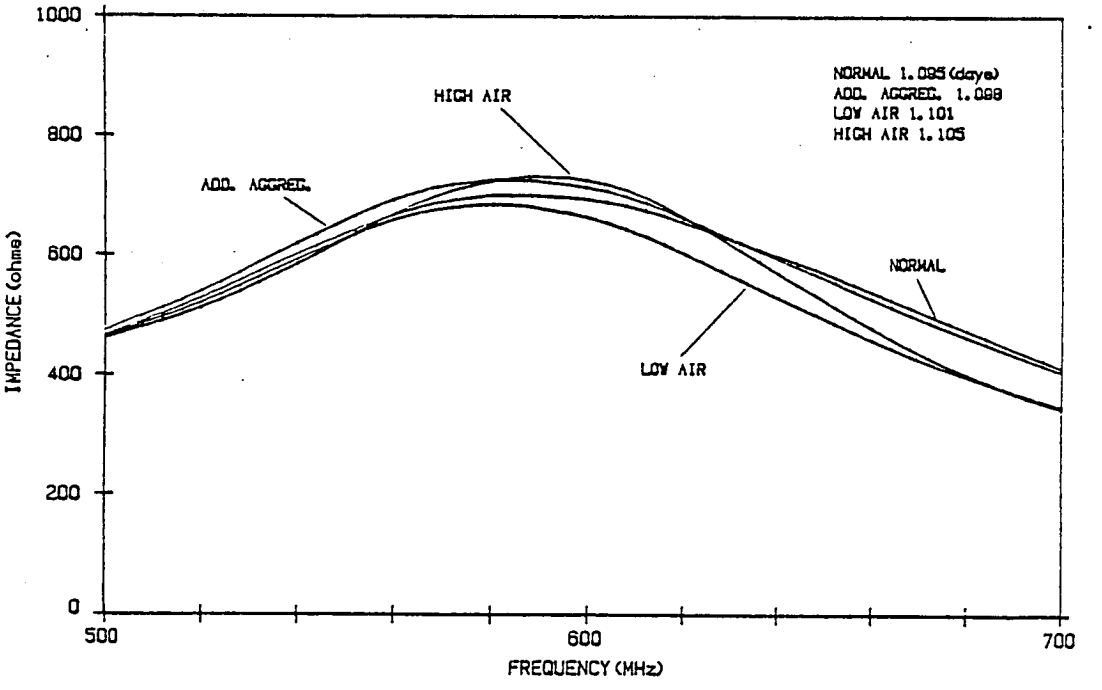

Figure 7.12.
High Freq. 1.10 Days

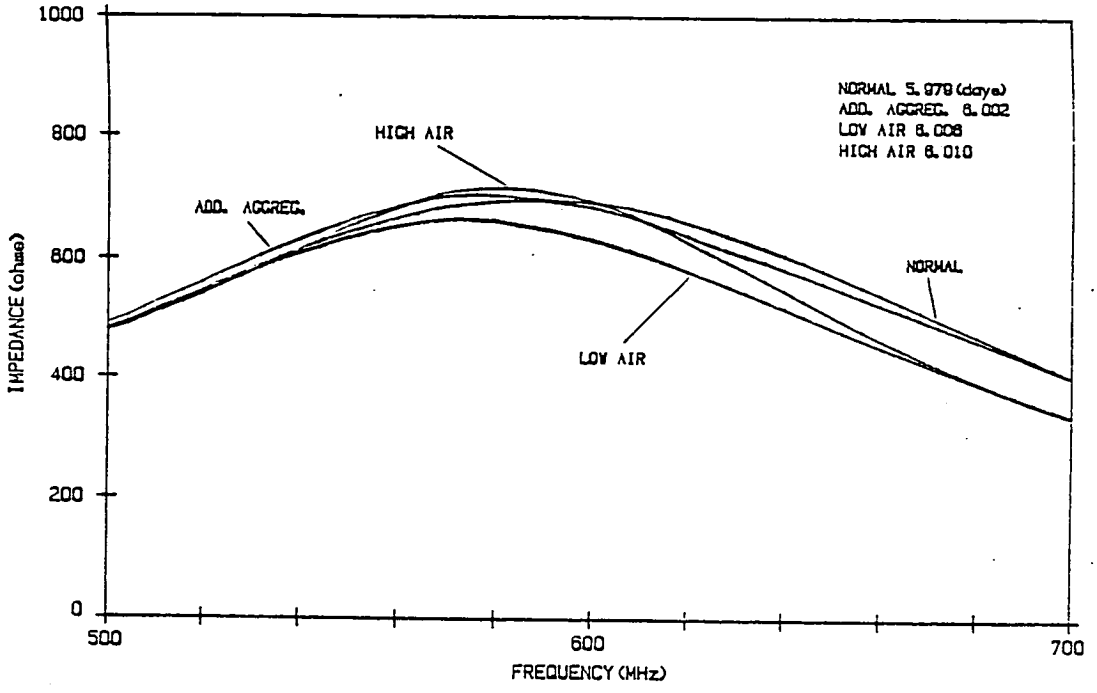

Figure 7.13.
High Freq. 6.01 Days

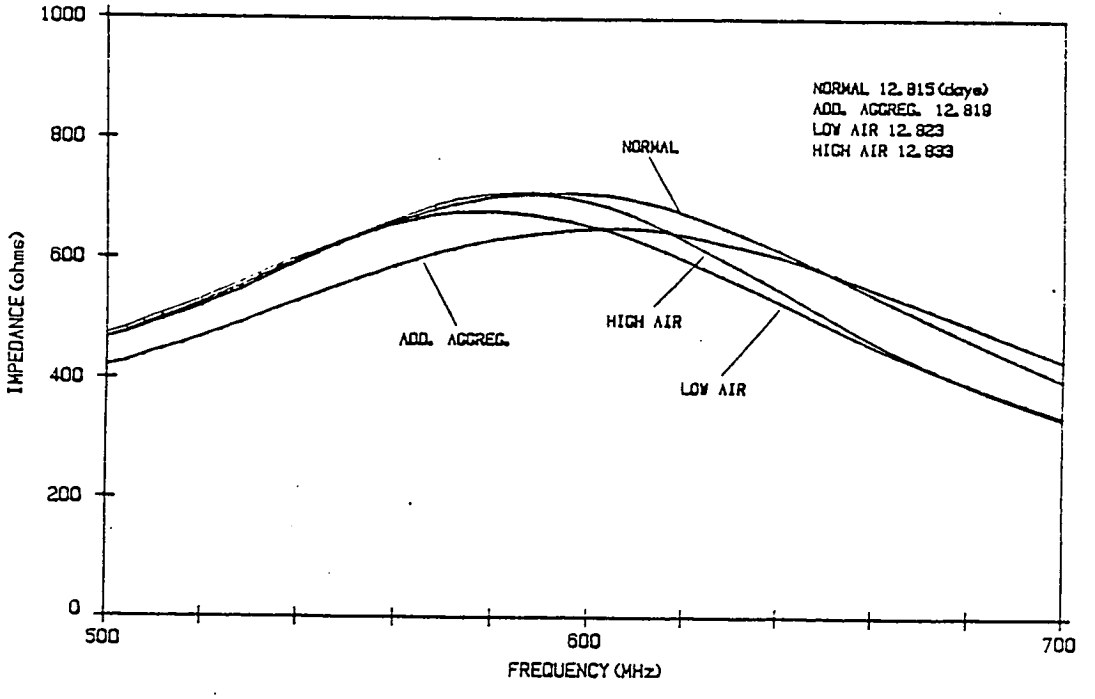

Figure 7.14.
High Freq. 12.82 Days

Figure 7.14 however, that there is an unusual response for the sample with additional aggregate in that the resonant frequency has increased, and the magnitude of the impedance has decreased.

7.3.3. Summary of Data.

In view of the large amount of data obtained from the experiment (experiments were kept running up to 30 days) a method of summarising the data describing the shapes of the graphs was developed, concentrating on factors which might discriminate between samples containing additional aggregate and air. It was also known that many of the parameters are temperature sensitive (Chapter 3.), and so the temperature was also included on the graphs.

Figures 7.15 and 7.16. summarise the data. The time scales are logarithmic, and indicate the time since water was added to the mix.

For the frequency band 1 - 100 MHz, the ratio of the modulus of the impedance at 30 MHz to that at 1 MHz is significant. This graph is shown in Figure 7.15 along with the average temperature of the samples. From this graph, it appears that the impedance ratio places samples with entrapped air closer to a normal sample than a sample with additional aggregate. There is some indication that the impedance ratio is temperature sensitive.

In the frequency band 500 - 700 MHz, a fractional bandwidth has been defined as the frequency difference between the points at which the modulus of the impedance is 90% of maximum, divided by the frequency of the maximum. This function is plotted in Figure 7.16

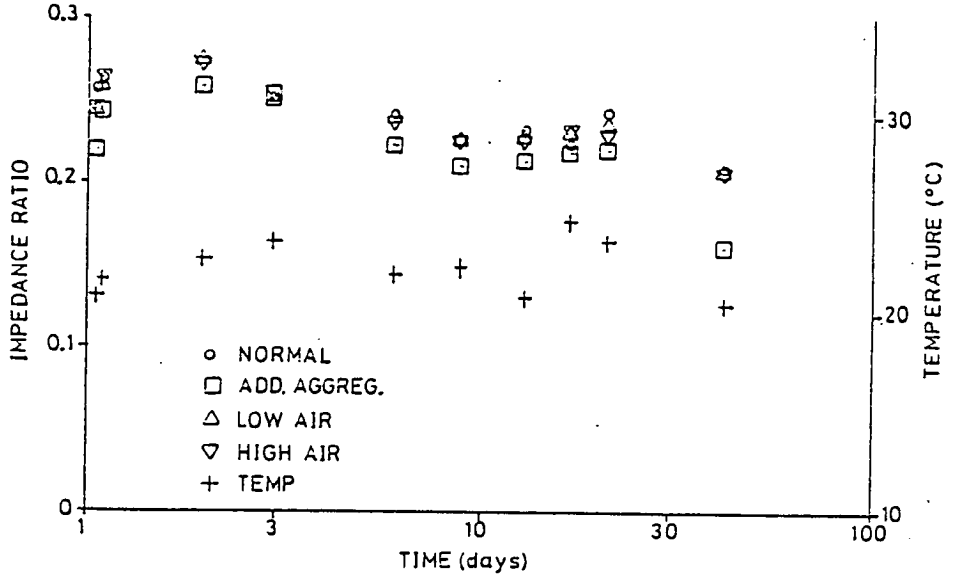

Figure 7.15.
Impedance Ratio

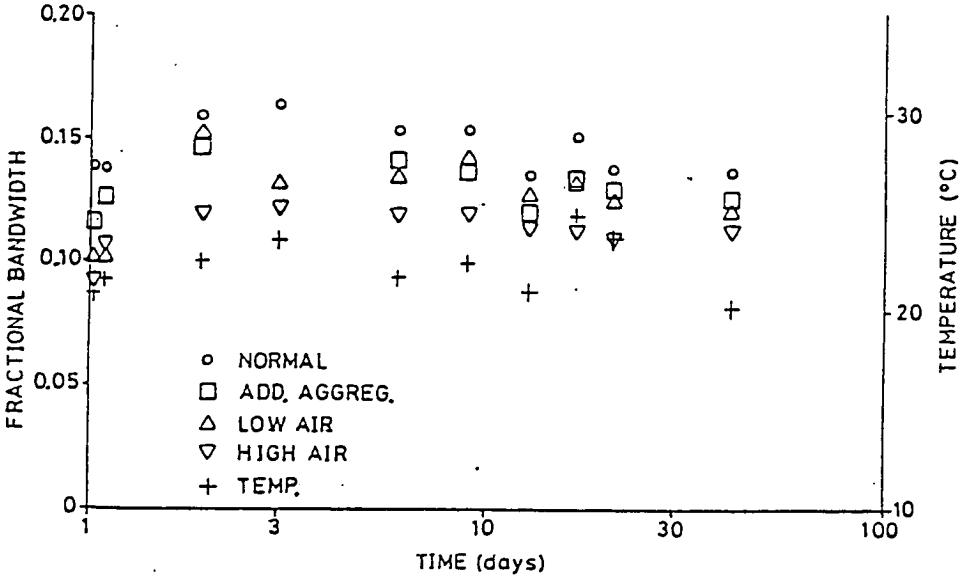

Figure 7.16.
Fractional Bandwidth

along with the average temperature. The fractional bandwidth parameter places the additional aggregate sample closer to a normal sample than those with entrapped air. The function again appears to be temperature sensitive.

The first two data points show discontinuities compared with the others. This is because, following these readings, the concrete is stored in water for a considerable time, and will be saturated, while for the first measurements, the samples have just been demoulded, and for the second they have only been stored in water for a very short time.

The following results have been taken from earlier trials using polystyrene chips to simulate air voids:-

TRIAL A

PARAMETER	ADD AGGREG	POLYSTYRENE
Time(days)	6.079	6.084
Imped. ratio	0.340	0.339
Temp. oC	22.2	21.5

TRIAL B

PARAMETER	ADD AGGREG	POLYSTYRENE
Time(days)	6.268	6.272
Frac. bandwidth	0.116	0.103
Temp. oC	23.7	23.5
Time(days)	6.254	6.258
Imped. ratio	0.215	0.243
Temp. oC	23.6	23.6

In trial B there was approximately twice the amount of polystyrene chips in the mix compared with trial A.

While these measurements largely confirm the relationships obtained from the later trial, except for the value of impedance ratio in trial A, it must be remembered that results obtained with expanded polystyrene may be modified by water present in the polystyrene.

7.3.4. Resistivity and Dielectric Constant.

A computer program has been designed which deduces the value of the resistivity and dielectric constant of the concrete from the impedance measurements. It is assumed that the electrode system forms a narrow open circuited parallel plate transmission line with the concrete as dielectric. Fringing effects are assumed to be negligible, as are the effects of the coaxial line to parallel plate transition. The derivation of the algorithm used is given in Appendix N.

The assumptions made cannot be justified by the sample geometry used. The calculation is however straightforward, and it is hoped that the use of the algorithm will give some indication of the feasibility of the technique.

This program was applied to the impedance measurements for the normal concrete sample at approximately 6 days. Figure 7.17 shows the results for the low frequency band, and Figure 7.18 those for the high-frequency band.

In the low frequency band, there is a progressive reduction in

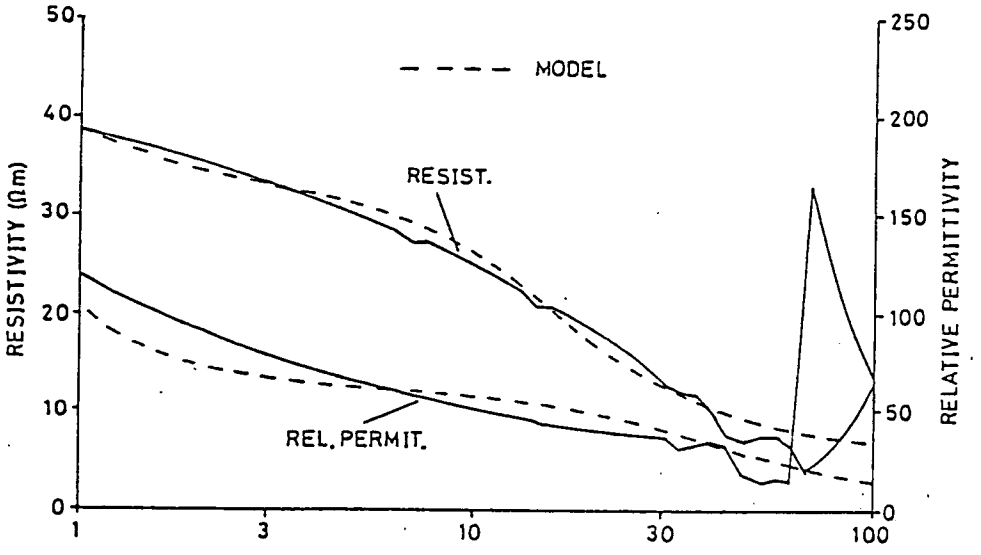

Figure 7.17.
Low Freq. Resistivity and Rel. Permit.

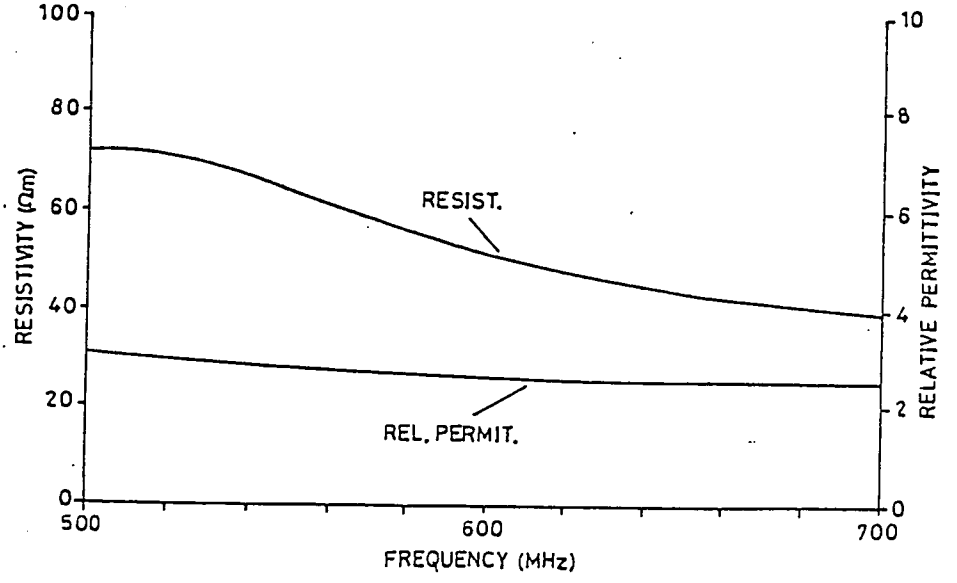

Figure 7.18.
High Freq. Resistivity and Rel. Permit.

resistivity and relative permittivity (dielectric constant) as frequency increases, with the relative permittivity having a value greater then 100 at 1 MHz. Discontinuities occur in the region of 70 MHz due to parameters in the parallel plate to coaxial line transition. The validity of these results must therefore be in question in this region.

The results for the high-frequency band give a relative permittivity of approximately 3, and a resistivity which is greater than that at 1 MHz. Since a study of the properties of the constituents of concrete (Chapter 3) show no mechanism which will cause a reduction in conductivity, and hence an increase in resistivity, in this frequency band, it is assumed that the validity of the algorithm is poor in this frequency range, and no further calculations have been carried out in this range.

Further calculations were carried out on a set of measurements taken over the frequency range 1 - 100 MHz after approximately 3 days. Values for resistivity are presented in Figure 7.19, and those for dielectric constant in Figure 7.20. An increase in resistivity is obtained for all samples compared with the normal sample. The samples with entrapped air show a fall in dielectric constant, the reduction being greater for the sample with a lower volume of entrapped air. This is not what might have been expected since the greater the volume of air, which has a dielectric constant of approximately 1, the lower the expected dielectric constant of the sample would be.

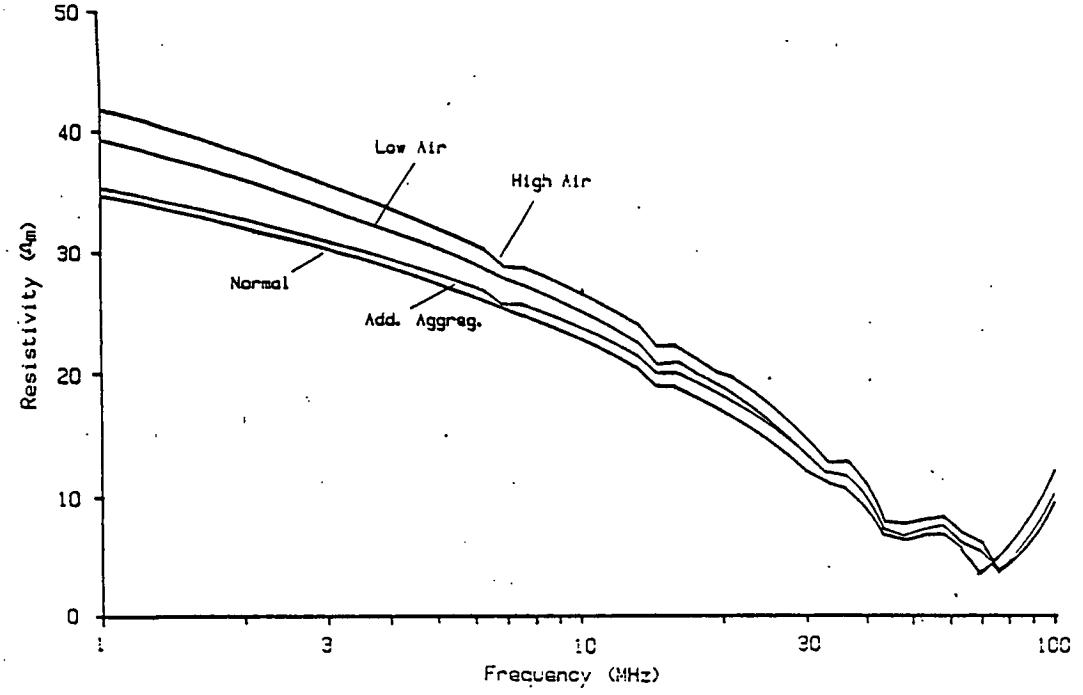

Figure 7.19.
Resistivity

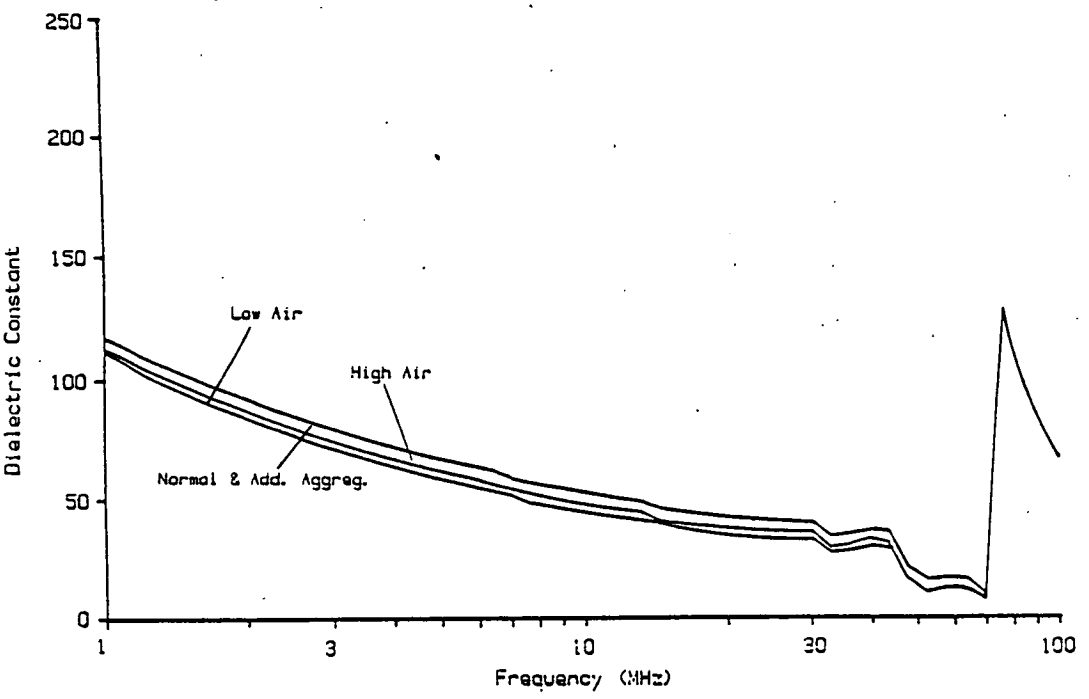

Figure 7.20.
Dielectric Constant

7.3.5. Electrical Model

The results for dielectric constant indicate very high values of dielectric constant at low frequencies. The dielectric constant of water is only in the region of 80, and the percentage of water by volume is in the range 3 - 18%. The dielectric constant of the aggregate and cement matrix without the water is thought to be about 7. (Section 3.7.3) The reason for the high value of measured relative permittivity is believed to be Maxwell-Wagner effects in the relatively high conductivity water pores imbedded in the low conductivity cement and aggregate structure. The equations developed by Fricke [53] (Section 3.5.2) for needle shaped conducting particles can give very high values of relative permittivity at low frequencies. This model could be applied to concrete where the needles are the conducting capillary pores.

Figure 7.17 also shows resistivity and dielectric constant results for a model consisting of a continuous water channel with a very thin insulating layer, and a channel consisting of randomly orientated conducting needles in a cement/aggregate matrix. The thin insulating layer models a layer of gas generated by electrolytic effects (Section 3.3.1.). It can be seen that, although the general shape is correct, there are considerable discrepancies.

This model is described by the equations:-

$$\varepsilon_r = \left\{ \varepsilon_{As} + \left(\frac{\varepsilon_{A\infty} - \varepsilon_{As}}{1+\omega^2 \tau_A^2} \right) \omega^2 \tau_A^2 \right\} x + \left\{ \varepsilon_{B\infty} + \frac{\varepsilon_{Bs} - \varepsilon_{B\infty}}{1 + \omega^2 \tau_B^2} \right\} (1-x) \qquad (7.1)$$

$$\frac{1}{\rho} = \frac{\omega^2 \tau_A^2 \sigma_{A\infty}}{1+\omega^2 \tau_A^2} x + \frac{\omega^2 \tau_B^2 \sigma_{B\infty}}{1+\omega^2 \tau_B^2} (1-x) \qquad (7.2)$$

where ε_r = dielectric constant

ρ = resistivity (Ωm)

ε_{As} = low frequency dielectric constant of the water channel - 10^4

$\varepsilon_{A\infty}$ = high frequency dielectric constant of the water channel - 8.0

ε_{Bs} = low frequency dielectric constant of the needle channel - 60

$\varepsilon_{B\infty}$ = high frequency dielectric constant of the needle channel - 2.5

$\sigma_{A\infty}$ = high frequency conductivity of water channel - 1 Sm^{-1}

τ_A = time constant of water channel - 4.0×10^{-7} s

τ_B = time constant of needle channel - 4.0×10^{-9} s

x = fractional volume of water channel - 0.03

The Fricke model assumes that the needles are all of the same length, but in concrete, the pore lengths will have a distribution probably approaching the Poisson distribution, with the part of the distribution with pores exceeding the length of the sample giving rise to the finite value of low-frequency resistivity.

From experiments described in Section 6.5.3, the relaxation frequency due to the gas layer is likely to be approximately 30 Hz, giving a relaxation time of 5.3 ms, which is very much larger than that assumed here.

7.4. Conclusions.

It is possible, by examining the shape of the impedance curves for the frequency ranges 1 - 100 MHz and 500 - 700 MHz, to assess whether an increase in low frequency resistivity is due to increased aggregate or to entrapped air in the sample. The fact that such differences can be detected shows that the measuring equipment is sufficiently sensitive for this kind of investigation.

Use of an algorithm to obtain resistivity and dielectric constant from impedance measurements shows little difference in dielectric constant over the frequency range 1 - 100 MHz between a normal sample and one with additional aggregate, but a significant reduction for the samples with entrapped air. These results do, however, require further investigation. The validity of the algorithm in the frequency range 500 - 600 MHz is doubted. While the assumptions made during the development of the algorithm are not adhered to, the results are believed to indicate that differences

between the dielectric constants of the different samples are significant.

While the model chosen to fit the resistivity and dielectric constant graphs in the frequency range 1 - 100 MHz is now known to be inappropriate, the graphs show that the measured effects are similar to those caused by heterogeneous relaxation.

7.4. Areas Requiring Further Investigation.

The experimental techniques used have raised a number of points with regard to measurement and the interpretation of results. In general the experiments described have established the feasibility of obtaining meaningful high-frequency impedance measurements on concrete samples. It is necessary however to refine the technique to obtain reliable numerical data on the resistivity and dielectric constant of the material over the available frequency range of the measuring equipment. The following points must therefore be investigated:-

(i) a method of external calibration of the impedance analyser for measurement of multiplexed impedances through switching units and cable assemblies, to allow measurements on multiple samples

(ii) determination of the terminating impedance of the parallel plate transmission line, including the effect of the sample support

(iii) theoretical calculation of the inductance of a parallel plate transmission line of the geometry used

(iv) calculation of the network parameters describing the coaxial line to parallel plate transition when treated as a two port network

(v) the possible radiative characteristics of the sample geometry, and its effect on results

(vi) development of a satisfactory iterative process for the calculation of dielectric constant and conductivity from impedance data

(vii) development of a suitable mathematical model of the dispersive effects in dielectric constant and conductivity which will allow mechanical properties to be inferred.

8. CONCLUSIONS FROM RESEARCH.

1. The Civil Engineering and Construction industries experience difficulties from time to time with concrete structures. Many of these problems result from poor supervision and inspection rather than design errors, and could be eliminated by better quality control. There is currently no equipment available, which could be used on-site by operators who are not specially skilled or qualified, for assessing the quality of concrete in the period between mixing and hardening.

2. A large number of workers have carried out electrical measurements on concrete. Their results and conclusions are frequently confusing and contradictory, and demonstrate the problem of the breadth of knowledge of Science and Engineering required to undertake a valid programme of research in this field. None of the techniques described have gained general acceptance for quality assurance purposes.

3. The electrical behaviour of concrete is complex, but is characterised by a low frequency relaxation process with a relaxation frequency of the order of 10 Hz, which might be due to a number of effects, but which is believed to be due primarily to electrolytic action. The high-frequency behaviour is governed by Maxwell-Wagner effects due to the heterogeneous nature of concrete, and in particular to the random distribution and dimensions of water filled capillary pores, which are ionic conductors, within an

aggregate/cement matrix. The frequency band over which these effects take place has not been determined accurately, but an approximate range is 100 kHz - 200 MHz. Over this frequency range, the dielectric constant falls, and the conductivity increases. No theoretical reasons have been established for further significant variations in conductivity or dielectric constant until frequencies much greater than 1000 MHz are reached, although some approximate calculations carried out in the frequency range 500 - 700 MHz indicate that further investigation is required in this band.

4. A prototype low-frequency resistivity measuring equipment has been developed which gives reliable measurements on up to 15 samples of concrete in the form of 150 mm cubes. The 15 samples can be organised as one experiment or as fifteen separate experiments, or any intermediate grouping. The measurements are carried out at 2 kHz. Data processing programs have been developed which produce tabulated data, or a graph of resistivity against time. The experiments can continue for up to 100 days. For experiments exceeding 1 day, the samples can be stored underwater, and withdrawn automatically for measurement. This equipment has been used in a research project in the Department of Civil Engineering and Building Science in the University of Edinburgh, to investigate the low frequency resistivity of concrete.

5. A developed version of the low-frequency resistivity equipment has been produced which has circuit improvements and refinements, making it more convenient to use in a Civil Engineering environment. The data produced by this equipment is stored on magnetic disc which eliminates the need to transcribe data for subsequent processing.

Initial measurements carried out using this equipment indicate that it might be possible to establish the water content available for conduction, during the induction period, and that the actual mix ratios of the samples might be established within 1 day. Limits on the resistivity profile might also be established as a quality assurance indicator.

6. During the design of the developed equipment, LSI techniques were used to produce most of the logic circuitry required. This has provided valuable experience in the application of such techniques.

7. Measurements of the electrical impedance of 150 mm cubes of concrete configured as open-circuited parallel plate transmission lines, have been carried out over the frequency range 1 - 1000 MHz, and more particularly in the bands 1 - 100 MHz and 500 - 700 MHz. It has been found that, by examining the shape of the impedance/frequency curves, it is possible to deduce whether a particular sample has additional aggregate or entrapped air, compared with a normal sample.

8. An approximate method has been developed to obtain the dielectric constant and resistivity as functions of frequency from transmission line impedance data. Over the frequency band 1 - 100 MHz, it is found that the presence of entrapped air or additional aggregate increases the resistivity, but while entrapped air reduces the dielectric constant, additional aggregate has little effect. Application of these techniques to the frequency band 500 - 700 MHz resulted in values of resistivity higher than those in the band 1 - 100 MHz. This might indicate that there is some mechanism which results in an increase in resistivity or reduction in conductivity in this frequency range.

9. The variations in dielectric constant and resistivity have been compared with those predicted by a particular Maxwell-Wagner model.

10. In general, aspects of the electrical behaviour of concrete have been clarified, and equipment and measuring techniques have been developed which allow the electrical properties to be determined. Controlled measurements of low-frequency resistivity, and refinement of the high-frequency technique to obtain accurate numerical data, are now required to establish the electrical properties of the material in the frequency bands considered, and to evaluate the application of such techniques to the practical situation.

APPENDIX A.

Lossy Dielectrics.

When an alternating electric field is applied to a lossy dielectric, electrical dipole polarization will take place within the material, but there will be a phase lag between the electric field and the orientation of the dipoles, and consequently the electric flux density will lag the electric field intensity by phase angle δ. An introduction to lossy dielectrics is given by Blythe [24].

Two dielectric constants can be deduced from this effect:-

$$\varepsilon' = \frac{D_1}{\varepsilon_o E} \qquad \varepsilon'' = \frac{D_2}{\varepsilon_o E} \qquad \text{(A.1)}$$

where ε' = real part of the complex dielectric constant or relative permittivity

ε'' = imaginary part of the complex dielectric constant or relative permittivity

D_1 = amplitude of the in-phase component of the electric flux density (Cm^{-2})

D_2 = amplitude of the quadrature component of the electric flux density (Cm^{-2})

E = amplitude of the applied electric field intensity (Vm^{-1})

ε_o = permittivity of free space (Fm^{-1})

The phase lag δ is given by the expression:-

$$\frac{\varepsilon''}{\varepsilon'} = \tan\delta \qquad (A.2)$$

The complex dielectric constant is given by:-

$$\varepsilon_v = \varepsilon' - j\varepsilon'' \qquad (A.3)$$

If the lossy dielectric is used in a parallel-plate capacitor of area A and plate separation d, and an alternating voltage of amplitude V is applied, then the complex current is:-

$$\underset{\sim}{I} = j\omega\varepsilon_o(\varepsilon' - j\varepsilon'')\frac{A}{d}V$$

$$= (G + j\omega C)V \qquad (A.4)$$

where G is conductance (S)

$$G = \omega\varepsilon_o\varepsilon''\frac{A}{d}V \qquad (A.5)$$

and C is capacitance (F)

$$C = \varepsilon_o\varepsilon'\frac{A}{d}V \qquad (A.6)$$

From the capacitor geometry, the value of conductivity necessary to give conductance G is:-

$$\sigma_D = G\frac{d}{A}$$

$$= \omega\varepsilon_o\varepsilon'' \qquad (A.7)$$

$$= \omega\varepsilon_o\varepsilon'\tan\delta \qquad (A.8)$$

If in addition, the material has a static value of

conductivity σ_s ($\omega = 0$) then, the total conductivity at frequency ω is:-

$$\sigma = \sigma_s + \sigma_D$$

$$= \sigma_s + \omega\varepsilon_o\varepsilon'' \qquad (A.9)$$

$$= \sigma_s + \omega\varepsilon_o\varepsilon' \tan\delta \qquad (A.10)$$

Thus

$$\varepsilon'' = \frac{\sigma - \sigma_s}{\omega\varepsilon_o} \qquad (A.11)$$

and

$$\tan\delta = \frac{\sigma - \sigma_s}{\omega\varepsilon_o\varepsilon'} \qquad (A.12)$$

The Debye Theory of dielectric relaxation [24], considers the dynamic aspects of the dipole polarization process, and assumes that the rate at which polarization takes place is proportional to the extent of the departure from equilibrium.

By applying this theory, it is possible to deduce that polarization must have a time factor of the form:-

$$1 - e^{t/\tau} \qquad (A.13)$$

associated with it , where τ is the dielectric relaxation time.

If an alternating electric field of radian frequency ω is considered, it is found that:-

$$\underset{\sim}{\varepsilon}(\omega) = \varepsilon_\infty + \frac{\varepsilon_s - \varepsilon_\infty}{1 + j\omega\tau} \qquad (A.14)$$

where ε_∞ = dielectric constant at infinite frequency

ε_s = static dielectric constant

Thus:-

$$\varepsilon'(\omega) = \varepsilon_\infty + \frac{\varepsilon_s - \varepsilon_\infty}{1 + \omega^2\tau^2} \qquad (A.15)$$

and

$$\varepsilon''(\omega) = \frac{\varepsilon_s - \varepsilon_\infty}{1 + \omega^2\tau^2}\ \omega\tau \qquad (A.16)$$

These are called the Debye dispersion equations.

Combining Expressions A.9 and A.16 gives:-

$$\sigma = \sigma_s + \frac{(\varepsilon_s - \varepsilon_\infty)\varepsilon_o\omega^2\tau}{1 + \omega^2\tau^2} \qquad (A.17)$$

When $\omega = 0$, $\sigma = \sigma_s$

and when $\omega = \infty$

$$\sigma = \sigma_\infty = \sigma_s + \frac{(\varepsilon_s - \varepsilon_\infty)\varepsilon_o}{\tau} \qquad (A.18)$$

Thus

$$(\varepsilon_s - \varepsilon_\infty)\varepsilon_o = (\sigma_\infty - \sigma_s)\tau \qquad (A.19)$$

$$\tau = \frac{\varepsilon_o(\varepsilon_s - \varepsilon_\infty)}{(\sigma_\infty - \sigma_s)} \qquad (A.20)$$

Substituting Expression A.19 in A.17 gives:-

$$\sigma = \sigma_s + \frac{(\sigma_\infty - \sigma_s)\omega^2\tau^2}{1 + \omega^2\tau^2} \qquad (A.21)$$

In the Debye case, $\varepsilon_\infty < \varepsilon_s$, thus from Expression A.19 $\sigma_\infty > \sigma_s$.

The relaxation frequency is given by:-

$$\omega_r \tau = 1$$

$$\omega_r = \frac{1}{\tau} \qquad \text{(A.22)}$$

and

$$f_r = \frac{1}{2\pi\tau} \qquad \text{(A.23)}$$

Sometimes a relaxation wavelength is considered. This is defined as:-

$$\lambda_r = \frac{c}{f_r}$$

$$= 2\pi c\tau \qquad \text{(A.24)}$$

where c = velocity of light.

APPENDIX B.

Effect of Insulating Layer.

Figure B.1 shows an equivalent circuit of an electrolytic solution which includes capacitance C_1 due to the insulating layer, resistance R due to the bulk conductivity of the material, and capacitance C_2 due to the dielectric constant of the bulk material.

$$C_1 = \varepsilon_o \varepsilon_1 \frac{A}{d_1} \qquad (B.1)$$

$$C_2 = \varepsilon_o \varepsilon_2 \frac{A}{d} \qquad (B.2)$$

$$R = \frac{1}{\sigma} \frac{d}{A} \qquad (B.3)$$

where ε_1 = dielectric constant of the gas

= 1

ε_2 = dielectric constant of the bulk material

σ = conductivity of the bulk material

d_1 = thickness of gas layer

d = thickness of the bulk material

A = cross sectional area

$d_1 << d$ and $C_1R = \tau_1 >> C_2R = \tau_2$

From Figure B.1, the electrical impedance of the equivalent circuit is:-

$$Z = \frac{1}{j\omega C_1} + \frac{R}{1 + j\omega C_2 R} \qquad (B.4)$$

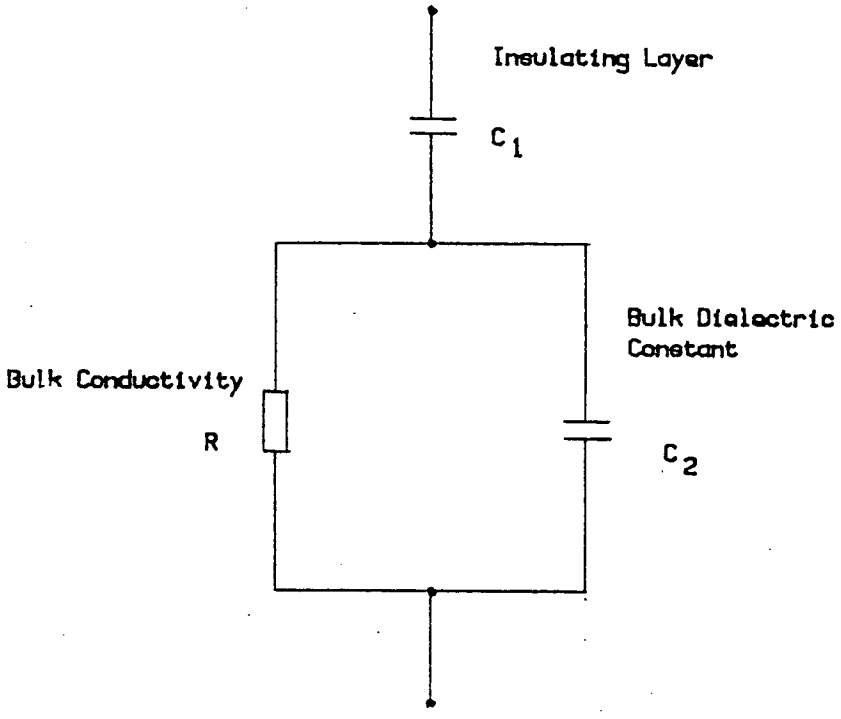

$$C_1 R = \tau_1$$

$$C_2 R = \tau_2$$

Figure B.1
Equivalent Circuit of an Electrolytic Solution.

$$\underset{\sim}{I} = \frac{\underset{\sim}{V}}{\underset{\sim}{Z}} = \frac{\underset{\sim}{V}}{\frac{1}{j\omega C} + \frac{R}{1 + j\omega C_2 R}}$$

$$\doteq j\omega C_1 \left\{ \frac{1 + \omega^2\tau_1\tau_2 - j\omega\tau_1}{1 + \omega^2{\tau_1}^2} \right\} \underset{\sim}{V}$$

$$= j\omega\varepsilon_o \left\{ \frac{d\varepsilon_1}{d_1} \frac{1 + \omega^2\tau_1\tau_2}{1 + \omega^2{\tau_1}^2} - j\frac{d\varepsilon_1}{d_1}\omega\tau_1 \right\} \frac{A}{d} \underset{\sim}{V} \qquad \text{(B.5)}$$

Thus from Expression A.4

$$\varepsilon' = \frac{d}{d_1}\varepsilon_1 \frac{1 + \omega^2\tau_1\tau_2}{1 + \omega^2{\tau_1}^2} \qquad \text{(B.6)}$$

$$\varepsilon'' = \frac{d}{d_1}\varepsilon_1 \frac{\omega\tau_1}{1 + \omega^2{\tau_1}^2} \qquad \text{(B.7)}$$

This has the appearance of a relaxation process with:-

$$\varepsilon_s = \frac{d}{d_1}\varepsilon_1 \qquad \text{(B.8)}$$

$$\varepsilon_\infty = \frac{d}{d_1}\varepsilon_1 \frac{\tau_2}{\tau_1}$$

$$= \frac{d}{d_1}\varepsilon_1 \frac{\varepsilon_2}{d} \frac{d_1}{\varepsilon_1}$$

$$= \varepsilon_2 \qquad \text{(B.9)}$$

and relaxation time

$$\tau_1 = C_1 R$$

$$= \varepsilon_o \frac{\varepsilon_1}{\sigma} \frac{d}{d_1} \qquad \text{(B.10)}$$

Thus at high frequency, the material exhibits the bulk properties, but at low frequencies there is an apparent dielectric constant:-

$$\varepsilon_s = \frac{d}{d_1} \varepsilon_1$$

Applying this to a 150 mm sample cube of concrete, and assuming that gas completely fills the capillary pores at the electrode, gives:-

$d = 150$ mm

d_1 = capillary pore diameter

$= 1.3$ μm

Thus

$$\varepsilon_s = 1.15 \times 10^5$$

APPENDIX C.

Ionic Dynamic Lag Effects.

Consider the following after Schwarz [45]. The movement of a particle with charge q in electric field E(t) is defined by the following differential equation:-

$$m\dot{v} + rv = qE(t) \qquad (C.1)$$

where v = velocity

m = mass

r = a frictional constant

If E(t) is held constant, then in the steady state condition:-

$$rv = qE \qquad (C.2)$$

The mobility μ of an ion is the mean velocity of the ion in an electric field of 1 Vm^{-1}.

$$\Rightarrow r = \frac{q}{\mu}$$

$$\Rightarrow m\dot{v} + \frac{q}{\mu}v = qE(t) \qquad (C.3)$$

The solution for an alternating field of radian frequency ω is:-

$$j\omega m \underset{\sim}{V} + \frac{q}{\mu} \underset{\sim}{V} = q\underset{\sim}{E} \qquad (C.4)$$

$$\Leftrightarrow \quad \underset{\sim}{V} = \frac{\mu \underset{\sim}{E}}{1 + j\omega \frac{m\mu}{q}} \qquad (C.5)$$

The conductivity and dielectric constant are related to this complex velocity, and the process will have a relaxation time:-

$$\tau = \frac{m\mu}{q} \qquad (C.6)$$

Consider the hydroxyl ion. From Blanchard et al [78]:-

atomic weight of hydrogen = 1.008

atomic weight of oxygen = 15.999

mass of a proton = 1.672×10^{-27} kg

electron charge = 1.602×10^{-19} C

$$\frac{m}{q} = \frac{(1.008 + 15.999) \times 1.672 \times 10^{-27}}{1.602 \times 10^{-19}}$$

$$= 1.775 \times 10^{-7} \text{kgC}^{-1}$$

From Glasstone [36], mobility μ for the hydroxyl ion is 20.5×10^{-8} $m^2v^{-1}s^{-1}$

$$\tau = 1.775 \times 10^{-7} \times 20.5 \times 10^{-8}$$

$$= 3.639 \times 10^{-14} \text{s}$$

The relaxation frequency is then:-

$$f_r = \frac{1}{2\pi\tau}$$

$$= 4.37 \times 10^{12}\text{Hz}$$

If there are 100 water molecules associated with each hydroxyl molecule, the mass will increase and the relaxation frequency will fall:-

$$\frac{m}{q} = \frac{(201 \times 1.008 + 101 \times 15.99) \times 1.672 \times 10^{-27}}{1.602 \times 10^{-19}}$$

$$= 1.897 \times 10^{-5}\text{kgC}^{-1}$$

$$\tau = 1.897 \times 10^{-5} \times 20.5 \times 10^{-8}$$

$$= 3.889 \times 10^{-12}\text{s}$$

Relaxation frequency

$$f_r = 4.09 \times 10^{10}\text{Hz}$$

Thus relaxation frequencies would be expected in the range 40 - 4000 GHz.

APPENDIX D.

Letter on "The Electrical Response Characteristics of Setting Cement Paste" - Reference 66.

The electrical response characteristics of setting cement paste*

W. J. McCarter and P. N. Curran

Contribution by J. G. Wilson

Department of Electrical and Electronic Engineering, Napier College, Edinburgh and

H. W. Whittington

Department of Electrical Engineering, University of Edinburgh

Regarding the estimated values of ε_r for the material, a value of 10^6 would seem to be very high, even considering polarization or non-homogeneous Maxwell-Wagner effects, when it is considered that the relative permittivity of water is only 80.

Whilst an a.c. bridge measurement gives the results for a parallel configuration of C and R, this does not imply that the physical configuration is either a series or a parallel combination. For a given electrical admittance, the two configurations are interchangeable at any one frequency. Consider series and parallel configurations (Figure I). For equivalence, the electrical admittances must be equal at any particular frequency.

$$Y_p = \frac{1}{R_p} + j\omega C_p$$

and

$$Y_s = \frac{1}{R_s + \dfrac{1}{j\omega C_s}}$$

Equating these admittance values and separating real and imaginary parts gives:

$$R_p = \frac{1 + \omega^2 C_s^2 R_s^2}{\omega^2 C_s^2 R_s}$$

and

$$C_p = \frac{C_s}{1 + \omega^2 C_s^2 R_s^2}$$

where $\omega = 2\pi f$;

f = frequency (Hz).

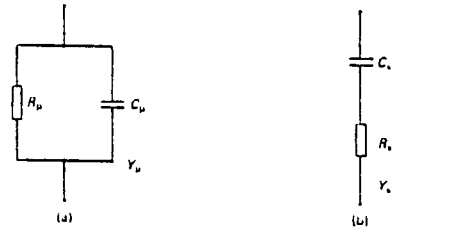

(a) Parallel configuration *(b) Series configuration*

Figure I: Electrical configuration.

Since C_s is generally very large, at higher frequencies

$$R_p = R_s$$

and

$$C_p = \frac{1}{\omega^2 C_s R_s^2}$$

Thus, if physically the circuit is a series circuit, C_p can be expected to decrease if f is increased.

Although the circuits are equivalent to any one frequency, over a range of frequencies, their performances are completely different and, in particular, if a square waveform is applied to the circuit of Figure II then, if the actual circuit is a series combination,

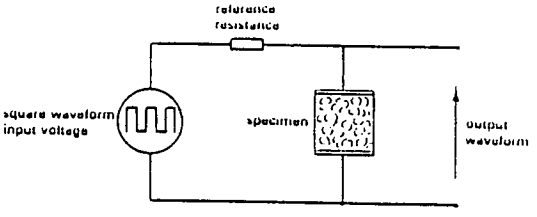

Figure II: Test circuit.

*Pages 42–49 of *MCR* 126.

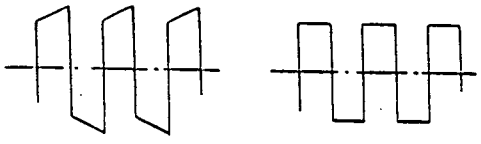

(a) Low frequencies *(b) High frequencies*

Figure III: Output waveforms: series circuit.

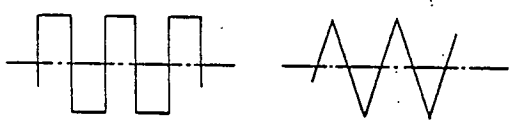

(a) Low frequencies *(b) High frequencies*

Figure IV: Output waveforms: parallel circuit.

the output waveform can be expected to follow the pattern of Figure III whereas, if the actual circuit is a parallel circuit, the output waveform will follow the pattern of Figure IV.

In experiments we have carried out[1] over the frequency range 2 Hz to 2 kHz, the waveform pattern for the series configuration is obtained.

We believe that the high value of series capacitance is due to the formation of a layer of gas at the electrodes because of electrolytic action. This gas layer will be of molecular thickness and, despite a relative permittivity of approximately 1, will result in a high value of capacitance because of its very small thickness. The value of capacitance also depends on area, and in this case the area will be the effective value for conduction A. Thus:

$$C_s \propto A$$

$$R_s = R_p \propto \frac{1}{A}$$

and

$$C_p \propto \frac{1}{C_s R_s^2} \propto A$$

Thus, for either the effective series or the parallel values of capacitance, the capacitance can be expected to fall as hydration progresses and the effective area for conduction, which is determined by free water paths, is reduced. This must also result in an increase in measured resistivity.

Although the relatively high value of capacitance can be explained in terms of a gas layer, the bulk material will still have a relative permittivity value associated with it. This value will, however, only become apparent at higher frequencies. Measurements carried out by ourselves and other workers[2,3] suggest values in the range 50–100 at high frequencies for concrete and cement paste.

Reply by the authors

Mr Wilson and Dr Whittington's contribution on our paper is appreciated and we would comment on the main points raised as follows.

(1) With regard to the series or parallel electrical models, both models are interchangeable; in other words, the equivalent parallel model can be calculated from the series values of C_s and R_s and vice versa. We have checked this to be the case in practice, as the component bridge we are using (Wayne Kerr B905) can give capacitive and resistive values for both models. The reason we have chosen the parallel model is that we are regarding the cement paste as a 'lossy dielectric', where there is not only a polarization current (quadrature component) but also a leakage of current through the resistive element (in-phase component).

(2) In measurements on electrolytic solutions the phenomenon of electrode polarization can be regarded as a piling-up of ions at the electrodes when a direct current is passed through the system. The same effect occurs with alternating current if the frequency is low enough to allow ions to concentrate at the electrodes during each half-cycle. It can be shown theoretically that, if electrode polarization is the only factor contributing to polarization capacity, the capacitance should decrease as the inverse square root of the frequency, i.e. $\propto (\text{frequency})^{-0.5}$. The build-up of ions at the electrodes, without discharge, or the formation of a thin layer of gas would result not only in high dielectric constants for the layer, but also in extremely high resistances for the sample–this resistance being frequency-dependent. The resistance would drop from virtually an infinite value at d.c. (direct current)–as no conduction can take place across the layer of 'gas'–to negligible proportions as the frequency of the applied electrical field increases. In fact, Mr Wilson and Dr Whittington must have noticed such an effect in their low-frequency work[1]. If, as they explain, high dielectric constants are due to the formation of a gas layer at the electrodes, then the impedance of their series model would be infinite. For the frequency employed in our work (1000 Hz), we have not found this to be the case for either model–signifying negligible electrode polarization.

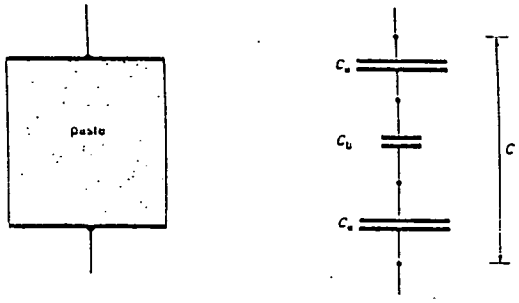

Figure V: Series combination of electrode and bulk capacitances.

(3) The drop in resistance (due to electrode polarization) with increasing frequency would predominate over very low frequencies. A significant drop in resistance with increasing frequency would indicate the existence of electrode polarization effects and a frequency must be reached at which electrode polarization effects become negligible. Work has advanced quite considerably since publication of our paper and we have investigated the effect of varying the frequency of applied electrical field over the range 100 Hz–10 kHz. Over this range we have found negligible change in resistance. If electrode polarization effects did predominate, one would expect noticeable changes in resistance.

(4) Mr Wilson and Dr Whittington claim that electrode polarization effects predominate over bulk effects. If this were the case, the dielectric constant would remain reasonably constant with time, as the capacitance of the 'air-gap' would remain constant. In fact, the variation of dielectric constant with time displays a marked fluctuation, which would suggest that it is the bulk effects (i.e. polarization mechanisms within the cement paste) that are having a considerable influence upon the over-all dielectric constant.

Furthermore if, as Mr Wilson and Dr Whittington suggest, a thin layer of gas is formed at the electrodes then, as they explain, this would result in a very high capacitance value for the layer. This capacitance, C_e, can be visualized as being in series with the bulk capacitance, C_b, of the cement paste (Figure V), the capacitance, C, of the combination being,

$$1/C = 1/C_e + 1/C_b + 1/C_e$$

If C_e (as is suggested) is very much greater than C_b, then $1/C_e$ will be negligible in comparison to $1/C_b$ and thus

$$C \simeq C_b$$

and bulk effects will control the measured capacitance C!

(5) As explained in (3), we have conducted extensive tests over the frequency range 100 Hz–10 KHz. The shapes of the curves (Figure VI) remain more or less the same over this frequency range, with only the magnitude of the dielectric constants decreasing with increasing frequency (dielectric dispersion). The fall in dielectric constant with increasing frequency is too great to be explained solely by an inverse square root relationship–see (2) above, assuming electrode polarization effects did predominate. This would suggest that other polarization mechanisms are becoming non-operative as the frequency increases–these being associated with the bulk material.

(6) Regarding the high dielectric constants for cement paste in its early hydration stages, it is not unusual for colloidal solutions to have high dielectric constants. Polarization of the double layer[4–6] around the cement grain can induce large effective dipole moments and result in high dielectric constants. The values of 50–100 quoted by Mr Wilson and Dr Whittington are for relatively mature concrete specimens at high frequencies; we are concerned with cement paste and mortars in the liquid state and very early stages of hardening at medium frequencies.

(7) Electrode polarization effects are visible when d.c. is applied to an electrolytic solution by the formation of gas bubbles at the electrodes. The formation of gas at the electrodes would not only be visible but also lead to honeycombing of the cement paste in the vicinity of the electrode and virtually zero bond between the electrode and the cement paste prism. No such physical evidence of these features has been found.

In conclusion, whilst we accept that electrode polarization effects do occur with d.c. and periodically reversed d.c., they are considerably reduced as frequency increases and have virtually been reduced to zero for frequencies in excess of about 50 Hz. The fluctuations in dielectric constant are attributable to polarization mechanisms within the bulk material. Both parallel and series models are interchangeable over the frequency range 100 Hz–10 kHz for the cement paste during the early stages of hydration and agree well with the simplified form of the equations:

$$R_s \simeq R_p$$

and

$$C_s \simeq \frac{1}{\omega^2 C_p R_p^2}$$

Experimental and calculated values using these equations are given in Table 1, the values being taken 10 minutes after mixing.

Whilst we also accept that the effective area available for conduction is decreased as the cement grains segment and the capillary pores become blocked, it must be remembered that the resistivity will increase due to a reduction in ionic concentrations within the capillary water due to the hydration process. It would be difficult to quantify the division between these mechanisms.

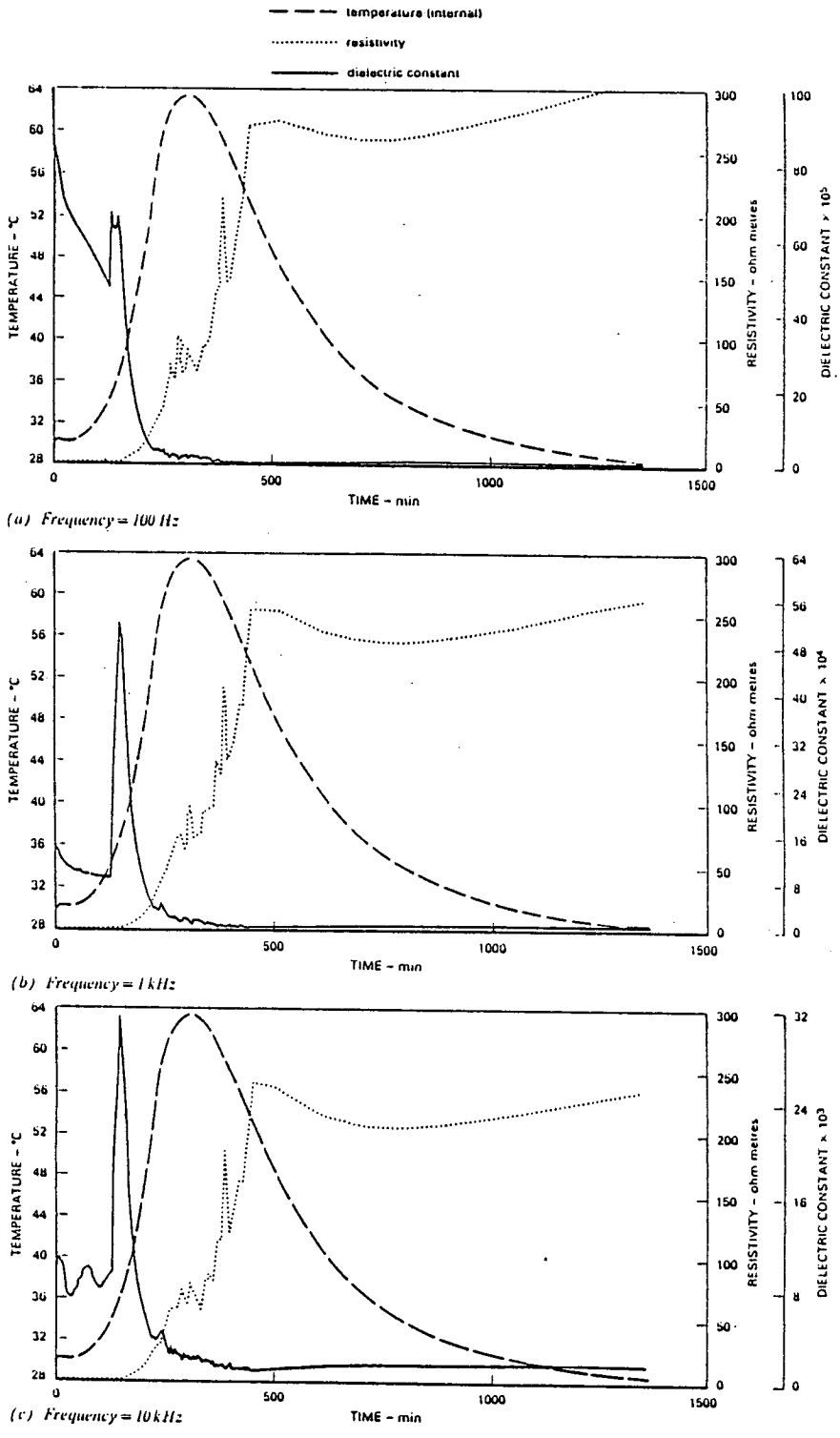

Figure V1: Variation of temperature, resistivity and dielectric constant during initial 24 h after gauging with water. Ordinary Portland cement paste, w/c = 0·25.

TABLE 1: Calculated and experimental values for series model.

Frequency (Hz)	Parallel model (measured)		Series model (calculated)		Series model (measured)	
	R_p (ohms)	C_p (Farads)	R_s (ohms)	C_s (Farads)	R_s (ohms)	C_s (Farads)
100	9·134	$8{\cdot}25 \times 10^{-6}$	9·134	$3{\cdot}67 \times 10^{-3}$	9·092	$3{\cdot}707 \times 10^{-3}$
400	8·866	696×10^{-9}	8·866	$2{\cdot}90 \times 10^{-3}$	8·857	$2{\cdot}914 \times 10^{-3}$
1000	8·915	142×10^{-9}	8·915	$2{\cdot}247 \times 10^{-3}$	8·905	$2{\cdot}256 \times 10^{-3}$
10 000	8·861	$6{\cdot}9 \times 10^{-9}$	8·861	468×10^{-6}	8·854	460×10^{-6}

REFERENCES

1. WILSON, J. G., WHITTINGTON, H. W. and FORDE, M. C. Microprocessor based system for automatic measurement of concrete resistivity. *Journal of Physics* E. Vol. 16, 1983. pp. 700–705.
2. WILSON, J. G., WHITTINGTON, H. W. and FORDE, M. C. Dielectric properties of concrete at different frequencies. *Proceedings of the Fourth International Conference on Dielectric Materials, Measurements and Applications, Lancaster*. London, Institution of Electrical Engineers, 1984. pp. 157–160.
3. TAYLOR, M. A. and ARULANANDAN, K. Relationships between electrical and physical properties of cement pastes. *Cement and Concrete Research*. Vol. 4, No. 6. November 1974. pp. 881–897.
4. SCHWAN, H. P., SCHWARZ, G., MACZUK, J. and PAULY, H. On the low-frequency dielectric dispersion of colloidal particles in electrolytic solutions. *Journal of Physics and Chemistry*. Vol. 66. 1962. p. 2626.
5. SCHWARZ, G. A theory of the low-frequency dielectric dispersion of colloidal particles in electrolyte solution. *Journal of Physics and Chemistry*. Vol. 66. 1962. p. 2636.
6. HASTED, J. B. *Aqueous dielectrics*. London, Chapman and Hall, 1973. pp. 172–173.

APPENDIX E

Analysis of the Equivalent Circuit for Low Frequency Resistivity Measurements

Fig. 5.1 shows the equivalent circuit of the low frequency measurement system.

The input voltage v_r is periodic in t such that

$$v_r = V_r \qquad NT < t < T/2+NT$$

$$v_r = -V_r \qquad T/2+NT < t < T+NT$$

where T is the period, and N = +0, 1, 2, 3, ...

The Laplace transform of v_r

$$L\{v_r\} = \frac{v_r}{s}\{1 - 2e^{-\frac{T}{2}s} + e^{-Ts}\}\{1 + e^{-Ts} + e^{-2Ts} + ...\}$$

The transfer function of the circuit of Fig. 5.1 is:

$$H(s) = \frac{R_s + \frac{1}{sC_s}}{R_r + R_s + \frac{1}{sC_s}}$$

$$= \frac{R_s}{R_r + R_s} \cdot \frac{s + \frac{1}{C_s R_s}}{s + \frac{1}{C_s(R_r + R_s)}}$$

Assuming that capacitance C_s is initially uncharged, the transform of the output voltage will be:

$$L\{v_0\} = H(s)\, L\{v_r\}$$

Letting $C_s(R_r + R_s) = \tau$ gives:

$$L\{v_0\} = V_r \left\{ \frac{1}{s} - \frac{R_r}{R_r + R_s} \cdot \frac{1}{s + \frac{1}{\tau}} \right\}$$

$$x \left\{ 1 - 2e^{-\frac{T}{2}s} + e^{-Ts} \right\} \left\{ 1 + e^{-Ts} + e^{-2Ts} + \ldots \right\}$$

The inverse transform:

$$L^{-1}\left\{ \frac{1}{s} - \frac{R_r}{R_r + R_s} \cdot \frac{1}{s + \frac{1}{\tau}} \right\} = 1 - \frac{R_r}{R_r + R_s} e^{-\frac{t}{\tau}}$$

For $NT < t < T/2+NT$ and letting $t = t_0 + NT$ gives

$$v_0 = V_r \left\{ 1 - \frac{2R_r}{R_r + R_s} e^{-\frac{t_0}{\tau}} \left(1 - e^{-\frac{0.5T}{\tau}}\right) \right.$$

$$\left. x \left[1 - e^{-\frac{T}{\tau}} + e^{-\frac{2T}{\tau}} + \ldots\right] \right\}$$

In the steady state this reduces to:

$$v_0 = V_r \left\{ 1 - \frac{2R_r}{R_r + R_s} e^{-\frac{t_0}{\tau}} \frac{\left(1 - e^{\frac{-0.5T}{\tau}}\right)}{\left(1 - e^{-\frac{T}{\tau}}\right)} \right\}$$

However:

$$\frac{1 - e^{\frac{-0.5T}{\tau}}}{1 - e^{-\frac{T}{\tau}}} = \frac{1}{1 + e^{\frac{-0.5T}{\tau}}}$$

Thus, the output can be rewritten as:

$$v_0 = V_r \frac{R_s}{R_r + R_s} \left\{ 1 + \frac{R_r}{R_s} \left[1 - \frac{2e^{-\frac{t_0}{\tau}}}{1 + e^{\frac{-0.5T}{\tau}}} \right] \right\}$$

(E.1)

If C_s did not exist the output voltage would be:

$$v_0 = V_r \frac{R_s}{R_r + R_s} \qquad (E.2)$$

Thus

$$\alpha = \frac{R_r}{R_s}\left[1 - \frac{2\,e^{-\frac{t_0}{\tau}}}{1 + e^{\frac{-0.5T}{\tau}}}\right] \qquad (E.3)$$

is the fractional deviation from the required value of v_0.

If $C_s (R_s + R_r) = \tau >> T/2$

$$\alpha \doteqdot \frac{R_r}{R_s}\left[1 - \frac{2\,(1 - \frac{t_0}{\tau})}{1 + (1 - \frac{0.5T}{\tau})}\right]$$

$$\doteqdot \frac{R_r}{R_s} \cdot \frac{2\frac{t_0}{\tau} - 0.5\frac{T}{\tau}}{2 - \frac{0.5T}{\tau}}$$

$$\doteqdot \frac{R_r}{R_s} \frac{(t - T/4)}{\tau} \qquad (E.4)$$

If $t_0 = T/4$ then $\alpha = 0$. Thus if the measurement is taken at the mid-point of the positive pulse, the fractional error will be zero.

The maximum value of α will occur when $t_0 = 0$ or $T/2$.

Taking the value when $t_0 = 0$ gives:

$$|\alpha|_{MAX} = \frac{1}{4} \frac{R_r}{R_s} \frac{T}{\tau} \qquad (E.5)$$

Thus if the value of T is reduced, and therefore the frequency of the waveform increased, the value of $|\alpha|_{max}$ will fall.

Thus, from E.1, and E.4, for a positive half cycle

$$v_0 \doteq \frac{V_r R_s}{R_r + R_s} \left\{ 1 + \frac{R_r}{R_s} \frac{(t_0 - T/4)}{\tau} \right\} \qquad (E.6)$$

and, from symmetry, for a negative half cycle

$$v_0 \doteq - \frac{V_r R_s}{R_r + R_s} \left\{ 1 + \frac{R_r}{R_s} \frac{(t_0 - T/4)}{\tau} \right\} \qquad (E.7)$$

APPENDIX F.

Microprocessor Based System for Automatic Measurement of Concrete Resistivity - Reference 71.

J. Phys. E: Sci. Instrum., Vol. 16, 1983. Printed in Great Britain

Microprocessor-based system for automatic measurement of concrete resistivity

J G Wilson†, H W Whittington‡ and M C Forde§
† Department of Electrical Engineering, Napier College, Edinburgh, UK
‡ Department of Electrical Engineering, Edinburgh University, Edinburgh, UK
§ Department of Civil Engineering and Building Science, Edinburgh University, Edinburgh, UK

Received 13 December 1982, in final form 31 January 1983.

Abstract. An automatic electronic system for measuring the electrical resistivities of a large number of concrete sample cubes over a period of up to 100 days is described. Results obtained using the equipment are presented and the possible applications to concrete quality control and fundamental research are briefly discussed.

1. Introduction

The importance of concrete as a structural material is evidenced by its widespread use in many applications. The traditional method of assessing the quality of a batch of concrete is by casting 150 mm cubes from the mix and later crushing them. The cubes are cured in a water tank at 293 K (20 °C), to prevent loss of moisture, for a period of 7 or 28 days prior to crushing. The date of crushing varies with structural design specifications.

The limitations of destructively testing concrete cubes are:
(i) the results of cube crushing tests are not available for 7 or 28 days depending upon the structural engineer's specification;
(ii) in civil engineering works this delay may disrupt subsequent construction schedules;
(iii) the quality of the compacted concrete in the cubes may not be representative of the concrete mass of the structure.

Therefore, it can be seen that an alternative technique which could test concrete at an earlier stage and eventually be applied to mass concrete *in situ* would be of substantial value to the civil engineering industry.

Alternatives to destructive testing have been studied. Other parameters of concrete have been monitored and their values related to the crushing strength. One such parameter is the electrical resistivity of the concrete (Hammond and Robson 1955, Monfore 1968, Whittington *et al* 1981).

To date, manual methods of resistivity measurement have been used, but to achieve statistical significance of results, many samples must be tested over extended periods of time. This paper describes an automatic system which will perform this function.

2. Standard test conditions

Normal strength measurements for concrete are described in BS1881. One of the sample geometries allowed in this specification is a 150 mm cube and this has been taken as the standard for the present resistivity measurements to allow correlation with crushing strength. BS1881 requires that the samples be kept in an atmosphere of not less than 90% relative humidity at 293 K for a period of 1 day. The samples are then demoulded and stored under water at a temperature of 293 K until they have reached the required maturity, usually 7 to 28 days, and then crushed.

3. Measurements technique

3.1. Representation of concrete

At low frequencies, the concrete sample can be represented by the equivalent circuit of figure 1. The capacitance C is due to polarisation caused by electrolytic action between the cement paste and the electrodes. This polarisation must be regarded as semi-permanent because of the difficulty in dispersing the gas which has been generated.

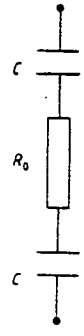

Figure 1. Equivalent circuit of concrete sample at low frequency.

3.2. Measurement of resistivity

The resistivity is measured by applying a square waveform of known amplitude, to the sample, in series with a known value of resistance (R) as shown in figure 2. The resistivity is calculated from the voltage measured across the concrete. The waveform obtained is shown in figure 3.

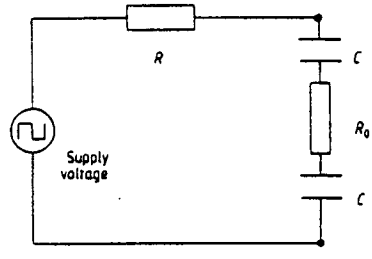

Figure 2. Test circuit for measuring concrete resistance R_0. R is a standard resistance.

The fractional increase in voltage during the pulse due to the polarisation capacitance is largely independent of the value of R, and will present an uncertainty in the measurement of the concrete resistance. The increase in voltage can be minimised by using as high a frequency as possible, and theoretically, the correct value of resistance will be obtained using the average value of voltage which is the voltage at the mid-point of the pulse.

The frequency used in the equipment is 2 kHz, and the

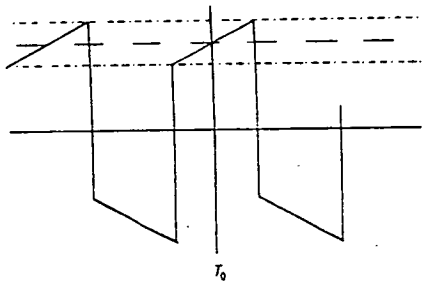

Figure 3. Waveform of voltage across concrete sample. T_0 = measurement point.

voltage is sampled at the mid-point of the pulse. Together, these reduce polarisation effects to a negligible level.

Because of the low values of resistivity involved, fringing effects are not significant.

$$R_0 = \frac{Rv_0}{E - V_0}$$

and resistivity

$$\rho = \frac{Rv_0}{E - V_0} l$$

where l is the length of a face of the cube.

4. Details of the automatic resistance-measurement system

The automatic resistance-measurement system is based on the Rockwell 6502 CPU with associated monitor and interfacing circuits, i.e. the Rockwell AIM65 microcomputer. Additional circuitry is located in the electronics unit shown in figure 4.

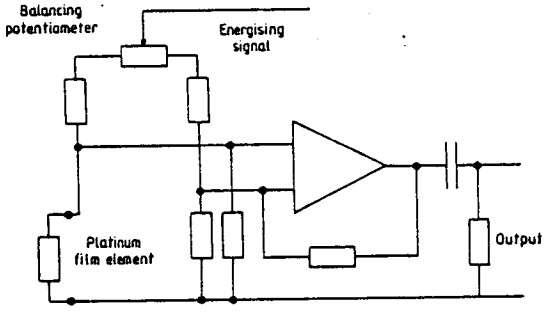

Figure 4. Temperature sensor and amplifier.

4.1. Timing circuits

Within the electronics unit, waveforms required are obtained by frequency-dividing the AIM65 clock of frequency 1 MHz, using a chain of four-bit binary counters. The lowest-frequency signal, the basic timing signal for the system, has a period of 43.2s, which corresponds to 0.0005 days. Other signals include 7.2 kHz to energise the temperature-monitoring system, 2.0 kHz to energise the resistivity-measurement system, and a frequency of 3.9 kHz to ensure that measurements take place at the centre of the resistivity energising pulse. A frequency of 0.95 Hz is used to control monitoring of the output of the A/D converter on the AIM65 electronic display.

4.2. Measurement of temperature

Since concrete has a relatively high value of temperature coefficient of resistivity (about 0.02 K^{-1}), the temperature of the samples is important. A platinum film temperature sensor is fixed to one of the electrodes on each sample. The measured resistivity is then corrected to a temperature of 293 K. The temperature coefficient of the platinum film element is only $3.85 \times 10^{-3}\ K^{-1}$. This will result in a very small change in voltage across the element for a fixed current over the temperature range 273–323 K. The element is used in the circuit of figure 5. Because of the variations in resistance between elements, and the very small signals involved, a separate amplifier is used for each element, and is positioned as close to the sample as possible. The energising signal is a square wave at 7.2 kHz. The output signals from the amplifiers are synchronously detected in the main electronics unit.

4.3. Sample measurement

The system is designed to accommodate 60 concrete samples arranged in groups of 15 in channels 0, 1, 2 and 3. Initially measurements were carried out using units 0 to 4 in channel 0 but this capability has been extended to allow all 15 units within channel 0 to be used.

Each channel has amplifiers to feed the resistivity and temperature energising signals to the concrete samples. The resistivity outputs are fed to the resistivity 16-channel multiplexer. The temperature outputs are fed to a similar multiplexer after having been synchronously detected. The 16th input for both the resistivity and temperature multiplexers is obtained from reference circuits which provide comparison standards for the sample.

The outputs from the resistivity and temperature multiplexers are buffered and then passed to an eight-channel multiplexer which selects the resistivity and temperature signals for the four channels. The ourput from the eight-channel multiplexer is again buffered and fed to an eight-bit successive approximation A/D converter to give a digital output to the computer. The A/D converter uses a 500 kHz clock signal obtained from the timing circuit. Selection of the output from the multiplexers is by the eight-bit binary signal from the computer VIA interface unit. In all cases, control of the A/D conversion is by the microcomputer software.

4.4. Electro-mechanical facility

For one day after mixing, the concrete remains in the moulds. The room temperature is kept at 293 K, and the samples are covered with polythene to maintain the required humidity.

After one day the concrete samples are demoulded and are stored in a controlled-temperature water bath as required by BS1881 (§ 2, above). These are then automatically removed from the bath by an electrically driven hoist, at appropriate times, for measurement purposes. Sufficient time is allowed for surface water to drain off the concrete cubes before measurements are made. After measurement the samples are returned to the water.

The system design allows for the control of a hoist on each channel of 15 samples, although at present only one hoist has been installed.

The hoist consists of a single-phase capacitor-start induction motor driving a hoist drum through reduction gearing. This allows a load of 200 kg to be lifted at approximately 0.5 m min^{-1}. Upper and lower limit switches are operated by cams on the drum shaft. A safety switch is also fitted which will switch off the mains supply to the motor in the event of the limit

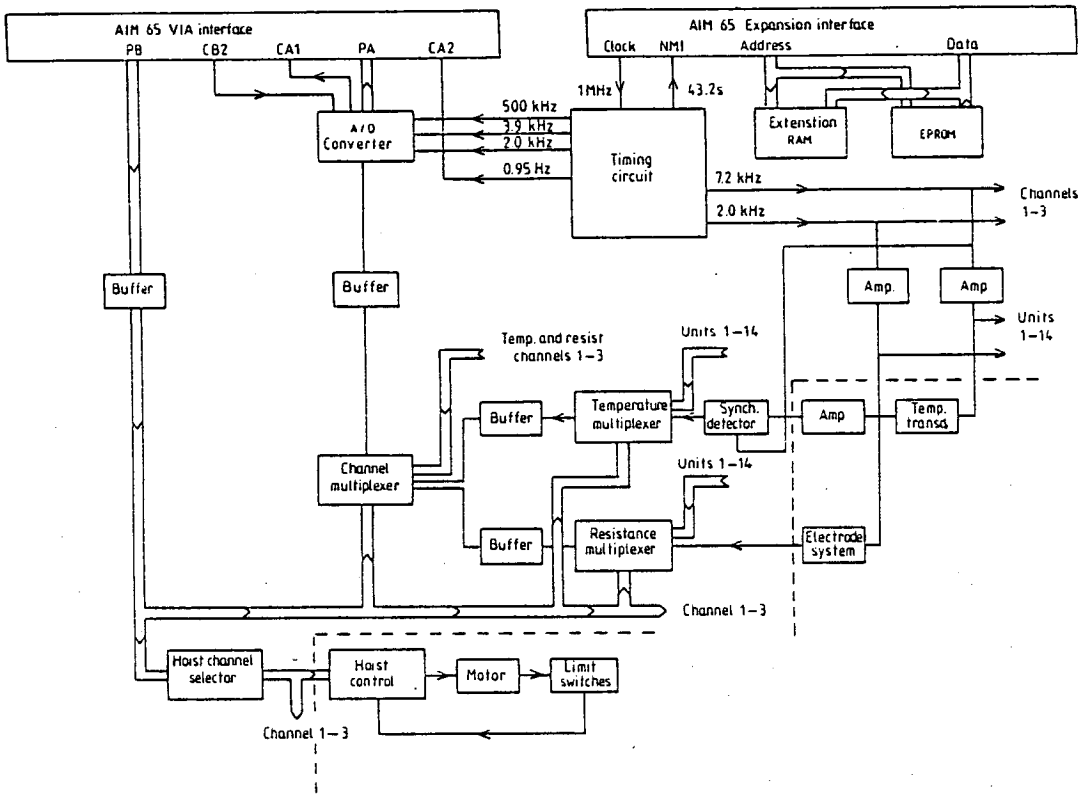

Figure 5. Electronic system; channel 0 units shown.

switches being overrun. Control of the hoist is by computer interface VIA, through the hoist control circuit.

5. Software

5.1. Program arrangement

In addition to the standard 4 k RAM available with AIM65, the present unit has 4 k RAM extension. Once developed, the operating programs were transferred to 2 × 4 k on-board EPROMs. The computer program organises the experiments being carried out by means of a timetable, which is updated after each set of measurements is taken. Because the early stages of setting of the concrete are of interest readings are taken relatively frequently during the first hours and days after casting.

Thereafter, the setting process is less rapid and consequently the period between readings increases.

To achieve this, measurements are carried out on a logarithmic time scale for 0.0015 days up to 100 days; the measurement points within a decade are 1.5, 2.5, 4, 6.5 and 10.

When a set of readings has been taken, the program calculates the resistivity, temperature, and resistivity at 293 K for each sample, and outputs this data on a dot matrix printer.

The program can monitor a maximum of 60 samples arranged in up to 40 separate experiments. Experiments can be inserted or removed at any time without switching down the system.

Control of the timetable, addressing of the multiplexers, and transfer of data from the A/D converter, is carried out by machine code program. System control, calculation of results, and control of output on the printer and electronic display, is by BASIC program.

5.2. Additional features

In addition to the normal running program controlling the timetable, measurement, calculation and output of data, the following facilities are also provided:

(a) Initiation of new experiments and removal of old.

(b) Measurement of an experiment sample set on demand, to supplement automatic measurement.

(c) Monitoring of any output available to the A/D converter on the electronic display.

(d) Monitoring of the calculated temperature of any sample on the electronic display.

(e) Operation of the hoist on demand, from the computer keyboard.

(f) Print-out of the list of experiments in the system, and the number of samples in each.

(g) Print-out of current system time.

(h) Correction of system time.

During normal operation, the electronic display presents the current system time, the code number of the next experiment to be measured, and the system time at which this measurement will take place.

6. Preparation of samples

The moulds used for preparing samples are made of cast steel,

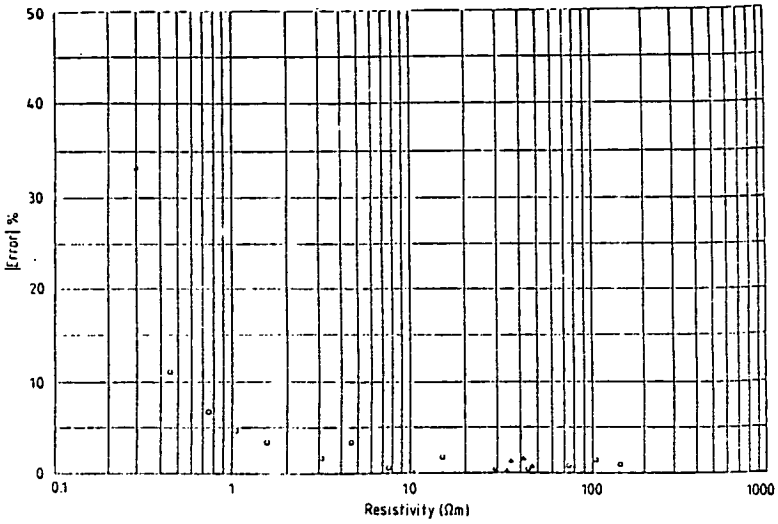

Figure 6. Accuracy of measurement. O, measurement on resistance; Δ, measurement on concrete.

and are insulated by a PVC liner with additional plastic film. Stainless steel electrodes are placed against two opposite sides of the mould before the concrete is poured. On demoulding it has been found that there is a good bond between the electrodes and the concrete. Oversized moulds are used, and these are shimmed such that a 150 mm cube of concrete is obtained between the electrodes.

7. System operation and results

7.1. System accuracy.

Comparison of resistivity measurements using the system and those obtained using a Wayne Kerr Universal Bridge Type B221, which has an accuracy of ±0.1% is shown in figure 6. Most of the measurements are with resistors, but a few are values obtained with concrete. At low values of resistivity, the error increases rapidly, and is due to the quantisation error of the A/D converter. At high values of resistivity, the percentage error is roughly constant at better than ±2%, and is largely due to the build up in resistance tolerance.

The values given are for uncorrected resistivity. The uncertainty for corrected resistivity depends on the uncertainty for the temperature coefficient of resistivity. The overall uncertainty will be greatest at the maximum temperature deviation from 293 K. This corresponds to a difference of 30 K when the temperature is 323 K. Assuming an uncertainty of ±15% in temperature coefficient, the total uncertainty at 323 K could be as high as ±7%.

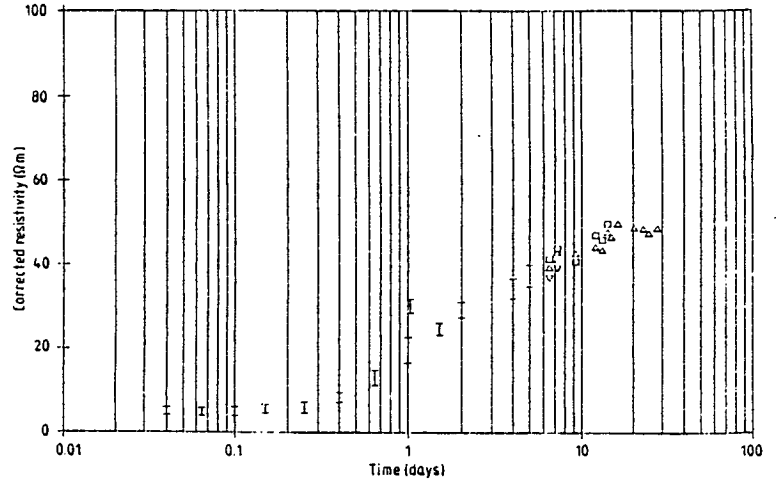

Figure 7. Second proving trial; temperature coefficient 0.022.

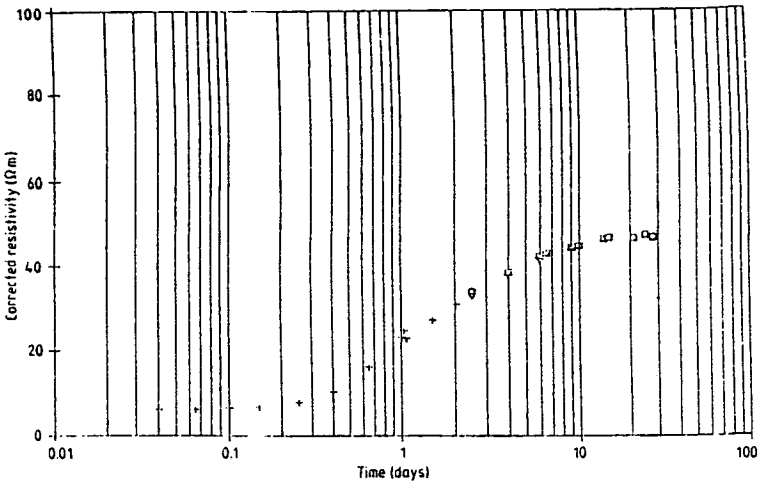

Figure 8. Third proving trial; temperature coefficient 0.022.

7.2. Results and discussion

Results using the equipment to measure resistivity for two experiments each of five samples with water: cement ratio 0.5:1, and cement:sand:coarse aggregate ratio 1:1.5:3, are presented in figures 7 and 8. On these graphs the symbol I is used to show the average value of resistivity if there are more than three samples. The height of the symbol indicates the 95% confidence limits for the average value. If the required height of the symbol becomes less than the horizontal dimension then the + symbol is used instead. If there are fewer than three samples, then individual points are shown, each with an identifying symbol. It can be seen that the uncertainties are greater, and that there is a significant discontinuity after demoulding at one day, for figure 7, as compared with figure 8. This is due to poor sampling of the concrete and poor insulation of the moulds. These were improved for the experiment whose results are shown in figure 8.

7.3. Applications

Some possible applications of the data obtained using this technique suggest themselves as follows.

7.3.1. Quality control of concrete. A test batch of concrete which is known to have the required crushing strength for the application in question could be characterised in term of its resistivity/time graph. This graph could then be taken as a reference and resistivity measurements on subsequent batches compared with it. Deviations would indicate suspect mixes.

7.3.2. Crushing strength prediction. The relationship between various parameters, derived from the resistivity/time graph, and the measured crushing strength is at present under investigation. Correlation already obtained indicates that parameters derived from the resistivity/time characteristic may be taken as some measure of the quality of the concrete.

7.3.3. Water:cement ratio estimation. The time at which setting occurs (the time at which the resistivity starts to increase significantly) will be largely determined by the water:cement ratio. The initial resistivity before setting will depend on both water:cement ratio and cement:aggregate ratio. If the relationships between these quantities can be reliably established, then the actual mix used for a particular sample can be deduced.

7.3.4. Pore investigation. The resistivity of concrete is largely due to ionic conduction through water-filled pores in the cement paste. The analysis of measured resistivity could be used in the investigation of these pores.

8. Future developments

The equipment is currently being modified to give a capability of measuring 15 samples. PVC moulds have been obtained and will be used instead of cast steel, to ease the insulation problem.

A series of intensive measurements using the modified equipment will start shortly. The aim of this programme is to estimate the water:cement ratio and cement:aggregate ratio from resistivity measurements, before the concrete is one day old, and to correlate long-term resistivity with crushing strength. The temperature coefficient of resistivity of concrete will also be investigated.

Design work is under way on new equipment which will measure 15 samples under the control of a Hewlett-Packard HP85 computer. This system will operate through an IEEE bus system, and will have the capability of expansion of up to 14 measurement units each with 15 samples.

Acknowledgments

The authors wish to thank Professor A W Hendry of the Department of Civil Engineering and Building Science and Professor J H Collins of the Department of Electrical Engineering at the University of Edinburgh, and Mr P H Beards of the Department of Electronic Engineering, Napier College of Commerce and Technology, Edinburgh, for placing the facilities of their respective departments at their disposal.

J G Wilson would also like to thank Lothian Regional Council for financial support.

References

Hammond E and Robson T D 1975 Comparison of electrical properties of various cements and concretes *The Engineer* **199** 21 January, pp 78–80

Monfore G E 1968 The electrical resistivity of concrete *J. PCA Research and Development Laboratories* **10** No 2 35–48

Whittington H W, McCarter J and Forde M C 1981 The conduction of electricity through concrete *Magazine of Concrete Research* **33** No 114 48–60

British Standards Institution 1970 (and amendments) *Methods of testing concrete BS1881*

APPENDIX G.

Circuit Diagrams - Prototype System.

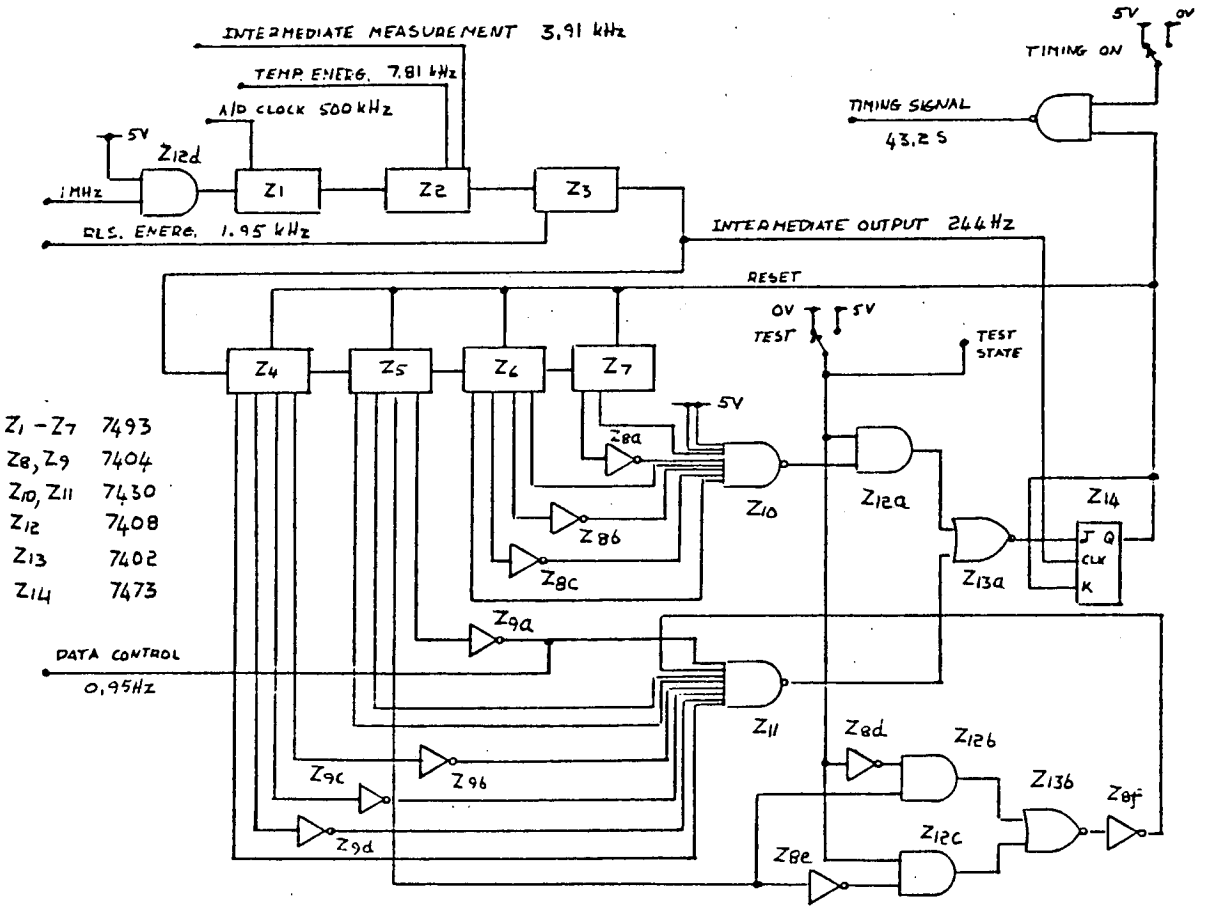

Figure G. 1.
Timing Circuit

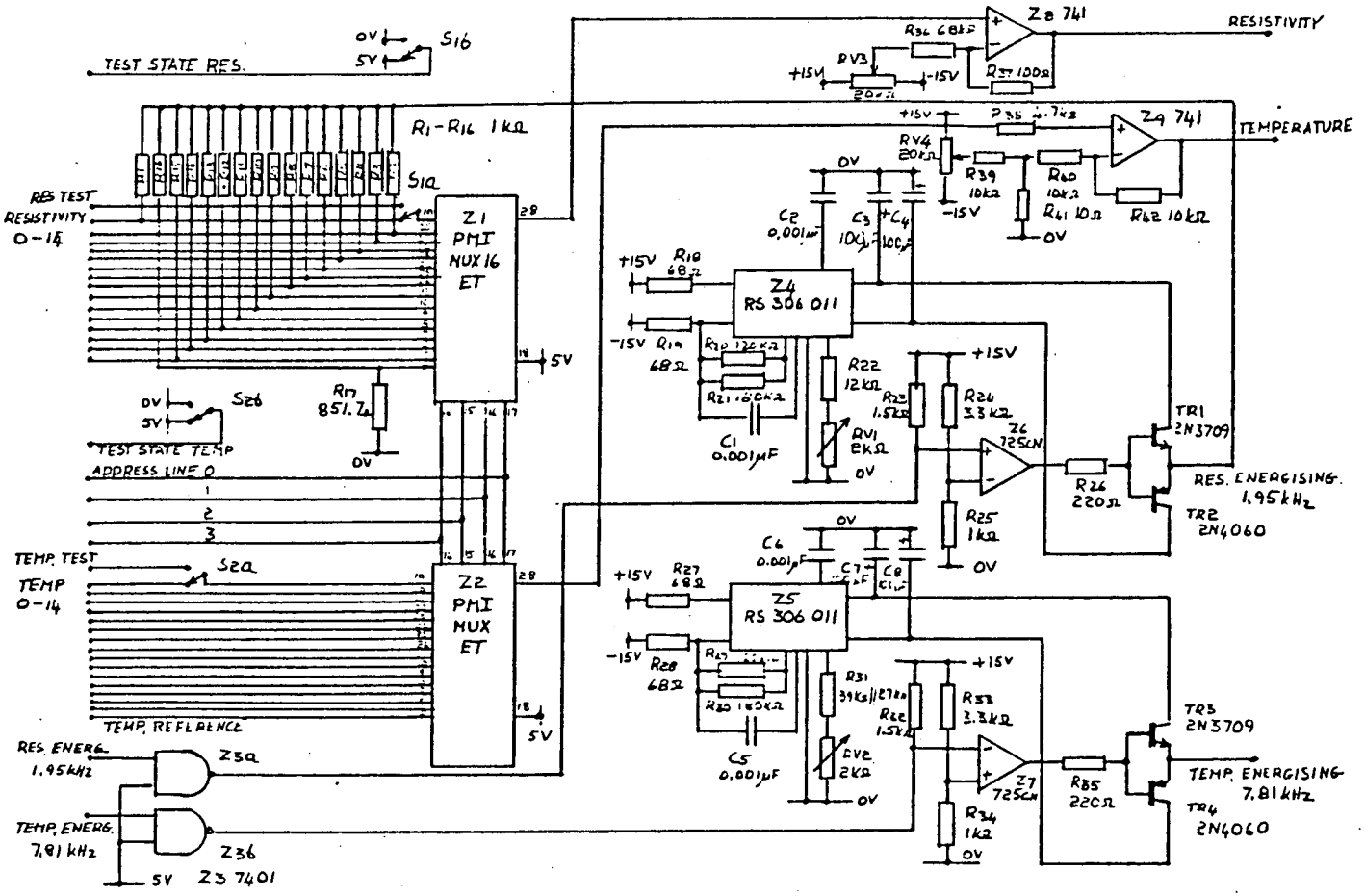

Figure C.2.
Multiplexer

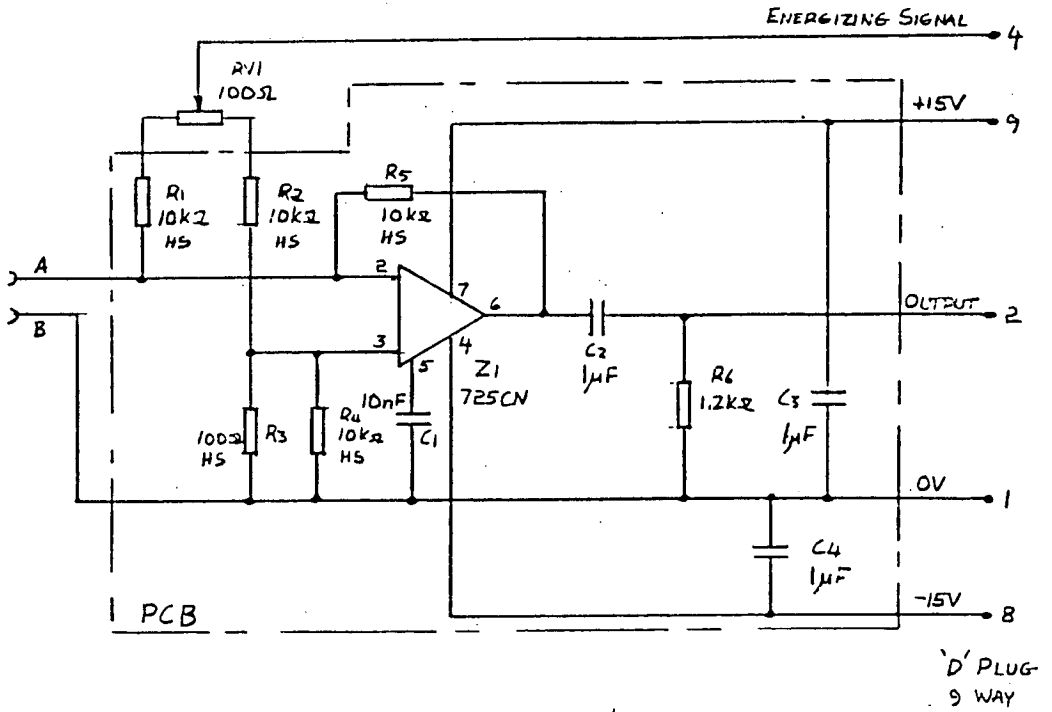

HS- HIGH STABILITY RESISTORS — TOLERANCE 0.1%.

Figure G. 3.
Temperature Amplifier

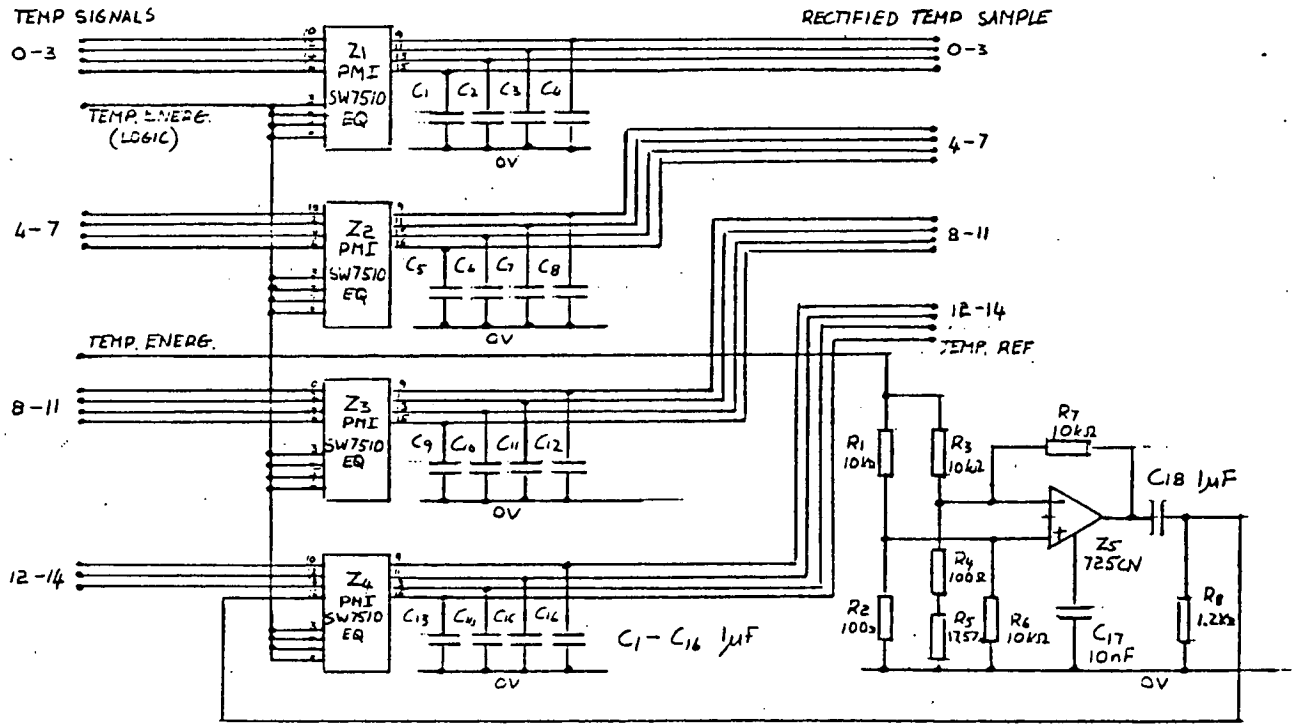

Figure G. 4.
Temperature Rectifier

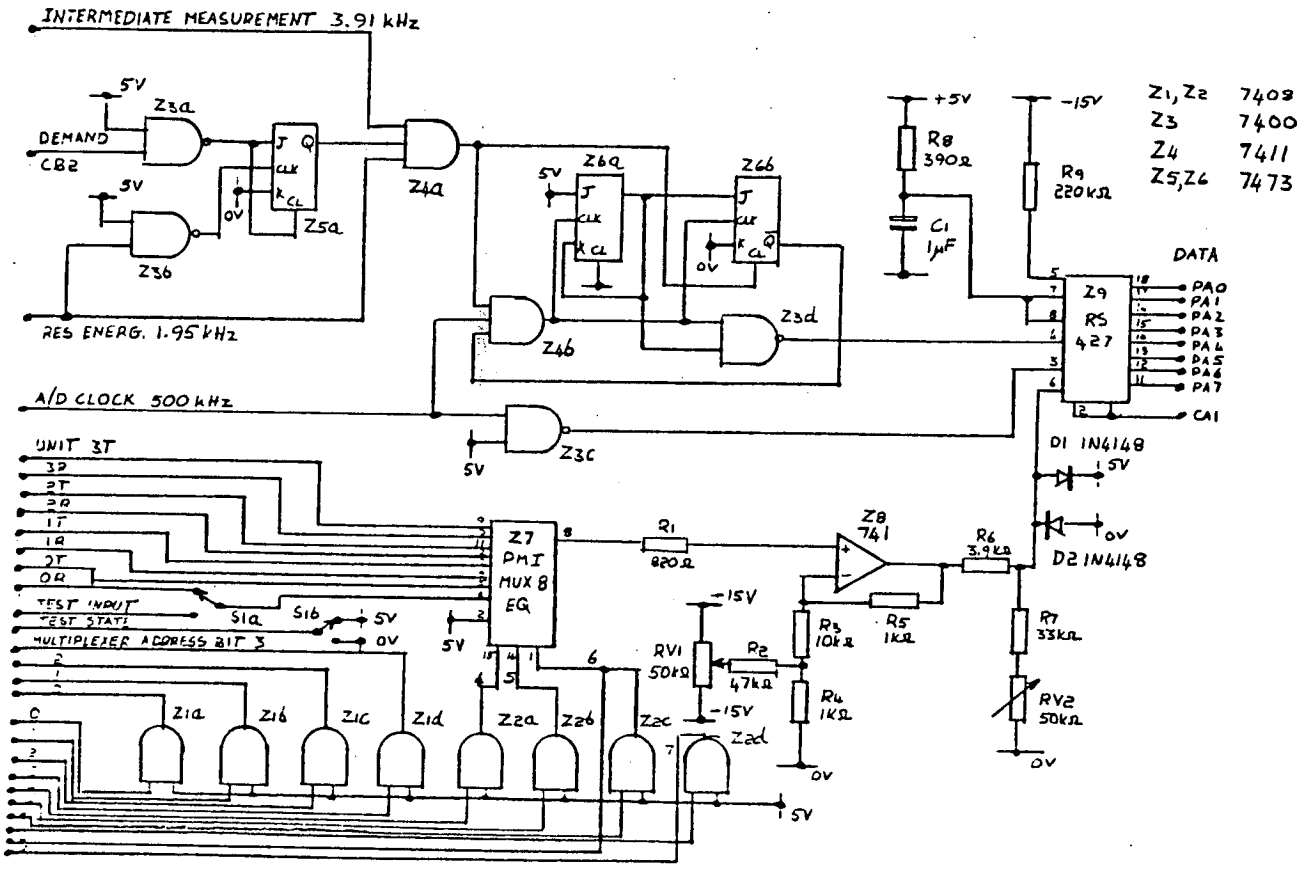

Figure 6.5.
A/D Converter

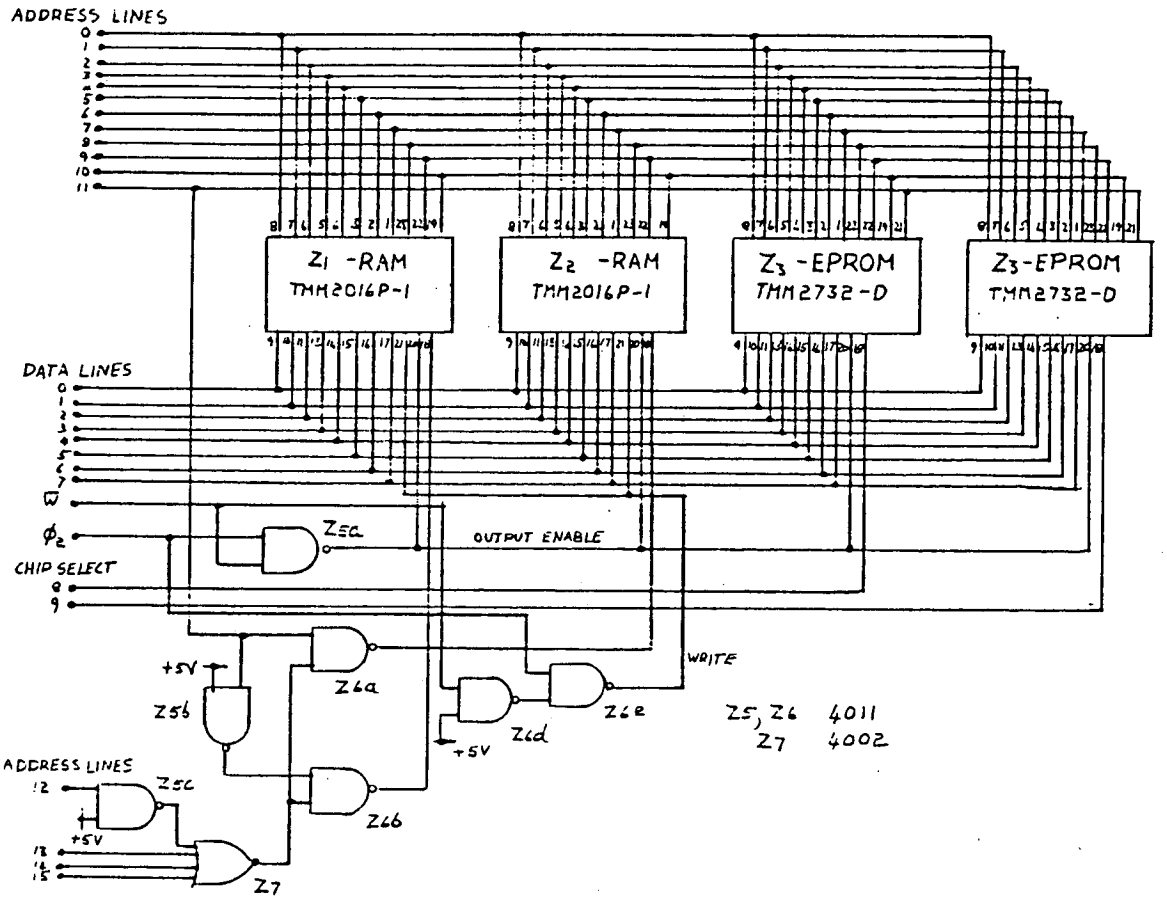

Figure C.6.
Memory Extension

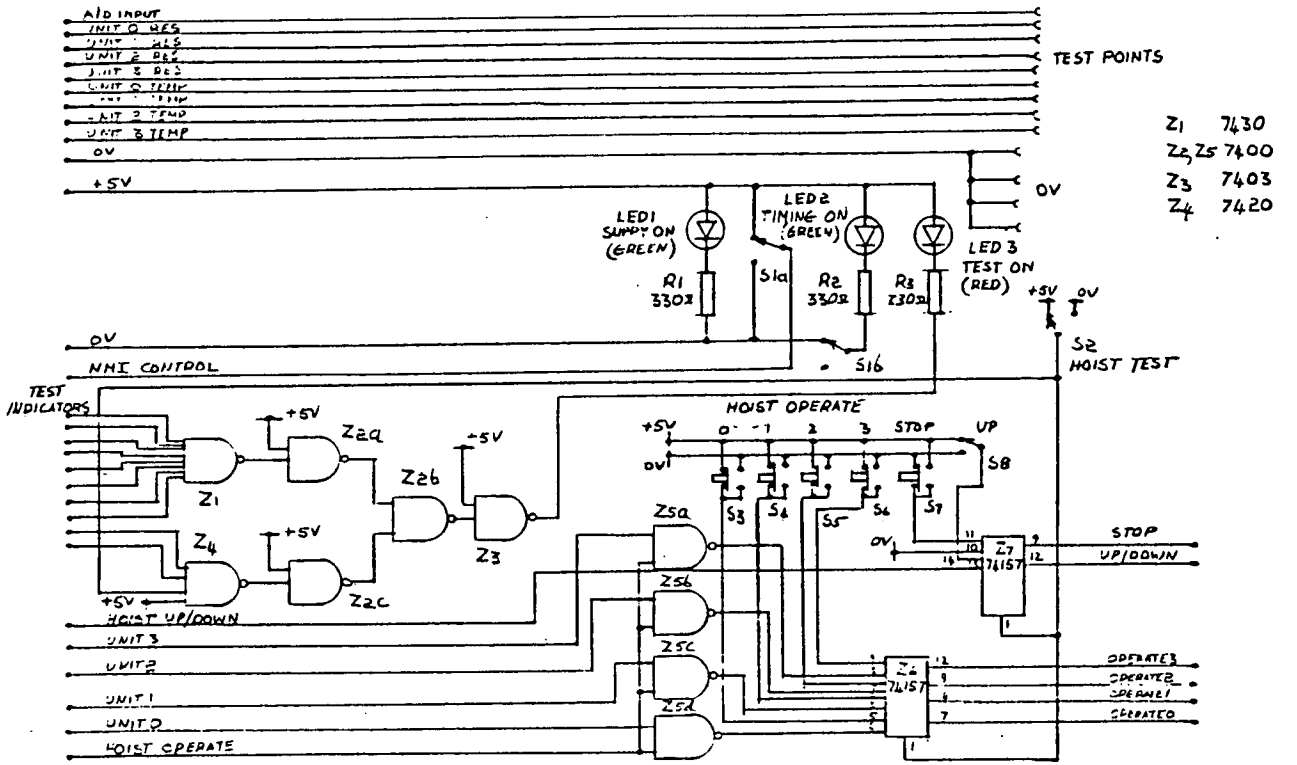

Figure 6.7.
Control Circuit

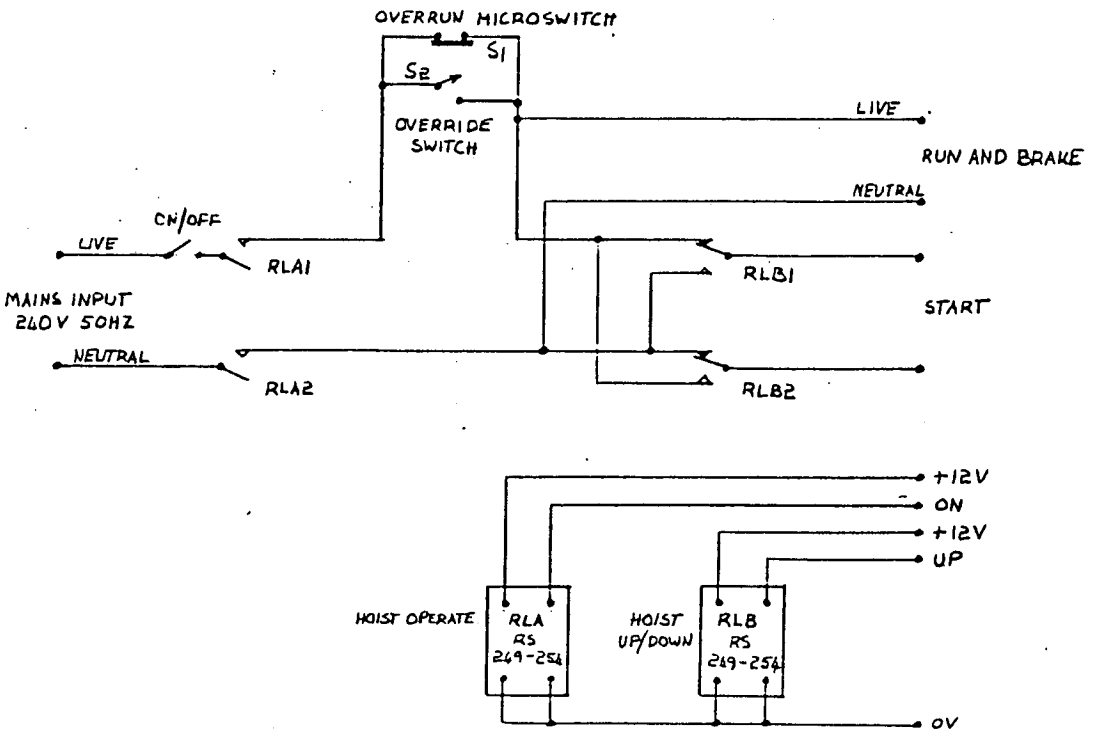

Figure G.8.
Hoist Circuit

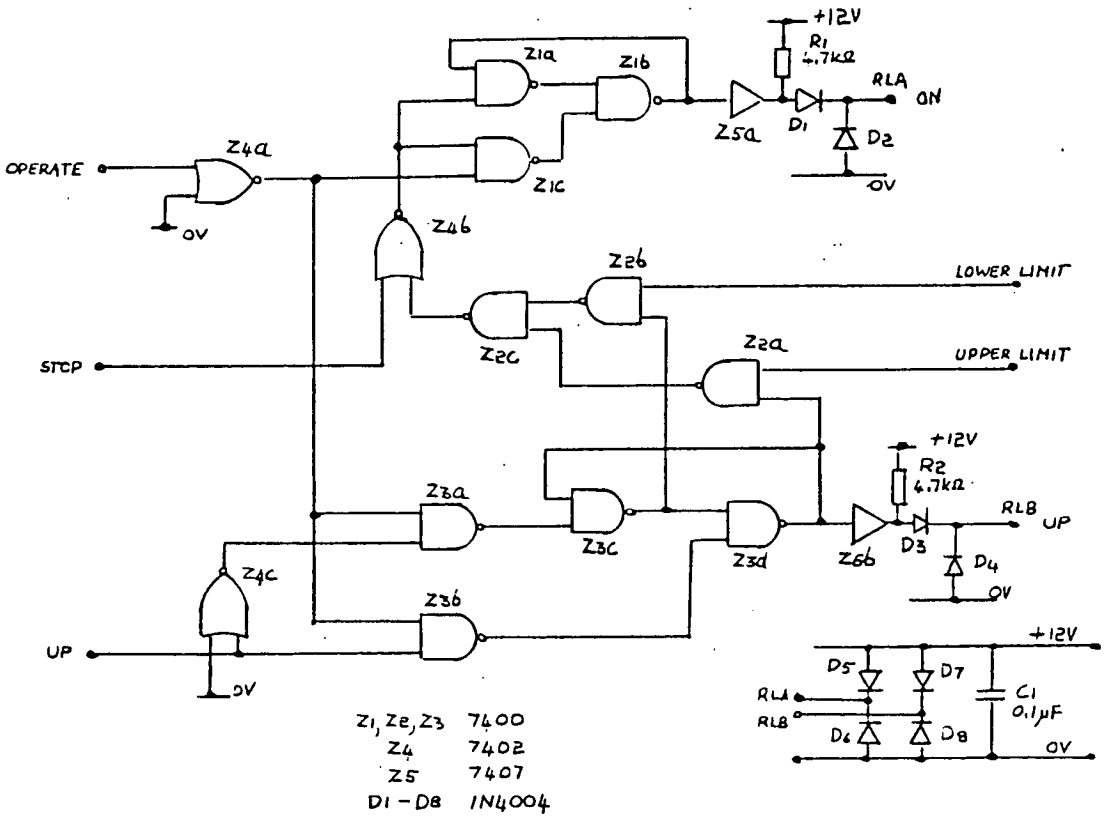

Figure 6.9.
Hoist Control Circuit

APPENDIX H

Uncertainty Analysis of Temperature Amplifier

The temperature amplifier is shown in Fig.H.1. This circuit can be simplified to that of Fig.H.2 by applying Thevenin's Theorem which gives:

$$V_1 = V_r \frac{R_T}{R_1 + R_T} = V_r \frac{R_T}{R_1}$$

$$V_2 = V_r \frac{\frac{R_3 R_4}{R_3 + R_4}}{R_2 + \frac{R_3 R_4}{R_3 + R_4}} = V_r \frac{R_3}{R_2}$$

$$R = \frac{R_1 R_T}{R_1 + R_T} = R_T$$

From Fig.H.2, assuming an ideal operational amplifier:

$$\frac{V_1 - V_2}{R_T} = \frac{V_2 - V_0}{R_5}$$

$$\Rightarrow V_0 = -\frac{R_5}{R_T} V_1 + \left(1 + \frac{R_5}{R_T}\right) V_2$$

$$= V_r \left\{ \frac{R_3}{R_2} - \frac{R_5}{R_1} + \frac{R_5 R_3}{R_2} \cdot \frac{1}{R_T} \right\}$$

Differentiating partially with respect to R_1, R_2, R_3, R_5 and R_T gives for small changes

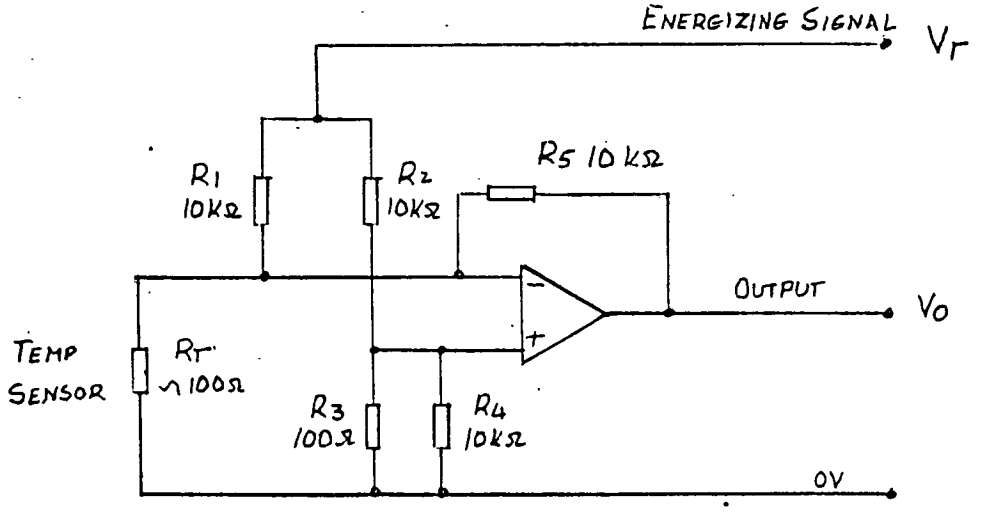

Figure H. 1.
Temperature Amplifier

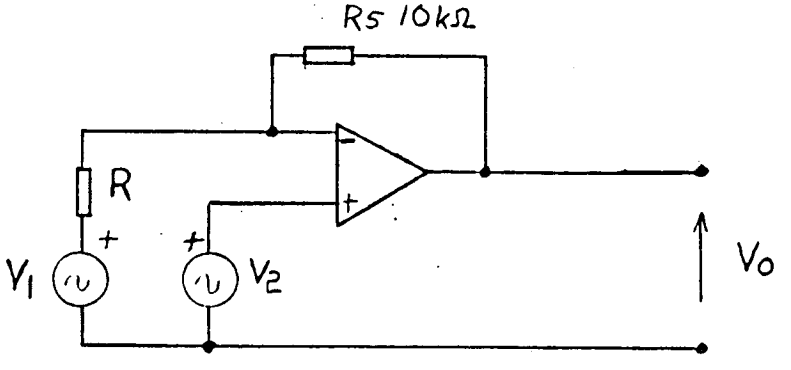

Figure H. 2.
Simplified Circuit

$$\Delta V_0 = V_r \left\{ \frac{R_5}{R_1^2} \Delta R_1 - \left[\frac{R_5 R_3}{R_2^2 R_T} + \frac{R_3}{R_2^2} \right] \Delta R_2 + \left[\frac{1}{R_2} + \frac{R_5}{R_2 R_T} \right] \Delta R_3 \right.$$

$$\left. + \left[\frac{R_3}{R_2 R_T} - \frac{1}{R_1} \right] \Delta R_5 - \frac{R_5 R_3}{R_2 R_T^2} \Delta R_T \right\}$$

$$= V_r \left\{ \frac{\Delta R_1}{R_1} - \left[\frac{10^2}{R_T} + 10^{-2} \right] \frac{\Delta R_2}{R_2} + \left[\frac{10^2}{R_T} + 10^{-2} \right] \frac{\Delta R_3}{R_3} \right.$$

$$\left. + \left[\frac{10^2}{R_T} - 1 \right] \frac{\Delta R_5}{R_5} - \frac{10^2}{R_T} \frac{\Delta R_T}{R_T} \right\} \qquad \text{(H.1)}$$

For the measurement channels, R_T is the variable being measured thus $\Delta R_T = 0$. The system is set correctly by adjustment of a balance potentiometer at some temperature at which $R_T = R_{T0}$. The error at this temperature must be zero. Thus:

$$\frac{\Delta R_1}{R_1} - \left[\frac{10^2}{R_{T0}} + 10^{-2} \right] \frac{\Delta R_2}{R_2} + \left[\frac{10^2}{R_{T0}} + 10^{-2} \right] \frac{\Delta R_3}{R_3} + \left[\frac{10^2}{R_{T0}} - 1 \right] \frac{\Delta R_5}{R_3} = 0$$

Subtracting this expression from Expression H.1 with $\Delta R_T = 0$ gives:

$$\Delta V_0 = V_r \left\{ \left[\frac{1}{R_{T0}} - \frac{1}{R_T} \right] 10^2 \frac{\Delta R_2}{R_2} + \left[\frac{1}{R_T} - \frac{1}{R_{T0}} \right] 10^2 \frac{\Delta R_3}{R_3} \right.$$

$$\left. + \left[\frac{1}{R_T} - \frac{1}{R_{T0}} \right] 10^2 \frac{\Delta R_5}{R_5} \right\}$$

$$= 10^2 V_r \left[\frac{1}{R_T} - \frac{1}{R_{T0}} \right] \left\{ - \frac{\Delta R_2}{R_2} + \frac{\Delta R_3}{R_3} + \frac{\Delta R_5}{R_5} \right\}$$

Taking V_r = 7.851V, assuming resistor tolerances ± 0.1% normally distributed, and allowing for a gain of 2 in the multiplexer gives for the standard deviation of the output voltage

$$\sigma_0 = 0.9056 \left| \frac{1}{R_T} - \frac{1}{R_{T0}} \right|$$

For the reference channel, R_T is replaced by the calibration resistance R_c = 117,562Ω, giving from Expression H.1

$$\Delta V_{0r} \doteq V_r \left\{ \frac{\Delta R_1}{R_1} - 0.851 \left[\frac{\Delta R_2}{R_2} - \frac{\Delta R_3}{R_3} + \frac{\Delta R_c}{R_c} \right] - 0.149 \frac{\Delta R_5}{R_5} \right\}$$

Assuming all resistor tolerances ± 0.1% normally distributed, and allowing for a gain of 2 in the multiplexer gives for the standard deviation in the output reference voltage:

$$\sigma_{0r} = 0.936 \times 10^{-3} \text{ V}$$

APPENDIX I.

Development of Microelectronic Circuits.

I.1. Introduction.

When developing an improved version of the equipment, it was decided to replace certain circuits by microelectronic devices designed by using an IC cell library.

The use of such libraries has overcome two of the major disadvantages of custom microcircuits, namely:-

(1) the cost and time involved in circuit design including silicon layout and mask production

(2) the necessity of using highly skilled designers for even the simplest circuit.

By using a computer based library of integrated circuit cells, and an interactive display to allow graphical development of the design, it is possible for a designer unfamiliar with microcircuit design, to develop an integrated circuit specifically for his own needs.

A set of large scale integration (LSI) predesigned cells known as the MAJIC cell library [75] had been developed in the Department of Electrical Engineering at Edinburgh University, and was offered to external groups to allow them to undertake dedicated microcircuit designs for their own purposes.

I.2. Prototype System.

Two areas of the prototype system were identified as being suitable for LSI using the cell technique. These were; the timing circuit which generates various waveforms from a 1MHz clock signal and the logic circuits which control the operation of the A/D converter; and the hoist control circuit.

The prototype circuits are described in Section 5.3.1. Figure G.1 is a diagram of the prototype timing circuit, Figure G.5 shows the additional A/D converter logic, and Figure G.9 is the diagram for the hoist control circuit.

I.3. Design Method Using MAJIC Cells.

I.3.1 Computer and Graphics.

The method uses the IC design software suite, GAELIC, developed by Compeda Limited. This allows information about the silicon layout for a microcircuit design to be defined either by providing coordinates, or by using an interactive display. The programs produce the masks necessary for manufacture of the microcircuits. A program is also available which will give check plots of the masks.

The programs are held on a PRIME C computer at the Science and Engineering Research Council's Rutherford Appleton Laboratory at Chilton, Oxfordshire. The University of Edinburgh LSI Design Facility is connected to this computer by a British Telecom private

line.

The design of the microcircuits was carried out using the interactive display (a Tektronix 4014A terminal). Checking was carried out using a Hewlett-Packard HP7221B A3 size plotter at Edinburgh, and a Benson drum plotter at the Rutherford Appleton Laboratory; this produces large plots (800 x 800 mm), and the plots were posted to Edinburgh in this case.

As described above, the silicon design information for certain logic functions is available within the MAJIC cell library. A silicon design for a complex logic circuit can be produced by using a combination of MAJIC cells, along with the necessary position and interconnection information. When the design is complete, a program in the GAELIC suite merges the data of the cells, with the position and interconnection information, and produces a language file. The complete masks are then produced at the Rutherford Appleton Laboratory from the GAELIC language file, using electron beam lithography.

I.3.2. Library Details.

The following cells from the original library were used:-

inverter

2 input NAND gate

2 input NOR gate

JK flip flop

2 input EXCLUSIVE OR

To simplify the design of the units, the following additional MAJIC cells were designed by the LSI design group:-

4 input AND gate

8 input AND gate

4 bit dynamic binary counter

4 bit static binary counter

2 channel multiplexer

1MHz crystal oscillator.

split cell (provides a two phase clock from single phase).

I.4. Experience of Design with the Cell Library.

I.4.1 Use of the Cell Library.

The cell library was designed by engineers with wide experience of LSI design, and reflected the techniques used in such designs, whereas the author was more familiar with the techniques used with discrete logic packages. This resulted in a number of changes being required to the prototype design as the microcircuit design progressed. e.g. the need for the split cell, since the counters were implemented using two phase clocks, whereas TTL discrete logic circuits use a single phase clock.

The documentation was difficult to follow with regard to the placement of input and output pads, and in the provision of a frame with test patterns. This was due to the level of knowledge assumed by the cell designer.

I.4.2 Graphics Package.

A number of practical difficulties became apparent once the design was underway. The engineers who prepared the documentation were expert in the use of the whole range of facilities available in the GAELIC interactive graphics package, and the documentation gave the full range of options available. In fact a relatively small sub-set of commands was all that was required for the design. The familiarisation time would have been very much shorter had this been appreciated from the start. The facilities used included:-

positioning cells

changing the orientation of cells

deleting cells

positioning groups of cells and interconnections

changing the orientation of groups of cells and interconnections

deleting groups of cells and interconnections

positioning rectangles

deleting rectangles

placing a dimensioning grid

changing the magnification of the display

locating part of the design on the display

I.4.3 Interactive Display.

There were also practical difficulties encountered when using the interactive display. Initially, when only small groups of cells were being used, there was no difficulty. As the size of the design group increased however, it became more difficult to place fairly long interconnections with narrow width, because of the need to change the magnification of the interactive display frequently, to locate the ends of the conductors.

A factor which increased the design time, and was due to the inexperience of the user, was the excessively high standard of placement of conductors which was attempted, for example in respect of butting of conductors. If simplifying procedures had been used, such as the deliberate use of overlaps at conductor joins, then the design would have been carried out much more quickly.

Access to the computer system was restricted on occasion mainly due to faults on the landline, and the implementation of new computer routines.

Familiarisation and design of the layout for the timing circuit took approximately five months, but some expertise had been gained, the design time became much shorter, and the basic design of the hoist control layout took only about two months.

The design work was carried out intermittently, and the actual hours using the interactive display probably amounted to no more than about six hours per month, giving a total of about 42 man-hours.

I.5. Mask Details.

The timing circuit had to be modified to accomodate the cell library that was available, along with the specially designed cells. The modified circuit is shown in Figure I.1. The hoist control circuit required no modification and is shown in Figure I.2.

The interactive display was used to place the required cells and then provide the necessary interconnections. This required working with four masks:-

cell outline mask

metal mask (used for X direction conductors)

polysilicon mask (used for Y direction conductors)

contact mask (used to connect between metal and polysilicon layers)

Since the metal and polysilicon tracks are at two different levels in the microcircuit, any kind of interconnection can be accommodated, including crossing conductors.

The design was carried out by grouping cells and providing interconnections for the groups, and then combining these groups to give the complete design. Figure I.3 shows the mask information for the timing circuit at the level at which design work was carried out, while Figure I.4 shows all the mask details for the timing circuit.

The microcircuits are both 5.08 x 5.08 mm.

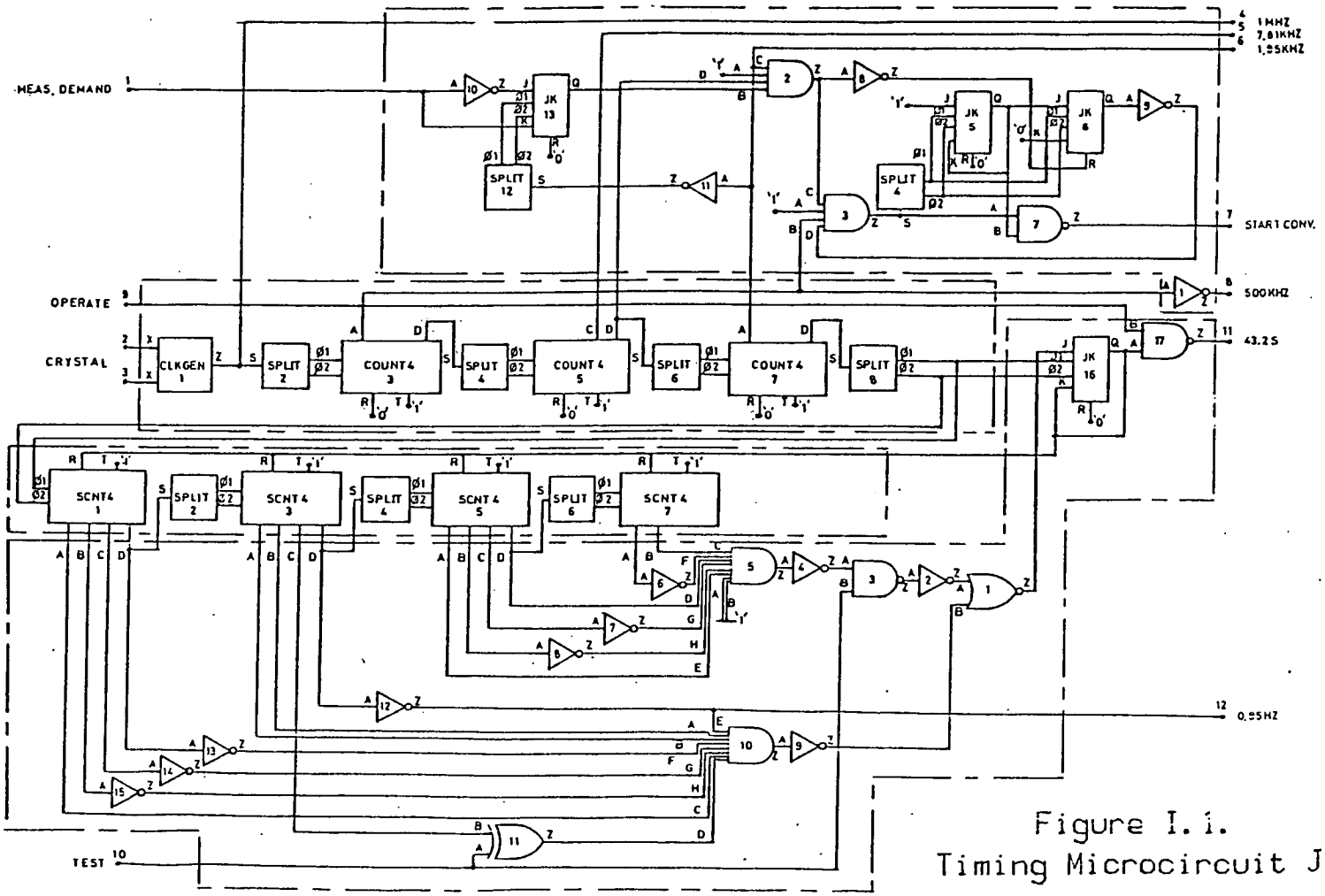

Figure I.1.
Timing Microcircuit JWD7

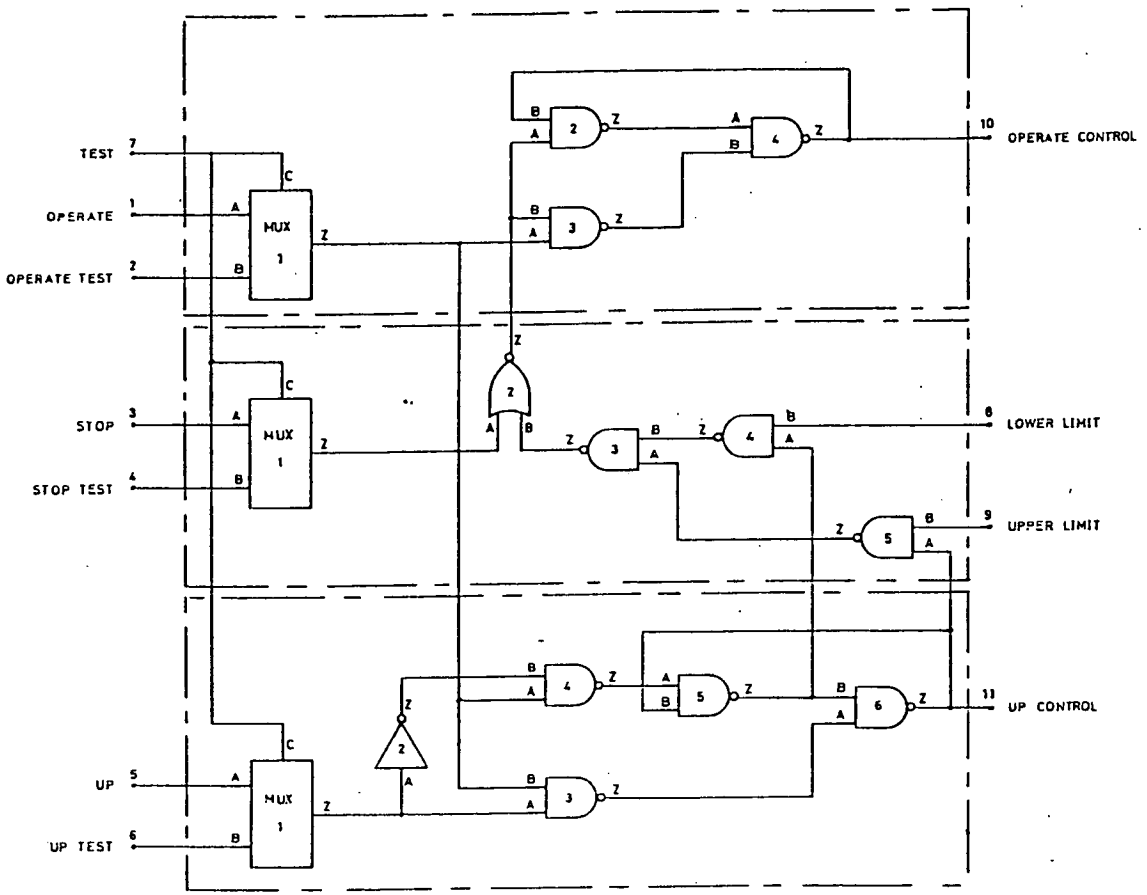

Figure I.2.
Hoist Control Microcircuit JW12

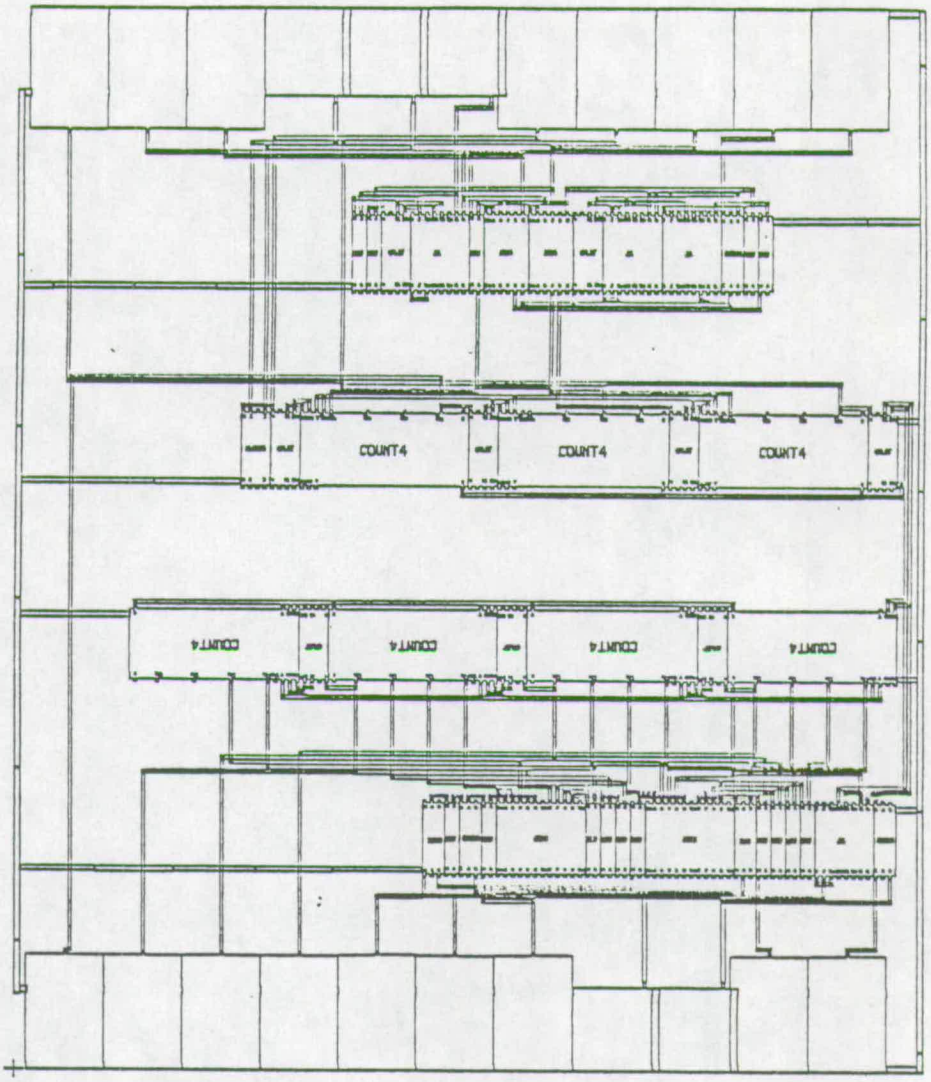

Figure I.3.
Timing Circuit Mask at
Design Level

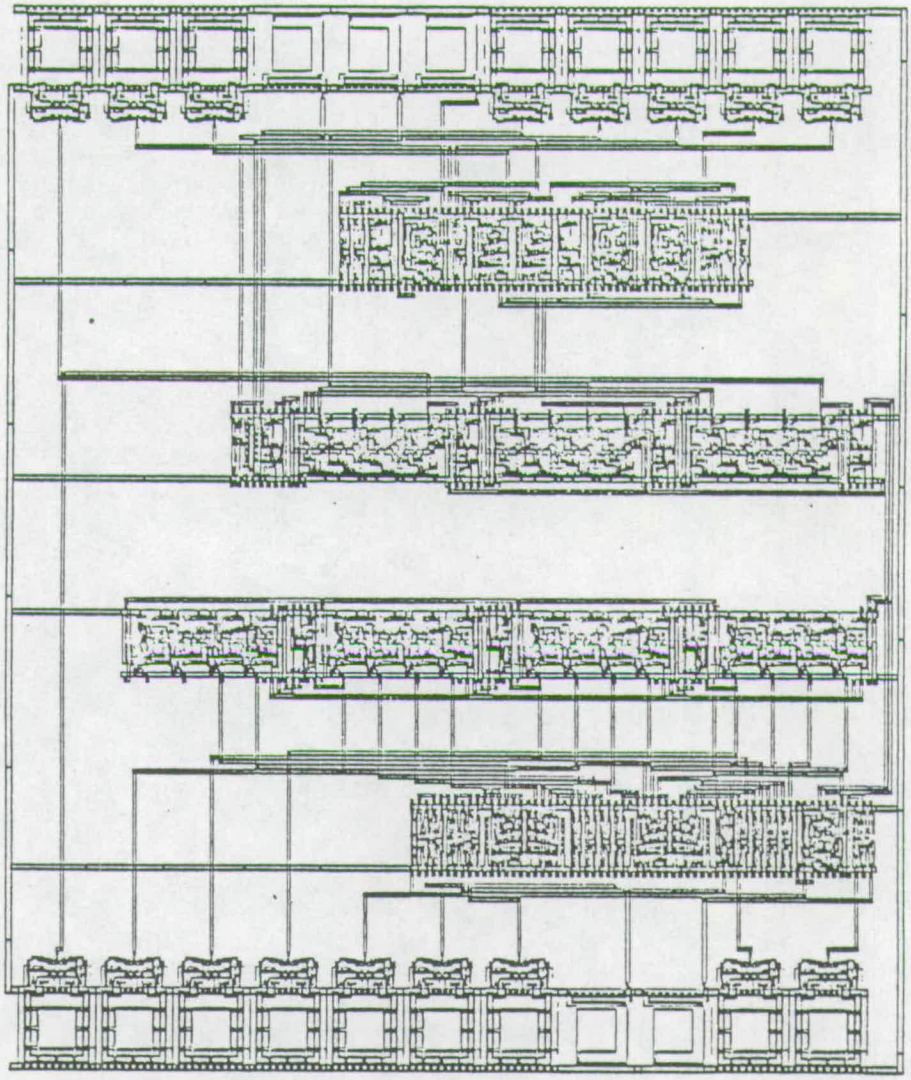

Figure I.4.
Timing Circuit; Complete
Mask Details

I.5. Performance.

On test, it was found that the timing interval produced by the timing microcircuit was 16.784 s rather than the required 43.2 s. On investigation, using monitoring points included in the design, it was found that the reset signal for the second set of binary counters was ineffective. Further investigation showed that a design change in the static binary counter has resulted in secondary errors which prevented the reset taking place. The counter was therefore operating in a free running mode. Since the new timing signal was still locked to the crystal frequency, it was decided to accept the new timing interval and to modify the software appropriately.

The hoist control circuit operated successfully.

I.6. Conclusions.

The cell library design method allowed the design of two separate custom microcircuits. After familiarisation with the documentation, the design time for the microcircuits was relatively short.

A major difference in approach to circuit design between the conventional TTL circuit designer and the custom microcircuit expert, has been identified. This incompatibility was largely overcome by the modification of the TTL designs and by the provision of extra functional elements by the cell designer.

Some communications problems remained which resulted in one of the circuits not operating to specification.

APPENDIX J.

The use of Microcircuits in a Computer Controlled System for the Measurement of the Electrical Resistivity of Concrete - Reference 76.

THE USE OF MICROCIRCUITS IN A COMPUTER CONTROLLED SYSTEM FOR THE MEASUREMENT OF THE ELECTRICAL RESISTIVITY OF CONCRETE

J.G. Wilson, BSc*, H.W.Whittington, BSc. PhD. C.Eng. MIEE**, M.C. Forde, B.Eng. MSc. PhD, C.Eng. MICunE, MIHE***

* Dept of Electrical & Electronic Engineering, Napier College, Edinburgh
** Dept of Electrical Engineering, University of Edinburgh
*** Dept of Civil Engineering & Building Science, University of Edinburgh

The measurement of the electrical resistivity of concrete provides an insight into the mix proportions and setting characteristics of concrete. Electrical resistivity measurements over an extended period of time can be very tedious. To overcome this problem a prototype computer controlled measurement system has been developed. The application of micro-electronic circuits, both proprietary and custom designed, to a developed model of the equipment is also described.

INTRODUCTION

The electrical properties of concrete depend on the amount of free water available within the concrete, the state of the cement matrix, and the proportion of aggregate present. These parameters, which are defined by the mix used, also control the strength of concrete. An investigation of the electrical properties might provide quality assurance indicators of mechanical strength, which can be applied at an earlier stage than current methods.

One practical difficulty with electical measurement is that, due to the heterogeneous nature of concrete, a large number of tests must be undertaken in order to obtain statistical significance. This process is extremely tedious if manually operated measuring equipment is used. The systems described allow automatic measurement of a large number of samples over an extended period of time.

CONDUCTION OF ELECTRICITY THROUGH CONCRETE

Two effects largely control the conduction process in concrete. These are, the effect of the aggregate, and the effect of capillary pores in the cement paste.

Aggregate-Cement Paste Model

The electrical resistivity of aggregate is generally very much higher than the resistivity of cement paste, e.g. 13 ohm metres as against 1000 ohm metres. Therefore, from an electrical point of view, concrete can be regarded as being made up of large numbers of relatively small volumes of insulating material imbedded in a conducting matrix of cement paste. This is shown in Figure 1.

A simple electrical model shown in Figure 2 assumes that the aggregate is distributed along the length of the conduction path. This model can be regarded as two electrical resistances connected in parallel, one of aggregate, and the other of cement paste. The cross sectional areas of these two components will be proportional to the volume ratios of the aggregate and cement paste. Whist the volume ratio of the cement paste will normally be lower than that of the aggregate (resulting in a lower cross sectional area for the cement paste), because the resistivity of the cement paste is very much less than that for the aggregate, the resistance of the cement paste path will be very much less than that for the aggregate. For resistances in parallel the combined resistance is less than the smaller value of resistance. In this case this means that the resistance of the paste is dominant, and if the resistivity of the aggregate is sufficiently high, the aggregate path can be neglected. The resistivity of the concrete is then controlled by the relative volume of the cement paste, and the resistivity of the paste.

Cement Matrix-Pore Model

Electrical conduction in the cement paste is very largely dependent on ionic conduction through the water filled capillary pores, since the resistivity of a dried cement paste is so high that it can be regarded as a very good insulator.

The resistivity of the cement paste must then depend on the relative volume proportions of cement matrix and free water, assuming that the sample is saturated. In this case, for conduction to occur, the water paths, and so the capillary pores, must be continuous in the direction of conduction. It can then be expected that the conduction process can be accurately described by the model with the aggregate replaced by the paste matrix, and the paste replaced by water filled capillary pores. The relative volumes of paste matrix and free water are controlled by the water/cement ratio of the mix. This model is shown in Figure 3.

The resistivity of the water in the capillary pores will be dependent on the species, concentration and mobilities of the ions present. If the solution is saturated, an equilibrium condition might exist, giving a constant value of resistivity dependent on the kind of cement used. This condition might well exist during the setting time. Once hardening has started, the equilibrium condition is less likely to exist.

RELATIONSHIP BETWEEN THE ELECTRICAL AND MECHANICAL PROPERTIES OF CONCRETE

The mechanical properties of concrete depend largely on the porosity of the cement paste, which in turn depends on the water/cement ratio of the mix. The electrical resistivity depends on the relative volume of free water to total paste volume, which is a measure of porosity, assuming that the concrete remains saturated with water, and on the relative volume of cement paste to total volume. This depends on the cement/aggregate ratio for a given water/cement ratio.

If the effects due to free water/paste volume ratio and paste/total volume ratio can be isolated using electrical resistivity measurements, then estimates of water/cement and cement/aggregate ratios can be made.

CONCRETE SAMPLE AND ELECTRODE GEOMETRY

The geometry of the concrete sample was chosen to conform with BS1881. The standard used is the 150mm cube. The moulding arrangements allow two 14 s.w.g. stainless steel electrodes to be placed on opposite faces of the cube. The electrodes cover the area of each face completely.

One of the pair of electrodes has a platinum film temperature sensor attached to it. Measurements taken by this sensor are used to correct the resistivity measurement to a temperature of 20°C.

Standard cast iron moulds will not give a 150 mm cube after electrodes had been fitted, and it was necessary to shim these moulds to give the correct dimensions. They also presented electrical insulation problems. PVC moulds were designed with dimensions such that a 150 mm cube is obtained after the electrodes are removed. These moulds also eliminate insulation problems.

PROTOTYPE AUTOMATIC RESISTIVITY MEASUREMENT SYSTEM

The prototype automatic measurement system has been designed and built to carry out measurements on up to 15 samples in the form already described.

The equipment is described in detail elsewhere (1), but a brief outline of its operation will be given. A block diagram of the system is shown in Figure 4.

The system is based on a Rockwell AIM65 microcomputer system. This computer has facilities for digital data input, data output on a dot matrix printer and on an electronic display, and calculation and control using machine code and BASIC programs.

The complete system comprises the computer, an electronics unit, power supply, amplifier units for temperature measurement of each sample, the hoist unit, temperature controlled water tank, and the samples with electrodes. The samples may be considered individually as 15 separate experiments or can be taken in groups; one experiment of 15 samples for example. New experiments can be added and completed experiments deleted without switching down the system. Measurements are carried out on a logarithmic time scale up to a maximum of 100 days. The zero time for a particular experiment is taken as the time at which the water is added to the mix. Samples which are more than one day old are removed from the water bath by an automatic hoist before a measurement is taken, and returned after the measurement.

System Operation

The Timing Circuit generates all the waveforms necessary for the system from the 1 MHz clock signal of the computer. In particular, a signal with period 43.2 s corresponding to 0.0005 days, which is the basic timing interval for the system, a signal at 2.0 kHz, which is the signal used to energise the resistivity measurement system, and a signal at 7.2 kHz, which energises the temperature transducers.

The 2.0 kHz square wave signal is amplified and fed to each sample through high accuracy resistors. The voltage across each sample is then used along with a measurement of input signal to calculate resistivity.

The 7.2 kHz signal is amplified and fed to the temperature transducers on each sample. As the temperature changes, the resistance of the transducer changes, and this results in a change in output voltage. The change in output is however very small, and it is necessary to amplify each output using amplifier units located near the samples.

The resistivity output voltage and the output signal from the temperature amplifier are selected for a particular sample by the computer using the Resistivity Multiplexer and the Temperature Multiplexer. Either the resistivity or the temperature signal is then selected by the Function Multiplexer. The signal which is finally selected, and which is still in analogue form, is then converted to a digital signal by the A/D Converter, and fed into the computer.

The computer program controls the timing of all measurement operations. When measurements are required, the computer sets up the correct addresses for the multiplexers and then reads the output from the A/D Converter. This is carried out for the resistivity and temperature of all the samples within a particular experiment. The computer then calculates the resistivity, temperature and resistivity corrected to 20°C for each sample, and outputs this information on the dot matrix printer.

The computer electronic display gives information to the operator about the occurrence of measurements, and the operating mode of the system.

The hoist system is also controlled by the computer. Upper and lower limit microswitches provide signals which ensure the correct height of lift.

The system program which includes both machine code and BASIC routines is contained in an erasable programmable read only memory (EPROM) located in the electronics unit.

System Accuracy

Figure 5 shows the result of accuracy measurements carried out on the system. Most of these measurements were carried out on resistors, which were used in place of the concrete samples, but a few were carried out on concrete samples. At high values of resistivity, the percentage uncertainty is approximately constant at better than 2%. This is largely due to the build up of resistor tolerance within the equipment. At low values of resistivity, the uncertainty increases rapidly. This is due to the quantization error of the A/D Converter. The resistivities to be measured are normally greater than 1 ohm metre.

Results

Figure 6 shows the results of one of the proving trials of the equipment. The experiment involved tests on 5 samples. The samples were all tested up to 1 day after pouring. Subsequently they were successively removed from the testing equipment and their crushing strength measured.

On the graph the + symbol indicates that an average of the sample readings has been taken. If the number of samples falls below 4, averages are no longer taken, and the individual readings are presented using identifying symbols.

The results are in agreement with those obtained by other workers. The corrected resistivity is practically constant during the setting period, which continues until about 0.3 day. Hardening then begins, and the resistivity rises progressively until about 20 days, when it reaches a limiting value.

There is a discontinuity at 1 day when demoulding occurs. The extent of this discontinuity depends on the mix being used.

DEVELOPED EQUIPMENT

A number of operational problems were experienced with the prototype equipment, and it was also considered that the equipment could be packaged in a more compact form. It was therefore decided to produce a developed model of the equipment.

The two operational points considered to be a problem were:

(1) the need to transcribe data from the paper tape of the AIM65 printer, to another computer for analysis, and

(2) problems in extending the system as necessary once the measurement programme is underway.

These problems can be overcome by using a standard instrumentation bus such as the IEEE bus. This provides address, data, and control lines using a standard format, and allows the interconnection of computer, disc storage and measurement devices. In principle, twelve measurement devices can be connected to the bus under the control of one computer, with all output data directed to a disc unit. This disc can then be removed at a suitable time for analysis of the data. The computer controlling the system will be a Hewlett-Packard HP85 rather than the AIM65 used for the prototype system.

When repackaging was being considered, the use of custom designed microcircuits was suggested as a method of reducing the volume of certain circuits, and also of simplifying manufacture.

Figure 7 shows a block diagram of the developed system.

IEEE Bus System

The flow of information to and from the measurement system by the IEEE bus, is most conveniently controlled using a microprocessor, in this case the Rockwell R6502. The microprocessor requires random access memory (RAM) as a working space, and a program which is held permanently in erasable read only memory (EPROM). Interface microcircuits allow control and data signals to be transferred from the measurement circuits to the microprocessor bus. A specialised interface microcircuit (Motorola M68488) interfaces the IEEE bus with the microprocessor bus and arranges all data transfer protocols.

Custom Designed Microcircuits

A significant proportion of the prototype equipment is logic circuitry, and this has been designed using 7400 series TTL discrete logic circuits. These circuits are largely contained within the timing and hoist control circuits.

For the engineered version of the prototype equipment, it was felt that packaging most of the logic circuitry as custom designed integrated circuits would present distrinct advantages. Viz:

(1) increased circuit reliability through reduced component count

(2) reduced physical size of circuits making equipment more portable

(3) reduced cost of any large-scale manufactured unit through reduced construction time.

Recent developments have, to a large extend overcome two of the major disadvantages of microcircuits for custom design, which are:

(1) the cost and time involved in circuit design including silicon layout and mask production

(2) the necessity of using highly skilled designers for even the simplest circuit.

It is now possible for a designer unfamiliar with microcircuit design, to contemplate developing an integrated circuit specifically for his own needs, by using a library of predesigned logic cells, and an interactive display to allow pictorial development of the design. Such a library has been prepared by the LSI Design Facility at the University of Edinburgh. A production unit for the manufacture of such microcircuits is also located at the University of Edinburgh.

The design of the masks for the production of the timing and hoist circuits was undertaken by the authors using the cell library. Production of the actual microcircuits is now complete, except for final packaging. Figures 8 and 9 show plots of the information used to produce the masks.

FURTHER INVESTIGATIONS

The effects of small variations in water and aggregate proportions on resistivity are being investigated using the prototype system, and work is continuing to establish the parameters necessary to predict the ratios used in the sample concrete mix from the resistivity measurements. This work will be augmented when the developed system becomes available.

Testing of the custom microcircuits and their integration into the developed system will begin shortly.

ACKNOWLEDGEMENTS

The authors wish to thank Professor A.W. Hendry of the Department of Civil Engineering and Building Science and Professor J.H. Collins of the Department of Electrical Engineering at the University of Edinburgh, and Mr. P.H. Beards of the Department of Electrical and Electronic Engineering, Napier College of Commerce and Technology, Edinburgh, for placing the facilities of their respective departments at their disposal.

J.G. Wilson would also like to thank Lothian Regional Council for financial support.

The development of the custom microcircuits was funded by the Science and Engineering Research Council.

REFERENCES

1. Wilson, J.G., Whittington, H.W., and Forde, M.C. 'Microprocessor-based system for automatic measurement of concrete resistivity', Journal of Physics E: Scientific Instruments, 1983, 16, pp. 700-705.

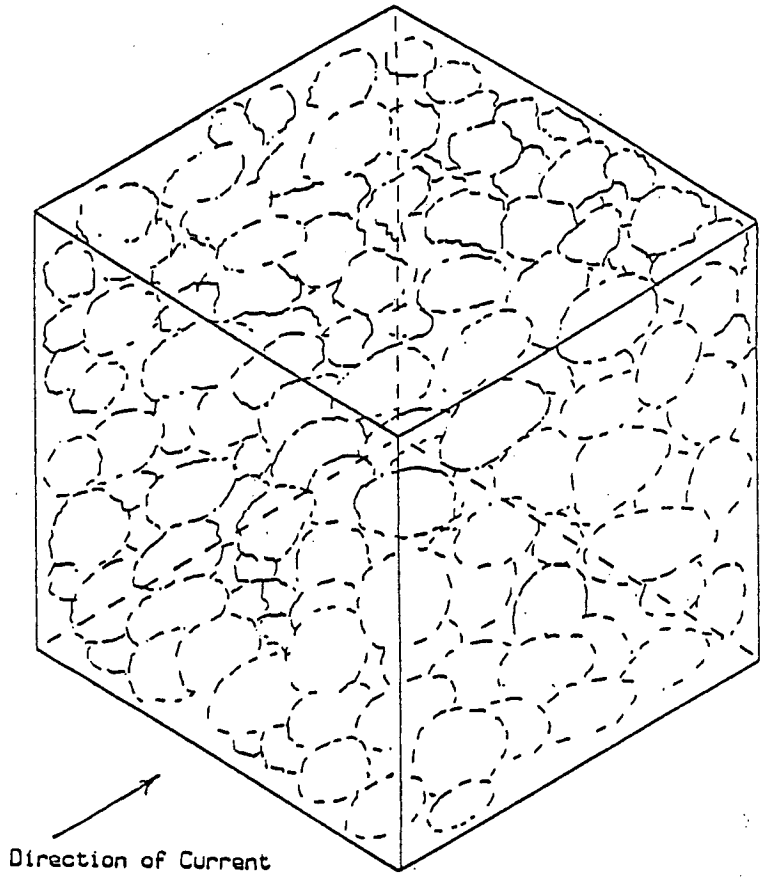

AGGREGATE IN CEMENT
MATRIX

Figure 1

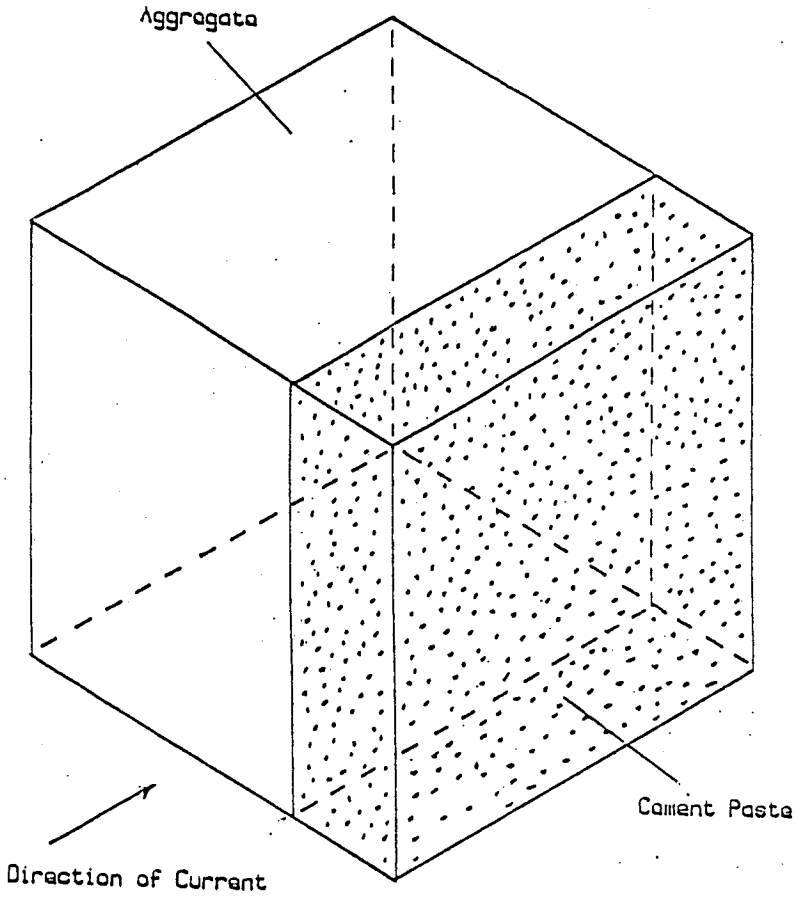

CEMENT-AGGREGATE MODEL

Figure 2

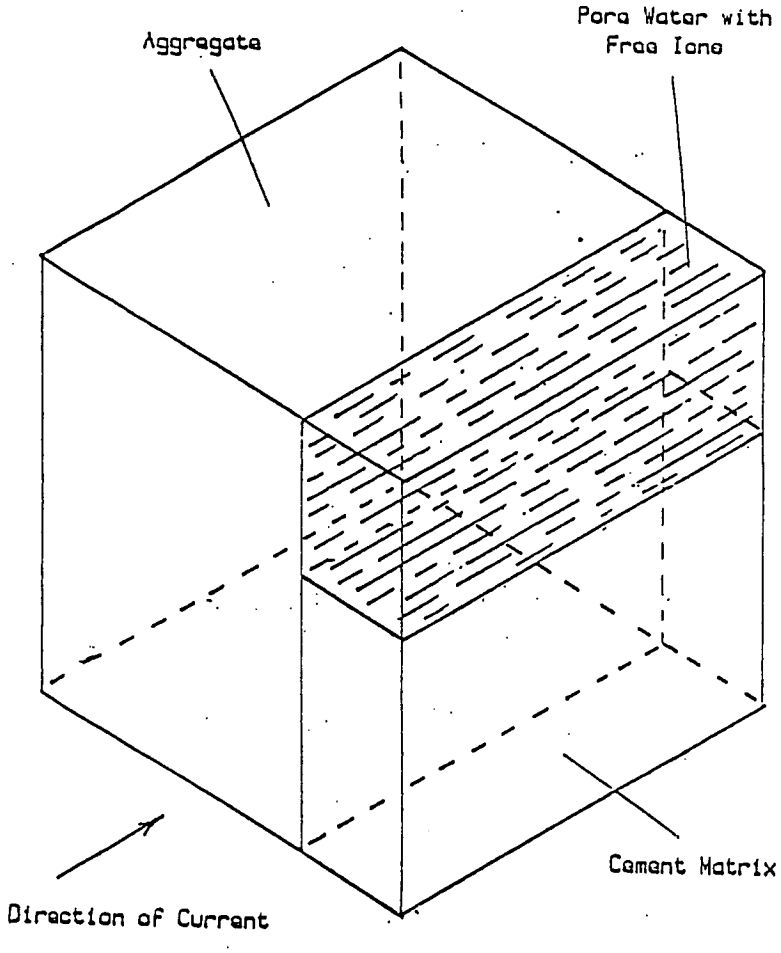

CEMENT MATRIX-PORE
MODEL

Figure 3

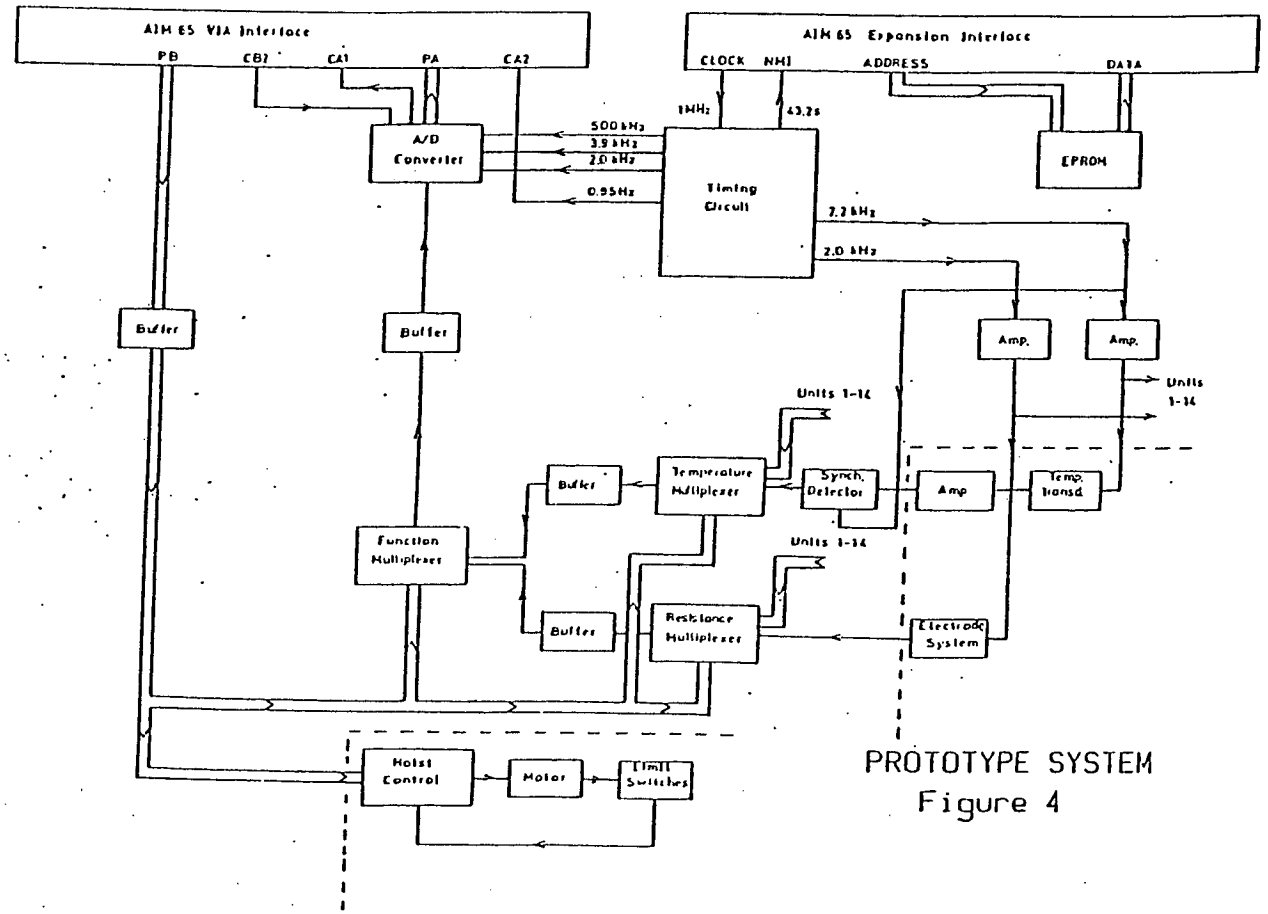

PROTOTYPE SYSTEM
Figure 4

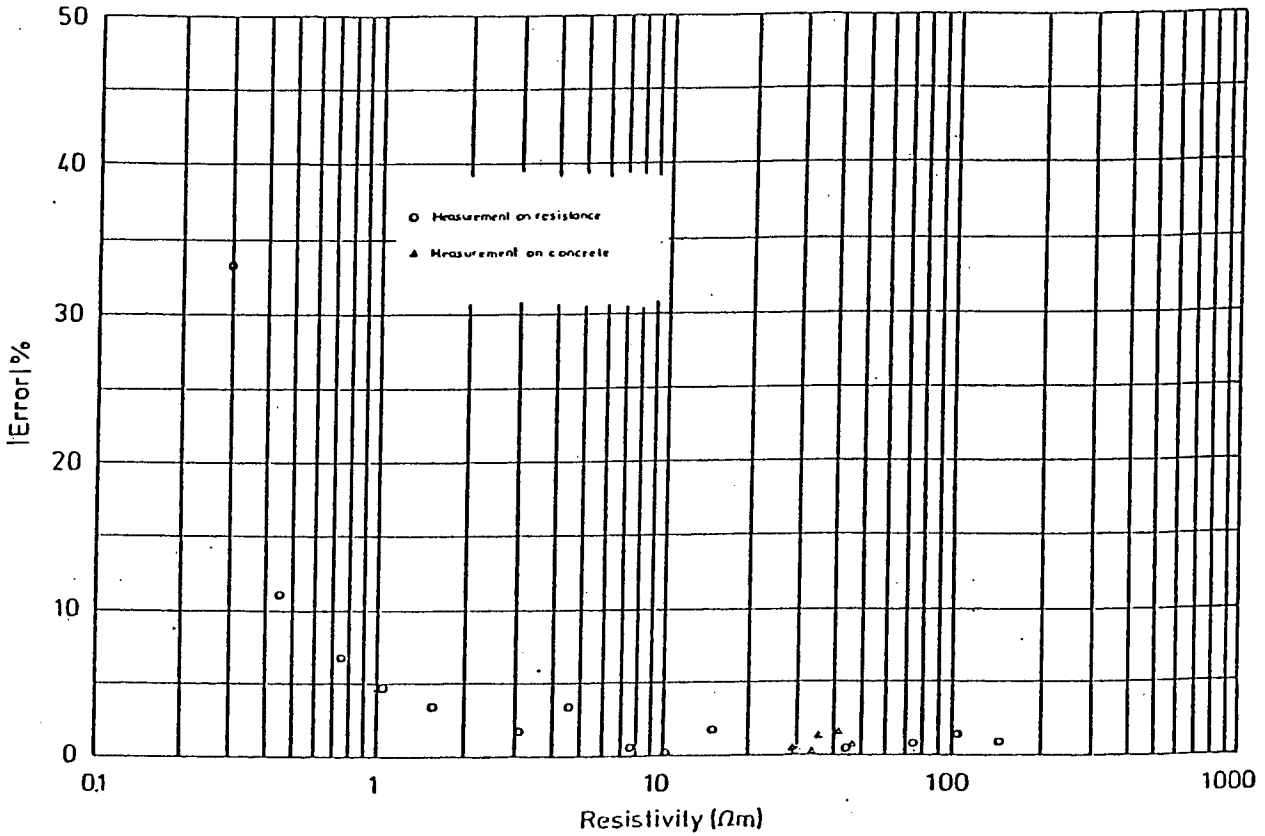

ACCURACY OF MEASUREMENT

Figure 5

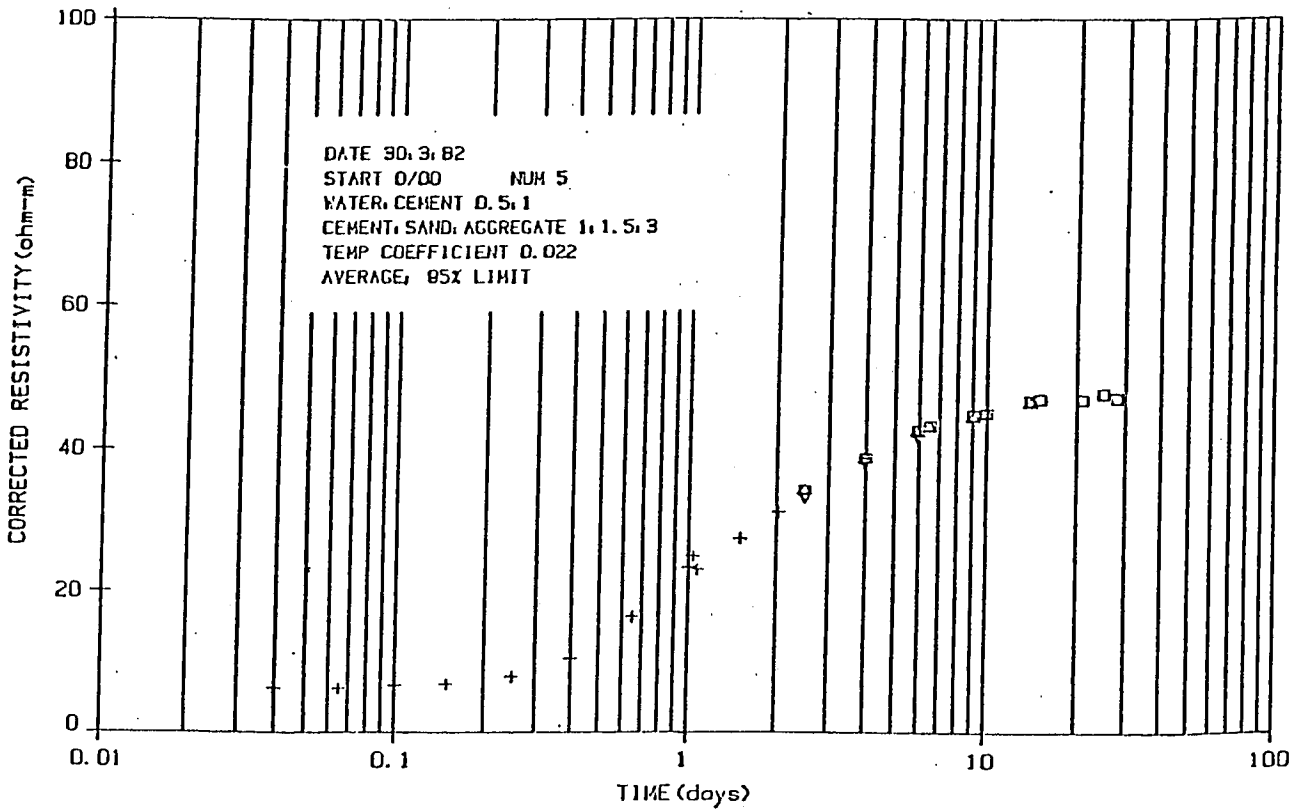

PROVING TRIAL

Figure 6

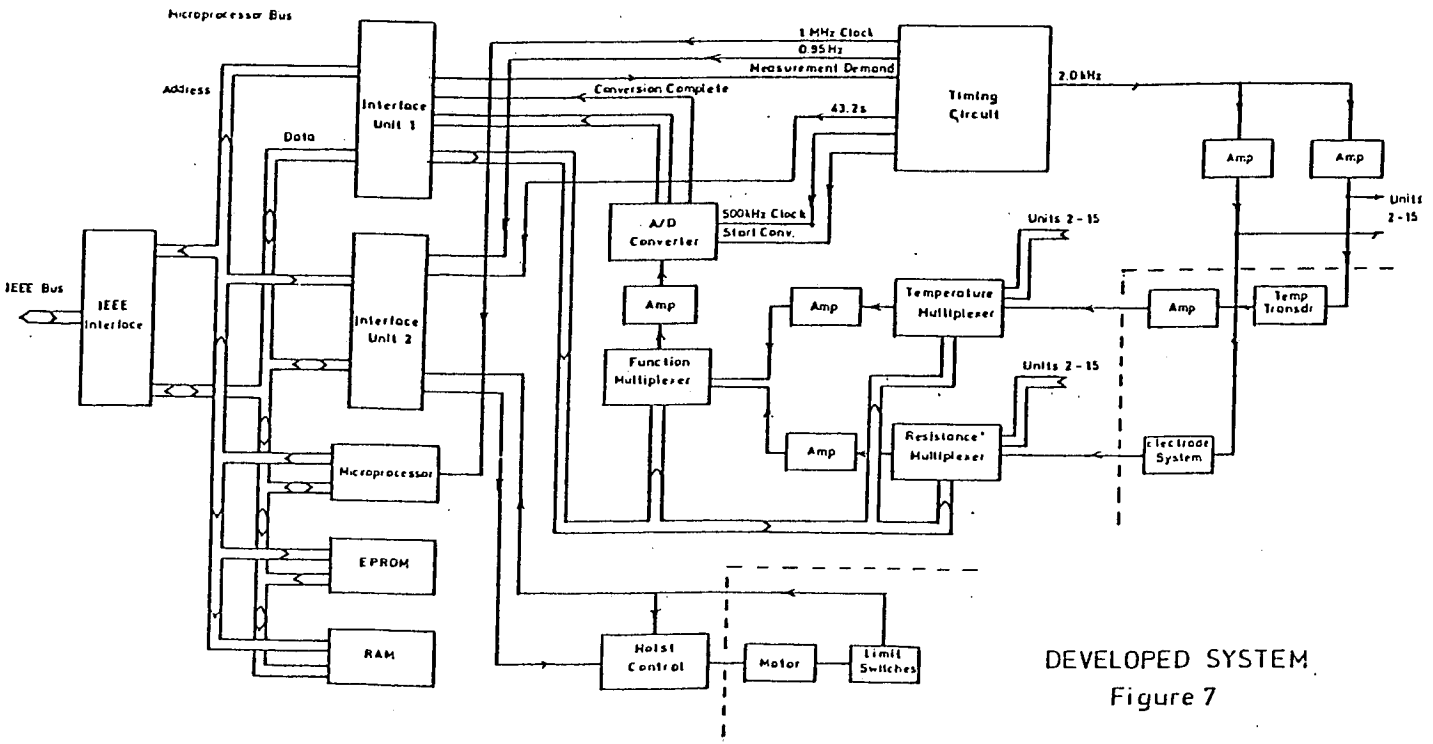

DEVELOPED SYSTEM
Figure 7

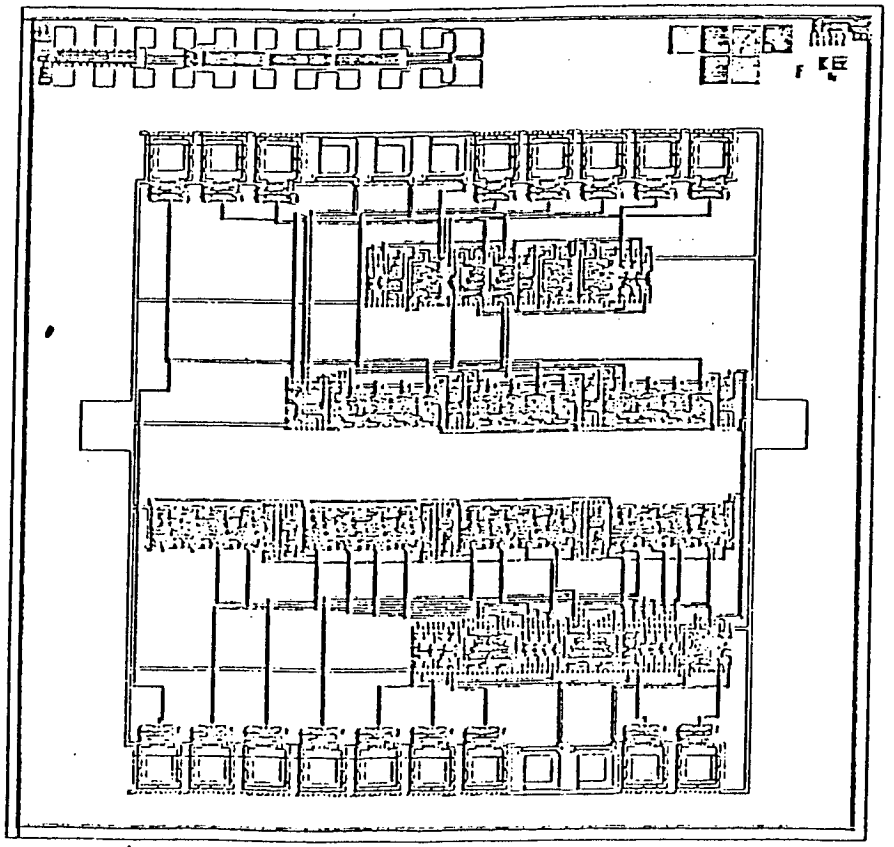

TIMING CIRCUIT
Figure 8

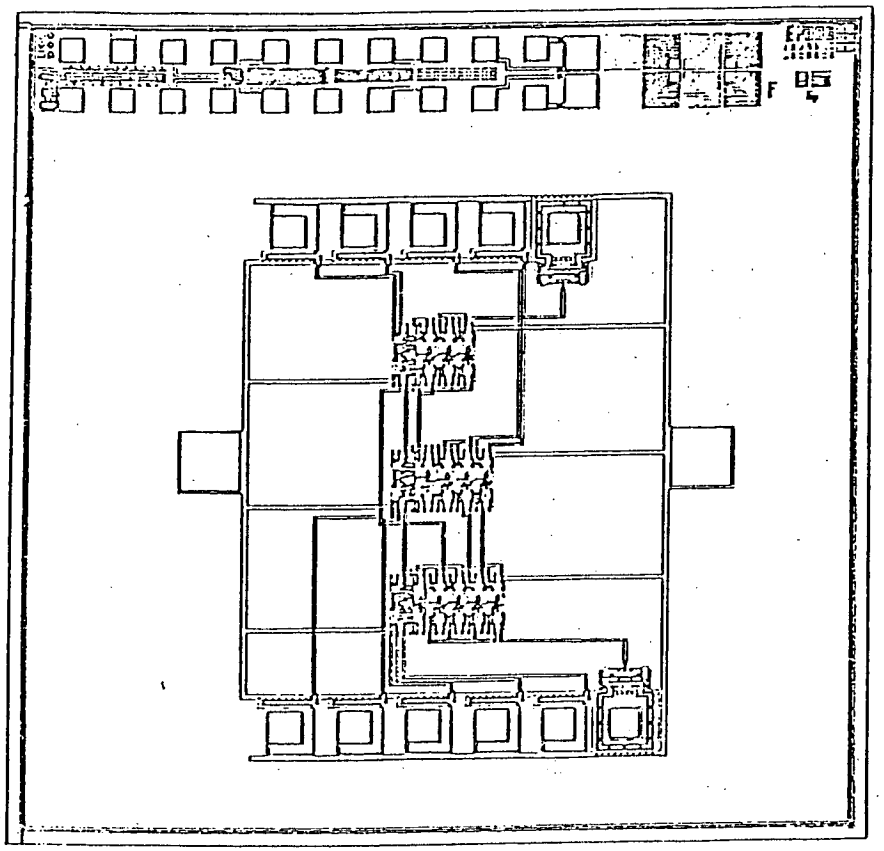

HOIST CONTROL
CIRCUIT
Figure 9

APPENDIX K.

Circuit Diagrams - Developed System.

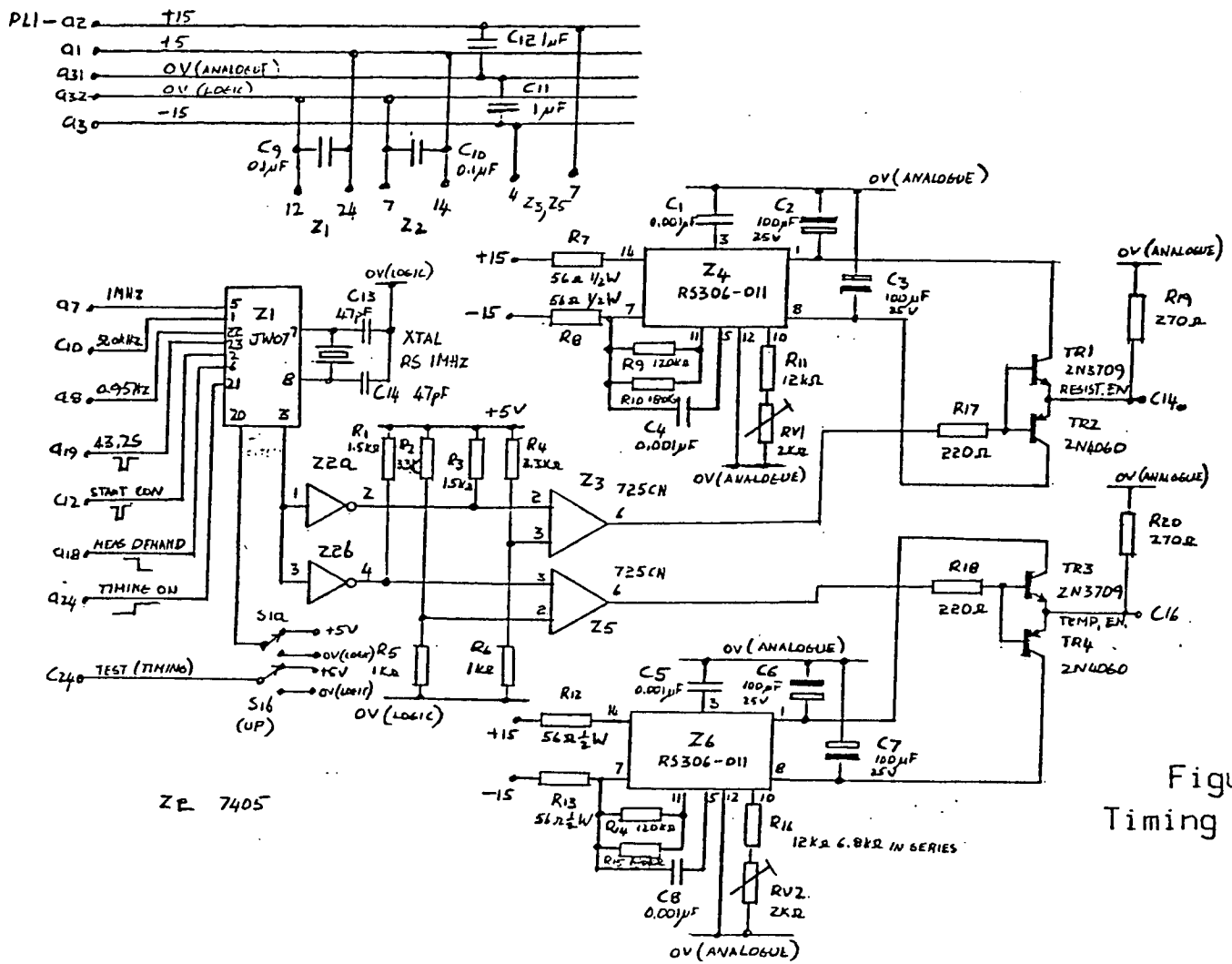

Figure K. 1.
Timing Circuit

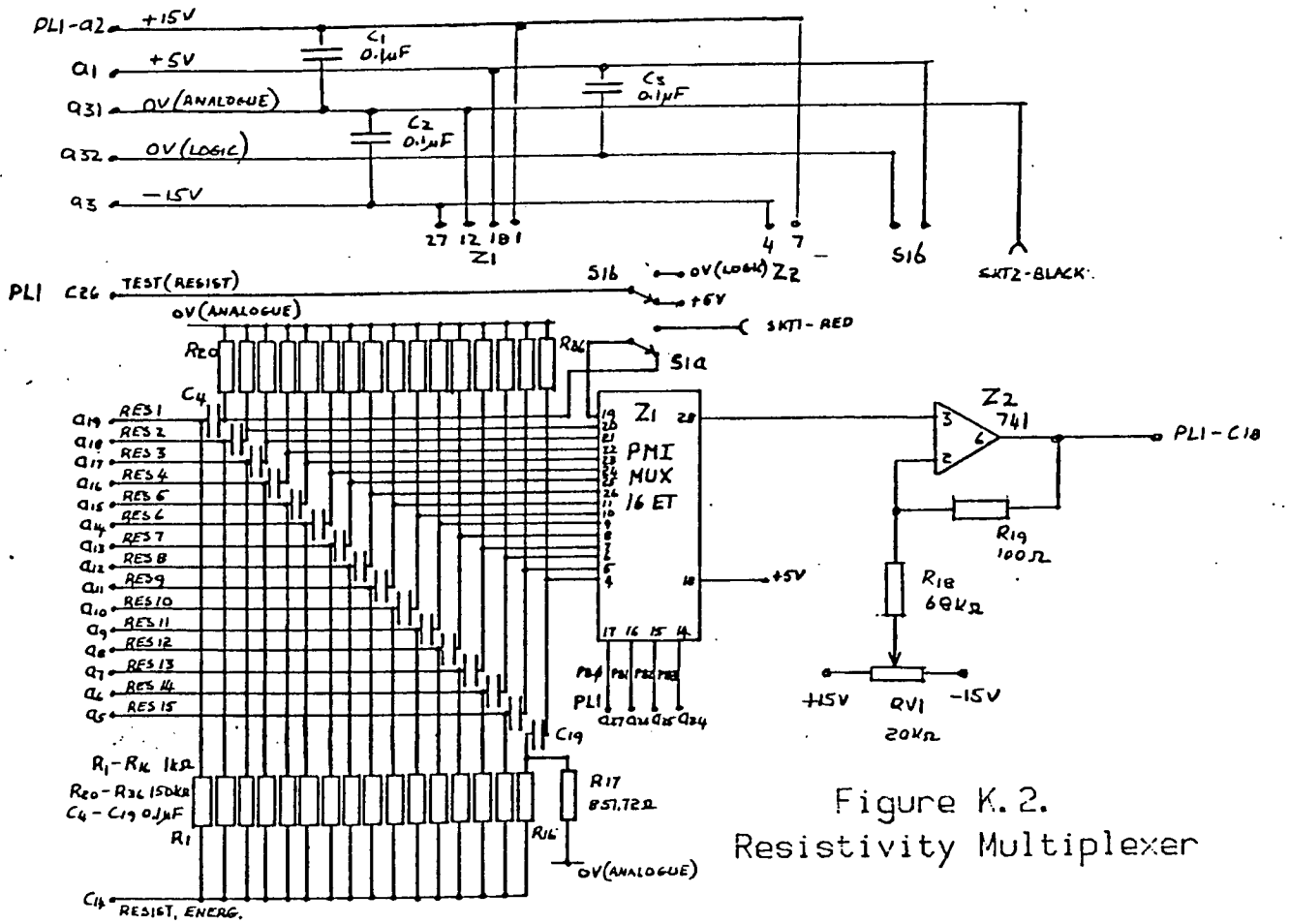

Figure K.2.
Resistivity Multiplexer

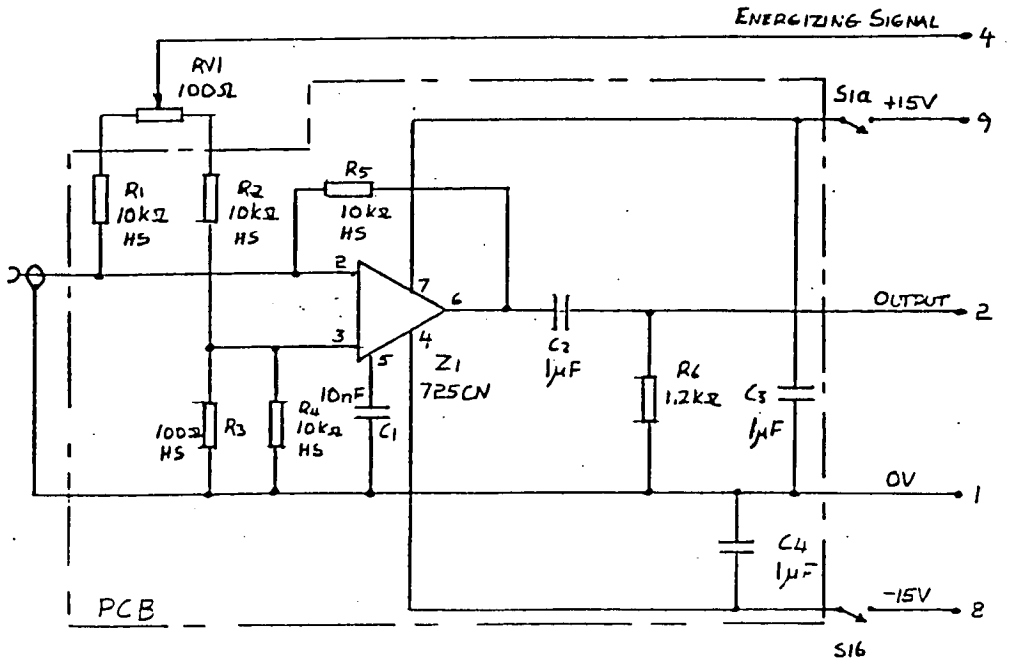

HS- HIGH STABILITY RESISTORS - TOLERANCE 0.1%.

Figure K. 3.
Temperature Amplifier

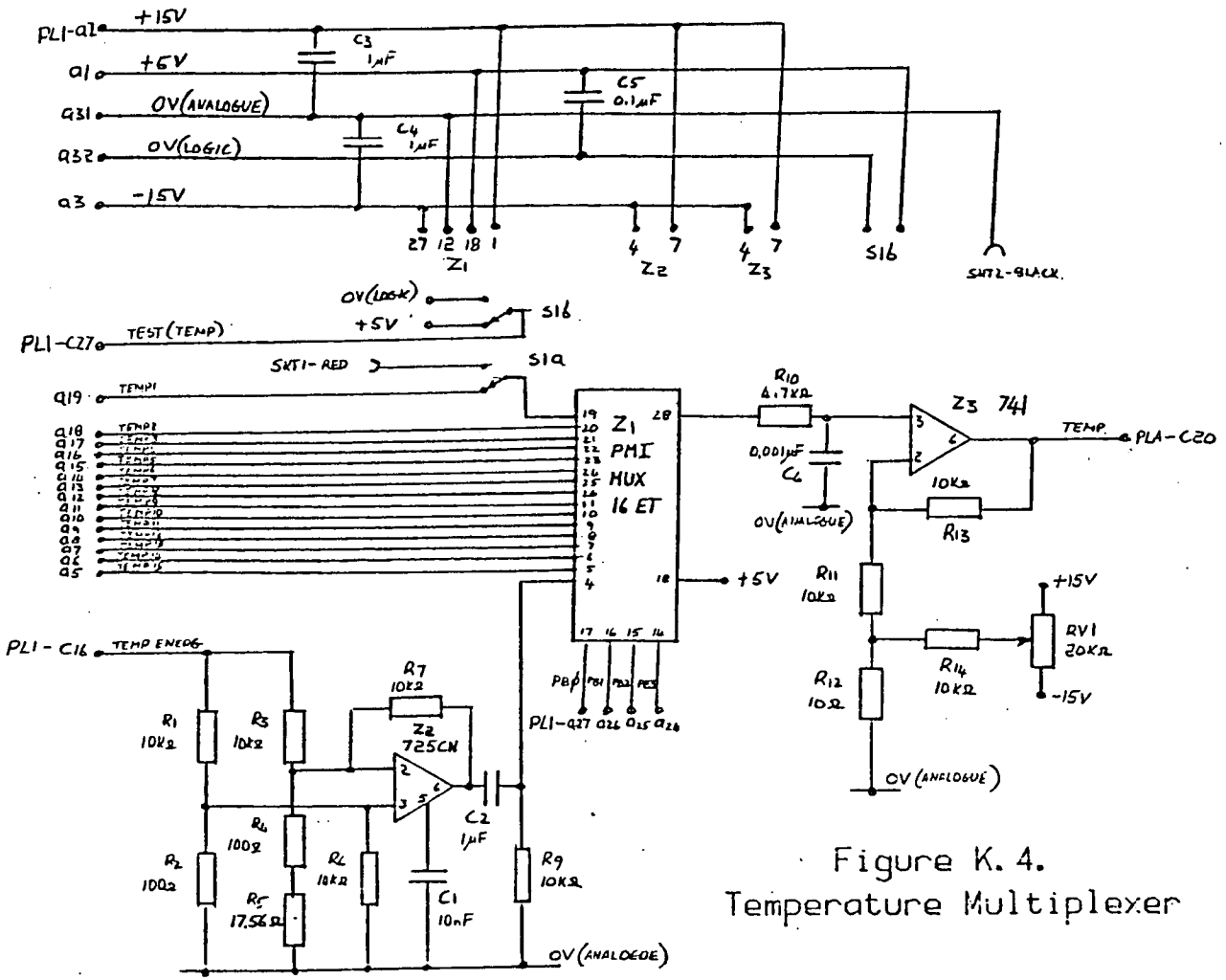

Figure K. 4.
Temperature Multiplexer

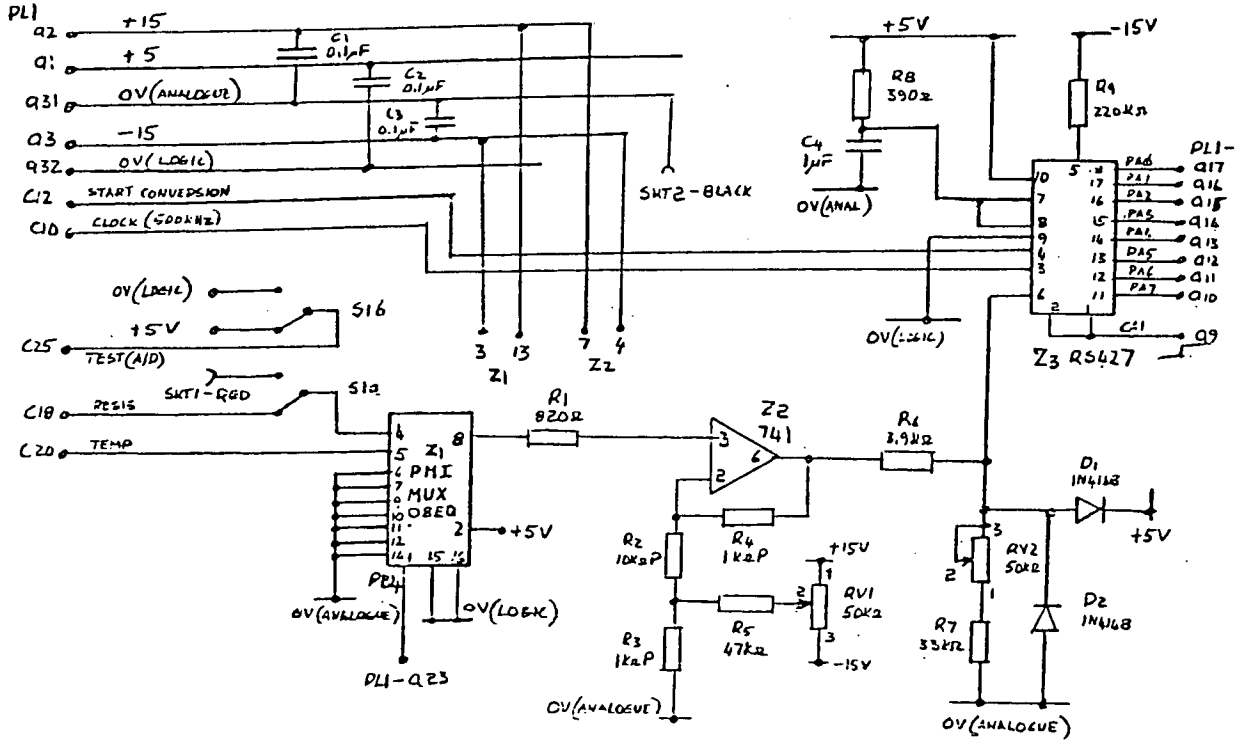

Figure K.5.
A/D Converter

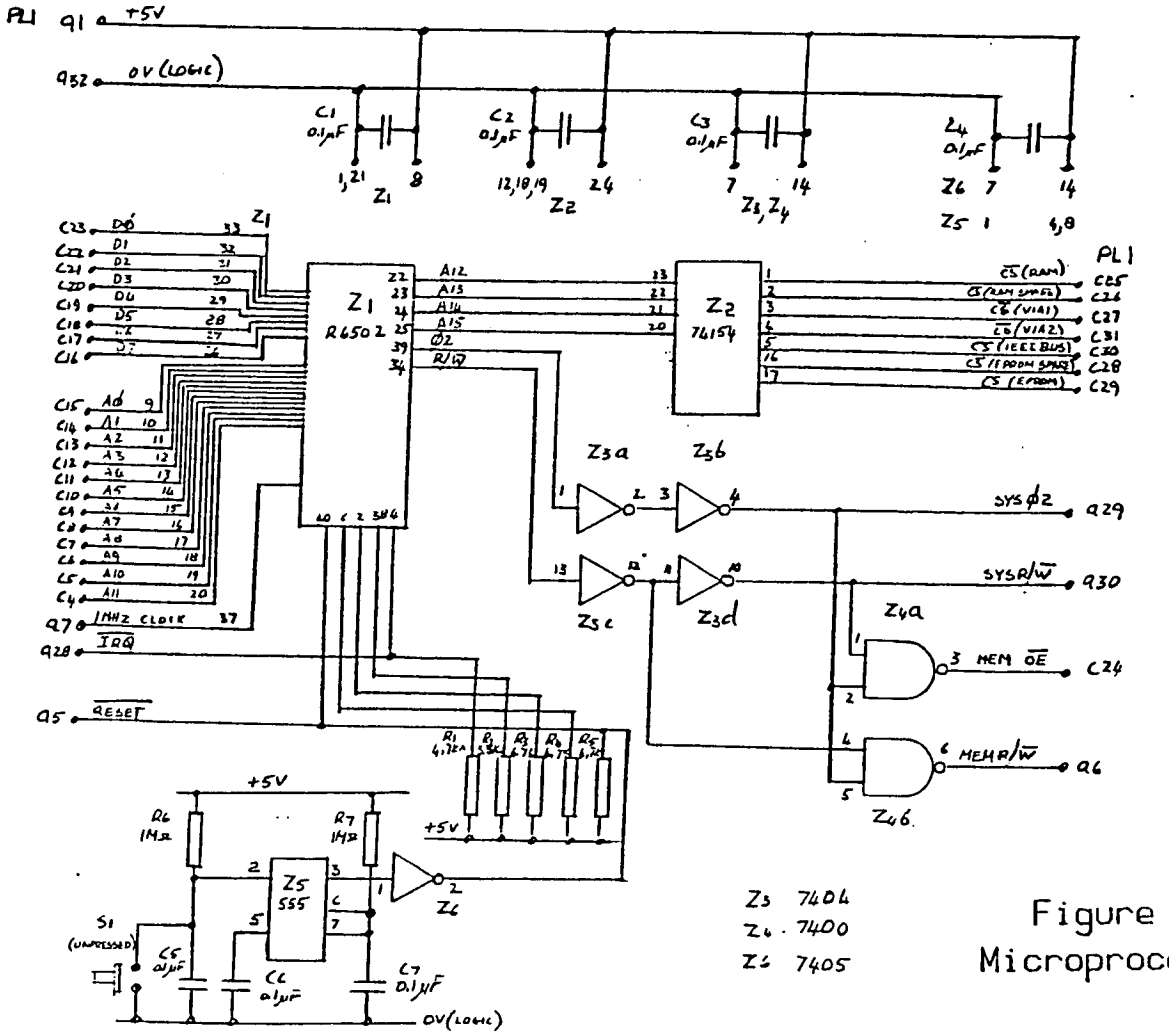

Figure K.6.
Microprocessor

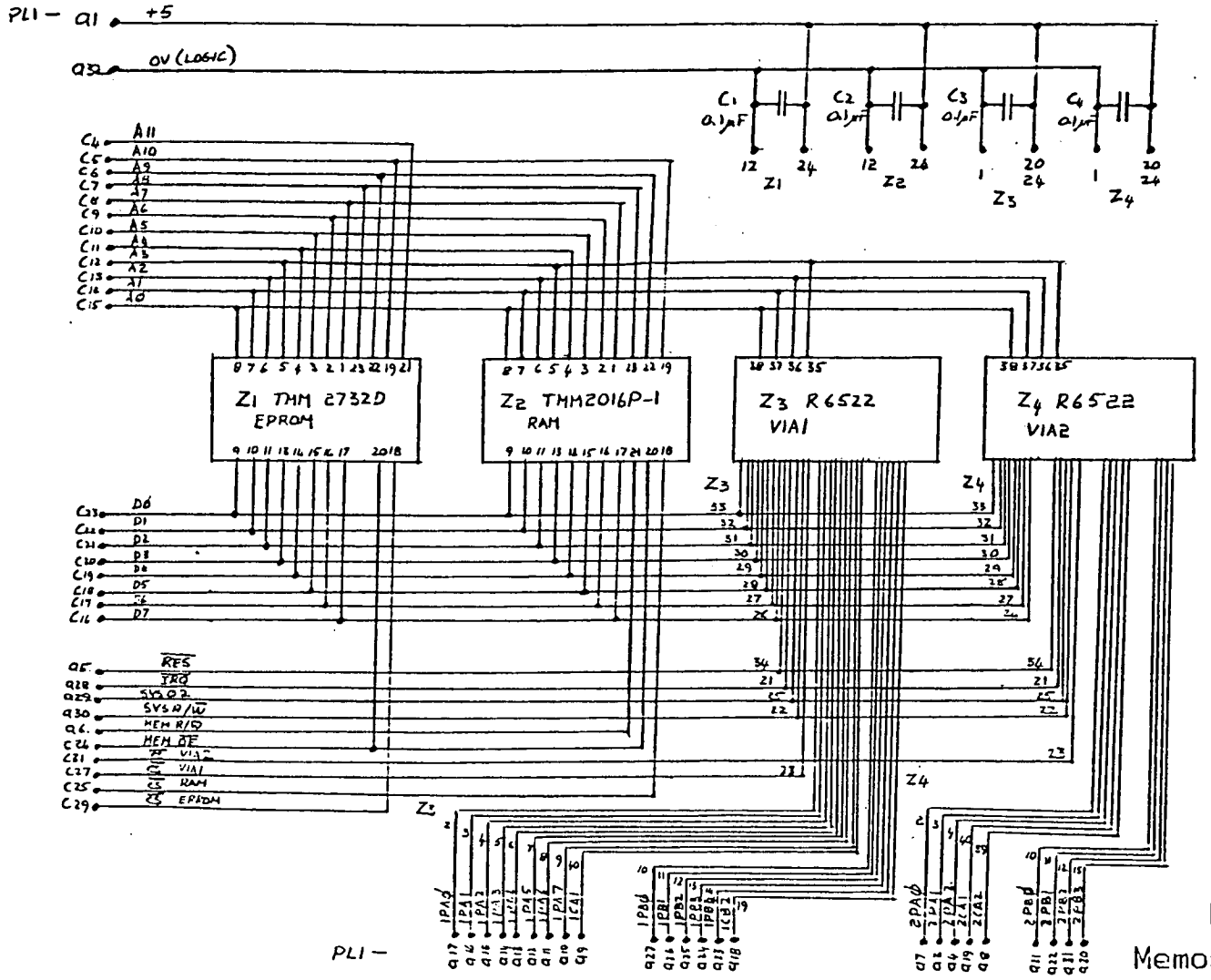

Figure K.7.
Memory and Interface

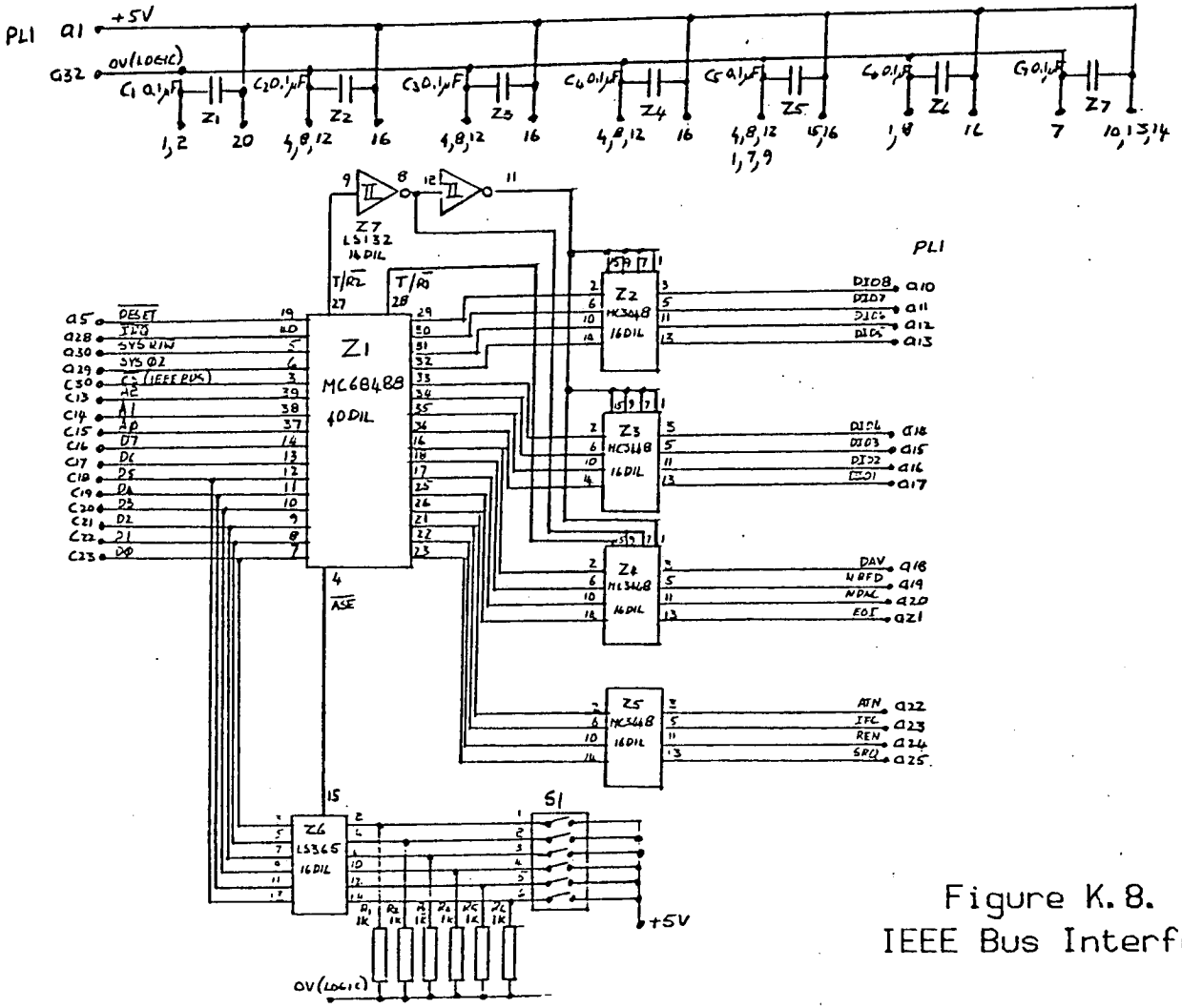

Figure K.8.
IEEE Bus Interface

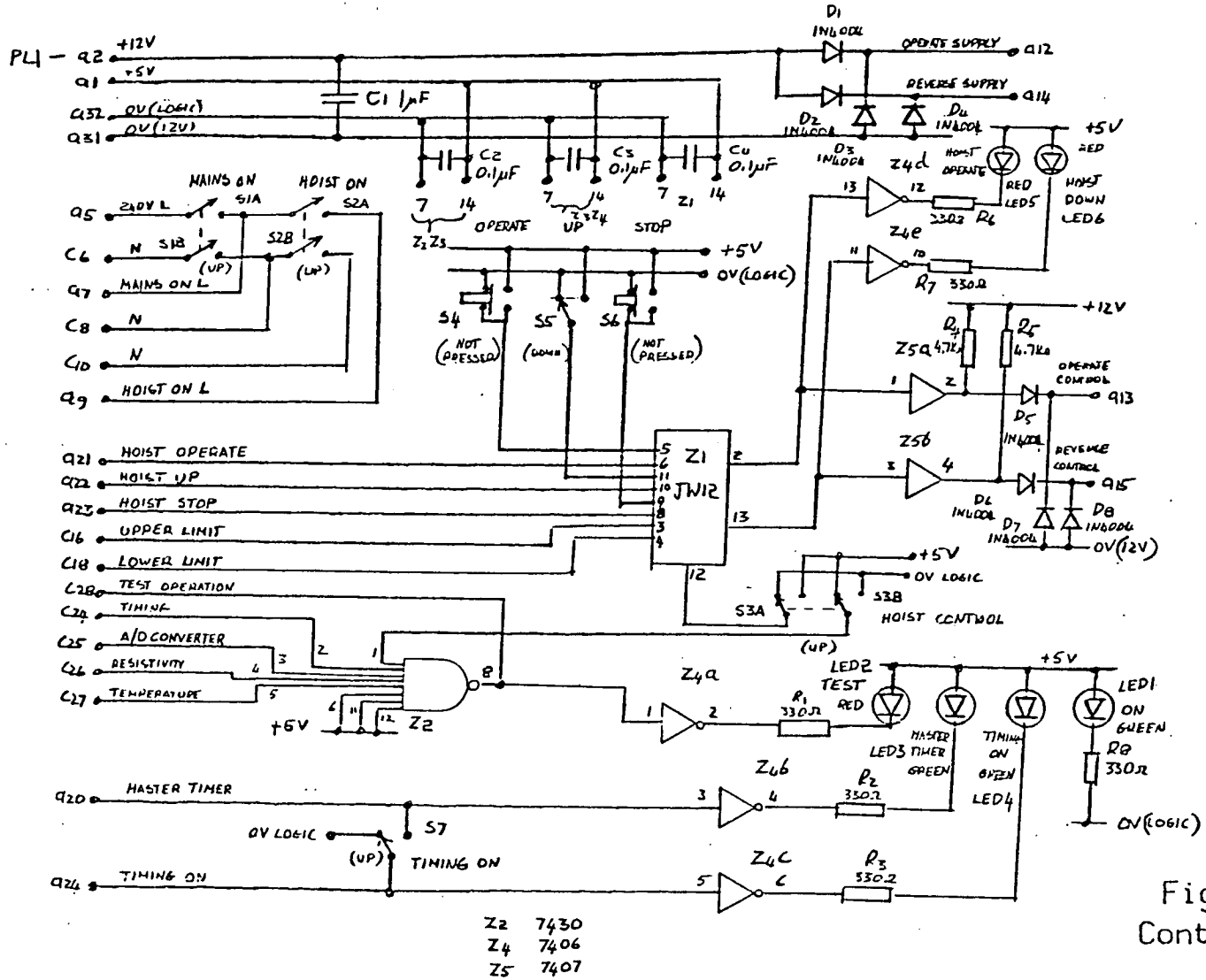

Z2 7430
Z4 7406
Z5 7407

Figure K.9.
Control Unit

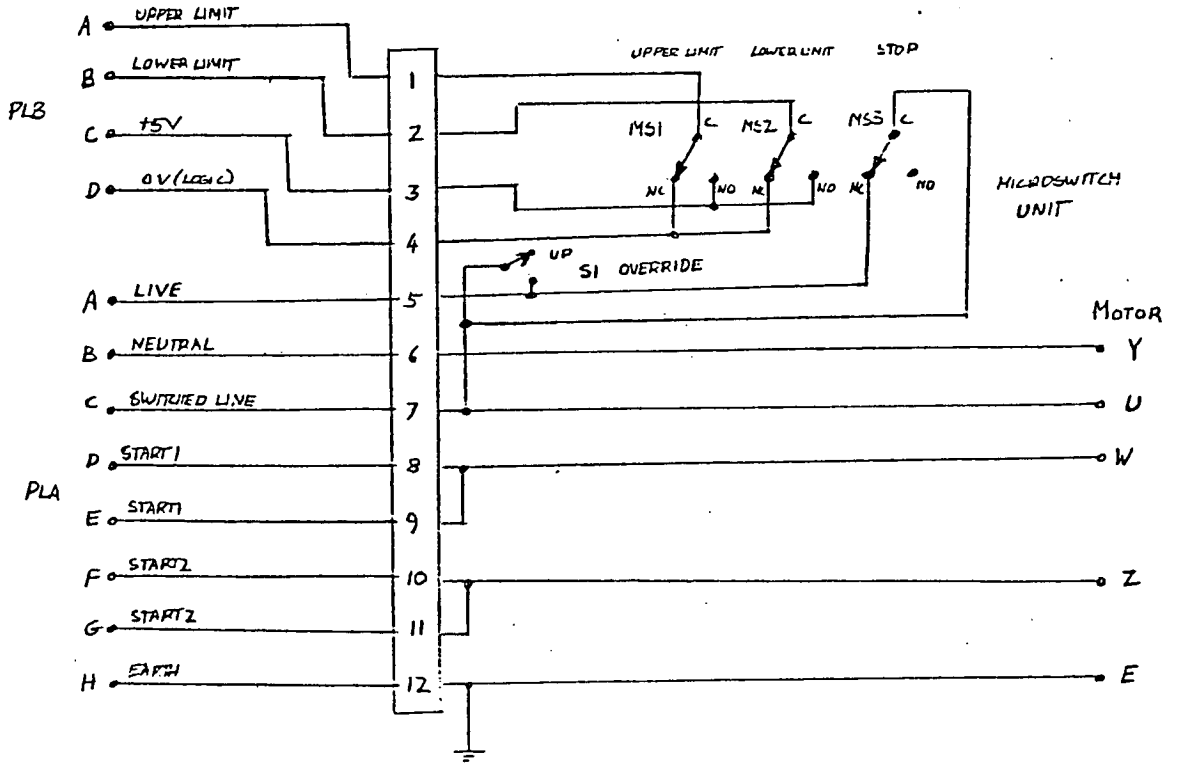

Figure K. 10.
Hoist

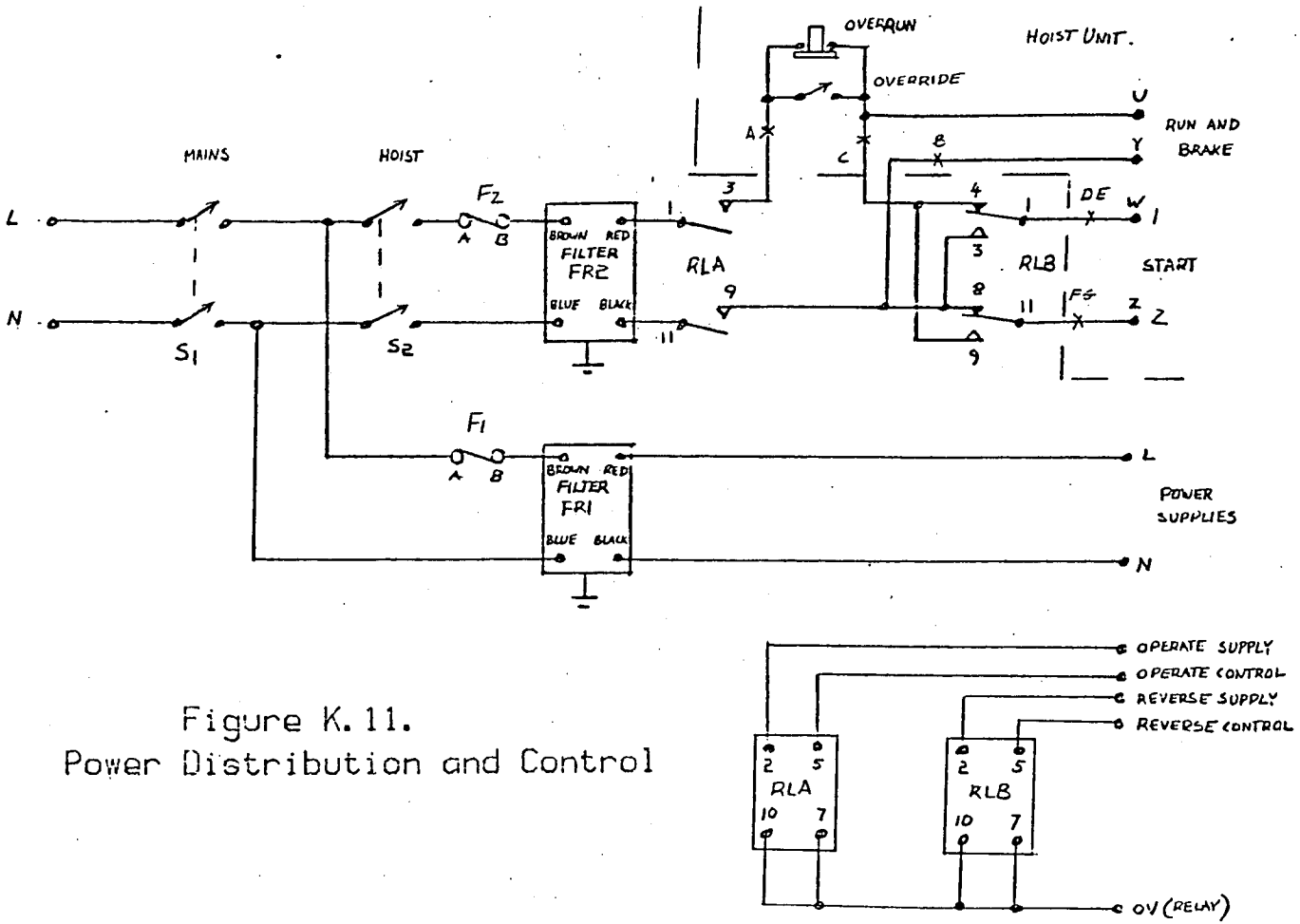

Figure K.11.
Power Distribution and Control

APPENDIX L.

Calibration Procedures.

A/D Converter.

1. Put the test switch for the A/D converter to the TEST state.
2. Monitor A/D converter output using the DATA program to monitor 01/01 resistivity, mode D.
3. Inject +9.766 mV at the input test point.
4. Adjust offset potentiometer RV_1 to give equal times at 0.5 and 1.5 on the CRT
5. Inject +2.490 V at the input test point.
6. Adjust gain potentiometer RV_2 to give equal times at 254.5 and 255.5 on the display.
7. Repeat 3 - 6 until satisfactory.
8. Return the A/D test switch to NORMAL.

Resistivity Multiplexer.

9. Monitor A/D converter output using the DATA program to monitor 01/01 resistivity reference, mode D.
10. Adjust RV_1 on the timing circuit to give equal time between 234.5 and 235.5 on the CRT.
11. Note the position of the potentiometer control, and adjust RV_1 to give equal times between 235.5 and 236.6, noting the increment required in the control position.
12. Reverse the position of the control on RV_1 by half the

total increment.

13. Monitor the A/D converter output using the DATA program to monitor 01/01 resistivity, mode D.

14. Short circuit the resistivity banana plug connectors on the lead for sample 01/01

15. Adjust RV_1 on the multiplexer to give equal time between 0.5 and 1.5.

16. Put the resistivity multiplexer test switch to the TEST state.

17. Inject a d.c. voltage at the resistivity multiplexer test point such that the indication has equal time at 1.5 and 2.5.

18. Adjust RV_1 to give equal time between 0.5 and 1.5.

19. Return the resistivity multiplexer test switch to the NORMAL state.

Temperature Multiplexer.

20. Monitor A/D converter output using the DATA program to monitor 01/01 temperature reference, mode D.

21. Adjust potentiometer RV_2 on the timing circuit to give equal times at 234.5 and 235.5 on the CRT.

22. Note the position of the control, and adjust RV_2 to give equal times at 235.5 and 236.5, noting the increment in the control position required.

23. Reverse the position of the control on RV_2 by half the increment.

24. Monitor the A/D converter output using the DATA program to monitor 01/01 temperature, mode D.

25. Put the temperature multiplexer test switch to the TEST position.

26. Inject a d.c. signal of +9.766 mV at the temperature multiplexer test point.

27. Adjust RV_1 on the multiplexer to give equal times at 0.5 and 1.5.

29. Return the test switch to the NORMAL position.

Temperature Amplifiers.

30. Place all O V electrodes in a draught free water bath at a temperature of approximately 20 ^{o}C. (water must not cover the temperature transducers and sockets).

30. Connect all transducer temperature output sockets to the corresponding temperature amplifiers, and switch on all amplifiers.

31. Measure the temperature of an electrode by placing the end of the contact probe near the temperature transducer.

31. Monitor the temperature indication on the CRT using the DATA program in mode C to monitor the temperature for the transducer being calibrated.

33. Adjust RV_1 on the temperature amplifier for the corresponding transducer (01/01 to 01/15) until the indicated temperature on the electronic display is as near the measured temperature as possible.

34. Repeat 31 - 33 for all transducers.

APPENDIX M.

Dielectric Properties of Concrete at Different Frequencies - Reference 77.

DIELECTRIC PROPERTIES OF CONCRETE AT DIFFERENT FREQUENCIES

J.G. Wilson, H.W. Whittington* and M.C. Forde*

Napier College, Edinburgh, *University of Edinburgh, U.K.

INTRODUCTION

Quality testing of structural concrete is traditionally carried out by making test cubes from the batch of concrete at the time at which it is placed, as described in BS1881 (1). These test cubes are cured, and submitted to a crushing strength test. The tests can be carried out at various intervals, but the earliest is normally 7 days after the concrete is placed. By this time the concrete has considerable strength, and if it is subsequently found to be faulty, removal can be very expensive.

To obtain results more quickly after the placement of the concrete, electrical methods of testing have been considered by a number of investigators (Hammond and Robson (2), Monfore (3), Whittington et al (4)). These methods generally depend on measuring the low-frequency resistivity of the concrete, and drawing conclusions from the measurements as to the quality of the concrete. For example, the resistivity value obtained during the setting process will be related to the porosity of the hardened concrete. Conduction through the concrete is by ionic conduction through the water filled capillary pores. High porosity concrete will have a low resistivity, and will also have relatively low strength.

The authors have designed test equipment to measure the low-frequency resistivity of concrete. This equipment described by Wilson et al (5), is currently in use in a research programme in the School of Engineering at the University of Edinburgh. It became clear early in the development of this equipment that there were certain conditions that the equipment could not detect. For example the presence of entrapped air in concrete cannot be differentiated from the presence of additional aggregate, since in general, aggregate has a very high value of resistivity, see Parkhomenko (6) for example.

Taylor and Arulanandan (7) measured the electrical impedance of cement pastes over the frequency range 1-100 MHz and derived values for conductivity and relative permittivity. They attempted to assess the proportion of free water in their samples as the hydration of the cement progressed. The authors have applied a similar technique to concrete with the initial aim of distinguishing between entrapped air and aggregate. Since the relative permittivity of air is 1, and that for aggregate is in the range 2.5-8, variations in impedance should be detectable.

The authors also intend using this technique to develop an electrical model of concrete which could be used on the assessment of quality.

EXPERIMENTAL METHOD

Measurement System

The experimental work has largely been directed to confirming that entrapped air can be detected by high-frequency impedance measurements, on the assumption that a low-frequency resistivity test has been carried out and has indicated a higher than normal value of resistivity.

The basis of the measuring system is the Hewlett-Packard RF Impedance Analyser Type HP4191A, which covers the frequency range 1 to 1000 MHz. The analyser is controlled by a Hewlett-Packard HP85 computer, and data is stored on a magnetic disc.

The geometry of the concrete samples is that which has been used by the investigators for low frequency experiments (5), i.e. a 150 mm cube, which is an industry standard for crushing strength measurement (1). Stainless steel plate electrodes are placed on two opposite faces of the cube to form a parallel plate transmission line with the concrete as dielectric. At one end of the electrode system there is a transition to 50 ohm coaxial line which is the form of connection required by the analyser. The temperature of one of the electrodes on each sample is also measured using an electronic thermometer.

After demoulding, the samples are stored in a water bath and withdrawn when measurements are required.

Impedance measurements were carried out over the frequency range 1-100 MHz, and also in the range 500-700 MHz, where half wave resonance occurs.

Concrete Samples

Four samples were used to obtain the results presented. These were:

(a) a normal sample of concrete with water/cement ratio 0.5:1 and cement/sand/coarse aggregate ratio 1:1.5:3

(b) a sample using the same basic mix, but with additional aggregate added to give an additional aggregate volume of 5%

(c) a sample using the same basic mix, but with holes moulded in the sample to give an air volume of 5%

(d) a sample using the same basic mix, but with holes moulded in the sample to give an air volume of 10%.

TRIAL RESULTS

Lower Frequency Band

Results of impedance measurements carried out over the frequency range 1-100 MHz are shown in Figure 1. These results were obtained about 6.01 days after the concrete was mixed.

The graphs show a progressive fall in impedance up to a frequency of 40 MHz. Above 40 MHz, minor resonances occur which are due to the coaxial to parallel plate transition. While the shape of the impedance/frequency graph for additional aggregate is similar to that for the normal mix, the slope is different from that for the low air content.

Higher Frequency Band

The results for measurements in the higher frequency range are given in Figure 2, and were taken about 6.01 days after the concrete was mixed.

The graph for the normal sample has a relatively broad maximum, with a relatively high resonant frequency. Additional aggregate causes the resonant frequency to be reduced, but still with a relatively broad response. A small amount of air causes a reduction in resonant frequency and narrowing of the response. A greater amount of air causes a higher resonant frequency with an even narrower response.

Derived Parameters

The authors have devised parameters which characterise the variations in the shapes of the impedance plots.

For the frequency band 1-100 MHz, the ratio of the impedance at 30 MHz divided by that at 1 MHz is significant. This graph is shown in Figure 3 along with the average temperature of the samples. From this graph it appears that the impedance ratio places samples with entrapped air closer to a normal sample than a sample with additional aggregate. There is some indication that the impedance ratio is temperature sensitive.

In the frequency band 500-700 MHz, a fractional bandwidth has been defined as the frequency difference between the points at which the impedance is 90% of maximum, divided by the frequency of the maximum. The function is plotted in Figure 4, along with the average temperature. The fractional bandwidth parameter places the additional aggregate sample closer to a normal sample than those with entrapped air. The function again appears to be temperature sensitive.

The first two data points show discontinuities compared with the others. This is because, following these readings, the concrete is stored in water for a considerable time, and will be saturated, while for the first measurements, the samples have just been demoulded, and for the second, they have only been stored in water for a very short time.

By comparing the signature parameters for a sample with a high value of low-frequency resistivity, it might be possible to distinguish between entrapped air or additional aggregate depending on the volume proportion involved.

RESISTIVITY AND RELATIVE PERMITTIVITY VALUES

A computer program has been designed which deduces the value of the resistivity and relative permittivity of the concrete from the impedance measurements. It is assumed that the electrode system forms an open circuited parallel plate transmission line with the concrete as dielectric. Fringing effects are assumed to be negligible.

This program was applied to the impedance measurements for the normal concrete sample at approximately 6 days. Figure 5 shows the results for the low frequency band, and Figure 6 those for the high-frequency band.

In the low-frequency band, there is a progressive reduction in resistivity and relative permittivity as frequency increases, with the relative permittivity having a value greater than 100 at 1 MHz. Discontinuities occur in the region of 70 MHz due to impedances in the parallel plate to coaxial line transition. The validity of these results must therefore be in question in this region.

The results for the high-frequency band give a relative permittivity of approximately 3, and a resistivity which is greater than 70 Ωm at 500 MHz, but falls with increasing frequency. The validity of these results might again be in question because of the effects of the transition impedances.

ELECTRICAL MODEL

The results for relative permittivity indicate very high values of relative permittivity at low frequencies. The relative permittivity of water is in the region of 80, and the percentage of water by volume is in the range 3-16%. The relative permittivity of the aggregate and cement matrix without the water is thought to be about 2.5. The reason for the high value of measured relative permittivity is believed to be due to Maxwell-Wagner effects in the relatively high conductivity water pores imbedded in the low conductivity cement and aggregate structure. Van Beck (8) gives various parameters for the Debye relaxation equations which describe the Maxwell-Wagner effect, depending on the geometry of the high conductivity particles. The equations attributed to Fricke (9) for needle shaped conducting particles can give very high values of relative permittivity at low frequencies. This model could be applied to concrete where the needles are the conducting capillary pores.

Figure 5 also shows resistivity and relative permittivity results for a model consisting of a continuous water channel with a very thin insulating layer, and a channel consisting of randomly orientated conducting needles in a cement/aggregate matrix. The water channel accounts for the finite low frequency resistivity of the concrete, while the thin insulating layer models a layer of gas generated by electrolytic effects (5). It can be seen that, although the general shape is correct, there are considerable discrepancies.

This model is described by the equations:

$$\varepsilon_r = \left\{ \varepsilon_{r\infty} + \frac{\varepsilon_{rs} - \varepsilon_{r\infty}}{1 + \omega^2 \tau_A^2} \omega^2 \tau_A^2 \right\} \chi + \left\{ \varepsilon_{r\infty} + \frac{\varepsilon_{rs} - \varepsilon_{r\infty}}{1 + \omega^2 \tau_B^2} \right\} (1 - \chi)$$

$$\frac{1}{\rho} = \frac{\omega^2 \tau_A^2 \sigma_{A\infty}}{1 + \omega^2 \tau_A^2} \chi + \frac{\omega^2 \tau_B^2 \sigma_{B\infty}}{1 + \omega^2 \tau_B^2} (1 - \chi)$$

where A refers to the water channel
B refers to the needle channel
χ is the fractional volume of the water channel.

The Fricke model assumes that the needles are all of the same length, but in concrete, the pore lengths will have a distribution probably approaching the Poisson distribution, with the part of the distribution with pores exceeding the length of the sample giving rise to the finite value of low-frequency resistivity. The authors are currently investigating this form of model.

CONCLUSIONS

Electrical impedance measurements can detect small variations in the constituents of concrete.

The electrical structure of concrete is complex, and exhibits Maxwell-Wagner effects. Models describing the electrical structure are being developed.

ACKNOWLEDGEMENTS

The authors wish to thank the School of Engineering, University of Edinburgh, and the Department of Electrical and Electronic Engineering, Napier College, Edinburgh, for the use of facilities.

This work was carried out on an SERC grant. Lothian Regional Council also gave financial support.

REFERENCES

1. British Standards Institution, 1970, "Methods of Testing Concrete", BS1881, and amendments.

2. Hammond, E. and Robson, T.D., 1975, "Comparison of Electrical Properties of Various Cements and Concretes", The Engineer, 199, 78-80.

3. Monfore, G.E., 1968, "The Electrical Resistivity of Concrete", J. PCA. Res. Dev. Labs., 10, 2, 35-48.

4. Whittington, H.W., McCarter, J. and Forde, M.C., 1981, "The Conduction of Electricity Through Concrete", Mag. Concr. Res., No.114, 48-60.

5. Wilson, J.G., Whittington, H.W. and Forde, M.C., 1983, "Microprocessor Based System for Automatic Measurement of Concrete Resistivity", J. Phys. E: Sci. Instr., 16, 700-705.

6. Parkhomenko, E.I., 1967, "Electrical Properties of Rocks", Plenum Press, New York.

7. Taylor, M.A. and Arulanandan, K., 1974, "Relationships Between Electrical and Physical Properties of Cement Pastes", Cem. Concr. Res., 4, 881-897.

8. Van Beek, L.K.H., 1967, "Dielectric Behaviour of Heterogeneous Systems", Prog. in Dielectrics, 7, 69-114, Heywood, London.

9. Fricke, H., 1953 "The Maxwell-Wagner Dispersion in a Suspension of Ellipsoids" J. Phys. Chem., 57, 934-937.

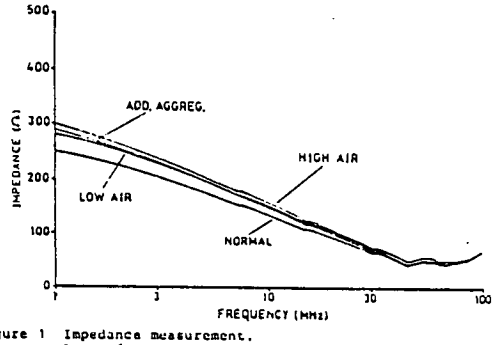

Figure 1 Impedance measurement. Lower frequency band.

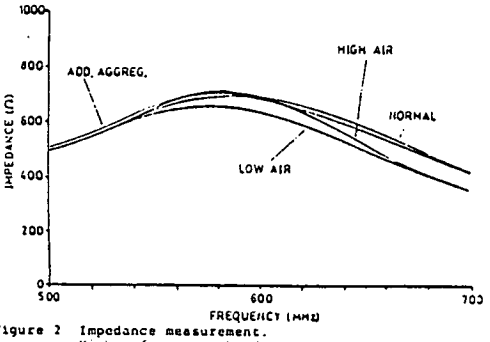

Figure 2 Impedance measurement. Higher frequency band.

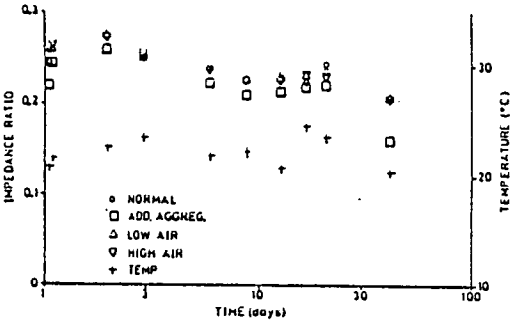

Figure 3 Impedance ratio.

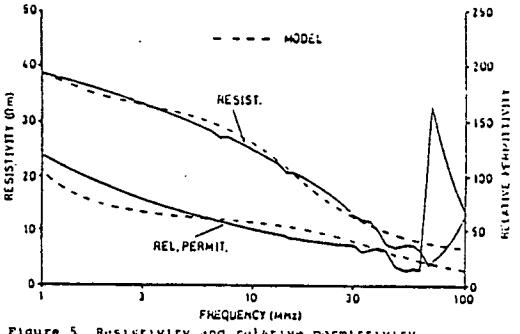

Figure 5 Resistivity and relative permittivity. Lower frequency band.

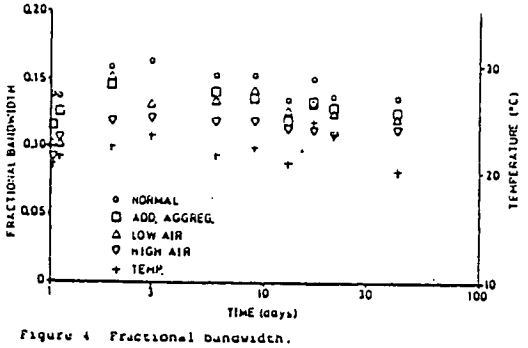

Figure 4 Fractional bandwidth.

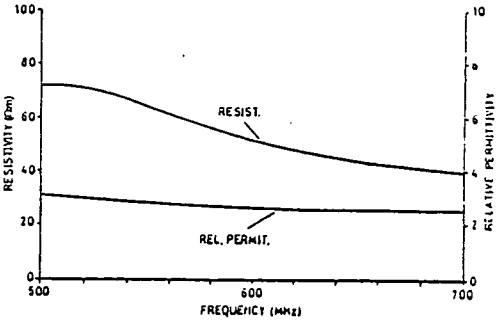

Figure 6 Resistivity and relative permittivity. Higher frequency band.

APPENDIX N

Calculation of Resistivity and Dielectric Constant

For an open circuited transmission line with a lossy dielectric

$$\tanh \gamma \ell = \frac{Z_o}{Z} \qquad \text{(N. 1)}$$

where $\gamma = \sqrt{j\omega L\ (G + j\omega C)}$

and $Z_o = \sqrt{\frac{j\omega L}{G + j\omega C}}$

Where γ = propagation constant

ℓ = length of transmission line (m)

Z_o = characteristic impedance (Ω)

Z = impedance measured at the input terminals of the transmission line (Ω)

ω = radian frequency (rad/s)

L = inductance per unit length (Hm^{-1})

G = conductance per unit length (Sm^{-1})

C = Capacitance per unit length (Fm^{-1})

For a narrow parallel plate transmission line

$$L = \mu_o \frac{a}{b}$$

$$G = \frac{1}{\rho} \frac{b}{a}$$

$$C = \varepsilon_o \varepsilon_r \frac{b}{a}$$

where μ_o = permeability of free space

$= 1.26 \times 10^{-6}$ (Hm^{-1})

ρ = resistivity of dielectric (Ωm)

ε_o = permittivity of free space

$= 8.85 \times 10^{-12} (Fm^{-1})$

ε_r = dielectric constant

a = separation between the plates (m)

b = width of plates (m)

Ignoring the limitation of a narrow parallel plate line, and making a = b gives

$$L = \mu_o$$

$$G = \frac{1}{\rho}$$

$$C = \varepsilon_o \varepsilon_r$$

$$\gamma = \sqrt{j\omega\mu_o \left(\frac{1}{\rho} + j\omega\varepsilon_o\varepsilon_r\right)} \qquad \text{(N. 2)}$$

$$Z_o = \sqrt{\frac{j\omega\mu_o}{\frac{1}{\rho} + j\omega\varepsilon_o\varepsilon_r}} \qquad \text{(N. 3)}$$

From Expression N. 1

$$\frac{Z_o}{Z} = \frac{e^{\gamma\ell} - e^{-\gamma\ell}}{e^{\gamma\ell} + e^{-\gamma\ell}}$$

$$= \frac{e^{2\gamma\ell} - 1}{e^{2\ell\gamma} + 1}$$

Thus $e^{2\gamma\ell} = \frac{Z + Z_o}{Z - Z_o}$ (N. 4)

Now $Z_o = \sqrt{\frac{j\omega\mu_o}{\frac{1}{\rho} + j\omega\varepsilon_o\varepsilon_r}}$

$$= \left\{\frac{\omega^2\mu_o^2}{\frac{1}{\rho^2} + \omega^2\varepsilon_o^2\varepsilon_r^2}\right\}^{\frac{1}{4}} e^{j\frac{1}{2}\left\{\frac{\pi}{2} - \tan^{-1}\omega\rho\varepsilon_o\varepsilon_r\right\}}$$

$$= \left\{ \frac{\omega^2 \mu_o^2}{\frac{1}{\rho^2} + \omega^2 \varepsilon_o^2 \varepsilon_r^2} \right\}^{\frac{1}{4}} \left\{ \cos\left(\frac{\pi}{4} - \frac{1}{2} \tan^{-1} \omega\rho\varepsilon_o\varepsilon_r\right) + j\sin\left(\frac{\pi}{4} - \frac{1}{2} \tan^{-1} \omega\rho\varepsilon_o\varepsilon_r\right) \right\}$$

Letting $Z_o = R_o + jX_o$ (N. 5)

where $R_o = \left\{ \frac{\omega^2 \mu_o^2}{\frac{1}{\rho^2} + \omega^2 \varepsilon_o^2 \varepsilon_r^2} \right\}^{\frac{1}{4}} \cos\left(\frac{\pi}{4} - \frac{1}{2} \tan^{-1} \omega\rho\varepsilon_o\varepsilon_r\right)$ (N. 6)

$$X_o = \left\{ \frac{\omega^2 \mu_o^2}{\frac{1}{\rho^2} + \omega^2 \varepsilon_o^2 \varepsilon_r^2} \right\}^{\frac{1}{4}} \sin\left(\frac{\pi}{4} - \frac{1}{2} \tan^{-1} \omega\rho\varepsilon_o\varepsilon_r\right) \quad \text{(N. 7)}$$

and $Z = R + jX$ (N. 8)

then from Expressions N.4 and N.8,

$$e^{2\gamma\ell} = \frac{R + jX + R_o + jX_o}{R + jX - R_o - jX_o}$$

$$= \frac{\sqrt{(R^2 + X^2 - R_o^2 - X_o^2) + 4(RX_o - R_oX)^2}}{(R - R_o)^2 + (X - X_o)^2}$$

$$\times e^{j\tan^{-1}\left\{\frac{2(RX_o - R_oX)}{R^2 + X^2 - R_o^2 - X_o^2}\right\}}$$

Thus $2\gamma\ell = \log\left\{ \frac{\sqrt{(R^2 + X^2 - R_o^2 - X_o^2)^2 + 4(RX_o - R_oX)^2}}{(R - R_o)^2 + (X - X_o)^2} \right\}$

$$+ j \tan^{-1}\left\{ \frac{2(RX_o - R_oX)}{R^2 + X^2 - R_o^2 - X_o^2} \right\}$$

and $\gamma = \frac{1}{2\ell} \log\left\{ \frac{\sqrt{(R^2 + X^2 - R_o^2 - X_o^2)^2 + 4(RX_o - R_oX)^2}}{(R - R_o)^2 + (X - X_o)^2} \right\}$

$$+ j \frac{1}{2\ell} \tan^{-1} \left\{ \frac{2(RX_o - R_oX)}{R^2 + X^2 - R_o - X_o^2} \right\}$$

$$= A + jB \qquad (N.9)$$

where $$A = \frac{1}{2\ell} \log \left\{ \frac{\sqrt{(R^2 + X^2 - R_o^2 - X_o^2)^2 + 4(RX_o - R_oX)}}{(R - R_o)^2 + (X + X_o)^2} \right\} \qquad (N.10)$$

$$B = \frac{1}{2\ell} \tan^{-1} \left\{ \frac{2(RX_o - R_oX)}{(R - R_o)^2 + (X - X_o)^2} \right\} \qquad (N.11)$$

From Expression N.9

$$\gamma^2 = A^2 - B^2 + j2AB \qquad (N.12)$$

From Expression N.2

$$\gamma^2 = j\omega\mu_o(\frac{1}{\rho} + j\omega \varepsilon_o \varepsilon_r)$$

$$= -\omega^2\mu_o\varepsilon_o\varepsilon_r + j \frac{\omega\mu_o}{\rho}$$

Equating with Expression N.12 gives

$$-\omega^2\mu_o\varepsilon_o\varepsilon_r = A^2 - B^2$$

$$\varepsilon_r = \frac{B^2 - A^2}{\omega^2\mu_o\varepsilon_o} \qquad (N.13)$$

and

$$\frac{\omega\mu_o}{\rho} = 2AB$$

$$\rho = \frac{\omega\mu_o}{2AB} \qquad (N.14)$$

The procedure followed to calculate ρ and ε_r is

(i) measure R and X at frequency

(ii) assume values for ρ and ε_r

(iii) calculate R_o and X_o using Expressions N.6 and N.7

(iv) calculate A and B using Expressions N.10 and N.11

(v) calculate ρ and ε_r using Expressions N.14 and N.13

(vi) take new trial values of ρ and ε_r as the arithmetic means of the previously assumed values and the calculated values.

(vii) iterate from (iii) until the variations in ρ and ε_r are within acceptable limits.

B as calculated by Expression N.11 is a multivalued function. The value which gives the smallest positive value for ε_r is taken.

REFERENCES.

1. Neville, A.M., "Properties of Concrete", Second Edition, Pitman, London, 1978.

2. Double, D.D., "New developments in understanding the chemistry of cement hydration", Philosophical Transactions of the Royal Society of London, Series A, Vol.310, 1983, pp53 - 66.

3. Pratt, P.L. and Ghose, A., "Electron microscope studies of Portland cement microstructures during setting and hardening", Philosophical Transactions of the Royal Society of London, Series A, Vol.310, 1983, pp93 - 103.

4. Schutz, R.J., "Handbook of Structural Concrete", Pitman, London, 1983, pp9-1 to 9-32.

5. Kendall, A., Howard, A.J. and Birchall, J.D., "The relation between porosity, microstructure and strength, and the approach to advanced cement-based materials", Philosophical Transactions of the Royal Society of London, Series A, Vol.310, 1983, pp139 - 153.

6. Harris, B. and Bunsell, A.R., "Structure and Properties of Engineering Materials", Longman, London, 1977.

7. Frohnsdorff, G. and Skalny, J., "Cement in the 1990s: challenges and oportunities", Philosophical Transactions of the Royal Society of London, Series A, Vol.310, 1983, pp17 - 30.

8. McArthur, H., "Design faults in Airey houses", Proceedings of the Conference on Structural Faults, March 1983, University of Edinburgh, pp235 - 241.

9. Tomsett, H.N., "The use of non-destructive testing in the control of concrete construction", Proceedings of the Conference on Non-Destructive Testing, November 1983, Heathrow, London, Engineering Technics Press, Edinburgh, pp88 - 99.

10. Bate, S.C.C., "Handbook of Structural Concrete", Pitman, London, 1983, pp2-1 to 2-56.

11. Parsons, P. and Melvin, J., "Two structures affected by inadequate cover and incompetent concrete", Proceedings of the Conference on Structural Faults, March 1983, University of Edinburgh, pp267 - 270.

12. British Standards Institution, "Methods of Testing Concrete", BS1881, 1970 (and amendments).

13. Tattersal, G.H. and Bloomer, S.J., "Further development of the two-point test for workability and extension of its range", Magazine of Concrete Research, Vol.31, No.109, December 1979, pp202 - 210.

14. Bungey, J.H., "The Testing of Concrete in Structures", Surrey University Press, 1982.

15. Dhir, R.K., Munday, J.G.L. and Ho, N.Y., "Analysis of fresh concrete; : determination of cement content by the rapid analysis machine", Magazine of Concrete Research, Vol.34, No.119, June 1982, pp59 - 73.

16. Bungey, J.H., "An appraisal of pull-out methods of testing concrete", Proceedings of the Conference on Non-Destructive Testing, November 1983, Heathrow, London, Engineering Technics Press, Edinburgh, PP12 - 21.

17. Keiller, A.P., "An investigation of test methods for the assessment of strength of in situ concrete", Proceedings of the Conference on Non-Destructive Testing, November 1983, Heathrow, London, Engineering Technics Press, Edinburgh, pp45 - 55.

18. Long, A.E., "A review of methods of assessing the in situ strength of concrete", Proceedings of the Conference on Non-Destructive Testing, November 1983, Heathrow, London, Engineering Technics Press, Edinburgh, pp56 - 76.

19. Swamy, R.N., and Ali, A.M.A.H., "Assessment of in situ concrete strength by various non-destructive tests", Proceedings of the Conference on Non-Destructive Testing, November 1983, Heathrow, London, Engineering Technics Press, Edinburgh, pp181 - 197.

20. Bungey, J.H., "The validity of ultrasonic pulse velocity testing of in-place concrete for strength", NDT International, Vol.13, No.6, December 1980, pp296 - 300.

21. Tomsett, H.N., "The practical use of ultrasonic pulse velocity measurements in the assessment of concrete quality", Magazine of Concrete Research, Vol.32, No.110, March 1980, PP7 - 16.

22. Elvery, R.H. and Ibrahim, L.A.M., "Ultrasonic assessment of concrete strength at early ages", Magazine of Concrete Research, Vol.28, No.97, December 1976, pp181 - 190.

23. Jones, R., "A review of the non destructive testing of concrete", Proceedings of the Symposium on Non-destructive Testing of Concrete and Timber, London, June 1969, ICE, pp1 - 7.

24. Blythe, A.R., "Electrical Properties of Polymers", Cambridge University Press, Cambridge, 1979.

25. Hasted, J.B., "Aqueous Dielectrics", Chapman and Hall, London, 1973.

26. Malmberg, G.G., and Maryott, A.A., J. Res. Nat. Bur. Standards, Vol.56,

27. Kay, R.L., Vituccio, T., Zawoyski, C., and Evans, D.F., Journal of Physical Chemistry, Vol.70, 1966, p2336.

28. Garside, J.E., and Phillips, R.F., "Pure and Applied Chemistry", Pitman, London, 1953.

29. Auty, R.P., and Cole, R.H., J. Chem. Phys., Vol.20, 1952, p1309.

30. Humbel, F., Iona, F., and Scherrer, P., Helv. Phys. Acta., Vol.26,

31. Bjerrum, N., Klg. Danske Videnskap. Selskab Mat-Fys. Medd., Vol.27,

32. Hasted, J.B., "Dielectric properties of water", Progress in Dielectrics, Vol.3, 1961, pp102 - 149.

33. De Loor, G.D., "The effect of moisture on the dielectric constant of hardened Portland cement paste", Appl. Sci. Res., Vol.11, 1961, PP297 - 308.

34. Van Beek, L.K.H., and Stein, H.N., "Low frequency dielectric behaviour of Portland cement paste", Kolloid-Zeitschrift und Zeitschrift fur Polymere, Vol.181, 1962, pp65 - 69.

35. Lovell, S.P., Firth, P., and Hasted, J.B., "Discontinuity in temperature variation of microwave dielectric properties of absorbed water", British Journal of Applied Physics, Vol.15, 1964, pp1439 - 1440.

36. Glasstone, S., "An Introduction to Electrochemistry", Van Nostrand, Princeton, 1942.

37. Monfore, G.E., "The electrical resistivity of concrete", Journal of the PCA Research and Development Laboratories Vol.10, Part 2, May 1968, pp35 - 48.

38. Johnson, J.F., and Cole, R.H., "Dielectric constant of liquid and solid formic acid", Journal of the American Chemical Society, Vol.73, Oct. 1951, pp4536 - 4540.

39. Gillespie, R.J., and Cole, R.H., "The dielectric constant of sulphuric acid", Transactions of the Faraday Society, Vol.52, 1956, pp1325 - 1331.

40. Schwan, H.P., Schwarz, G., Maczuk, J., and Pauly, H., "On the low frequency dielectric dispersion of colloidal particles in electrolyte solutions", Journal of Physical Chemistry, Vol.66, 1962, pp2626 - 2635.

41. Collie, C.H., Ritson, D.M., and Hasted, J.B., J. Chem. Phys., Vol.16,

42. Pottel, R., "Water: A Comprehensive Treatise", Vol.II, Ed.F, Franks, Plenum Press, New York - London, 1973.

43. Debye, P. and Falkenhagen, H.,"Dispersion der Leitfahigkeit und der Dielectrizitatskonstante starker Elektrolyte"., Physikalische Zeitschrift, Vol.29, No.13, July 1928, pp401 - 426.

44. Hasted, J.B., and Roderick, G.W., J. Chem. Phys., Vol.29, 1958, p17.

45. Schwarz., G., "A theory of the low-frequency dielectric dispersion of colloidal particles in electrolyte solutions", Journal of Physical Chemistry, Vol.66, 1962, pp2636 - 2642.

46. Arulanandan, K., and Smith, S.S., "Electrical dispersion in relation to soil structure", Journal of the Soil Mechanics and Foundation Division, ASCE, Vol.99, Part SM12, Dec. 1973, pp1113 - 1133.

47. Springer, M.M., Korteweg, A., and Lyklema, J., "The relaxation of the double layer around colloid particles and the low-frequency dielectric dispersion. Part II, experiments", Journal of Electroanalytical Chemistry, Vol.153, 1983, pp55 - 66.

48. McCarter, W.J., and Curran, P.N., "The electrical response characteristics of setting cement pastes", Magazine of Concrete Research, Vol.36, No.126, March 1984, pp42 - 49.

49. Whittington, H.W., McCarter, J., and Forde, M.C., "The conduction of electricity through concrete", Magazine of Concrete Research, Vol.33, No.114, March 1981, pp48 - 60.

50. Van Beek, L.K.H., "Dielectric behaviour of heterogeneous systems", Progress in Dielectrics, Vol.7, 1967, pp69 - 114.

51. Wagner, K.W., Arch. Elektrotech., Vol.2, 1914, p378.

52. Sillars, R.W., Journal of the Institute of Electrical Engineers, Vol.80,

53. Fricke, H., "The Maxwell-Wagner dispersion in a suspension of ellipsoids", Journal of Physical Chemistry, Vol.57, 1953, pp934 - 937.

54. Sachs, S.B., and Spiegler, K.S., "Radio frequency measurements of porous conductive plugs", Journal of Physical Chemistry, Vol.68, 1964, pp1214 - 1222.

55. Parkhomenko, E.I., "Electrical Properties of Rocks", Plenum Press, New York, 1967. (English translation).

56. Keller, G.V., and Licastro, P.H., "Dielectric constant and electric resistivity of natural state cores", Geol. Survey Bull., 1052-H, 1959.

57. Hammond, E., and Robson, T.D., "Comparison of the electrical properties of various cements and concretes", The Engineer, Jan.21, 1955, PP78 - 80.

58. Morelli, R., Private communication, Department of Civil Engineering and Building Science, University of Edinburgh, March 1983.

59. Spencer, R.W., "Measurement of the moisture content of concrete", Journal of the American Concrete Institute, Proceedings, Vol.34, Sept. - Oct. 1937, pp45 - 61.

60. Calleja, J., "New techniques in the study of setting and hardening of hydraulic materials", Journal of the American Concrete Institute, Proceedings, Vol.48, March 1952, pp525 - 536.

61. Calleja, J., "Effect of current frequency on measurement of electrical resistance of cement pastes", Journal of the American Concrete Institute, Proceedings, Vol.49, Dec. 1952, pp329 - 332.

62. Hammond, E., and Robson, T.D., "Comparison of electrical properties of various cements and concretes, No.2", The Engineer, Vol.199, No.5166, Jan.28, 1955, pp114 - 115.

63. Bell, J.R., Leonards, G.A., and Dolch, W.L., "Determination of moisture content of hardened concrete by its dielectric properties", Proceedings ASTM, Vol.63, 1963, pp996 - 1007.

64. Efimenko, Yu. V., and Ivanov, V.A., "Automatic instrument for measuring conductance of concrete", Ind. Lab. (USA), Vol.42. Part 8, August 1976, pp1285 - 1286, Translated from Zavodskaya Laboratoriya, Vol.42, No.8, August 1976, pp977 - 978.

65. McCarter, W.J., and Curran, P.N., "The electrical response characteristics of setting cement paste", Magazine of Concrete Research, Vol.36, No.126, March 1984, pp42 - 49.

66. Wilson, J.G., and Whittington, H.W., Letter on "The electrical response characteristics of setting cement paste" by McCarter and Curran, Magazine of Concrete Research, Vol.37, No.130, March 1985, pp52 - 53. (Appendix D)

67. Buenfeld, N.R., and Newman, J.B., "The permeability of concrete in a marine environment", Magazine of Concrete Research, Vol.36, No.127, June 1984, pp67 - 80.

68. Rzepecka, M.A., Hamid, M.A.K., and Soliman, A.H., "Monitoring of concrete curing process by microwave terminal measurements", IEEE Transactions on Industrial Electronics and Control Instrumentation, Vol. IECI-19, No.4, Nov. 1972, pp120 - 125.

69. Taylor, M.A., and Arulanandan, K., "Relationships between electrical and physical properties of cement pastes", Cement and Concrete Research, Vol.4, No.6, Nov. 1974, pp881 - 897.

70. Misra, D.K., "Permittivity measurement of modified infinite samples by a directional coupler and a sliding load", IEEE Transactions on Microwave Vol.MTT-29, No.1, Jan. 1981, pp65 - 67.

71. Wilson, J.G., Whittington, H.W., and Forde, M.C., "Microprocessor based system for automatic measurement of concrete resistivity", Journal of Physics E: Scientific Instruments, Vol.16, 1983, pp700 - 705. (Appendix F)

72. Data sheet, "Platinum resistance temperature detectors 158-238 & 158-244", R.S. Components, R/3914, July 1980.

73. Hermach, F.L., "An analysis of errors in the calibration of electrical instruments", Trans. Amer. IEE (Comm. and Electronics), Vol.54, May 1961, pp90 - 95.

74. Morelli, R., "Resistivity Testing of Concrete", Ph.D Thesis, Department of Civil Engineering, University of Edinburgh, May 1985.

75. Blackley, W.S., and Jack, M.A., "Semi-custom design in academic research and teaching", Proceedings of the 2nd. International Conference on Semi-custom Integrated Circuits, London, 1982, Prodex Limited in association with IEE.

76. Wilson, J.G., Whittington, H.W., and Forde, M.C., "The use of microcircuits in a computer controlled system for the measurement of the electrical resistivity of concrete", Proceedings of the International Conference on Civil and Structural Engineering Software and Applications, Heathrow, London, 15th - 17th November, 1983, Engineering Technics Press, Edinburgh, pp336 - 350. (Appendix J)

77. Wilson, J.G., Whittington, H.W., and Forde, M.C., "Dielectric properties of concrete at different frequencies", Fourth International Conference on Dielectric Materials, Measurements and Applications, 10 - 13 September, 1984, University of Lancaster, IEE Conference Publication No. 239, pp157 - 160. (Appendix M)

78. Blanchard, C.H., Burnett, C.R., Stoner, R.G., and Weber, R.L., "Introduction to Modern Physics", Second Edition, Pitman, London, 1969.